



Investigating the role of the transducin-like enhancer
of split proteins in maintenance of pancreatic beta cell
phenotype

Sarah Louise Armour

BSc, MRes

Thesis submitted for the degree of Doctor of Philosophy

Newcastle University

Faculty of Medical Sciences

Institute of Cellular Medicine

April 2019

Declaration

I hereby declare all work submitted in this thesis is entirely my own. All work was performed by me unless otherwise stated and all sources of information have been acknowledged by means of a reference.

Sarah Armour

Abstract

The relative contribution of pancreatic beta cell dysfunction and cell death to the decline in insulin production in type 2 diabetes (T2D) is debated. Although, undoubtedly, some cell death is occurring, studies have shown, in times of high metabolic stress, beta cells undergo changes to less mature cells (dedifferentiation) or even gain characteristics of other endocrine cell types (transdifferentiation) to 'hide away' from the constant demand for insulin secretion.

Our first aim was to assess the impact of glucotoxicity on beta cell phenotype and function. To achieve this, INS1E cells were cultured in high glucose and gene expression and functional assays were performed. A reduction in beta cell genes and insulin content were observed alongside upregulation of glucagon gene expression and protein levels, suggesting a transition to an alpha-cell phenotype.

Next, we aimed to assess the role particular proteins play in this phenotypic shift. Tle3, a member of the Groucho family of co-repressors, has been implicated as a repressor of the alpha-cell fate and has a potential role in beta cell function through interaction with transcription factor Pdx1. To investigate this further, Tle3 knockdown was performed *in vitro* using INS1E cells and isolated rodent islets. Both cell types showed a loss of beta cell phenotype and function and gain of alpha-cell characteristics.

Finally, we aimed to determine whether transdifferentiation is occurring in human T2D and what role TLE1, the human functional equivalent of Tle3, plays in this process.

Immunohistochemistry techniques were used to analyse beta-, alpha- and bihormonal cells in relation to TLE1 expression in control and diabetic patients. Our findings demonstrated an overall loss of beta cells and TLE1 expression in diabetic donors alongside increases in both alpha- and bihormonal cells.

Together, these studies provide evidence for transdifferentiation during T2D and show a potential role for Tle3/1 in the maintenance of the beta cell phenotype and function.

Acknowledgements

Firstly, I would like to thank my supervisors, Michael White and James Shaw for all their help and guidance over the past few years. I would also like to thank everyone else in the Shaw/diabetes group including Rashmi, Najwa, Xuefei, Nicole and Scott, along with Anne and Ally from the Wright group, who have always been there if I needed advice or a drink.

I would also like to thank the lab of Noel Morgan, University of Exeter and the MacDonald lab, University of Alberta, for kindly gifting me human tissue to use in my studies. It contributed some great findings to my work and, despite it resulting in endless hours of counting cells, it was well worth the effort!

Finally, I would like to thank my friends, in particular Clare and Katherine who live closest so took the brunt of my stressing. Most of all I would like to thank my family; my mum and dad (Gwen and John) and siblings (Katherine and Euan), for their constant support and for listening to me moan when science wasn't going my way, and to my gran for all the Sunday roasts I got when I showed up on her doorstep after a hard week.

Published Papers:

(Manuscript in submission) **Sarah, L. Armour**, Scott, J. Anderson, Sarah, J. Richardson, Yuchun Ding, James Lyon, Rashmi Maheshwari, Najwa Al. Jahdhami¹, Natalio Krasnogor, Noel, G. Morgan, Patrick Macdonald, James, A, M. Shaw, Michael, G. White. *Reduced beta cell expression of the transcriptional co-factor TLE1 is associated with increased islet alpha cell numbers in type 2 diabetes.*

Anderson SJ, White MG, **Armour SL**, Maheshwari R, Tiniakos D, Muller YD, et al. *Loss of end-differentiated beta cell phenotype following pancreatic islet transplantation.* Am J Transplant. 2018;18(3):750-5

Published Abstracts:

American Diabetes Association (Poster Presentation). '*A novel role for Tle3 in maintaining beta cell identity.*' **Sarah L Armour**, Scott Anderson, James A Shaw, Michael G White. June 2016 Diabetes.

American Diabetes Association. '*Evidence for beta cell dedifferentiation as a cause for sustained graft dysfunction following peri-engraftment hypoxia in clinical islet transplantation.*' Scott Anderson, **Sarah L Armour**, Michael G White, James A Shaw. June 2016, Diabetes.

Diabetes UK Professional Conference (Oral and Poster presentation). '*Limitation of glucotoxicity-induced beta cell dedifferentiation and alpha cell transition following Nkx6.1 overexpression.*' **Sarah L Armour**, James A Shaw, Michael G White. March 2016, Diabetic Medicine

Diabetes UK Professional Conference (Poster Presentation). '*An in vitro model of beta cell dedifferentiation and potential alpha cell reprogramming.*' **Sarah L Armour**, James A Shaw, Michael G White. March 2015, Diabetic Medicine

Diabetes UK Professional Conference (Poster Presentation). '*Limiting human beta cell dedifferentiation by small molecule inhibitors of the transforming growth factor beta (TGF-beta) pathway.*' Michael G White, **Sarah L Armour**, James A Shaw. March 2015, Diabetic Medicine

Table of Contents

1	Introduction	1
1.1	Glucose Homeostasis	2
1.1.1	Glucose metabolism in skeletal muscle	4
1.1.2	Glucose and the liver	4
1.1.3	Glucose regulation and adipocytes.....	5
1.1.4	The pancreas	5
1.1.5	Hormonal regulation of glucose	6
1.1.6	Insulin secretion from the pancreatic beta cell	8
1.2	Diabetes Mellitus.....	8
1.2.1	Type 1 diabetes	8
1.2.2	Type 2 Diabetes.....	10
1.3	Glucose toxicity and diabetic complications.....	11
1.4	Current Treatments for Diabetes	12
1.4.1	Type 1 Diabetes treatment	12
1.4.2	Type 2 Diabetes treatment	12
1.5	Pancreatic development	13
1.5.1	Differentiation of cell types within the pancreas	14
1.5.2	Pdx1.....	15
1.5.3	Nkx6.1	16
1.5.4	Groucho family of co-repressors	17
1.5.5	Tle proteins in the pancreas.....	18
1.6	Regulation of beta cell mass	19
1.7	Beta cell death in diabetes	19
1.8	Beta cell dysfunction	20
1.9	Beta cell plasticity.....	21
1.9.1	Dedifferentiation.....	21

1.9.2	Transdifferentiation.....	22
1.10	Aims.....	23
2	Materials and Methods.....	25
2.1	Materials.....	26
2.1.1	General Materials.....	26
2.1.2	Cell Culture Materials.....	26
2.2	Methods.....	27
2.2.1	INS1E cell culture.....	27
2.2.2	Subculture of cell lines.....	27
2.2.3	Generation of stable Tle3 knockdown cell line.....	27
2.3	Collection of Primary Tissue.....	28
2.3.1	Rodent Islet Isolations.....	28
2.3.2	Rodent Islet Culture.....	29
2.3.3	Human islet culture.....	29
2.4	Glucotoxicity treatments.....	29
2.5	Viral expansion, harvesting and treatments.....	29
2.5.1	Viral Expansion and harvesting.....	29
2.5.2	Viral treatments.....	30
2.6	Viral vectors.....	30
2.6.1	Transformation of viral vectors.....	30
2.6.2	Glycerol stocks of DNA plasmids.....	32
2.6.3	Miniprep purification of plasmid DNA.....	32
2.6.4	Agarose Gel electrophoresis.....	32
2.6.5	Maxiprep purification of plasmid DNA.....	33
2.7	Transfections.....	34
2.7.1	Small interfering RNA (siRNA) mediated knockdown of INS1E cells.....	34
2.7.2	Transfection of intact islets.....	35

2.7.3	Transfection of rodent and human islets.....	35
2.8	Staining of cells and tissue	36
2.8.1	Immunofluorescence staining of cell lines (ICC).....	36
2.8.2	Proximity Ligation Assay (PLA).....	37
2.8.3	PI-Hoechst staining	39
2.9	Staining of Tissue sections.....	39
2.9.1	Immunofluorescence staining of tissue sections.....	39
2.9.2	TSA assay.....	39
2.10	Cell counting.....	41
2.10.1	Manual counts	41
2.10.2	Automated counting	43
2.11	RNA extraction and cDNA synthesis.....	46
2.11.1	RNA extraction	46
2.11.2	RNA quantification	46
2.11.3	First strand cDNA synthesis	46
2.12	Polymerase Chain Reaction (PCR)	47
2.12.1	Quantitative Polymerase Chain Reaction (q-PCR)	47
2.12.2	Data Analysis of q-PCR	49
2.13	Glucose Stimulated Insulin Secretion (GSIS)	49
2.13.1	GSIS of cell lines	49
2.13.2	GSIS of rodent and human islets.....	50
2.14	Enzyme-linked Immunosorbent Assay (ELISA).....	50
2.15	Bradford Assay	51
2.16	Gel Electrophoresis and Western Blotting.....	51
2.16.1	Gel Electrophoresis	51
2.16.2	Western Blotting	52
2.16.3	Analysis of western blotting.....	53

2.17	Statistics	53
3	Results (1).....	55
3.1	Introduction	56
3.2	Aims	58
3.3	Results.....	59
3.3.1	Generation of an in vitro model of glucotoxicity in the rodent pancreatic INS1E cell line.....	59
3.3.2	Impact of glucotoxicity on beta cell function	63
3.3.3	Effect of glucotoxicity on beta cell phenotype.....	65
3.3.4	Effect of restoration of Pdx1 on changes observed in high glucose	72
3.4	Discussion	80
4	Results (2).....	85
4.1	Introduction	86
4.2	Aims	88
4.3	Results.....	89
4.3.1	The effect of high glucose culture on Tle3 expression.....	89
4.3.2	Interactions between Tle3 and Pdx1.....	90
4.3.3	siRNA mediated knockdown of Tle3	93
4.3.4	Generation of a stable Tle3 knockdown cell line	104
4.3.5	114
4.4	Discussion	123
5	Results (3).....	129
5.1	Introduction	130
5.2	Aims	131
5.3	Results.....	132
5.3.1	Cohort 1- Donor information	133
5.3.2	Cohort 1- Counting and analysis.....	135

5.3.3	Cohort 1- Does glucagon expression increase in type 2 diabetes?	135
5.3.4	Cohort 1- Is there an increase in bihormonal cells in type 2 diabetes?	137
5.3.5	Images of islets from tissue with and without type 2 diabetes.....	140
5.3.6	Cohort 1- Is TLE1 reduced in Type 2 diabetes?.....	144
5.3.7	Cohort 2- Donor information	146
5.3.8	Cohort 2- Staining of TLE1.....	147
5.3.9	Cohort 2- Determining the validity of the automated counting method.....	152
5.3.10	Cohort 2- Does the number of glucagon expressing cells increase in type 2 diabetes?.....	155
5.3.11	Cohort 2- Do the number of bihormonal cells increase in diabetes?.....	157
5.3.12	Cohort 2- Choosing a percentage confidence to continue with.....	161
5.3.13	Cohort 2- Localisation of TLE1.	162
5.3.14	Cohort 2- Is TLE1 lost in type 2 diabetes?.....	162
5.3.15	Cohort 2- Does the loss of TLE1 correlate to increased glucagon expression?.....	166
5.3.16	Cohort 2- Is there a link between loss of TLE1 and other donor information?.....	167
5.3.17	Cohort 2- Is there a link between loss of TLE1 and bihormonal cells?.....	170
5.3.18	Development of an in vitro model of TLE1 knockdown in intact human islets.....	175
5.4	Discussion	178
6	General discussion	183
6.1	Discussion	184
6.2	Future work	195
7	Bibliography	197
7.1	References.....	198
8	Appendix A. Published Papers	207

Table of Figures

<i>Figure 1.1 A diagram to summarise regulation of glucose levels in the fed and fasted states.</i>	3
<i>Figure 1.2 Simplified transcription factor map depicting different transcription factors required for mammalian pancreas differentiation.</i>	15
<i>Figure 2.1 Plasmid map of the lentiviral GFP vector containing either scrambled or TLE1 shRNA constructs used for transformations.</i>	31
<i>Figure 2.2 Transformation of E.coli with TLE1 shRNA plasmid.</i>	31
<i>Figure 2.3 Agarose gel to check for successful transformation.</i>	33
<i>Figure 2.4 Summary diagram of the Proximity Ligation Assay (PLA) technique.</i>	38
<i>Figure 2.5 Manual counting method.</i>	42
<i>Figure 2.6 Image acquisition using Vectra slide scanner.</i>	43
<i>Figure 2.7 Analysis of images using InForm software.</i>	46
<i>Figure 3.1 Morphology of the INS1E cells following normal or high glucose culture.</i>	59
<i>Figure 3.2 Cell viability assay.</i>	60
<i>Figure 3.3 Caspase counts were carried out on cells incubated in either 11 or 25 mM glucose medium.</i>	62
<i>Figure 3.4 Western blotting analysis for cells in normal and high glucose culture.</i>	63
<i>Figure 3.5 Glucose stimulated insulin secretion (GSIS).</i>	64
<i>Figure 3.6 Stimulation Index for GSIS.</i>	65
<i>Figure 3.7 qPCR analysis of insulin and glucagon mRNA levels following culture in high glucose.</i>	66
<i>Figure 3.8 Insulin content ELISA from cells cultured in normal (11 mM) or high (25 mM) glucose.</i>	67
<i>Figure 3.9 Glucagon content ELISA from cells cultured in normal (11 mM) or high (25 mM) glucose.</i>	67
<i>Figure 3.10 Western blot analysis of glucagon expression in cells cultured in normal glucose medium (NG) or high glucose medium (HG).</i>	68
<i>Figure 3.11 Glucagon counts were carried out on INS1E cells cultured in normal (11 mM) or high (25 mM) glucose. Cells were seeded on cover slips in 24 well plates.</i>	69
<i>Figure 3.12 ICC analysis of glucagon expression in INS1E cells cultured in 11 mM and 25 mM glucose.</i>	70
<i>Figure 3.13 qPCR analysis of transcription factor mRNA levels following exposure to 25 mM glucose.</i>	70
<i>Figure 3.14 Representative Western blot analysis of Nkx6.1 and Pdx1 expression in cells cultured in normal glucose medium (NG) or high glucose medium (HG).</i>	71
<i>Figure 3.15 Analysis of Nkx6.1 and Pdx1 western blots following high glucose culture.</i>	72
<i>Figure 3.16 ICC of Pdx1 overexpression in INS1E cells. Infection with Pdx1 adenovirus caused increase in Pdx1 expression.</i>	73
<i>Figure 3.17 qPCR data of Pdx1 expression following 48 hour treatment with increasing volumes of adenovirus.</i>	74
<i>Figure 3.18 Western blot analysis of Pdx1 expression in cells treated with increasing volumes of Pdx1 adenovirus.</i>	74
<i>Figure 3.19 qPCR analysis of INS1E genes following high glucose culture and treatment with Pdx1 overexpression virus.</i>	76

Figure 3.20 Insulin content following 48 hours in high glucose medium and treatment with Pdx1 overexpression virus or B-gal control virus.	77
Figure 3.21 Glucagon content following 48 hours in high glucose medium and treatment with Pdx1 overexpression virus or B-gal control virus.	77
Figure 3.22 Glucose stimulated insulin secretion (GSIS) following normal glucose culture and treatment with Pdx1 overexpression virus.	78
Figure 3.23 Glucose stimulated insulin secretion (GSIS) following high glucose culture and treatment with Pdx1 overexpression virus.	79
Figure 4.1 Gene expression of Tle3 in INS1E cell line following high glucose culture.	89
Figure 4.2 Tle3 gene expression following overexpression of Pdx1 in INS1E cells.	90
Figure 4.3 Proximity ligation assay assessing interactions between Pdx1 and Tle3 in INS1E cell line.	92
Figure 4.4 Gene expression analysis of Tle3 following siRNA mediated knockdown at 48 and 72 hours of 11 mM glucose culture using 3 different siRNA probes.	94
Figure 4.5 Gene expression analysis of Tle3 following siRNA mediated knockdown at 48 and 72 hours of 11 mM glucose culture using siRNA probe 3.	95
Figure 4.6 Gene expression analysis of p80+ INS1E cells following siRNA mediated Tle3 knockdown at 48 and 72 hours of 11 mM glucose culture.	96
Figure 4.7 Insulin content ELISA from p80+ INS1E cells following 48 or 72 hours of Tle3 knockdown.	97
Figure 4.8 Glucagon content of p80+ INS1E cells following 48 or 72 hours of Tle3 knockdown.	97
Figure 4.9 Glucose stimulated insulin secretion of p80+ INS1E cells following 48 or 72 hours of Tle3 knockdown.	99
Figure 4.10 Gene expression for Tle3 following 48 hours knockdown in p40+ INS1E cells.	100
Figure 4.11 Gene expression in (p40+) INS1E cells following 48 hours Tle3 knockdown.	100
Figure 4.12 Insulin content ELISA from p40+ INS1E cells following 48 hours of Tle3 knockdown.	102
Figure 4.13 Glucagon content of p40+ INS1E cells following 48 hours of Tle3 knockdown.	102
Figure 4.14 Glucose stimulated insulin secretion of p40+ INS1E cells following 48 hours of Tle3 knockdown.	103
Figure 4.15 Stimulation Index of young INS1E cells following 48 hours of Tle3 knockdown.	104
Figure 4.16 Puromycin kill curve.	105
Figure 4.17 Images of INS1E cells following infection with lentivirus containing shRNA for Tle3.	107
Figure 4.18 Western blot of lentiviral mediated knockdown of INS1E cells with no knockdown, a control vector and four different Tle3 vectors.	108
Figure 4.19 qPCR analysis of stable cell lines.	109
Figure 4.20 Gene expression analysis of INS1E cells following shRNA mediated Tle3 knockdown.	110
Figure 4.21 Insulin content ELISA from stable knockdown INS1E cells.	111
Figure 4.22 Glucagon content of INS1E cells following stable Tle3 knockdown.	112
Figure 4.23 Glucose stimulated insulin secretion of INS1E cells following stable Tle3 knockdown.	113
Figure 4.24 Stimulation index of control, and Tle3 knockdown cell lines.	114
Figure 4.25 PI staining of isolated islets following different culture periods and treatments.	116
Figure 4.26 Assessment of cell viability following isolation and transfection.	117

Figure 4.27 Gene expression analysis of <i>Tle3</i> following siRNA mediated knockdown in intact rodent islets.	118
Figure 4.28 Gene expression analysis of islet genes following siRNA mediated knockdown in intact rodent islets.	118
Figure 4.29 Insulin content following <i>Tle3</i> knockdown in intact rodent islets.	119
Figure 4.30 Fold change in insulin content following siRNA mediated knockdown of <i>Tle3</i> in rodent islets.	120
Figure 4.31 Glucagon content following <i>Tle3</i> knockdown in intact rodent islets.	120
Figure 4.32 Fold change in glucagon content following siRNA mediated knockdown of <i>Tle3</i> in rodent islets. ...	121
Figure 4.33 Glucose stimulated insulin secretion of rodent islets following siRNA mediated <i>Tle3</i> knockdown. .	122
Figure 4.34 Fold change in glucagon content following siRNA mediated knockdown of <i>Tle3</i> in rodent islets. ...	122
Figure 4.35 Effects of <i>Tle3</i> knockdown on rodent beta cells and potential mechanisms by which these effects may occur.	128
Figure 5.1 Average percentage of glucagon expressing cells per islet in control and diabetic patients.	136
Figure 5.2 Average percentage of cell types in control and diabetic donors for Observer 1.	138
Figure 5.3 Average percentage of cell types in control and diabetic donors for Observer 2.	139
Figure 5.4 Representative images from a range of donors in Cohort 1.	141
Figure 5.5 Example islet from control donor (top line) and diabetic donor (bottom line).	142
Figure 5.6 Images of insulin and glucagon co-localisation Cohort 1.	143
Figure 5.7 Islets showing TLE1 and insulin staining in 3 islets from a single donor.	145
Figure 5.8 Islets from control and diabetic donors of cohort 2.	148
Figure 5.9 Islet from control donor of cohort 2.	149
Figure 5.10 Islet from diabetic donor of cohort 2.	150
Figure 5.11 Co-expression of insulin and glucagon in human type 2 diabetes.	151
Figure 5.12 Comparison of manual counts versus automated counts at 50, 70 and 90% confidence for control donor.	153
Figure 5.13 Comparison of manual counts versus automated counts at 50, 70 and 90% confidence for diabetic donor.	154
Figure 5.14 Average number of glucagon positive cells in control vs diabetic donors.	156
Figure 5.15 Average percentages of all insulin expressing cells, all glucagon expressing cells and bihormonal cells in control and diabetic donors for 50% confidence counts.	158
Figure 5.16 Average percentages of all insulin expressing cells, all glucagon expressing cells and bihormonal cells in control and diabetic donors for 70% confidence counts.	159
Figure 5.17 Average percentages of all insulin expressing cells, all glucagon expressing cells and bihormonal cells in control and diabetic donors for 90% confidence counts.	160
Figure 5.18 Localisation of TLE1 in human control and diabetic donors.	162
Figure 5.19 Total percentage of all Tle1+ cells in donors with and without type 2 diabetes.	164
Figure 5.20 The percentage of TLE1 negative cells for each cell type in control versus diabetic tissue.	164
Figure 5.21 The average percentage of TLE1 negative insulin expressing cells.	165
Figure 5.22 Average percentage of TLE1 negative beta cells per donor.	166
Figure 5.23 Relationship between the loss of TLE1 in insulin+ cells and increased glucagon expression.	167

<i>Figure 5.24 Relationship between the percentage of TLE1 expressing beta cells and glycosylated haemoglobin levels.</i>	<i>168</i>
<i>Figure 5.25 Loss of TLE1 expression with disease duration in diabetic donors.</i>	<i>169</i>
<i>Figure 5.26 Relationship between disease duration and TLE1 expression.</i>	<i>169</i>
<i>Figure 5.27 Average percentage of bihormonal cells per donor in control and diabetic donors.</i>	<i>171</i>
<i>Figure 5.28 The relationship between loss of TLE1 expression and presence of bihormonal cells in islets from control and diabetic donors.</i>	<i>172</i>
<i>Figure 5.29 Relationship between percentage of bihormonal cells and disease duration.</i>	<i>173</i>
<i>Figure 5.30 Relationship between percentage of bihormonal cells and Body Mass Index (BMI) in control and type 2 diabetic donors.</i>	<i>173</i>
<i>Figure 5.31 Relationship between HbA1c and presence of bihormonal cells.</i>	<i>174</i>
<i>Figure 5.32 Relationship between HbA1c and presence of bihormonal cells per donor.</i>	<i>175</i>
<i>Figure 5.33 Knockdown of TLE1 in intact human islets by transfection with shRNA plasmids.</i>	<i>176</i>
<i>Figure 5.34 Changes in gene expression following knockdown of TLE1 in intact human islets.</i>	<i>177</i>
<i>Figure 6.1 A suggested role for Tle3 in regulating insulin secretion in the pancreatic beta cell.</i>	<i>192</i>

Table of Tables

<i>Table 1.1 Summary of hormones involved in regulation of blood glucose levels.....</i>	<i>7</i>
<i>Table 2.1 Kits used for general laboratory experiments.....</i>	<i>26</i>
<i>Table 2.2 Different methods of gene knockdown used.....</i>	<i>34</i>
<i>Table 2.3 List of transfection reagents used.....</i>	<i>35</i>
<i>Table 2.4 Volumes of transfection reagents used per reaction for siRNA mediated Tle3 knockdown in both INS1E cells and rodent islets.....</i>	<i>35</i>
<i>Table 2.5 Volumes of transfection reagents used for TLE1 knockdown in intact human islets.....</i>	<i>36</i>
<i>Table 2.6 Buffers used for IHC and ICC.....</i>	<i>37</i>
<i>Table 2.7 List of all primary antibodies used in experiments.....</i>	<i>40</i>
<i>Table 2.8 List of all secondary antibodies used in experiments.....</i>	<i>41</i>
<i>Table 2.9 List of Taqman probes used for analysis of mRNA levels in qPCR experiments.....</i>	<i>49</i>
<i>Table 2.10 Volume of glucose needed to make up basal and stimulatory solutions for GSIS.....</i>	<i>50</i>
<i>Table 2.11 Reagents and volumes needed to make up SDS-PAGE gels.....</i>	<i>52</i>
<i>Table 2.12 Buffers used for Gel Electrophoresis and Western Blotting.....</i>	<i>52</i>
<i>Table 5.1 Cohort 1- Donor information for control pancreas sections sourced from Exeter Archival Diabetes Biobank.....</i>	<i>133</i>
<i>Table 5.2 Cohort 1- Donor information for diabetic pancreas sections sourced from Exeter Archival Diabetes Biobank.....</i>	<i>134</i>
<i>Table 5.3 Donor information from control tissue in cohort 2 sourced from University of Alberta Islet Core Biobank.....</i>	<i>146</i>
<i>Table 5.4 Donor information from diabetic tissue in cohort 2 sourced from University of Alberta Islet Core Biobank.....</i>	<i>146</i>
<i>Table 5.5 Determining the percentage confidence to use.....</i>	<i>161</i>

List of abbreviations

Arx	- Aristaless Related Homeobox
ASP	- Acylation Stimulating Protein
Bcl2	- B-cell Lymphoma 2
Bcl2l1	- Bcl2-Like 1
B-gal	- β -Galactosidase
BMI	- Body Mass Index
BSA	- Bovine Serum Albumin
cDNA	- Complementary DNA
DAPI	- 4', 6'-Diamidino-2-Phenylindole
DDP-IV	- Dipeptidylpeptidase-IV
DNA	- Deoxyribose Nucleic Acid
EGFR	- Epidermal Growth Factor Receptor
ELISA	- Enzyme Linked Immunosorbent Assay
ER	- Endoplasmic Reticulum
FFA	- Free Fatty Acids
FOXO1	- Forkhead Box Protein O1
GAD	- Glutamic Acid Decarboxylase
Gcg	- Glucagon
GFP	- Green Fluorescent Protein
GLP-1	- Glucagon Like Peptide-1
GLUT2	- Glucose Transporter Type 2
GLUT4	- Glucose Transporter Type 4

GSIS	- Glucose Stimulated Insulin Secretion
HbA1c	- Glycosylated Haemoglobin A1c
HDACs	- Histone Deacetylases
Hes1	- Hairy and Enhancer of Split-1
Hnf6	- Hepatocyte Nuclear Factor-6
HLA	- Human Leukocyte Antigen
HRP	- Horseradish Peroxidase
ICC	- Immunocytochemistry
IHC	- Immunohistochemistry
INS1	- Insulin 1
INS2	- Insulin 2
Ipf1	- Insulin promotor factor-1
IRS-1	- Insulin Receptor Subtrate-1
LCF	- Lymphoid Enhancer-Binding Factor
MafA	- MAF bZIP Transcription Factor A
MafB	- MAF bZIP Transcription Factor A
MAPK	- Mitogen-Activated Protein Kinase
mRNA	- Messenger RNA
Ngn3	- Neurogenin 3
Nkx2.2	- NK2 Homeobox 2
Nkx6.1	- NK6 Homeobox 1
Nkx6.2	- NK6 Homeobox 2
Pax4	- Paired Box 4
PBS	- Phosphate Buffered Saline

Pdx1	- Pancreatic and Duodenal Homeobox 1
PI	- Propidium Iodide
PPARY	- Peroxisome Proliferator Activated Receptor γ
PPY	- Pancreatic Polypeptide
Ptf1a	- Pancreatic Transcription Factor 1a
qPCR	- Quantitative Polymerase Chain Reaction
RNA	- Ribonucleic Acid
RPLP0	- Ribosomal Protein Lateral Stalk Subunit P0
ROS	- Reactive Oxygen Species
Rxf6	- Regulatory X-Box Binding 6
SDS-PAGE	- Sodium Dodecyl Sulphate Polyacrylamide Gel Electrophoresis
SEM	- Standard Error of the Mean
shRNA	- Small Hairpin RNA
SI	- Stimulation Index
siRNA	- Small Interfering RNA
SRE	- Sterol Regulatory Element
SREBPc	- Sterol Regulated Element Binding Protein-1c
SST	- Somatostatin
STUbls	- SUMO-Targeted Ubiquitin Ligases
SUM	- Small Ubiquitin-Like Modifier Proteins
TBS	- Tris Buffered Saline
TGF- β	- Transforming Growth Factor- β
TLE1	- Transducin Like Enhancer of Split 1
Tle3	- Transducin Like Enhancer of Split 3

TZDs	- Thiazolidinediones
VEGF	- Vascular Endothelial Growth Factor
WT	- Wild Type
YFP	- Yellow Fluorescent Protein

1 Introduction

1.1 Glucose Homeostasis

Glucose is a vital source of energy for most organisms. In the human body, glucose is required for cellular metabolism in many different cell types and is the sole energy source used in red blood cells and, during non-starvation conditions, the brain (1). Alongside this it is used in muscle cells to enable contraction (2) and in the liver to help regulate the blood glucose levels in both fed and fasted states through lipogenesis and glycolysis, and gluconeogenesis and glycogenolysis respectively (3).

The regulation of blood glucose is largely controlled by two opposing pathways; glycolysis and gluconeogenesis. Glycolysis involves the breakdown of glucose into pyruvate to be used in the citric acid cycle, muscle contraction and the synthesis of fatty acids. Gluconeogenesis is the conversion of pyruvate and other 3-carbon compounds into glucose to maintain blood glucose and allow sufficient glucose to reach the brain (3).

In the fasted state, glucose leaves the circulation at a continuous rate as it is used up in basal respiration and cellular metabolism, requiring replacement through glycogen breakdown (4). In the fed state, glucose is in excess and is taken up by cells in the liver to be converted to glycogen or fatty acids (3) in order to maintain the blood glucose levels between 4-7 mM. The regulation of blood glucose is highly complex and is affected by numerous tissues which all contribute to glucose uptake or synthesis, glycogen breakdown and synthesis and hormone secretion in both the fed and fasted states (Figure 1.1) to ensure the body has sufficient glucose to utilize for energy.

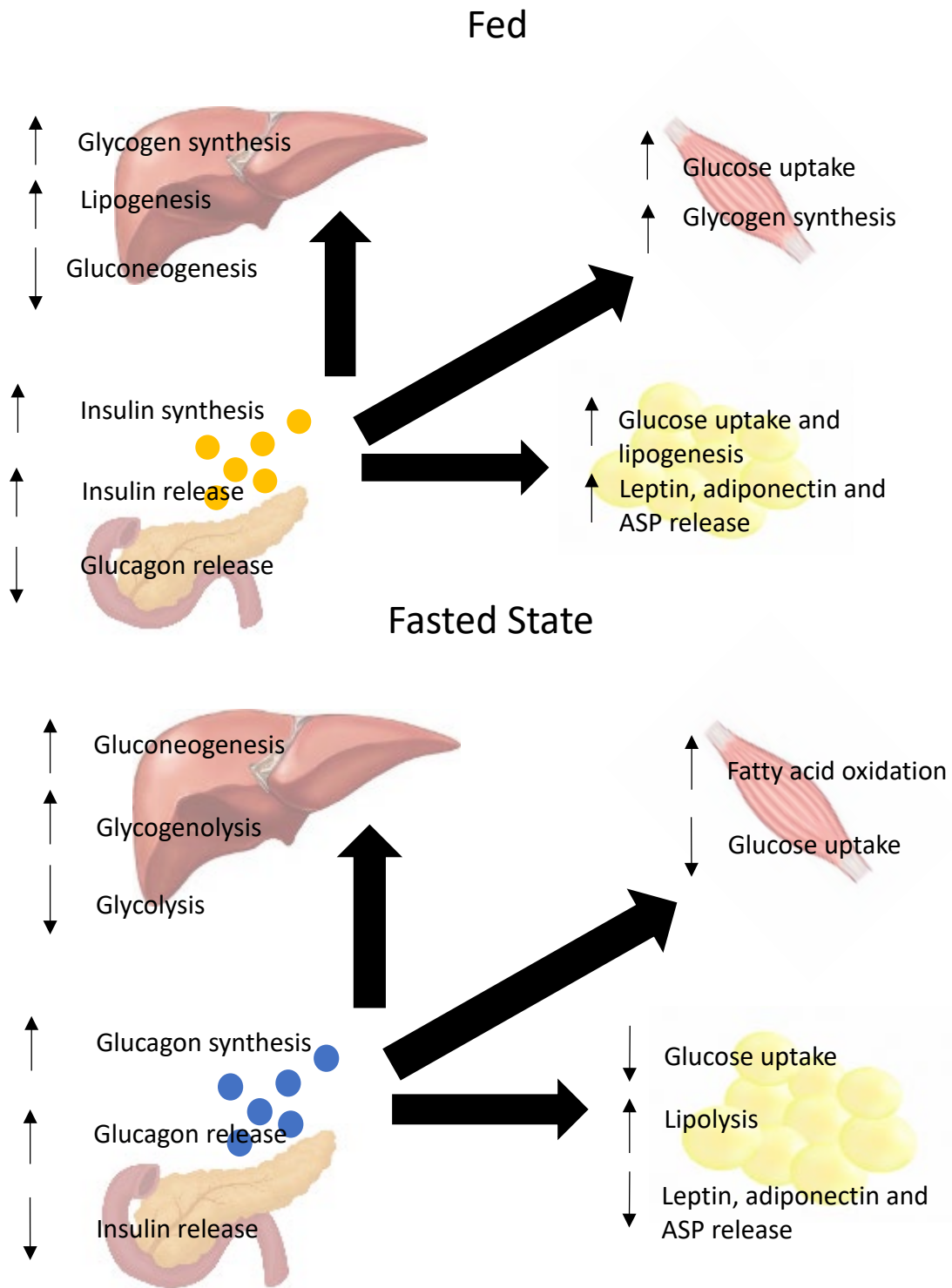


Figure 1.1 A diagram to summarise regulation of glucose levels in the fed and fasted states.

Detection of glucose and release of insulin or glucagon from the pancreas initiates different pathways in different cell types from increasing or decreasing glucose production in the liver, the oxidation of glucose or fatty acids for energy in the muscle and the up- or down-regulation of hormones controlling appetite in adipose tissue including leptin, ASP (acetylation stimulating protein) and adiponectin.

1.1.1 Glucose metabolism in skeletal muscle

A large proportion of glucose in the human body is required by skeletal muscle. As a result, skeletal muscle plays a significant role in maintaining glucose homeostasis. Skeletal muscle is a highly insulin-sensitive tissue and can account for up to 80% of postprandial glucose uptake. Under euglycaemic conditions, skeletal muscle plays an important role in maintaining physiological glucose levels and is one of the first tissue sites to encounter insulin resistance. Insulin signalling in skeletal muscle triggers phosphorylation of tyrosine molecules on the Insulin receptor substrate-1 (IRS-1), resulting in activation of downstream kinase molecules which facilitate translocation of the GLUT4 to the cell membrane and the uptake of glucose from the blood (5). During the fasted state, skeletal muscle oxidizes free fatty acids (FFA) as an energy source, leaving glucose free for utilisation by the brain (5). In the fed state, when glucose is in surplus, skeletal muscle switches from lipid to glucose oxidation as the primary energy source. Alongside this, the increase in plasma insulin levels activates synthesis of glycogen which accounts for ~90% of glucose disposal following feeding (6).

1.1.2 Glucose and the liver

The liver is the primary site of energy metabolism in the body. Glucose, fatty acids and amino acids are transported to the liver after digestion where nutrient, hormonal and neuronal signals help to determine the metabolic pathways in which they are used. Dysregulation of these signals can cause numerous problems, including type 2 diabetes (3). In the fasted state, the liver can generate glucose through hydrolysis of glycogen by the enzyme glycogen phosphorylase and, once glycogen stores have been depleted, through gluconeogenesis (7). Gluconeogenesis initially converts lactate to pyruvate which is taken into the mitochondria to be converted to oxaloacetate. After numerous biochemical reactions in both the mitochondria and cytoplasm, the product, glucose-6-phosphate, is then dephosphorylated to produce glucose (3). In the fed state, GLUT2 transporters take up glucose from the blood to be phosphorylated by glucokinase and used to synthesize glycogen by glycogen synthase in a multistep reaction (8). In 'times of plenty', the liver also converts some of the abundant carbohydrates into fatty acids to replenish stores that were used during the fasting state. Lipogenesis is driven by the availability of dietary carbohydrates. Increased flux through the glycolytic pathway after feeding causes elevated levels of malonyl-CoA, which is used in *de novo* fatty acid

synthesis (9) to produce palmitic acid. Palmitic acid can then be elongated by fatty acyl-CoA elongase enzymes to produce longer chain fatty acids (3). Alongside activating synthesis of glycogen, insulin signalling is a potent repressor of hepatic glucose production through the gluconeogenesis pathway (3).

1.1.3 Glucose regulation and adipocytes

Adipocytes play an important role in the regulation of both lipid and carbohydrate metabolism through secretion of a wide range of hormones. These hormones help to control many aspects of dietary regulation, such as energy intake and expenditure. One such hormone is leptin, which is secreted in response to food intake to suppress the appetite and increase energy expenditure (10). In the fed state, insulin-mediated glucose metabolism has been shown to induce leptin expression in rodent adipocytes (11) which, in turn, prevents hyperphagia (excessive hunger). Some studies also suggest that leptin may inhibit insulin secretion through interactions with the cAMP protein kinase A signalling pathway or through activation of ATP-dependent potassium channels (12) in the beta cell. Alongside the regulation of leptin, adipocytes also produce acylation stimulating protein (ASP) which acts to stimulate glucose uptake in adipocytes and promotes efficient synthesis and storage of triglycerides. The production and secretion of ASP is thought to be regulated, in part, by circulating insulin levels which increase its production following food intake (10). Another hormone released by adipocytes which has been shown to have a role in regulating blood glucose is adiponectin. There is a strong correlation between adiponectin levels and insulin sensitivity and studies have shown that both gene expression and circulating levels of adiponectin are reduced in patients with insulin resistance (10).

1.1.4 The pancreas

The pancreas is a relatively small but vital organ in the human body. Situated under the stomach and connected to the duodenum, the exocrine portion of the pancreas secretes digestive enzymes which are transported to the duodenum via the pancreatic ducts where they are involved in food breakdown.

The pancreas also secretes regulatory hormones including insulin and glucagon from endocrine tissue. The endocrine tissue accounts for only 1-5% of the pancreas but requires rich vascularisation to ensure proper function (13). Within the endocrine compartment are the islets of Langerhans, which are made up of multiple cell types, including glucagon-

secreting alpha cells, insulin-secreting beta cells, somatostatin-secreting delta cells, ghrelin secreting epsilon cells and pancreatic polypeptide-secreting PP cells. In contrast to rodent islets where there is a core of beta cells surrounded by alpha cells, in humans, these cells are randomly distributed throughout the islets (14). Although the proportion of beta cells per islet can be very variable in humans (14) a typical human islet will be comprised of ~60% beta cells, ~30% alpha cells and the remaining ~10% consisting of somatostatin, pancreatic polypeptide and ghrelin cells (15). Although some of the exact functions of these cell types remain incompletely understood, the roles that both the alpha and beta cells play in glucose homeostasis are well established.

1.1.5 Hormonal regulation of glucose

There are several hormones involved in the maintenance of the blood glucose levels. Insulin is a hormone produced by the beta cells and is critical to the regulation of tissue glucose utilisation. Beta cells secrete insulin in response to a rise in blood glucose level to promote glucose uptake, drive glycogen storage and prevent glucose production and glycogen breakdown in the liver (16). Insulin alone, however, is not sufficient to keep the blood glucose tightly regulated between 4-7 mM. Glucagon, another endocrine hormone, is secreted by alpha cells in response to amino acids (17) and functionally opposes insulin, promoting glycogen breakdown and gluconeogenesis in the liver (4). Far less is known about the role of the other islet cell types however studies looking at the role of somatostatin have shown it acting as a negative regulator of insulin and glucagon during the fed state (18). Pancreatic polypeptide has been implicated in the prevention of glucagon release following food intake as levels of pancreatic polypeptide have been shown to rise in response to glucose and prevent glucagon release by acting on the pancreatic polypeptide receptor (PPYR1) in rodent alpha cells (19). Ghrelin has been shown to have a negative impact on insulin secretion in both human and rodents and, whilst further investigation is required, it may also be implicated in regulating glucagon, pancreatic polypeptide and somatostatin secretion (15). The role of these hormones, alongside other hormones that play a role in regulation of the endocrine system are summarised in Table 1.1.

Cell Type	Hormone Production	Function
Pancreatic Alpha cell	Glucagon	Secreted in times of fasting to counter insulin action, encouraging glucose production in the liver, breakdown of glycogen and metabolism of lipid stores to raise blood glucose levels
Pancreatic Beta cell	Insulin	Secreted following feeding to promote uptake of glucose from the blood and production of glycogen and lipid stores. Also encourages release of insulin sensitising and satiety hormones from adipose tissue
Pancreatic Delta cell	Somatostatin	Inhibits glucose- and arginine- stimulated insulin and glucagon release respectively to prevent over production of the hormones during fed and fasted states
Pancreatic PP cell	Pancreatic polypeptide	Release stimulated by glucose resulting in inhibition of glucagon secretion by the alpha cells
Pancreatic Ghrelin cell	Ghrelin	Increased secretion during fasting resulting in inhibition of insulin secretion. Potential regulator of other endocrine hormones glucagon, PP and somatostatin
Intestinal L cells	Glucagon-like peptide-1 (GLP-1)	Stimulation of glucose dependent insulin release from the beta cells. Stimulation of somatostatin release and suppression of glucagon release
Intestinal K cells	Glucose-dependent insulinotropic peptide (GIP)	Secreted in response to glucose and meals to stimulate insulin secretion from the beta cells

Table 1.1 Summary of hormones involved in regulation of blood glucose levels.

1.1.6 Insulin secretion from the pancreatic beta cell

Insulin secretion is stimulated following a chain of events that begins with the phosphorylation of glucose by the glucokinase enzyme and subsequent entry into the glycolysis and Krebs cycle pathways (20). The resultant rise in intracellular ATP levels from this chain of events results in closing of the K_{ATP} channels and depolarisation of the cell membrane. This leads to opening of the voltage gated Ca^{2+} channels and the influx of calcium in the cells causes translocation of the insulin vesicles to the cell membrane to enable secretion (20). The secretion of insulin is carried out using two pools of insulin granules, the readily releasable pool (RRP) accounting for ~5% of granules which are released during the first phase of insulin secretion and the reserve pool (RP) which is used during the second phase of insulin secretion allowing for a pulsed insulin secretion which is more effective for lowering blood glucose (21, 22).

1.2 Diabetes Mellitus

Resulting from an insufficient production of and/or response to insulin, diabetes mellitus is a chronic heterogeneous metabolic disease characterised hyperglycaemia (23). Encompassing both the clinical and aetiological characterisations, diabetes mellitus is classified into two major forms: Type 1 and Type 2 diabetes. These two main forms of the disease account for ~5-10% and ~90-95% of diabetes respectively (23). The estimated number of people living with diabetes in 2013 was 382 million worldwide, a number which is predicted to increase to 592 million by 2035 (24).

1.2.1 Type 1 diabetes

Type 1 diabetes, or insulin dependent diabetes mellitus, is an autoimmune disease whereby the immune system initiates cellular-mediated destruction of the insulin producing beta cells in the pancreas (23) resulting in absolute dependence on exogenous insulin for the patient. The majority of type 1 diabetes patients present at a young age; however, diagnosis during adolescence and adulthood is not uncommon. Patients manifest symptoms such as polyuria (excessive urination), polydipsia (excessive thirst), unexplained weight loss and occasionally polyphagia (excessive eating), blurred vision and muscle cramps. Continued hyperglycaemia in combination with insulin deficiency results in ketonuria (presence of ketone bodies in the urine), glycosuria (presence of glucose in the urine) and ketoacidosis (lowered pH of blood due to presence of ketone bodies) (23). Type 1 diabetes is influenced by genetic,

environmental and acquired factors. For example, antibodies raised against viral proteins such as the coxsackie B4 virus, which shares a large degree of sequence homology with the beta cell enzyme glutamic acid decarboxylase (GAD), provide evidence for environmental factors influencing disease onset (25). Although molecular mimicry has been suggested to be one way in which enterovirus infection can cause the onset of diabetes, there is conflicting evidence in support of this theory. One study looking at peptide binding of a conserved sequence between the GAD protein and the 2c protein of the enterovirus showed that the two proteins bound in the same way to the HLA-DR3 receptor (but not DR1 or 4) of the MHC class II receptor group, providing a potential explanation for why only certain people who encounter enterovirus infections develop type 1 diabetes (26). More recent studies however, have suggested that spread of viral infection from other parts of the body triggers the immune response. This chain of events differs from person to person and production of proteins such as Mda5, an RNA helicase enzyme that senses enteroviral proteins and triggers the immune response (27), have been found to be increased in some people with type 1 diabetes. Studies looking at the immune response of the beta cell following enteroviral infection found that those patients who failed to initiate a strong immune response were less likely to develop diabetes and people with a certain haplotype for the IHIF1 gene, resulting in reduced efficiency of the Mda5 enzyme, show some degree of protection against diabetes onset as a result of viral infection (28). Although increased susceptibility to type 1 diabetes has been linked to genetic make-up at the human leukocyte antigen (HLA)-D genes, these have been shown to impact on both predisposition and protection, indicating the potential involvement of other chromosome regions (non-HLA genes) (23, 25). Evidence suggests certain HLA haplotypes, such as HLA-DR3-DQ2 and HLA-DR4-DQ8, are thought to account for roughly half of the genetic predisposition to type 1 diabetes and acquisition of other autoimmune diseases (29), however, genome-wide association studies identified over 40 loci that indicated a predisposition for diabetes including SNPs in the immunoregulatory cytokine genes *IL10*, *IL19* and *IL20* (30) and *INS* gene (31). Although many different factors have been shown to influence the development of the disease, the consensus remains that multiple factors are involved in the onset of Type 1 diabetes.

1.2.2 Type 2 Diabetes

Type 2 diabetes is caused by insulin resistance (an inability of target tissues to respond to the insulin signal) alongside reduced insulin secretion in response to glucose. The incidence of type 2 diabetes is rapidly rising on a global scale, with an increasing prevalence in children and adolescents posing serious life-long health risks and increasing mortality (32). The exponential increase in type 2 diabetes over the last few decades is thought to be largely due to adverse lifestyle changes i.e. lack of physical activity and an unhealthy diet. (32). Insulin resistance causes many issues at its target tissues, affecting all tissues that play a role in the maintenance of the blood glucose levels. In insulin responsive skeletal muscle, after glucose ingestion, plasma concentration of insulin rises, stimulating the translocation of GLUT4 vesicles to the plasma membrane to mediate glucose uptake, which is then stored as glycogen (6). As insulin resistance develops in skeletal muscle, the primary metabolic change that can be observed is the decline in glucose uptake and glycogen synthesis (5). In the liver, the detection of insulin signal suppresses gluconeogenesis in hepatocytes and therefore insulin resistance promotes continuous gluconeogenesis which contributes further to hyperglycaemia (3).

In the human body, adipocytes are responsible for the maintenance and release of free fatty acids (FFA) into the blood stream, preventing elevated plasma FFA levels and abnormal communication between adipocytes and other tissues such as skeletal muscle, liver and pancreatic beta cells (33). An increase in nutrient consumption coupled to a decrease in energy expenditure can result in dysfunctional adipocytes and subsequent systemic problems, including desensitisation to insulin, due to increased signalling from FFA, adipokines and other inflammatory molecules (34) demonstrating one way in which obesity can lead to onset of the diabetic state.

Although the link between environmental and lifestyle factors is well documented, there is also a genetic susceptibility to type 2 diabetes with evidence suggesting that the risk of developing type 2 diabetes in individuals with 1 parent with type 2 diabetes is 40% and this increases to 70% if both parents have it (35). Monogenic polymorphisms in several genes such as PPAR γ , TCF7L2 and KCNJ11 (playing roles in adipogenesis, Wnt signalling and insulin secretion through ATP-sensitive potassium channels respectively) have been shown to increase the risk of type 2 diabetes, however these monogenic polymorphisms account for only a small proportion (~5%) of incidences (35). Recent studies looking into lower frequency variants associated with type 2 diabetes have found several risk variants associated with

global origin such as PAX4 (involved in beta cell differentiation and function), SLC16A11 (membrane transporter) and TBC1D4 (regulation of GLUT4 vesicle trafficking) variants in people from East Asia, Native America and Greenland Inuits respectively (36).

The general consensus is that type 2 diabetes is likely caused or worsened by multiple factors, as other environmental, ethnic and even socioeconomic factors have been shown to contribute to increased risk and complications of type 2 diabetes including fat distribution (37), education level and job status (38) and stress (39).

1.3 Glucose toxicity and diabetic complications

Despite the vital role glucose plays in maintaining cellular function, if concentrations are excessive for prolonged periods of time there are many detrimental implications that can occur. The complications that arise from extended hyperglycaemia are both numerous and severe, with macro- and micro-vascular problems including an increased risk of cardiovascular disease and retinopathy (40).

Microvascular complications of diabetes include neuropathies, which are very common in diabetic patients, with a prevalence of ~50%. Peripheral neuropathy is the most common form of neuropathy in diabetic patients and predominantly affects the lower extremities. With suboptimal control of the blood glucose levels over prolonged periods of time, patients are at risk of developing ulceration of the feet, which can ultimately lead to amputation (41). Persistent hyperglycaemia is also a major contributor to the incidence of renal failure, with a 30% mortality rate in diabetic patients compared to 11% in non-diabetic patients. Although the pathophysiology of diabetic nephropathy is not completely understood, hyperglycaemia is thought to contribute to dysregulation of vascular growth factors. These include the vascular endothelial growth factor (VEGF) and angiotensin II. Alongside this, hyperglycaemia also increases reactive oxygen species (ROS), inflammation and expression of transforming growth factor- β (TGF- β). These changes in cell signalling cause problems within the vasculature of the kidney, resulting in thickening of the glomerular basement membrane and a subsequent decline in the glomerular filtration (42).

With diabetes mellitus increasing on a global scale, incidences of its complications are also dramatically rising. As much as 80% of type 2 insulin-treated and 50% of non-insulin-treated patients with type 2 diabetes will present some form of diabetic retinopathy after prolonged disease duration (43). Diabetic retinopathy is one of the major microvascular complications seen in diabetes and accounts for ~5% of cases of blindness worldwide (44).

The numerous complications that can arise from all forms of diabetes contribute to the growing burden on health services worldwide. Thus, a better understanding of the pathophysiology of type 2 diabetes is imperative.

Alongside the extensive list of micro- and macro-vascular complications, glucotoxicity has been shown to contribute to beta cell dysfunction through mechanisms such as increased reactive oxygen species in beta cells (45), resulting in further dysregulation of the blood glucose levels. Several studies have suggested that glucotoxicity drives beta cell dysfunction and worsened diabetic state (46, 47). These studies only showed inhibition of insulin gene expression in the beta cells following exposure to palmitate and high glucose concentrations compared to treatment with palmitate only (46) and that hyperglycaemia, but not hyperlipidaemia, caused increases in islet triacylglyceride (TAG) content (47).

1.4 Current Treatments for Diabetes

1.4.1 Type 1 Diabetes treatment

Type 1 diabetes requires life-long treatment with exogenous insulin injections to maintain the blood glucose at near-physiological levels. Patients must administer short-acting insulin (at meal times) and a long-acting (basal) insulin to help maintain consistent blood glucose levels. Although it is the most effective treatment for type 1 diabetes, administration of exogenous insulin remains inadequate to replicate the tight control of the beta cell (48). Patients with severe fluctuation in glucose levels and persistent hypoglycaemia are considered for the option of a pancreas transplant (often done in combination with a kidney transplant) (49) or an islet transplant (50). The latter involves isolation of islets from the donor pancreas and delivery into the well-vascularised portal vein. Although this is a viable option and can result in reduced insulin therapy, it rarely offers long-term independence from insulin and is limited by the number of adequate donors.

1.4.2 Type 2 Diabetes treatment

Type 2 diabetes is a progressive degenerative condition which will often result in patients eventually requiring insulin injections. Several classes of drug are used to improve beta cell function and insulin sensitivity. The majority of these drugs fall into two categories: insulin sensitizers (used to increase response to the insulin signal) and insulin secretagogues (used to help beta cells release more insulin). One of the most widely used drugs to treat type 2 diabetes is metformin. As an insulin sensitizer, metformin is known to work by improving

lipid and glucose metabolism, however the exact mechanisms by which this occurs remain unknown. It is thought that one of the mechanisms by which this is achieved is through activation of AMP kinase (AMPK). Specifically, AMPK has been implicated in the inhibition of hepatic glucose production and glucose uptake in skeletal muscle, providing a potential mechanism through which metformin, as an AMPK activator, acts to help maintain normoglycemia (51).

Alongside insulin sensitizers, sulphonylureas are a group of drugs used to increase insulin secretion. The mechanism by which this occurs is through binding to sulphonylurea receptor (SUR) subunits of the K_{ATP} channels in the beta cell, preventing their opening. The resultant membrane depolarisation causes calcium channels to open and the subsequent Ca^{2+} ion influx stimulates translocation of insulin granules to the plasma membrane for release. In this way, these drugs promote improved blood glucose levels through increased insulin release from the beta cell (52).

There are other drugs available to treat type 2 diabetes that do not fall into the category of insulin sensitizers or secretagogues. One example is the incretin mimetics, or GLP-1 receptor agonists. Glucagon-like peptide-1 (GLP1) is a hormone secreted from intestinal L-cells with potent insulinotropic effects. These drugs, alongside dipeptidylpeptidase-IV (DPP-IV) inhibitors (which prevent the enzyme DPP-IV from breaking down GLP-1), work to increase circulating levels of GLP-1 and prolong the action of endogenous GLP-1 respectively. As such, these drugs can help to better regulate blood glucose levels and reduce HbA1c (glycosylated haemoglobin) readings in patients with type 2 diabetes (53).

Alongside insulin sensitising and secretory drugs, recent advances in research has shown that endogenous beta cell function can be recovered in type 2 diabetes by bariatric surgery (54) and even through a calorie restricted diet (55, 56) providing another means of treating the disease.

1.5 Pancreatic development

The endocrine pancreas is composed of the islets of Langerhans, which contain several cell types that are designated to the production of different hormones. Each of the cell types has a different role to play in the endocrine system and therefore requires expression of specific transcription factors to ensure proper development and function.

1.5.1 Differentiation of cell types within the pancreas

During pancreatic development, there are several different pathways leading to expression of specific transcription factors enabling the formation of the multiple cell types found in the islets of Langerhans. Figure 1.2, adapted from a previous publication (13), shows some of the transcription factors involved in development of the rodent pancreas. In order for the pancreas to develop properly, numerous transcription factors need to be expressed sequentially. Progenitor cells containing the Oct4 and Nanog transcription factors are highly pluripotent cells and downregulation of these markers of pluripotency leads to the differentiation of the progenitor pool (57). Gene knockout studies in mice have shown that mice lacking the pancreatic and duodenal homeobox 1 (Pdx1), a transcription factor expressed in pancreatic beta cells, completely lack a pancreas and die shortly after birth suggesting that this transcription factor is also required for pancreas organogenesis (58). Alongside Pdx1, knockout studies for hepatocyte nuclear factor 6 (Hnf6) have shown that mice lacking this gene develop pancreas hyperplasia (59). Following establishment of the pancreatic progenitor pool, another transcription factor, neurogenin 3 (Ngn3), acts to direct differentiation towards the endocrine cell types, triggering the expression of cell-specific transcription factors which determine endocrine cell fate. Paired Box 4 (Pax4) and Aristaless Related Homeobox (Arx) for example, control different regulatory networks within the pancreas. Their expression is induced in Ngn3-positive progenitors, however they become mutually exclusive at later stages of pancreas development with Pax4 being expressed alongside Pdx1 to determine a beta- or delta-cell lineage and Arx being expressed in cells adopting the alpha- or ghrelin-cell lineage (13). Knockout studies looking at other important endocrine progenitor transcription factors identified the regulatory X-box binding-6 (Rxf6) transcription factor as important in development of the endocrine pancreas with null mice showing reduced numbers of all endocrine cell types (59). Expression of certain co-repressors such as the transducin-like enhancer (Tle) family have also been reported to co-localise with a subset of Ngn3 progenitor cells during development to help determine endocrine cell fate (60). Slight differences occur between development of the pancreatic cell types in humans, for example TLE1 is important in the human pancreatic beta cell and is considered the functional equivalent of Tle3 in rodents (61), however many of the important transcription factors, for example Pdx1 and Nkx6.1, overlap between species. Each of the endocrine cell types within the islet has its own, complex, transcriptional regulatory network

that allows production of the different endocrine hormones and proper development and function of each cell lineage.

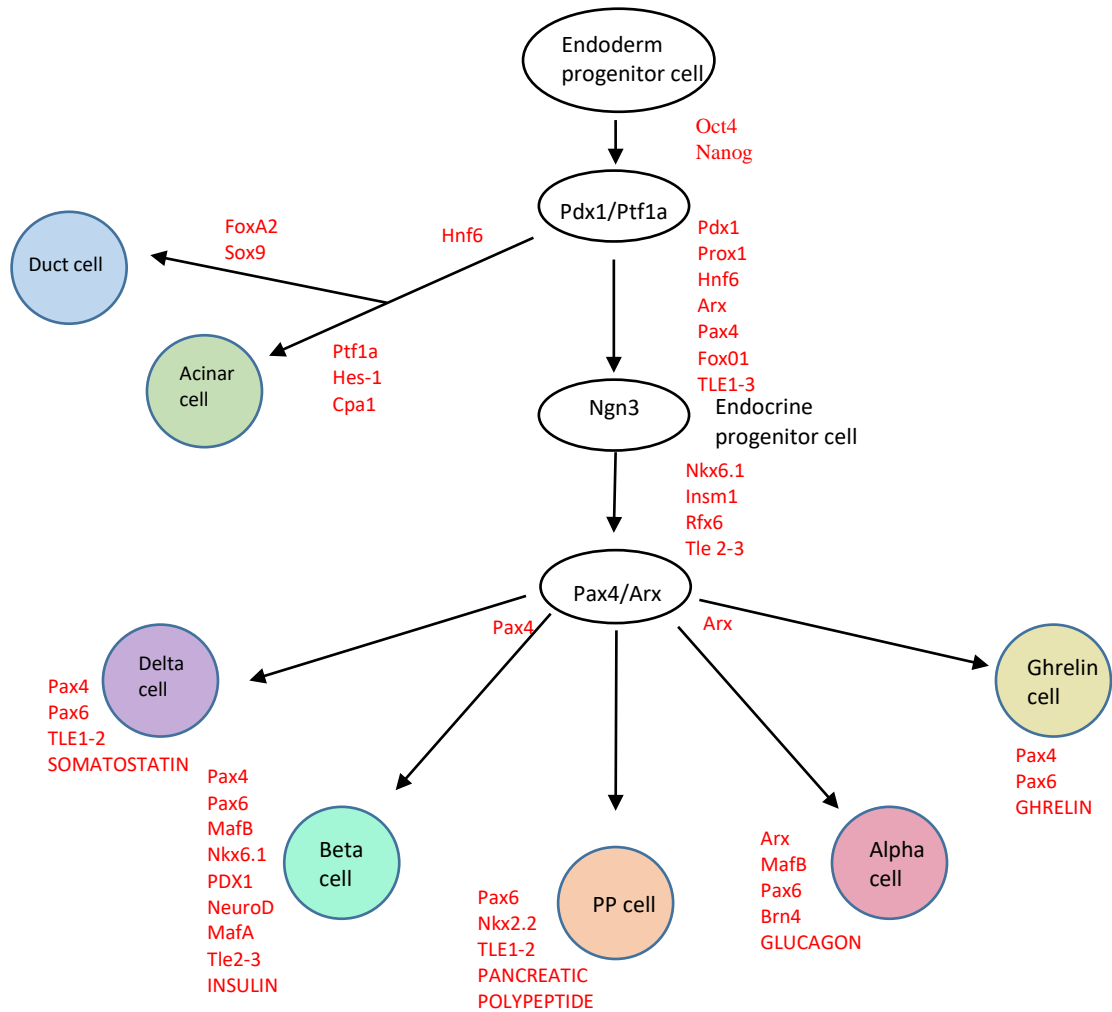


Figure 1.2 Simplified transcription factor map depicting different transcription factors required for mammalian pancreas differentiation.

Multiple transcription factors are required for proper differentiation of all pancreatic cell types in rodents. This map shows just some of the transcription factors required for the different cell fates and production of the endocrine hormones insulin, glucagon, somatostatin, pancreatic polypeptide and ghrelin (shown in capitals).

1.5.2 Pdx1

There are numerous transcription factors that provide the beta cell with its identity, affecting both the production and secretion of insulin alongside glucose sensing. PDX1 not only plays a role in the early development of the pancreas but it is also constitutively expressed in the adult beta cell. Rodent studies using heterozygous *Pdx1* knock out mice (*Pdx1*^{+/-}) have identified several roles for Pdx1 in beta cell function. *Pdx1*^{+/-} mice have

impaired glucose tolerance and show both reduced insulin plasma levels and glucose clearance compared to wild type (WT) mice (17). Furthermore, Pdx1 has been shown to be a potent regulator of many beta cell genes. A host of studies have shown a potential role for Pdx1 in the regulation of *Glut2*, *Glucokinase*, *Ins1 and 2*, *Pax4*, *Nkx6.1*, *MafA* genes alongside self-regulation of its own expression (62). This study demonstrates that Pdx1 plays a vital role in the orchestration of the functional beta cell.

The role Pdx1 plays in maintaining beta cell identity has also been shown, in part, to be through the repression of the alpha cell phenotype. Pdx1 deficient mice showed physiological responses of alpha cells and loss of beta cell function when changes in calcium flux were measured. In these experiments lineage tracing methods were employed using RIP-CreER and Rosa^{YFP} to knock out Pdx1 exclusively in adult beta cells and to label these cells with yellow fluorescent protein (YFP). Calcium flux was then measured in YFP⁺ beta cells and YFP⁻ non-beta cells in response to glucose (stimulates insulin secretion in a beta cell) or glycine (stimulates glucagon secretion in an alpha cell). In control islets, cells responded to either glucose (~85% cells) or glycine (~5% cells) whereas in Pdx1 deficient mice (expressing YFP) a third category of cells were detected which responded to both stimuli (~40% cells) alongside a marked increase in cells responding to mixed amino acids rather than glucose (17). Pdx1 repression in beta cell lines such as in the INS1 cell line, causes an increase in glucagon expression (12-fold) which supports other evidence that one way in which Pdx1 maintains beta cell function and phenotype is through the repression of the alpha cell program (63).

1.5.3 Nkx6.1

Three of the NKX family members, NKX6.1, NKX6.2 and NKX2.2 play a role in the development of pancreatic endocrine lineages. NKX2.2 expression is initially widespread throughout the pancreas and its expression is maintained in maturing alpha, beta and pancreatic polypeptide cells (64). *Nkx2.2*^{-/-} knock out mice show reduced numbers of both alpha and pancreatic polypeptide cells and, although there is a subset of cells showing markers of beta cells, they remain insulin-negative, suggesting that *Nkx2.2* plays a role in the terminal differentiation of the functional beta cell (64). A study by Sussel *et al.* also showed that deletion of part of the *Nkx2.2* tinman (TN) domain prevented interactions with other proteins leading to loss of beta cell differentiation and beta- to alpha-cell conversion (64).

Nkx6.1 and Nkx6.2 are other members of the Nkx family that impact on beta cell differentiation.

Although displaying significant homology with Nkx6.1, Nkx6.2 appears to be more involved in the development of alpha and acinar cells. In the absence of Nkx6.1 however, the pancreas has a much reduced beta cell number, indicating a proliferation-inducing role during beta cell development. This has been shown in studies by Schisler *et al.* who showed that Nkx6.1 is involved in both repression and activation of transcription factors such as cdk and cyclin which are involved in regulation of the cell cycle (65). This study also showed Nkx6.1 repression resulted in a reduction of beta cell mass with no apparent effect on other endocrine cell types (65). Another study by Taylor *et al.* showed that loss of Nkx6.1 in mature murine beta cells (*Nkx6.1^{Δadultβ}*) resulted in reduced glucose tolerance, reduced insulin secretion and increased fasting blood glucose levels compared to control mice (66). In contrast to the study by Schisler *et al.* this study also showed that Nkx6.1 knockout lead to increased delta cell characteristics in some cells (66), suggesting that Nkx6.1 is important in the function of the beta cell and repression of other endocrine cell types. Another study that used siRNA to silence *Nkx6.1* expression resulted in a 2-fold increase in expression of the alpha cell hormone glucagon, whereas overexpression of Nkx6.1 using an adenoviral vector caused a decrease in glucagon expression through binding and repression at the glucagon promoter (63).

Although the exact mechanism by which Nkx6.1 functions remains unclear, recent evidence suggests a possible interaction of Nkx6.1 with Groucho family of corepressors (Gro/Grg/Tle) which are known to interact with many different transcription factors (60). One such interaction in beta cells may be between transducin-like enhancer of split 3 (Tle3) and Nkx6.1 to repress the alpha cell fate (61).

1.5.4 Groucho family of co-repressors

The Groucho family of co-repressors have been shown to be important in animal development, interacting with a number of different pathways to influence pancreas, kidney and heart development (67). In mammals, the Groucho family of proteins are known as transducin-like enhancers or Tle proteins. There are four full length Tle genes (1-4) and two truncated Tle proteins (5 and 6), the latter of which are thought to help regulate Tle1-4 (67). These proteins do not contain a DNA-binding domain so are recruited to promotor regions of genes by other transcription factors to help regulate gene expression, often in a repressive

role (67). There are several mechanisms through which the Tle family members repress gene transcription. One mechanism is through the recruitment of histone deacetylases (HDACs), which are a family of enzymes that remove acetyl groups from histones allowing DNA to be more compact, preventing transcription factor binding and transcription (68). Tle3 has been shown to be recruited by Nkx2.2 alongside HDAC1 in the beta cell to repress transcription of the *Arx* gene (69). The other mechanism through which they are thought to work is through binding to histones directly, causing modifications and preventing activation of transcription (67). The function of the Groucho proteins is regulated by specific post-translational modifications such as phosphorylation and ubiquitination (67, 70). One such example is in the epidermal growth factor receptor signalling pathway (EGFR) where phosphorylation of Groucho proteins occurs in response to mitogen-activated protein kinase (MAPK) signalling and results in attenuation of its repressor capabilities (71). Post-translational modification by ubiquitination has been shown to be used in relation to interaction with the Hairy family of proteins and can work in different ways. Ubiquitination of the Hairy proteins prevents recruitment of the Groucho family of co-repressors without affecting binding of other co-factors. Binding of small ubiquitin-like modifier proteins (SUMO) to Groucho proteins targets them for ubiquitination by SUMO-targeted ubiquitin ligases (STUbLs) which, in turn, prevents binding between the Hairy and Groucho proteins and antagonises the repression of their target genes (70).

1.5.5 Tle proteins in the pancreas

In relation to the development of the pancreas, Tle2 and 3 are known to play roles in endocrine cell fate in rodents. Tle2 has been shown to interact with Nkx2.2, Nkx6.1, *Arx* and Hairy and enhancer of split-1 (*Hes1*) to maintain the beta cell phenotype and to help regulate the expression of progenitor markers found in the developing pancreas (60). Alongside Tle2, Tle3 has been shown to have an important role in the beta cell. Specifically, Nkx6.1 recruits Tle3 to the *Gcg* promoter where it acts to repress gene transcription, thereby helping maintain the beta cell identity (61). This is highlighted by rodent knock out studies where heterozygous *Tle3*^{+/-} mice showed a greater alpha cell to beta cell ratio compared to wild type mice (61). Furthermore, Metzger *et al.* showed that analysis of rare live *Tle3*^{-/-} embryos showed robust staining for Pdx1; however the numbers of both alpha and beta cells were dramatically reduced. Cells that were present after Tle3 knockout were shown to favour transition to an alpha cell phenotype (68) suggesting a role for Tle3 in both the initial

development of endocrine cell fates and in the maintenance of the beta cell lineage. This study also showed that combined overexpression of Tle3 and Pdx1 in the alpha cell line α TC1-6 caused insulin secretion in response to glucose stimulation whereas individual overexpression of these proteins did not (68). This suggests that a potential interaction between these two proteins may be important in the function of the beta cell.

1.6 Regulation of beta cell mass

Whilst generally thought of as having limited capacity to regenerate once adulthood is reached, pancreatic beta cell mass has been shown to occur under certain metabolic demands such as pregnancy (72) and obesity (73) and even following certain injuries such as subtotal pancreatectomy (74). This suggests that beta cells are capable of a certain degree of replication. Where these beta cells are sourced from however is still debated. Firstly, a study using lineage tracing techniques in mice showed that following a pancreatectomy, the regeneration of the beta cell population was mainly sourced from replication of remaining beta cells (74). Other studies have shown that following loss of the beta cell population, generation of new beta cells came from conversion of other endocrine cell types. Thorel et al. demonstrated this through use of a mouse model containing a transgene encoding diphtheria toxin receptor under the control of the insulin promoter to induce near total (>99%) beta cell ablation upon treatment with the diphtheria toxin. This study showed that although there was no apparent replication of the few remaining beta cells, there was an appearance of bihormonal cells after beta cell ablation, from which 32-81% were shown to be derived from alpha cells using lineage tracing methods (75).

1.7 Beta cell death in diabetes

Together with insulin resistance, type 2 diabetes is characterised by inadequate insulin secretion by the pancreatic beta cells. For many years, beta cell dysfunction was thought to be primarily due to a loss of beta cell mass through apoptosis following the continuous demand for insulin secretion and subsequent 'burn out'. Pathology studies assessing the beta cell mass in obese non-diabetic, type 2 diabetic and lean non-diabetic patients found a ~50% increase in relative beta cell volume in obese non-diabetic patients compared to lean control patients (76). Rodent studies on different strains of insulin resistant, obese non-diabetic and obese diabetic rats also provided evidence of beta cell hypertrophy (increased cell volume) compared to non-obese controls (77). This phenomenon is likely to be due to

the increased demand for insulin secretion following establishment of insulin resistance in peripheral tissues. In addition, type 2 diabetic subjects showed a decrease of up to 65% beta cell volume (76), which is in accordance with the view that there is a beta cell deficit and increased apoptosis during type 2 diabetes. Although there is, undoubtedly, a certain degree of beta cell death in type 2 diabetes, other pathology studies have shown that within the first 5 years of onset, the reduction in beta cell mass is not sufficient enough to explain the dramatic dysregulation of the glucose levels when compared to BMI matched controls. In light of this evidence, Rahier and colleagues suggest that the failure of the beta cell to respond to glucose may be largely due to dysfunction rather than death (78). Other studies have shown that the loss of beta cell mass in type 2 diabetes may be overestimated if determined by insulin production and detection and that ultrastructural and morphological studies can give a more accurate determination of beta cell loss (79). This outlines the need for further understanding of the mechanisms involved in the onset of type 2 diabetes.

1.8 Beta cell dysfunction

Although there is evidence of beta cell death in diabetes, studies have shown that beta cell dysfunction has a role to play in the dysregulation of glucose levels and that, particularly in the earlier stages of the disease, this dysfunction may be reversible. During the onset of type 2 diabetes, basal insulin levels in patients tend to be upregulated to compensate for the insulin resistance at target tissues. This hyperinsulinemia, even under fasting conditions, has been suggested to be due to reduced cell membrane cholesterol under diabetic conditions which helps to regulate hormone release (80). This study found that reduced membrane cholesterol resulted in constitutively open Ca^{2+} channels, resulting in continued influx and resulted in increased translocation of insulin granules to the membrane for secretion (80). Another early sign of beta cell dysfunction in patients with type 2 diabetes is loss of first phase insulin secretion. A study looking at 66 patients with a range of fasting glucose concentrations showed that when patients were administered an intravenous glucose tolerance test there was a loss of first phase insulin response in patients with a fasting glucose of >6.4 mmol/l and, as a result, impaired glucose clearance (81). These studies provide evidence for the contribution of beta cell dysfunction in the pathogenesis of type 2 diabetes.

1.9 Beta cell plasticity

The relative contributions of reversible beta cell dysfunction and true decreases in beta cell mass in type 2 diabetes remain unresolved. A study looking at the effect of bariatric surgery on type 2 diabetes showed persistent improvements in plasma glucose levels, HbA1c and insulin levels in 80-100% of patients. The apparent reversal of type 2 diabetes appeared too fast to be accounted for by beta cell regeneration (54) and therefore suggests that it may be the function of the beta cells that was restored during the surgery. In agreement with this, a study by Lim *et al.* showed that a calorie restricted diet caused a marked increase in hepatic sensitivity to insulin, the restoration of normal fasting blood glucose and improvements in beta cell function (55). Further analysis showed that the ability of beta cells to recover function remains several years after diagnosis (56). These studies provide evidence for rapid reversal of beta cell dysfunction, suggesting that rather than undergoing apoptosis, beta cells may have lost the molecular machinery necessary to respond appropriately to glucose, which, upon insult removal, is regained. This concept, in which cells lose their hallmark characteristic state that identifies them as terminally differentiated, is termed dedifferentiation. Potentially offering a metabolic 'hideaway' from stresses associated with diabetes, dedifferentiation may prevent beta cell apoptosis through overwork and stress.

1.9.1 Dedifferentiation

Rodent studies have shown that by knocking out Foxo1, a transcription factor which plays a role in beta cell fate, there is a marked decline in expression of beta cell transcription factors including NKX6.1, MafA and Pdx1 following metabolic stress. In addition, beta cell dedifferentiation was associated with the re-expression of progenitor markers such as Ngn3, Oct4 and Nanog (82). This dedifferentiated state allows the beta cells to become more similar to endocrine progenitor cells and provides the opportunity for re-differentiation to a different endocrine lineage. This concept has been observed in several rodent studies which noted an increase in other endocrine cell numbers in the presence of the dedifferentiated phenotype, suggesting that a degree of fate-switching can occur under stressed conditions (17, 66, 82).

1.9.2 Transdifferentiation

Transdifferentiation from beta to alpha cell phenotype has been shown by several groups and provides a potential mechanism for the hyperglucagonemia seen in the diabetic state. One explanation for this is the downregulation of transcription factors such as Pdx1. The Pdx1 transcription factor is vital in the early development of the pancreas, with Pdx1 knock-out mice showing impaired pancreatic development (83), and its continued expression is important in the progression to a beta cell lineage (84). Gao and colleagues have shown, through Pdx1 knock-out, that beta cells have reduced function, and begin to develop both ultrastructural and physiological features of an alpha cell (17). This change in ultrastructural components of the beta cell has also been observed by Brereton *et al.* who used a mouse model with a defect in the K_{ATP} channel to induce rapid onset of hyperglycaemia through the prevention of insulin secretion (85). In mice with the mutated K_{ATP} channel a reduced number of insulin granules were observed in cells compared to control littermates. This study also showed that the diabetic mice showed reduced staining for insulin of as much as 70%, and a corresponding increase in glucagon staining compared to control mice after exposure to chronic hyperglycaemia (85). Interestingly, with insulin or sulphonylurea (glibenclamide) treatment and the subsequent restoration of euglycaemia, these changes were reversed (85) suggesting that changes in the beta cell, as a result of hyperglycaemia, may be reversed when the metabolic stress is removed.

The previously mentioned role Nkx6.1 plays in the suppression of the alpha cell phenotype may also contribute to the transdifferentiation process. Downregulation of this transcription factor during extended periods of hyperglycaemia could be partially responsible for the loss of beta cell phenotype and gain of alpha cell characteristics. A study using recombinant adenovirus vectors to knock down Nkx6.1 expression showed a resultant 2-fold increase in glucagon mRNA levels and a significant impairment in glucose stimulated insulin secretion. In agreement with this, overexpression of Nkx6.1 in the alpha cell line α TC1.6 was shown to significantly repress the activity of the glucagon promoter (63).

Transdifferentiation between endocrine cell types has been shown in many models looking at different beta cell transcription factors and their importance in maintaining the beta cell phenotype. In an Nkx2.2 knockout study evidence was presented that demonstrated a role in not only activation of beta cell genes, but also in the repression of other endocrine gene programs (86). A similar role was shown by Swisa *et al.* for Pax6, which demonstrated a role in activation of beta cell genes alongside the repression of Ghrelin, Somatostatin and

Glucagon genes (87). These studies not only show the importance in the tight regulation of beta cell transcription factors to maintain the beta cell phenotype but also highlight the dual role that single transcription factors can have in activating genes associated with the beta cell phenotype whilst also repressing genes associated with other endocrine phenotypes. Although the theory of pancreatic endocrine cell transdifferentiation is still disputed, the plasticity between endocrine cell types is an exciting concept, and one that may potentially provide a therapeutic target through which an endogenous source of replacement beta cells can be generated as a transformative therapy for diabetes.

1.10 Aims

Informed by the accumulating evidence for beta cell plasticity playing a large role in beta cell dysfunction and hyperglucagonemia in type 2 diabetes, the following studies aimed to develop an *in vitro* model of hyperglycaemic stress to elucidate the mechanisms involved. Alongside this, these studies aimed to further investigate the role of transdifferentiation in beta cell dysfunction and to determine the specific role of Tle3/1 in this process.

Specific objectives were:

1. To characterise changes in gene expression and beta cell function under glucotoxic conditions using the rodent INS1E cell line as a model of hyperglycaemia
2. To investigate the role of transcriptional co-repressor, Tle3, in maintaining the beta cell phenotype in rodent cell lines and primary islets
3. To investigate whether there is an association between loss of TLE1 and transdifferentiation of beta cells in human type 2 diabetes

2 Materials and Methods

2.1 Materials

2.1.1 General Materials

General laboratory chemicals were supplied by Sigma-Aldrich Company Ltd. (Poole, Dorset UK) unless specified otherwise. Kits used are specified in Table 2.1.

Kit	Supplier	Catalogue number
GenElute Mammalian Total RNA Miniprep Kit/ On Column DNase-1 digestion set	Sigma	RTN350-1KT/DNASE70
ABI High Capacity cDNA Kit	Thermo Fisher (Applied Biosystems)	4368814
Mercodia High Range Rat Insulin ELISA	Diagenics	10-1145-01
Mercodia Glucagon ELISA - 10µl	Diagenics	10-1281-01
Alexa Fluor 555 Tyramide SuperBoost Kit (Goat anti-mouse IgG)	Thermo Fisher	B40913
Duolink Insitu red starter kit mouse/rabbit- Proximity Ligation Assay	Sigma	DUO92101-1KT
QIAprep Spin Miniprep Kit (50)/ QIAGEN Plasmid plus Maxi kit	QIAGEN	27104 /12965

Table 2.1 Kits used for general laboratory experiments.

2.1.2 Cell Culture Materials

Cell culture flasks and multiwell plates were supplied by Greiner (Gloucestershire, UK). All culture medium was supplied by Life Technologies (Thermo Fisher- Cramlington, UK).

2.2 Methods

2.2.1 INS1E cell culture

INS1E cells were cultured in RPMI medium 1640 glucose (11 mM) supplemented with 5% Foetal Bovine Serum (FBS), 100 U/ml penicillin and 100 µg/ml streptomycin, 1% Sodium pyruvate and 5 µl β-mercaptoethanol. Cells were cultured in 75 cm² (T75) tissue culture flasks. All cells were incubated at 37°C with 5% CO₂.

2.2.2 Subculture of cell lines

INS1E cells were passaged upon reaching approximately 80-90% confluence. Cells were washed with Phosphate Buffered Saline (PBS) and detached using trypsin. Following detachment, complete INS1E medium was added and cells were transferred to a 50 ml universal tube and subjected to centrifugation at 548 g for 3 minutes. Following centrifugation, the medium was aspirated and the cell pellet re-suspended in appropriate medium prior to transfer in to the required tissue culture flasks/plates.

2.2.3 Generation of stable Tle3 knockdown cell line

Short hairpin RNA (shRNA) is a valuable tool for generation of knockdown cell lines. Utilising viral vectors, shRNA can be delivered into cells where it integrates with host DNA. Following transcription shRNA is processed in the cells in a similar mechanism to host micro RNA, through use of the DICER complex which processes the shRNA into siRNA (88). The resulting generation of siRNA allows knockdown of the desired gene whilst the integration into the DNA allows the shRNA to maintain knockdown in dividing cells (88). INS1E cells were grown to ~80% confluence. Cells were treated with 0.8 µg/ml polybrene and infected with lentivirus containing shRNA to knockdown Tle3 or a scrambled control. Cells were incubated for 2 days at 37 °C, 5% CO₂ before replacement with fresh, complete INS1E medium. Cells were then grown up until a ~80% of cells were GFP+. Cells were then passaged as normal with complete INS1E medium containing 0.02 µg/ml puromycin to prevent growth of non-knockdown cells as shRNA plasmid contained puromycin resistance. Cells were grown up and passaged for at least 4 weeks prior to assessment in studies to establish a model of long-term knockdown.

2.3 Collection of Primary Tissue

2.3.1 Rodent Islet Isolations

Black 6 (C57BL/6) mice purchased from Charles Rivers (Wilmington, MA- USA) were euthanized by dislocation of the neck in the Comparative Biology Centre, Newcastle University following local ethical committee approval. The pancreas was distended through ductal or parenchymal injection using 1 mg/ml Collagenase Type V from Clostridium (Sigma Aldrich).

1X Hanks' Balanced Salt Solution (HBSS) with 350 mg sodium bicarbonate and 4 ml 30% Bovine Serum Albumin (BSA) per litre, was prepared prior to isolation and kept at 4 °C until required.

Mouse pancreata were put in a 50 ml Falcon tube in a 37 °C water bath for 7 minutes to digest the pancreas. Tubes were then shaken 7 times to re-distribute the collagenase and placed back in the water bath for a further 1 minute. Volume was then made up to 25 ml with the previously made Hanks' Balanced Salt Solution (HBSS)+ BSA and tubes were shaken 30 times to dissociate the pancreas. Volume was made up to 50 ml using Hank's + BSA and tubes were spun down for 2 minutes at 339 g, 4°C.

Supernatant was discarded and pellet re-suspended in 20 ml Hank's + BSA. Solution was passed through an islet screen (CD-1 size 60 mesh, S1020-5EA- Sigma Aldrich) using 20 ml syringe and 18G needle. All equipment for this step had been rinsed with Hanks' for coating (34 ml HBSS + 6 ml 30% BSA) to prevent loss of islets. A further 10 ml Hanks' + BSA was used to rinse the Falcon tubes and passed through the screen. Tubes were spun for 2 minutes at 339 g, 4°C. Supernatant was discarded and this step was repeated twice. After the third spin, tubes were left inverted on absorbent paper to dry. The interior of the tubes was then wiped to absorb excess Hank's buffer without disturbing the pellet and placed on ice.

For the gradient, the pellet was re-suspended with 5 ml Histopaque (Thermo Fisher) using a pipette that had been rinsed with Hanks' for coating. A further 5 ml was added to make up to 10 ml. 10 ml of complete rodent medium was slowly added on top of the Histopaque, ensuring the two solutions did not mix. Tubes were then centrifuged for 30 minutes at 339 g, 4°C with the brake turned off.

Following centrifugation, the supernatant was collected and the pellet was placed on ice until the islets had been picked.

The supernatant was then made up to 50 ml with Hanks' buffer+ BSA and spun down for 3 minutes at 339 g, 4°C. Supernatant was discarded and the pellet, containing the islets, was

re-suspended in 5-10 ml complete rodent medium and placed on ice until picked. Islets were combined in one petri dish and hand-picked for use in studies. To hand-pick, the islets were pooled in a petri dish and tubes were washed with a further 5 ml complete medium to ensure no islets were lost. A light microscope was used to identify the islets, which appeared darker in comparison to exocrine tissue, which appeared slightly transparent.

2.3.2 Rodent Islet Culture

Rodent islets were cultured in RPMI medium 1640 glucose (11 mM) supplemented with 10% Foetal Bovine Serum (FBS) and 100 U/ml penicillin and 100 µg/ml streptomycin. Cells were cultured in 12 well tissue culture plates. All islets were incubated at 37°C with 5% CO₂ until required.

2.3.3 Human islet culture

Human islets were obtained from the Alberta Diabetes Institute Islet Core Laboratory, University of Alberta (Edmonton, Canada) and cultured in Dulbecco's Modified Eagle Medium, 4.5g/L D-glucose, L-Glutamine and 25 mM HEPES supplemented with 10% FBS. All islets were incubated at 37°C with 5% CO₂ until required.

2.4 Glucotoxicity treatments

Plates were prepared for treatment with high and low glucose for use in staining, PCR and glucose stimulated insulin secretion (GSIS) studies (see below for methods). For the glucotoxicity studies cells were seeded and cultured overnight in complete medium prior to culture in INS1E media with 11 mM or 25 mM glucose for 48hrs. Both high and low glucose conditions were set up in technical triplicate.

2.5 Viral expansion, harvesting and treatments

2.5.1 Viral Expansion and harvesting

Pdx1 and β-galactosidase (β-gal) adenovirus were kindly gifted by Professor Sarah Ferber (89). HEK293 cells, derived from human embryonic kidney cells, were treated with 5 µl β-gal or Pdx1 virus and grown in T75 flasks for 48 hrs, when ~50% cells had lifted, cells were harvested by lysing cells through freeze-thaw cycles in a methanol/dry ice bath and 37°C water bath 4 times. Samples were centrifuged at 6000 rpm for 5 minutes at 4°C. Supernatant

was passed through an 18g needle and mixed 1:4 with virus storage buffer (10 mM Tris pH8.0, 100 mM NaCl, 0.1% BSA, 50% glycerol, filter sterilised).

2.5.2 Viral treatments

INS1E cells were treated with 1 µl/ml of Pdx1 virus for 1 hour before medium was replaced with 1 ml fresh, complete medium. Control cells were treated with 1 µl/ml of β-gal before being put into either normal (11 mM) or high (25 mM) glucose culture.

2.6 Viral vectors

2.6.1 Transformation of viral vectors

TLE1 Human short hairpin RNA (shRNA) transfer vectors were purchased from OriGene (Maryland, USA) containing four shRNA constructs to TLE1 and a scrambled shRNA cassette in pGFP-C-shLenti Vector (Figure 2.1).

For the transformation, NEB® Stable Component *E.coli* (C3040H) cells were thawed on ice and mixed with 3 µl of each DNA plasmid which were re-suspended at 10 µg/ml. Each vial was mixed gently and incubated on ice for 30 minutes. Cells were then heat-shocked for 30 seconds in a water bath at 42 °C, removed, then placed on ice for a further 5 minutes. 950 µl of NEB 10-beta/Stable Outgrowth Medium was added to the mixture with incubation for 60 minutes at 30 °C on a rotator. 50 µl of each vial was plated onto individual LB (Luria broth- 10 g NaCl, 10 g Tryptone, 5 g yeast in 1 L dH₂O) selective plates containing chloramphenicol (34 µg/ml) which were left to incubate overnight at 37 °C. Four cultures for each plasmid were selected and grown up for glycerol stocks and miniprep culture. The method is summarised in the flow chart in Figure 2.2.

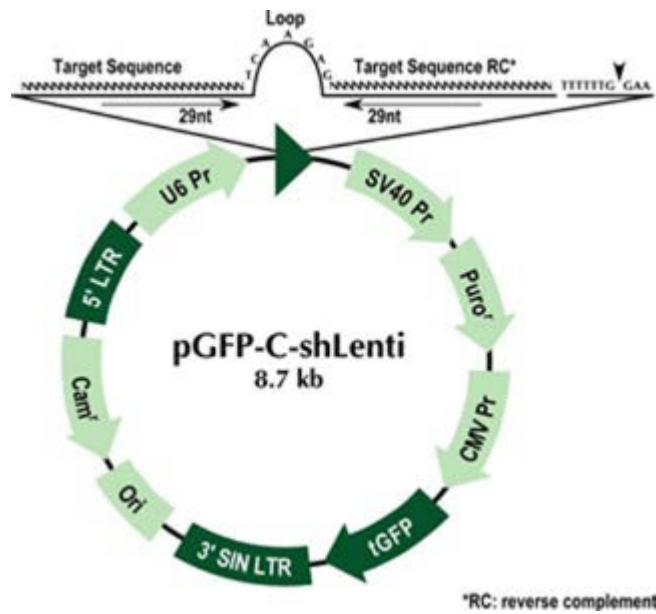


Figure 2.1 Plasmid map of the lentiviral GFP vector containing either scrambled or TLE1 shRNA constructs used for transformations.

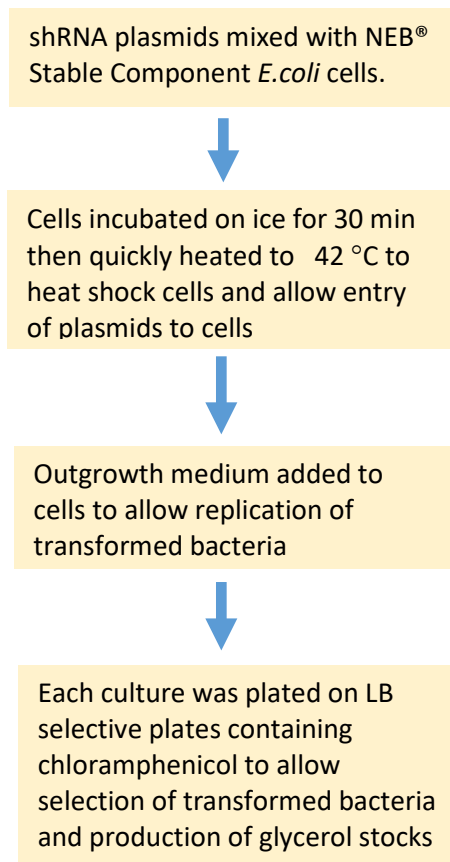


Figure 2.2 Transformation of *E. coli* with TLE1 shRNA plasmid

2.6.2 Glycerol stocks of DNA plasmids

Stocks of plasmid DNA were stored by adding 500 μ l of culture stock with 500 μ l glycerol. Stocks were stored at -80 °C until required. To grow plasmids, a small sample of stock was added to 5 ml of LB medium containing selection antibiotic. The solution was incubated overnight on a shaker at 220 rpm and 37 °C.

2.6.3 Miniprep purification of plasmid DNA

The miniprep kit was purchased from Qiagen (Hilden, Germany) and purification of plasmid DNA was carried out as instructed. 1 ml of overnight culture was spun down at 10,000 rpm for 1 minute to pellet bacteria. The pelleted cells were re-suspended in 250 μ l Buffer P1. 250 μ l Buffer P2 was added and solution was gently mixed by inverting tube 4-6 times. 350 μ l Buffer N3 was then added and immediately mixed by inverting tube. Samples were centrifuged for 10 minutes at 16,100 rcf and supernatant was transferred to the QIAprep spin column. Columns were centrifuged for 30-60 seconds and flow-through was discarded. Spin columns were washed with 750 μ l Buffer PE, flow through discarded and columns were spun for a further minute to remove residual buffer. Samples were then eluted into a clean micro-centrifuge tube by adding 50 μ l Buffer EB, allowing to sit for 1 minute before spinning for 1 minute. Purified DNA was quantified using Nanodrop to read absorbance at 260 and 280 nm.

2.6.4 Agarose Gel electrophoresis

The principle of agarose gels is to separate DNA fragments based on their size. As DNA is negatively charged, the samples are loaded at one end of a polymerised agarose gel and will move through the gel to the positively charged anode at the other end. As larger fragments of DNA will migrate through the gel slower than smaller fragments it allows the DNA to be separated. These can then be visualised under UV light by adding Ethidium Bromide into the gel when preparing it, as it intercalates with nucleic acids and fluoresces under UV light, giving a visual representation of the DNA bands. Using this technique we ran the DNA from each of the colonies taken forward for the miniprep on an agarose gel to see if the insert was present. First, samples were cut with restriction enzymes EcoR1 and Xba1 (New England BioLabs #R0145, #R0101) by incubating at 37°C for 5-15 minutes. Once the digest was complete DNA was loaded into 1.5% agarose w/v gel (made by dissolving the agarose

powder in 1x Tris acetate-ethylenediaminetetraacetic acid (TAE) by heating and allowing to cool to ~50 °C before adding Ethidium Bromide at 1 µl/100 ml and leaving to set at room temperature with the appropriate comb). Gels were run for ~45-60 minutes at 90 volts before being visualised under UV light (Figure 2.3).

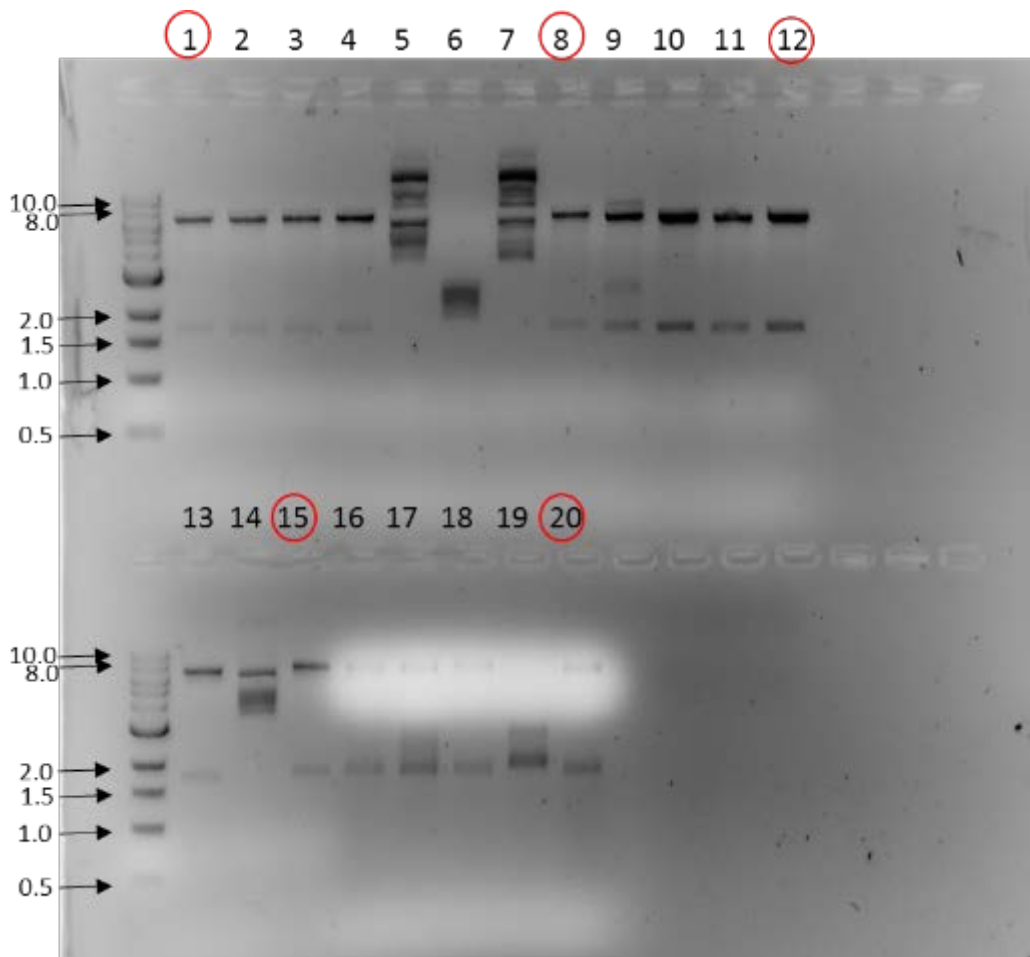


Figure 2.3 Agarose gel to check for successful transformation.

Wells 1-4 contain samples from the scrambled control, 5-7, 8-12, 13-16 and 17-20 contain samples from the 4 shRNA TLE1 constructs purchased from Origene. The highlighted samples were the sample chosen for each construct to be taken forward for maxipreps.

2.6.5 Maxiprep purification of plasmid DNA

Maxipreps were carried out to yield high quantities of plasmid DNA. The Qiagen maxiprep protocol was followed which works on the same principle as the miniprep protocol. As the maxiprep works on a larger scale, 500 ml of overnight culture was used for the Qiagen maxiprep protocol for each of the colonies chosen from the agarose gel. The bacterial pellet was spun down (3,300 rcf for 15 minutes, 4°C) and lysed by adding Buffer P1 and P2 and

mixed thoroughly by inverting the tube. Tubes were incubated at room temperature for 5 minutes before Buffer P3 was added and immediately mixed by inversion. Tubes were incubated on ice for 15 minutes. Tubes were spun down at 16,100 rcf for 30 minutes at 4°C. Supernatant was removed and spun for a further 15 minutes. Supernatant was promptly added to an equilibrated QIAGEN-tip 500 and left to move through the column by gravity flow. 2x 30ml Buffer QC was added and allowed to pass through the column by gravity flow before the purified DNA was eluted in 15 ml Buffer QF. DNA was then precipitated using isopropanol, mixed and centrifuged at 11,200 x g for 30 minutes at 4 °C. DNA pellet was then washed in 70% ethanol and centrifuged for a further 10 minutes. Supernatant was discarded and pellet was air-dried before being re-dissolved in TE buffer, pH 8.

2.7 Transfections

Transfection methods for the different experiments are summarised in the table below.

Experiment	Knockdown system used
Short term knockdown in INS1E cells	Transfection using siRNA
Generation of stable knockdown cell lines	Infection using lentiviral vector and shRNA
Knockdown in rodent islets	Transfection using siRNA
Knockdown in human islets	Transfection using shRNA plasmid

Table 2.2 Different methods of gene knockdown used.

2.7.1 Small interfering RNA (siRNA) mediated knockdown of INS1E cells
 siRNA is a useful tool for studying gene function. siRNA are small ~20 nucleotide sequences that are complementary to the target gene. They contain a 3' overhang which activates the RNAi pathway in cells, resulting in degradation of the target protein (90). siRNA differ from shRNA as they are not integrated into the DNA of the host therefore are usually used or assessing short term impacts of gene knockdowns. All transfection reagents can be found in Table 2.3. Cells were plated onto 12 well plates and incubated until 60-80% confluent. RNAiMAX Lipofectamine solution (Thermo Fisher, 13778-075) and siRNA was prepared as in Table 2.4. Solutions were left at room temperature for 5 min. Each siRNA solution was mixed with a Lipofectamine solution and incubated at room temperature for 20 min. Cells were washed with PBS and 350 µl of antibiotic free medium was added to each well. 150 µl of the

respective Lipofectamine-siRNA mix was added to the control and Tle3 siRNA wells. Cells were incubated at 37 °C 5% CO₂ for 16-18 hours before 1 ml fresh complete INS1E medium was added and cells were left for the remainder of the 48 or 72 hour culture period. Knockdown efficiency was assessed using qPCR before functional studies were carried out.

Reagent	Supplier	ID number	Cells used
Silencer Select negative control #1 siRNA	Ambion	190098	All cells
Tle3 silencer pre-designed siRNA (siRNA 1)	Ambion	190098	INS1E
Tle3 silencer pre-designed siRNA (siRNA 2)	Ambion	190099	INS1E (young- full studies)
Tle3 silencer pre-designed siRNA (siRNA 3)	Ambion	190100	INS1E (old- full studies)
Tle3 silencer pre-designed siRNA	Ambion	54928	Mouse islets
Lipofectamine RNAiMAX Transfection Reagent	Thermo Fisher	13778-075	INS1E, mouse islets, human islets
Opti-mem reduced serum medium	Thermo Fisher	31985070	INS1E, mouse islets, human islets

Table 2.3 List of transfection reagents used.

Reagent	Volume added per reaction (μl)	Volume Optimem per reaction (μl)
Lipofectamine	2.5	75
siRNA	3	75

Table 2.4 Volumes of transfection reagents used per reaction for siRNA mediated Tle3 knockdown in both INS1E cells and rodent islets.

2.7.2 Transfection of intact islets

Protocols for intact islet transfection were adapted from a previously published paper (91) and is described below.

2.7.3 Transfection of rodent and human islets

For transfections, an average of 100 rodent islets or 500 human islet equivalents (IEQ) were needed per well of a 12-well or 6-well plate respectively. Following isolation, islets were

washed once in PBS prior to 2 minute incubation at 37 °C in 0.5X trypsin. Cells were spun down at 100 g and re-suspended in 350 µl antibiotic free medium per well for rodent islets or 700 µl for human islets.

For rodent islets, transfection reagents were made up as shown in Table 2.4 and 150 µl was added to each.

For human islet transfections reagents were made up as shown in Table 2.5. For human islets 300 µl lipofectamine-DNA mix was added to each well.

Both rodent and human islets were then incubated in transfection reagents for 2 days prior to re-transfection for a further 2 days before being used for final experiments.

Reagent	Volume added per reaction (µl)	Volume optimum added per reaction (µl)
Lipofectamine	8	300
Control pGFP (2 µg DNA)	5.50	300
shRNA A (2 µg DNA)	6.36	300
shRNA B (2 µg DNA)	5.38	300
shRNA C (2 µg DNA)	4.86	300
shRNA D (2 µg DNA)	6.66	300

Table 2.5 Volumes of transfection reagents used for TLE1 knockdown in intact human islets.

2.8 Staining of cells and tissue

Buffers used for immunocytochemistry (ICC) and immunohistochemistry (IHC) are listed in Table 2.6.

2.8.1 Immunofluorescence staining of cell lines (ICC)

Cells were fixed using 4% paraformaldehyde before being permeabilised using 0.4% Triton in PBS for 20 minutes. Blocking of non-specific binding was achieved by incubating cells for an hour with 20% FBS in PBS at room temperature. Subsequent to blocking, cells were incubated with primary antibodies diluted in 0.05% FBS (Table 2.7 for dilutions) overnight at 4 °C. For negative controls, primary antibody was omitted and replaced with appropriate serum. After overnight incubation, cells were washed 3 x 5 minutes in PBS Tween (PBSTw) and incubated with appropriate secondary antibodies (Table 2.8) at room temperature for one hour. Cells were then washed 3x5mins in PBSTw and counterstained with 4, 6-

diamidino-2-phenylindole (DAPI) at a concentration of 0.1 µg/mL prior to mounting with Vectorshield (Vector Labs) and sealing with nail varnish.

Buffer	Composition	Use
PBS-Tween	100 mL PBS (10X), 1 mL Tween in 1L H ₂ O	IHC/ICC
Sodium Citrate Buffer	2.49g sodium citrate buffer in 1L H ₂ O, pH6	IHC

Table 2.6 Buffers used for IHC and ICC

2.8.2 Proximity Ligation Assay (PLA)

PLA assays are used to visualise protein-protein interactions. The process is summarised in Figure 2.4. Antibodies against the proteins of interest have complementary oligo-sequences bound to them. If these two proteins are in close proximity, the oligo probes will bind each other. This reaction can then be amplified and visualised in a PCR-type reaction, resulting in visualisation of the interaction. Duolink[®] Insitu red starter kit Mouse/Rabbit (Sigma) was used to detect interactions between proteins. INS1E cells were permeabilised with 0.2% triton before 1 drop of blocking solution was added to each cover slip. Slides were incubated at 37°C for 1 hour. Primary antibodies were diluted 1:100 with Duolink[®] Antibody Diluent and added to the cover slips and incubated for 90 minutes at 37 °C. Slides were washed 2x 5 min in wash solution A. Plus and Minus probes were diluted as per manufacturer's instructions and added to slides for 1 hour at 37 °C. Ligase was added to the slides at a 1:40 dilution in ligation buffer following 2 washes with wash buffer A. Slides were incubated for 30 minutes at 37 °C. Slides were then washed twice in wash buffer A before polymerase was added to each slide in a 1:80 dilution with amplification buffer. Slides were then incubated for 100 minutes at 37 °C. Slides were washed 2x 10 minutes with 1X wash buffer B before 1 minute wash with 0.01X wash buffer B. Slides were mounted with DAPI at a concentration of 0.1 µg/mL and imaged as previously described.

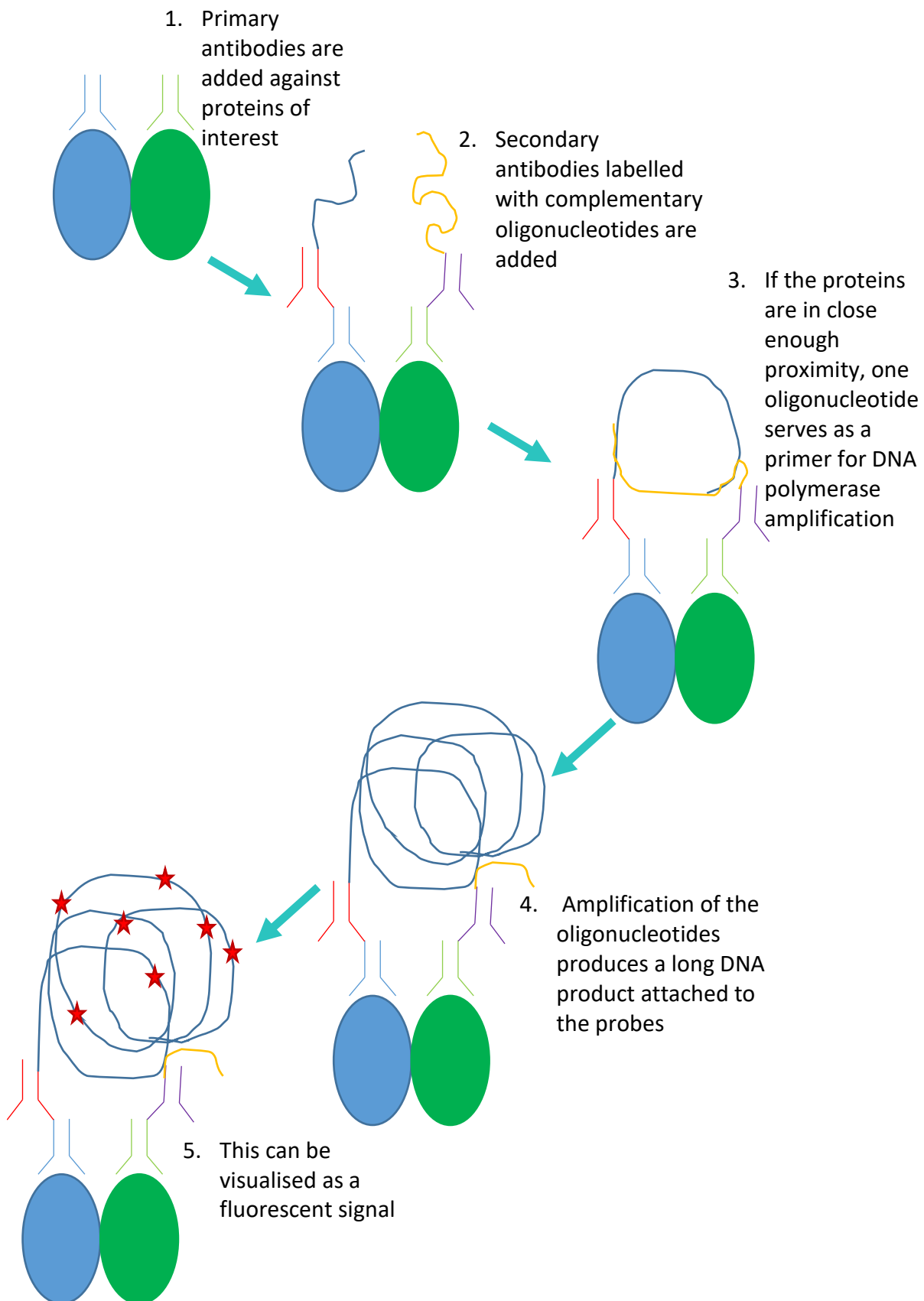


Figure 2.4 Summary diagram of the Proximity Ligation Assay (PLA) technique.

Image is adapted from previously published schematic of Duolink PLA assay (92).

2.8.3 PI-Hoechst staining

Propidium Iodide (PI) is a dye taken up through the membrane of dying cells but cannot permeate the membrane of living cells. This makes it a useful technique to study changes in cell death (both necrosis and late-stage apoptosis) (93) following treatment. Cells were stained with PI and Hoechst at a concentration of 10 µg/ml for 20 minutes. Cells were then washed with PBS and fixed in 4% formaldehyde for 20 min. Each condition was set up in technical triplicate.

A total of 4 images were taken across each well to image ~1000 cells. Image J software was used to analyse the percentage of PI positive cells.

2.9 Staining of Tissue sections

2.9.1 Immunofluorescence staining of tissue sections

All studies on human tissue had appropriate ethics in place before studies began. Human tissue sections were kindly gifted by the University of Exeter, UK (Cohort 1), for donor information see Table 5.1 and Table 5.2. Cohort 2 was gifted by the University of Alberta, Canada, for donor information see Table 5.3 and Table 5.4. Paraffin embedded sections were dewaxed in histoclear prior to rehydration in decreasing alcohol concentrations. Antigen retrieval was performed with 10 mM sodium citrate buffer pH 6 (2.49g sodium citrate in 1L water) heated in the microwave for 20 min before the slides were left to cool to 40 °C. Slides were blocked for 1 hour in 20% FBS in PBS before incubating overnight at 4 °C with primary antibody diluted in 0.05% FBS in PBS (Table 2.7). For negative controls, primary antibody was omitted and slides were incubated in 0.05% FBS in PBS only. After overnight incubation, cells were washed 3 x 5 minutes in 1X PBS Tween (PBSTw) and incubated with appropriate secondary antibodies (Table 2.8) at room temperature for one hour. Cells were then washed 3x5mins in PBSTw and counterstained with 4, 6-diamidino-2-phenylindole (DAPI) prior to mounting with Vectorshield (Vector Labs) and sealed with nail varnish.

2.9.2 TSA assay

Paraffin embedded sections were dewaxed in histoclear prior to rehydration in increasing alcohol concentrations. Antigen retrieval was performed with sodium citrate buffer pH 6 and slides left to cool to 40 °C. Slides were blocked in 10% goat serum for 5 minutes. TLE1 primary antibody was diluted in solution B signal enhancer and incubated overnight at 4 °C before Alexa Flour™ 555 Tyramide SuperBoost™ Kit Goat Anti-Mouse IgG (Thermo Fisher) was used to further enhance the TLE1 signal. For this, Poly-HRP secondary antibody was

mixed 1:1 with solution B and left at room temperature for 1 hour. The amplification step was optimised as per the manufacturer's instructions and the tyramide working solution was added for 8 minutes before stop solution was added. The insulin and glucagon primary antibodies were then added overnight at 4°C and staining was finished as previously mentioned.

Primary Antibody	Species	Supplier/ Catalogue number	Use
Cleaved caspase-3	Rabbit	Cell Signalling/ 9661s	Staining (1: 100)/ Western blot (1: 1000)
Tle3	Rabbit	Santa Cruz/ sc-514798	Staining (1:50)/ Western blot (1: 100)
Glucagon	Rabbit	Abcam/ ab92517	Staining (1: 500)/ Western blot (1: 1000)
Insulin	Guinea-pig	Abcam/ ab7842	Staining (1: 100)
Pdx1	Mouse	DSHB/ F6A11	Staining (1: 100)/ Western blot (1: 1000)
Nkx6.1	Mouse	DSHB/ F55A10-c	Staining (1: 100)/ Western blot (1: 1000)
Beta galactosidase	Rabbit	Abcam/ ab4751	Staining (1: 100)
TLE1	Mouse	Origene/ TA800301	Staining (1: 50)
B-actin	Mouse	Sigma/ A541p1	Western Blot (1:10 000)
GAPDH	Mouse	HyTech/ 5G4	Western Blot (1:10 000)

Table 2.7 List of all primary antibodies used in experiments.

Fluorochrome/ Conjugate	Species	Raised in	Supplier/ Catalogue number	Use
Alexa Fluor 568	Anti- rabbit IgG	Donkey	Life Technologies/A10042	Staining (1:500)
Alexa Fluor 488	Anti- guinea pig IgG	Donkey	Life Technologies/A11073	Staining (1:500)
Alexa Fluor 647	Anti- rabbit IgG	Donkey	Life Technologies/A31573	Staining (1:500)
Alexa Fluor 568	Anti- mouse IgG	Donkey	Life Technologies/A10037	Staining (1:500)
Alexa Fluor 488	Anti- mouse IgG	Donkey	Life Technologies/A21202	Staining (1:500)
Alexa Fluor 488	Anti- rabbit IgG	Donkey	Life Technologies/A21206	Staining (1:500)
Polyclonal HRP	Anti- rabbit Immunoglobulin	Goat	DAKO/ PO448	Western blot (1: 5000)
Polyclonal HRP	Anti- mouse Immunoglobulin	Goat	DAKO/ PO447	Western blot (1: 5000)

Table 2.8 List of all secondary antibodies used in experiments.

2.10 Cell counting

2.10.1 Manual counts

Nikon Elements software or Zen pro software was used following capture images of 50 islets per section using the Nikon A1 confocal microscope or the Zeiss AxioImager with Apotome microscope respectively. Blinded manual counts were carried out on all images from all donors (Cohort 1) and one control donor and one diabetic donor (Cohort 2). For the counting, Nikon Elements and Fiji software was used. The same counting method was used in both software as depicted in Figure 2.5. All cells were first marked with DAPI using the insulin and glucagon channels to mark out the boundary of the islet (A). Each channel was put on individually and positive cells marked with a different colour marker for each channel (B-C). The number of cells with each combination of markers were gathered for each islet and entered manually into spreadsheets to use for analysis (D).

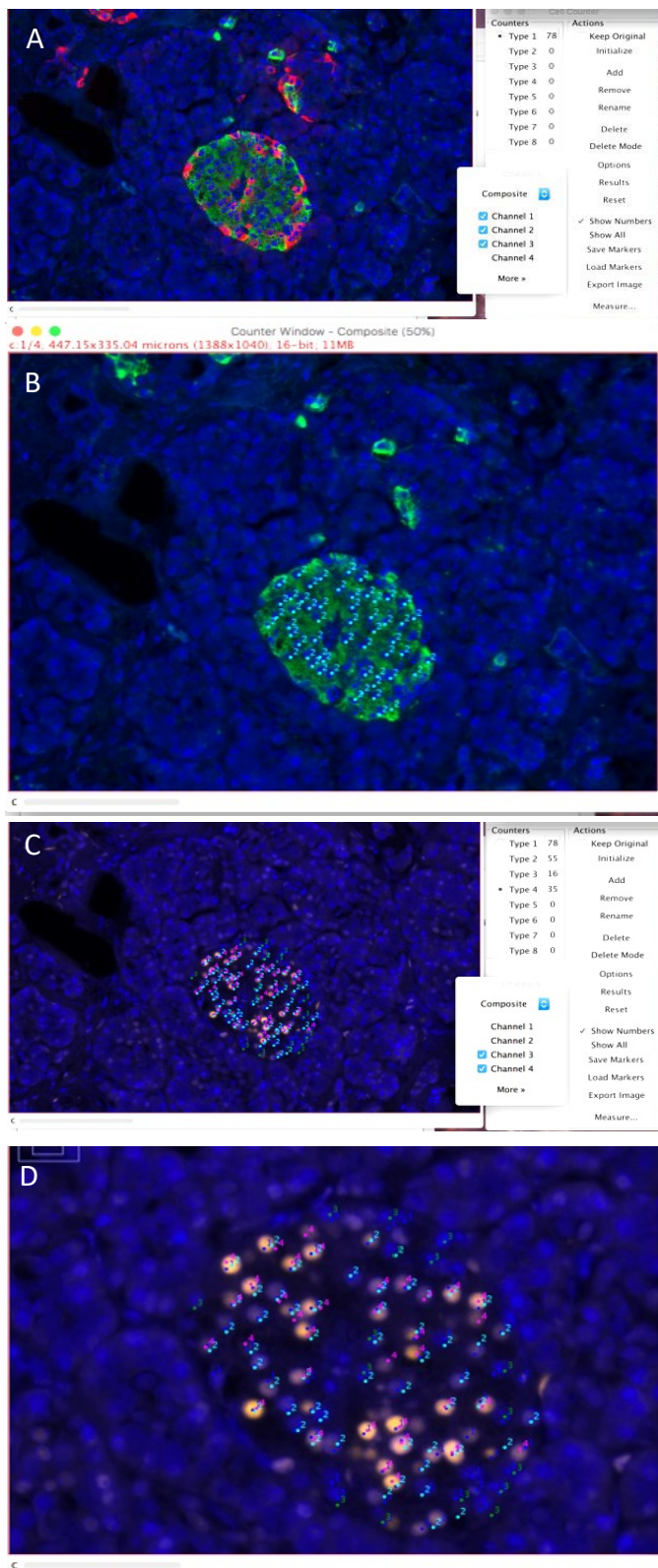


Figure 2.5 Manual counting method.

Manual counting method using Nikon elements and Fiji Software. All cells in islet were marked for DAPI using insulin and glucagon channels to outline the boundaries of islets (A). Individual channels were then put on and all positive cells marked with different counters per channel (B-C). Numbers of each phenotype were counted once all cells had been marked on individual channels (D).

2.10.2 Automated counting

Slides were scanned in using the Vectra slide scanner at 4x magnification. Islets were then marked by 'stamping' using the Phenochart 1.0.7 software (Figure 2.6) which identified islets through use of the insulin channel and marked out the area to enable further imaging. 'Stamped' islets were then imaged individually at x20 magnification for subsequent analysis.

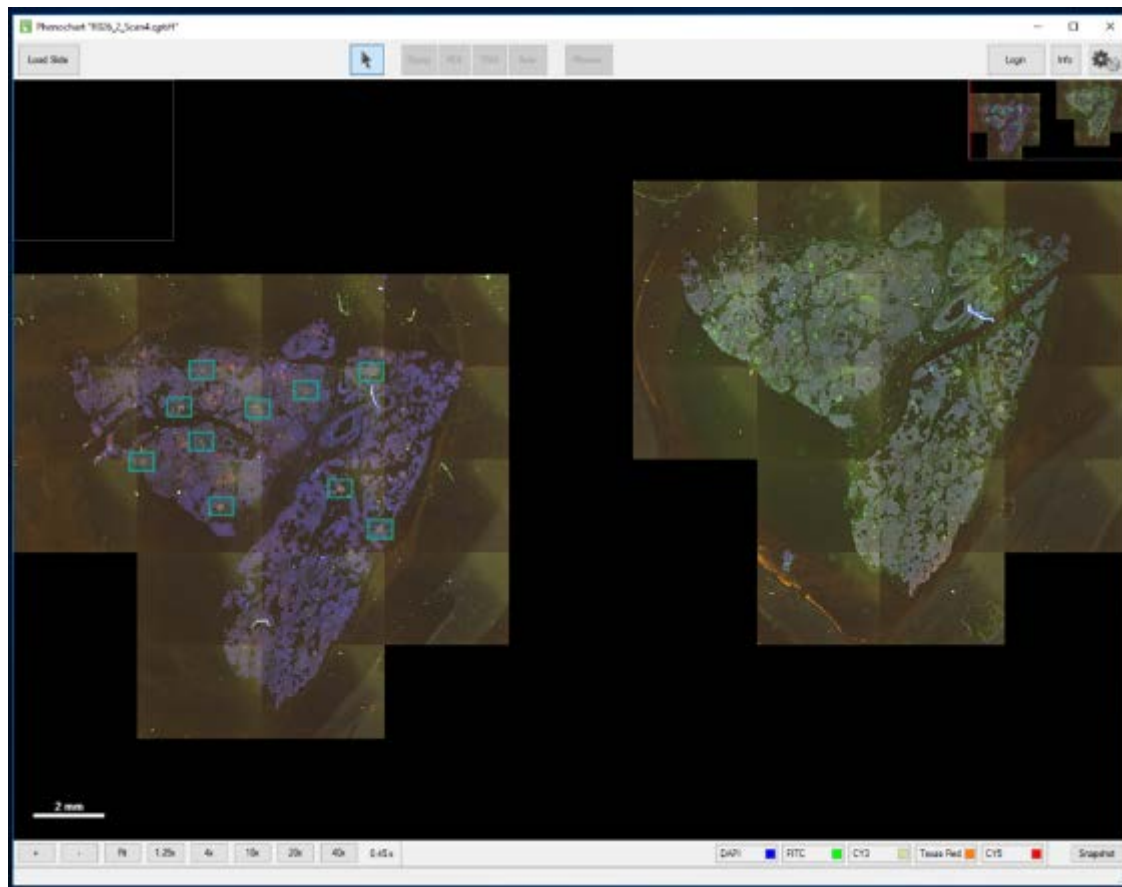
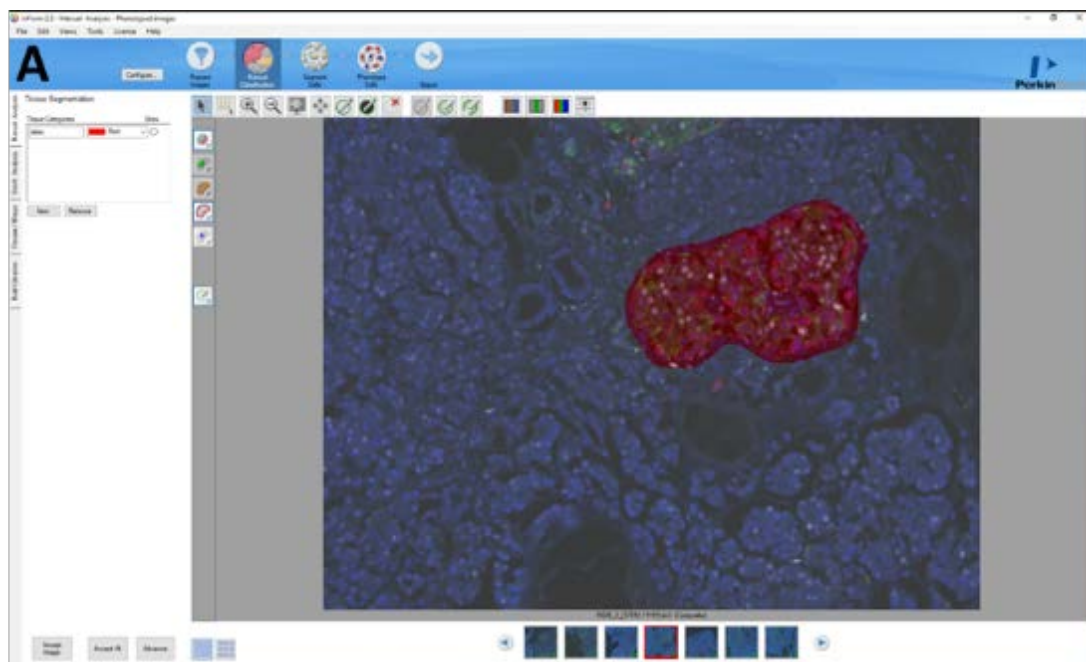


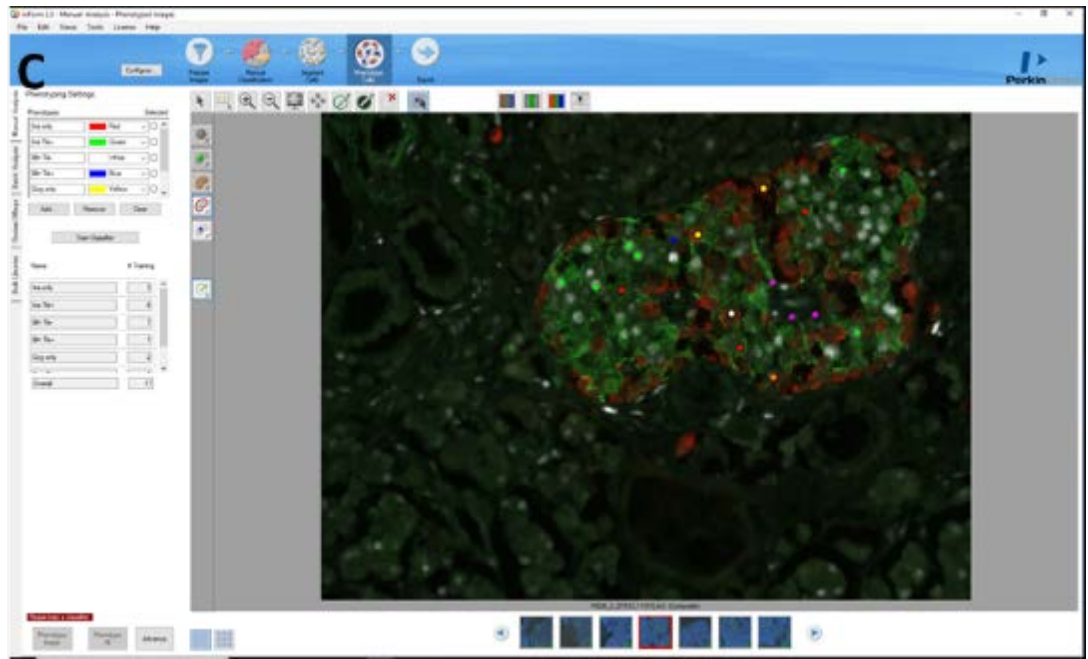
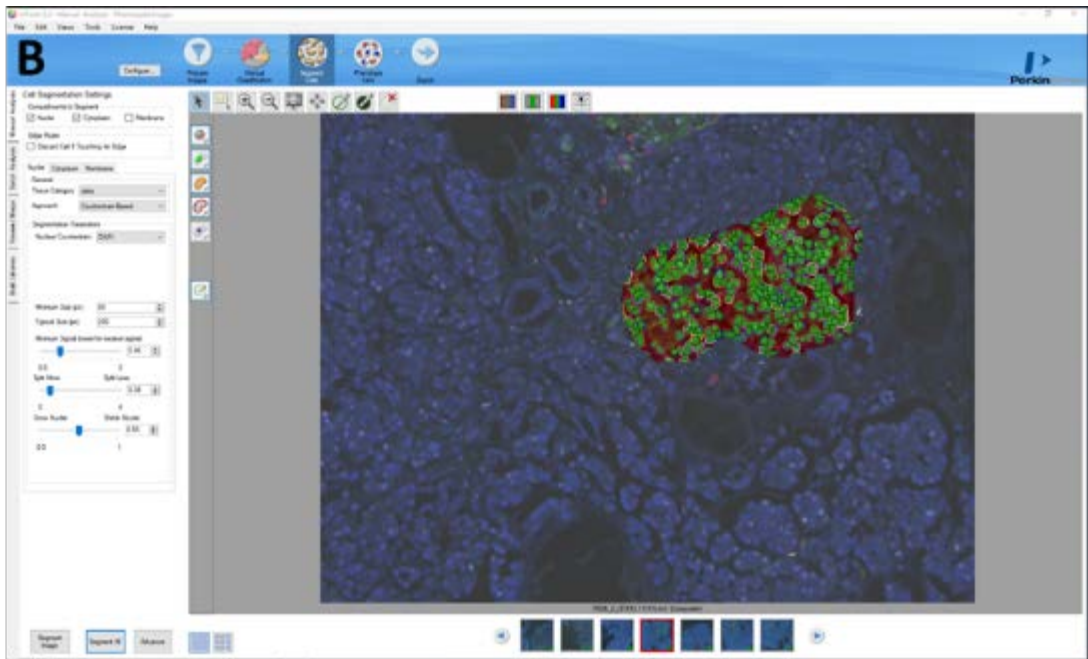
Figure 2.6 Image acquisition using Vectra slide scanner.

Whole tissue sections were scanned by Vectra Slide Scanner and islets were identified marked by 'stamping' as shown in the left hand image. Sections were then scanned at a higher magnification to enable further analysis.

The software InForm 2.3 (PerkinElmer, Massachusetts USA) was used to create an algorithm to identify individual cells in the islet. Individual islets within each x20 image were selected as regions of interest (Figure 2.7A). Minimum and typical pixel size for nuclei was set at 80 and 200 respectively to allow the nuclei of each cell to be identified and a minimum signal threshold was set at 0.46 (range 0-1). Split and grow nucleus settings were used to finalise

nuclei size as this parameter sets the outer boundary of the nucleus. Cells were then segmented based on these parameters (Figure 2.7B). Selected islets then undergo supervised machine learning to 'phenotype' the cells, which included: Ins only, Ins Tle+, Bih only, Bih Tle+, Gcg only, Gcg Tle+, DAPI only. Each phenotype is assigned a different colour marker to identify them. A subgroup of cells are manually assigned to each phenotype (training phase) (Figure 2.7C) and phenotypes are then assigned to all remaining cells, according to the relative fluorescent markers (testing phase) (Figure 2.7D). The accuracy of the algorithm is improved by using interactive training/testing process and the confidence of the assigned phenotype is reported for each cell. Following a testing phase, selected islets are reassessed for the accuracy of phenotype assignment and confirmed manually where confidences are low. This enables the algorithm to improve its accuracy and confidence during further testing phases. Following completion of the final testing phase, the project was exported and all data collected for 50, 70 and 90% confidence to be taken forward for analysis.





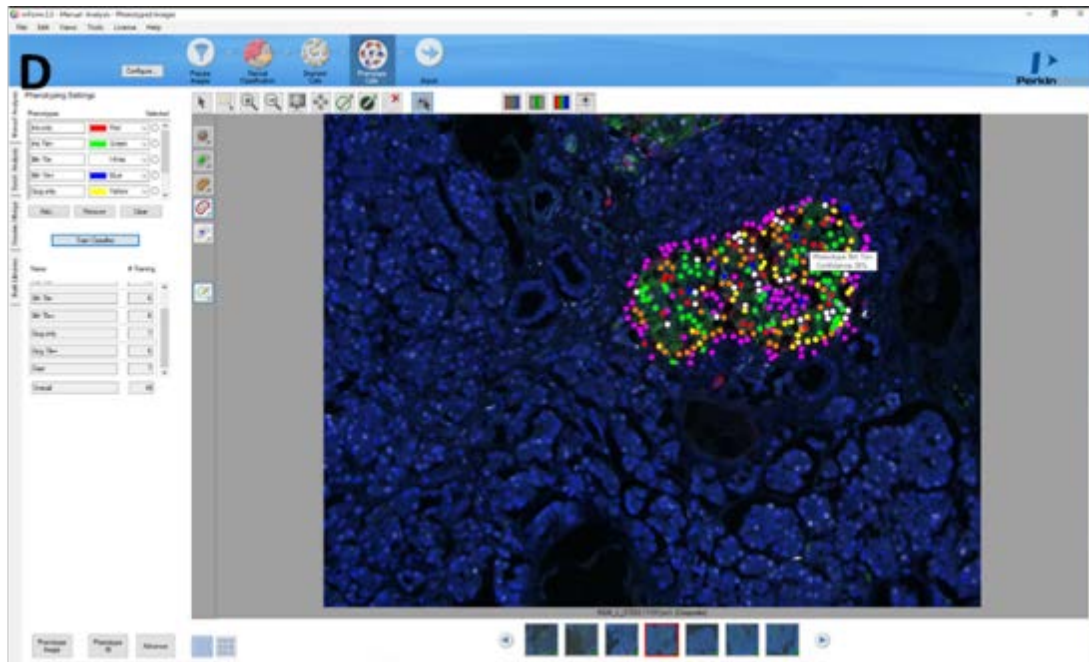


Figure 2.7 Analysis of images using InForm software.

InForm software was used to produce an algorithm that could identify different phenotypes within islets. Islets were first highlighted as regions of interest (A) before being segmented using different parameters based typical nuclear size and signal strength (B). Phenotypes were then entered into the algorithm and examples of each were identified (C) allowing the software to assign phenotypes to each cell across all islets based on these examples (D). A selection of cell phenotypes could be adjusted if the software was incorrect, or alternatively, correct but with low confidence to ‘train’ the software before re-phenotyping.

2.11 RNA extraction and cDNA synthesis

2.11.1 RNA extraction

Following detachment, cells were washed with PBS and centrifuged for 3 minutes at 16 100xg in a mini-centrifuge to obtain a cell pellet. RNA was then extracted using GenElute Mammalian Total RNA Miniprep Kit (Sigma) according to the manufacturer’s instructions.

2.11.2 RNA quantification

Initially, the concentration and quality of the RNA samples was measured on a NanoDrop (Thermo Scientific). Concentration was determined using the absorbance at 260 nm, with a reading of 1 being equivalent to ~ 40 µg/ ml. The ratio of absorbance at 260 and 280nm was used to measure the purity, with a ratio of ~ 2.0 indicating the sample to be free from protein, phenol and other contaminants.

2.11.3 First strand cDNA synthesis

The reverse transcriptase step was conducted using the ABI High Capacity cDNA kit (Applied Biosystems). All 20 µl reactions required preparation of a RT master mix (10 µl/reaction) that

included: 2 μ l RT random primers, 2 μ l RT buffer, 1 μ l Multiscribe™ reverse transcriptase and 4.2 μ l nuclease-free water. RNA samples were normalised to the lowest RNA concentration and the appropriate volume of nuclease-free water was added to make a final volume of 10 μ l before 10 μ l of the master mix was added. A negative Reverse Transcriptase (-RT) reaction was also set up for use as a negative control. This reaction contained 2 μ l RT random primers, 2 μ l RT buffer and 5.2 μ l nuclease-free water. Reactions were mixed by flicking the tube and centrifuged briefly at 13,000 rpm prior to incubation at 25 °C for 10 minutes followed by 37 °C for 120 minutes and finally 85 °C for 5 minutes.

2.12 Polymerase Chain Reaction (PCR)

2.12.1 Quantitative Polymerase Chain Reaction (q-PCR)

Changes in gene expression were analysed during the treatments using the Taqman-based method (Applied Biosystems). Each reaction consists of: 2 μ l cDNA, 0.5 μ l TRIS-EDTA buffer, 0.5 μ l Taqman probe (Table 2.9), 10 μ l of 10X Taqman master mix and 7 μ l nuclease-free water. The master mix for each probe, excluding cDNA, was prepared and 18 μ l was dispensed into the appropriate wells of a 96 well PCR plate prior to adding 2 μ l cDNA. Each of the samples was run in technical triplicates using the Lightcycler480 real-time PCR machine (Roche Diagnostics Ltd).

Species	Gene of Interest	Probe ID.
Rat	Rplp0	Rn03302271_gH
	Ins1	Rn02121433_g1
	Ins2	Rn01774648_g1
	Pdx1	Rn00755591_m1
	Nkx6.1	Rn0145007_m1
	Gcg	Rn00562293_m1
	Tle3	Rn00584575_m1
	Pax4	Rn00582529_m1
	Pax6	Rn00689608_m1
	Arx	Rn01419077_m1
Mouse	GAPDH	Mm99999915_g1
	Ins1	Mm01950294_s1
	Ins2	Mm00731595_gH
	Pdx1	Mm00435565_m1
	Nkx6.1	Mm00454961_m1
	Gcg	Mm01269055_m1
	Tle3	Mm00437097_m1
	Arx	Mm00545903_m1
	MafB	Mm00627481_s1
	Sst	Mm00436671_m1
Ppy	Mm01250509_g1	
Human	Rplp0	Hs99999902_m1

Ins	Hs02741908_m1
Pdx1	Hs00236830_m1
Nkx6.1	Hs00232355_m1
Gcg	Hs0131536_m1
TLE1	Hs00270768_m1
Arx	Hs00292465_m1
MafB	Hs00534343_s1
Sst	Hs00356144_m1
Ppy	Hs00358111_g1

Table 2.9 List of Taqman probes used for analysis of mRNA levels in qPCR experiments

2.12.2 Data Analysis of q-PCR

The comparative Ct ($\Delta\Delta Ct$) method was employed for quantification of real-time PCR data. This entails comparing the Ct values of the samples of interest with non-treated samples. The reference gene used to compare the Ct values of both the controls and the samples was RPLP0. This method relies on the housekeeping gene and gene of interest having similar efficiencies.

2.13 Glucose Stimulated Insulin Secretion (GSIS)

2.13.1 GSIS of cell lines

Function of treated and non-treated adherent INS1E cells was assessed using glucose stimulated insulin secretion. All samples were run in triplicate. The cells were washed with PBS prior to being starved for 1 hour in Krebs-hepes buffer pH7.4 (119 mM NaCl, 4.74 mM KCl, 2.54 mM CaCl₂, 1.19 mM MgCl₂, 1.19 mM KH₂PO₄, 25 mM NaHCO₃, 10 mM HEPES, 0.5% BSA) at 37 °C. Cells were then treated with 200 µl of either Krebs-HEPES with 2 mM glucose or Krebs-HEPES with 25 mM glucose for 1.5 hours at 37 °C and supernatant was collected and subjected to centrifugation at 13,000 rpm for 2 minutes to pellet any cells. These were stored at -20 °C until required. The pellets were re-suspended in 100 µl protein extraction buffer and stored at -20°C.

2.13.2 GSIS of rodent and human islets

The recommended concentrations of glucose solutions used for GSIS are 2.8 mM and 16.7 mM for rodent islets and 1 mM and 16.7 mM for human islets. These solutions were made up as shown in Table 2.10.

Glucose concentration	Volume (μ l) 1M glucose added to 50 ml Krebs-HEPES
1 mM	50
2.8 mM	140
16.7 mM	835

Table 2.10 Volume of glucose needed to make up basal and stimulatory solutions for GSIS

The function of isolated rodent and human islets was assessed by GSIS. 100 rodent islets or 500 human IEQ were used per well for functional studies following Tle3 and TLE1 knockdown respectively (see section 2.7.3 for method). Islets were first washed with 1 ml Krebs-HEPES buffer without glucose before pre-incubating for 2 hours at 37 °C, in appropriate low glucose Krebs-HEPES buffer (Table 2.10). Buffer was replaced halfway through this pre-incubation to allow cells to get to a basal level of insulin secretion. Following the pre-incubation, the buffer was removed and 500 μ l low glucose Krebs-HEPES was added to each well. Islets were incubated for 1 hour at 37 °C with lids opened to allow CO₂ to reach cells. Tubes were then inverted and spun down at 179 rcf to pellet islet. Supernatant was collected and replaced with 500 μ l high glucose Krebs-HEPES buffer (Table 2.10). Islets were incubated for another hour at 37°C with lids opened. Following the incubation, islets were spun down and supernatant collected and stored at -20 °C until needed. To harvest content, 500 μ l islet extraction buffer (150 ml 95% ethanol, 47 ml Acetic acid, 3 ml concentrated HCl) was then added to each tube of islets and stored at -20 °C until required.

2.14 Enzyme-linked Immunosorbent Assay (ELISA)

Mercodia ELISA kits were supplied by Diagenics Ltd (Bletchley, UK). ELISAs were carried out using the supernatant collected from GSIS experiments to quantify the amount of insulin secreted in response to treatment with different glucose concentrations. A dilution ELISA was carried out initially to determine what dilution factor would be used to assess each sample. Concentrations tested were undiluted, 1:5 and 1:10. The appropriate dilution was

chosen and the full ELISA was carried out according to the manufacturer's instructions (Mercodia High Range Rat Insulin ELISA). All samples were diluted using Krebs-HEPES buffer.

Insulin content ELISAs were run by harvesting samples in 100 μ l water, sonicating for 15 seconds and adding 300 μ l acid ethanol (0.18 M HCl in 96% ethanol) for INS1E cell line or harvesting in islet extraction buffer for rodent and human islets. Samples were then kept in the fridge overnight, vortexed and stored at -80 °C. Glucagon content samples were harvested in protein extraction buffer in the same method as GSIS pellets. Glucagon ELISAs were carried out using Mercodia Glucagon ELISA 10 μ l kit.

2.15 Bradford Assay

Bradford assays were run for each GSIS sample to quantify the amount of protein, the results of which were used to normalise the corresponding ELISA data. Cell pellets in protein extraction buffer were sonicated for 15 seconds each prior to being subjected to centrifugation at 13,000 rpm for 5 minutes to pellet cell debris. A standard curve was set up using BSA at known concentrations and 10 μ l of each sample was loaded into appropriate wells of a 96 well plate. 200 μ l of Coomassie Protein Assay Reagent (Thermo Scientific) was added to each well and the plate was read immediately at 595nm using Softmax Pro5.3 software on Molecular devices SpectraMAX190 plate reader. Any samples outlying the standard curve were diluted in protein extraction buffer and a further reading was taken.

2.16 Gel Electrophoresis and Western Blotting

2.16.1 Gel Electrophoresis

Cells were lysed in Protein Extraction Buffer. Samples were run by SDS-PAGE (sodium dodecyl sulfate–polyacrylamide gel electrophoresis) 10% running gels and 4% loading gels (Table 2.11). Gels were run for ~1 hour at 40 mA per gel and 250 V. Samples were loaded at a concentration of 40 μ g protein per lane. Composition of buffers used for GEP and Western blotting are listed in Table 2.12.

	10% gel	4% gel
dH ₂ O	11.8 ml	9.4 ml
Acrylamide (40%)	6.4 ml	1.5 ml
Buffer B	6.3 ml	-
Buffer D	-	3.8 ml
10% SDS	250 µl	150 µl
10% APS	250 µl	150 µl
TEMED	12.5 µl	7.5 µl

Table 2.11 Reagents and volumes needed to make up SDS-PAGE gels

2.16.2 Western Blotting

Following running the samples on the gel. The protein was transferred onto a nitrocellulose membrane by putting in 1x transfer buffer (100 ml 10xCAPS, 100 ml methanol and 800 ml dH₂O) and running for 2 hours at 200 V, 250 mA. Once the transfer was complete, nitrocellulose was blocked in 5% Marvel in TBS and then the membrane was incubated overnight at 4 °C in primary antibody (Table 2.7). Membranes were washed 3x 5 minutes in 1x TBS-T and incubated for 2 hours in secondary antibody (Table 2.8).

The membrane was probed with Thermo Scientific SuperSignal West Pico Chemiluminescent substrate for 5mins before development. Blots were stripped with Thermo Scientific Restore PLUS Western blot stripping buffer before re-probing with a second antibody.

Buffer	Composition	Use
Buffer B (1.5M Tris)	27.2g Tris in 150 mL H ₂ O	Acrylamide gels
Buffer D (0.5M Tris)	6.05g Tris in 100 mL H ₂ O	Acrylamide gels
Running Buffer	29.8g Tris, 144g Glycine, 10g SDS in 1L H ₂ O	Gel electrophoresis
CAPS (10X)	22.13g CAPS in 1L H ₂ O	Western Blot
Transfer Buffer	100 mL CAPS (10X), 100 mL methanol in 800 mL H ₂ O	Western Blot
TBS (10X) (1.5M NaCl, 100 Mm Tris)	87.6g NaCl, 12.1g Tris in 1L H ₂ O	Western Blot
TBS-Tween	100 mL TBS (10X), 1 mL Tween in 1L H ₂ O	Western Blot

Table 2.12 Buffers used for Gel Electrophoresis and Western Blotting

2.16.3 Analysis of western blotting

Western blots were analysed using Fiji software to calculate the area under the curve for each band. An average was taken over 3 experimental repeats and normalised to the loading control to see whether protein levels were changed in the different conditions. Significant changes were worked out using an un-paired student's t-test.

2.17 Statistics

All statistics were analysed using either paired or un-paired students t-test where appropriate. Coefficient of Determination and Pearson's Correlation Coefficient were worked out for analysis of scatter plots. Statistics were performed using Microsoft Excel.

3 Results (1)

Characterising phenotypic and functional changes in
pancreatic beta cells following chronic exposure to high
glucose

3.1 Introduction

For many years, it has been established that type 2 diabetes is a disease of insulin resistance and a gradual decline in functional beta cell mass as the disease progresses. Evidence of this has been shown in pancreatic autopsy tissue, from both obese and lean cases of type 2 diabetes, that show a deficit of up to 63% and 41% (obese and lean type 2 diabetes respectively) in relative beta cell volume compared to their non-diabetic controls. These studies proposed that this deficit was due to increased apoptosis (76). Other studies looking at beta cell deficit in type 2 diabetes show that relative beta cell mass of patients with clinical type 2 diabetes for <5 years and >15 years show a 24% and 54% reduction respectively when compared to their respective controls (78). This study found however, that the beta cell deficit alone was not sufficient to cause diabetes without considering a role for beta cell dysfunction (78). Although the gradual decline in beta cell mass is widely accepted, and provides an explanation as to why some patients with type 2 diabetes eventually rely on treatment by exogenous insulin injections, there is mounting evidence to suggest that in the early years of the disease, beta cell dysfunction may have a bigger role to play than apoptosis in the dysregulation of blood glucose levels.

The evidence of reversal of type 2 diabetes following bariatric surgery or a restricted calorie diet suggest that, at least in the earlier stages of the disease, the beta cells do not undergo apoptosis but instead stop secreting insulin in response to glucose intake. The aforementioned studies showed that following 1 week post-bariatric surgery, clinical diabetes was reversed with insulin sensitivity increased and total insulin output reduced (94). Similarly, following one week on a restricted calorie diet, fasting plasma glucose was reduced from 9.2 ± 0.4 to 5.9 ± 0.4 mmol/l and the maximal insulin response recovered to near control values (0.62 ± 0.15 nmol min⁻¹ m⁻²), rising from 0.19 ± 0.02 to 0.46 ± 0.07 nmol min⁻¹ m⁻² (55). The rapid reversal of symptoms suggest that regeneration is not responsible for the regain of blood glucose control but instead, it is likely caused by recovery of function. Further studies on the calorie restricted diet showed that return to normal blood glucose control was achieved in 46% of patients who were diagnosed with type 2 diabetes up to 6 years previously (56). This gives strong evidence for the ability of the beta cell to recover following removal of metabolic stress.

There are many potential contributors to beta cell dysfunction in type 2 diabetes. Pancreatic beta cells respond to high glucose levels through increasing flux through the glycolytic and TCA cycle, which increases the ATP:ADP ratio and encourages closure of the ATP-sensitive K⁺ channels and subsequent secretion of insulin (95). In times of hyperglycaemia, when increased flux through the glycolytic and TCA pathways is heightened in pancreatic beta cells, this can also lead to an increase in production of Reactive Oxygen Species (ROS) through increased mitochondrial activity (95). Increased ROS levels have been shown to impair the stimulated secretion of insulin from pancreatic beta cells treated with H₂O₂. This study demonstrated a reduction in the ATP:ADP ratio in treated cells, resulting in hyperpolarisation of the cell membrane and loss of stimulated insulin secretion (96). Excess levels of oxidised-Low Density Lipoproteins (LDLs) have also been shown to cause oxidative stress and can result in reduced insulin content and cell death (97).

Some evidence suggests that the resistance to, or impaired secretion of incretin hormones (such as GLP-1) during diabetes may also contribute to beta cell dysfunction, as these hormones play roles in glucose stimulated insulin secretion, upregulation of beta cell specific genes and prevention of apoptosis (98).

Alongside dysregulation of beta cell functional pathways, many studies have suggested pancreatic beta cells are susceptible to changes in phenotype following metabolic insult, resulting in a dysfunctional cell. Mounting evidence suggests that in times of high metabolic stress the beta cells revert to a more progenitor-like state as a way of avoiding the increased functional demand for insulin secretion, which stresses the cell and is thought to contribute to entry into the apoptosis pathway. This mechanism was first proposed in studies looking at FoxO1 deficiency. FoxO1 has been shown to play a role in cell differentiation and stress response (82). Ablation of the FoxO1 gene in the beta cell caused reduced beta cell mass through 'dedifferentiation', that is, a loss of mature beta cell markers and gain of progenitor markers (82). Several studies also provide evidence that some cells are 'transdifferentiated' to the alpha cell lineage, showing evidence of co-localisation of insulin or other beta cell markers with glucagon (82, 99, 100). This mechanism is potentially another way of avoiding the stress of constant insulin production, as other endocrine cell types do not have to respond to glucose in the same way as the beta cell.

Alternatively, transdifferentiation could be a result of downregulation of beta cell transcription factors, such as Pdx1, which results in de-repression of alpha cell genes such as

glucagon. The hypothesis of beta cell plasticity provides a possible explanation for the dysregulation of the blood glucose levels in type 2 diabetes and can also account for the rapid reversal of symptoms by suggesting that beta cell dysfunction plays a bigger role in the first stages of the disease than cell death. Alongside this, studies have shown that other examples of metabolic stress, such as lipotoxicity, also impairs the beta cell secretory ability and sensitivity to insulin, resulting in impaired beta cell function (101). This suggests that beta cell plasticity may be a common default pathway to deal with numerous metabolic stresses.

3.2 Aims

The hypothesis that different metabolic stresses seen in type 2 diabetes, such as lipotoxicity and glucotoxicity, can cause beta cell dysfunction is an interesting one. The following studies aimed to further investigate the effects of glucotoxic stress on pancreatic beta cell phenotype and function.

The specific aims of these studies were:

1. To develop an *in vitro* model of glucotoxicity using the rodent pancreatic INS1E cell line
2. To determine changes in beta cell phenotype and function following exposure to high glucose
3. To determine the role of beta cell specific transcription factors in maintenance of beta cell identity/function

3.3 Results

3.3.1 Generation of an in vitro model of glucotoxicity in the rodent pancreatic INS1E cell line

Type 2 diabetes is considered a metabolic disorder resulting in elevated glucose levels and progressive dysfunction of the pancreatic beta cell. In light of the recent evidence demonstrating loss of beta cell specific markers causing transition to an alpha cell phenotype through de-repression of glucagon gene expression (63, 102), studies were set up to investigate whether these changes can occur as a direct result of sustained high glucose levels. To investigate the impact of high glucose on pancreatic beta cells, the rodent INS1E cell line was incubated for 48 hours in either normal medium (11 mM glucose), or a high glucose medium containing 25 mM glucose. Cells could then be assessed for changes in phenotype and function, reflecting the changes that may occur in pancreatic beta cells under hyperglycaemic conditions. Figure 3.1 shows cells cultured in normal (A) or high (B) glucose medium. No changes in morphology of the cells were observed after 48 hours of culture.

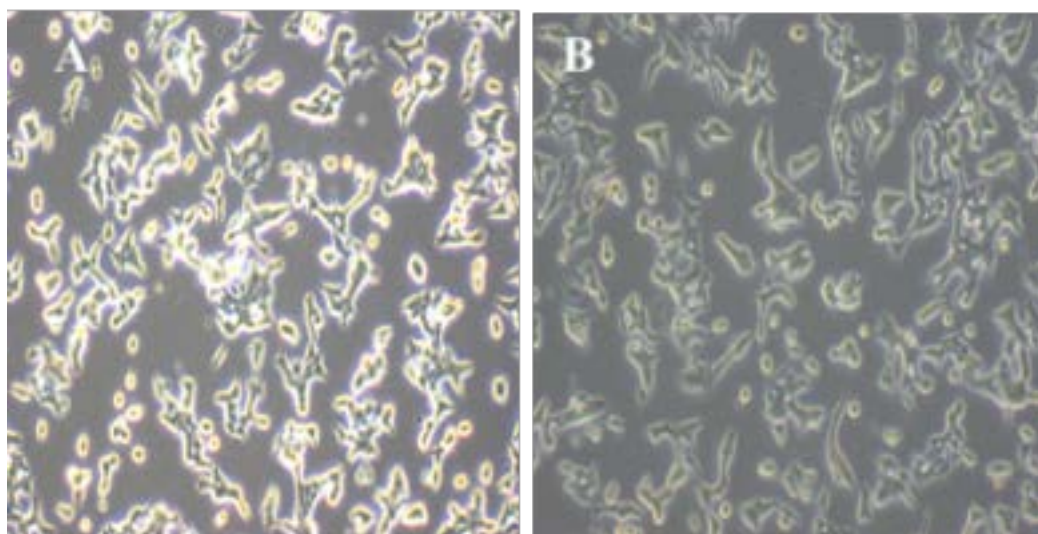


Figure 3.1 Morphology of the INS1E cells following normal or high glucose culture.

Following culture in either normal (A) or high (B) glucose medium for 48 hours no difference in morphology was observed. Images were taken at 10x magnification.

To ensure any changes seen in the function of the cells was not due to glucose-induced cell death, viability studies were carried out on cells cultured in both glucose conditions (Figure 3.2). Cells were stained with propidium iodide (PI), a dye which cannot permeate the membrane of live cells and thus identifies necrotic and apoptotic cells (93). No significant differences in cell viability were observed across the two culture conditions and cells showed a ~90% viability in both culture conditions.

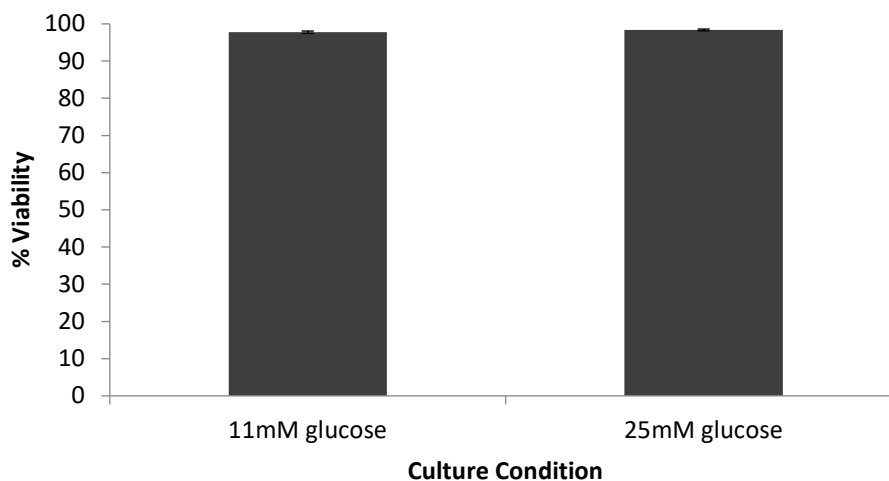


Figure 3.2 Cell viability assay

Cells from 11 or 25 mM glucose culture were stained with PI to mark dying cells. Cells were counterstained with DAPI nuclear stain and cell viability was worked out as a percentage of total cells. Data represent average value \pm SEM. n=3 biological repeats. For each study 4 images were taken for 3 wells of each condition and all cells were analysed using Image J software. P=0.185 using unpaired students t-test.

To substantiate these findings and confirm there was no ongoing apoptosis, cells were also stained with an antibody for cleaved caspase-3, a marker of apoptosis. Caspase counts were then carried out to see whether there was an increase in apoptosis following high glucose culture (Figure 3.3). No significant increase in apoptosis was observed between the two glucose cultures. Although levels of apoptosis were higher than the cell death in the viability assay, PI staining may only pick up late stage apoptosis as during the first stages of apoptosis the cell membranes remain uncompromised, preventing penetration of PI into the cell (93). Western blot analysis for total and cleaved caspase-3 was also carried out to confirm these observations using protein samples from the 11 and 25 mM cultures, alongside a positive control (6 hour Staurosporine treatment). Total caspase-3 is an inactive form of the

apoptotic protein. When cells undergo apoptosis, caspase-3 is cleaved to its active form (103). Figure 3.4 shows cleaved caspase 3 in the positive control but no cleaved caspase could be detected in the two culture conditions. Together these data suggest that culturing the INS1E cell line in high glucose for 48 hours does not significantly increase cell death.

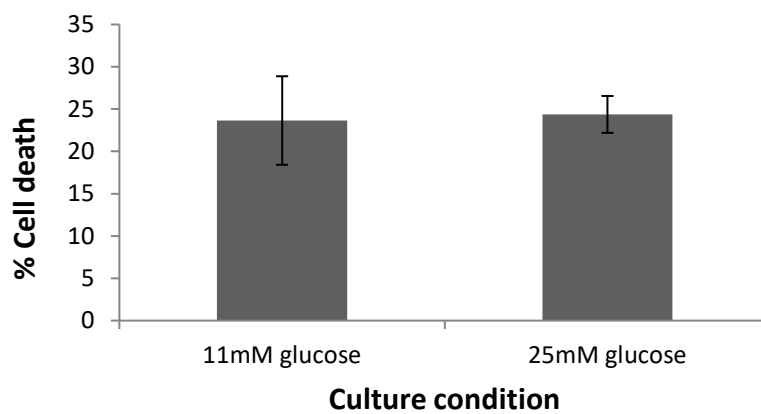
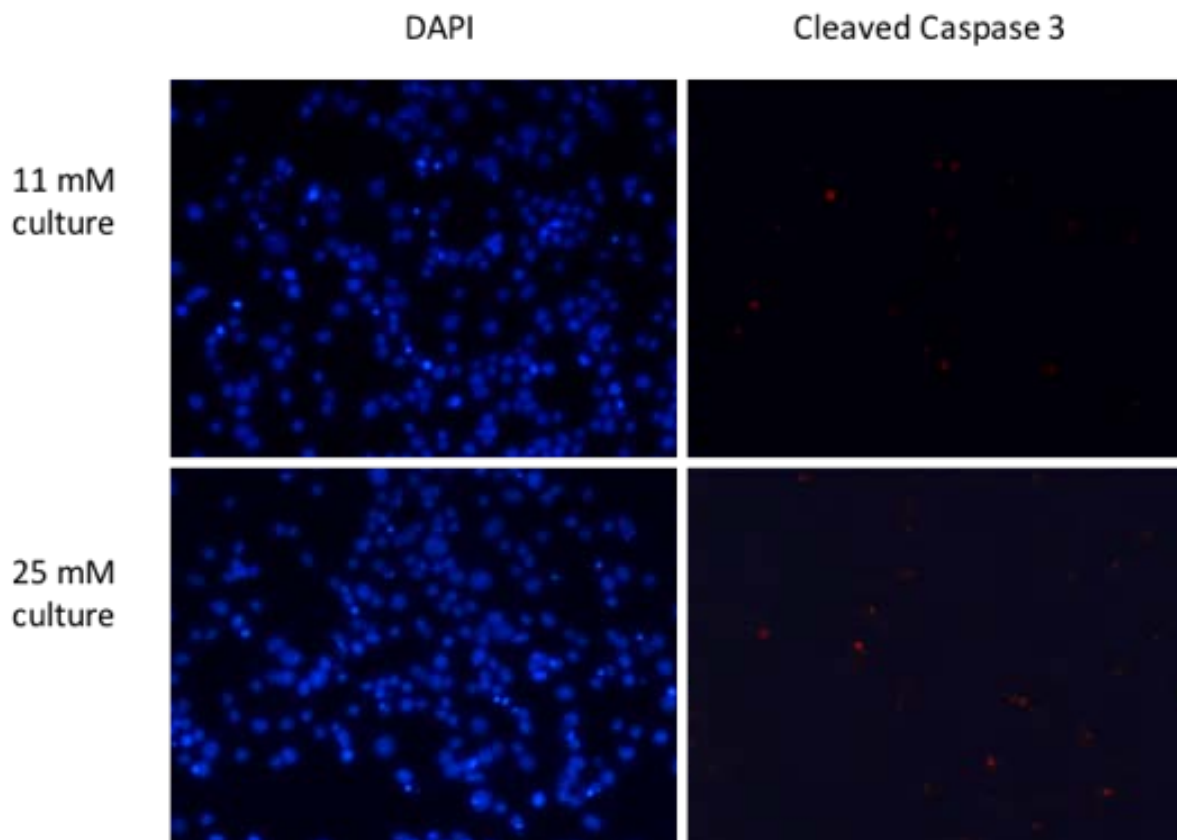


Figure 3.3 Caspase counts were carried out on cells incubated in either 11 or 25 mM glucose medium.

Images were taken at 10x magnification. DAPI was used as a nuclear stain to mark all cells. Cleaved caspase 3 antibody was used to mark cells undergoing apoptosis. Cell death counts were compared between the two culture conditions. 3 images were taken per well for each individual experiment. Data represent mean \pm SEM. n=3 from 3 biological repeats.

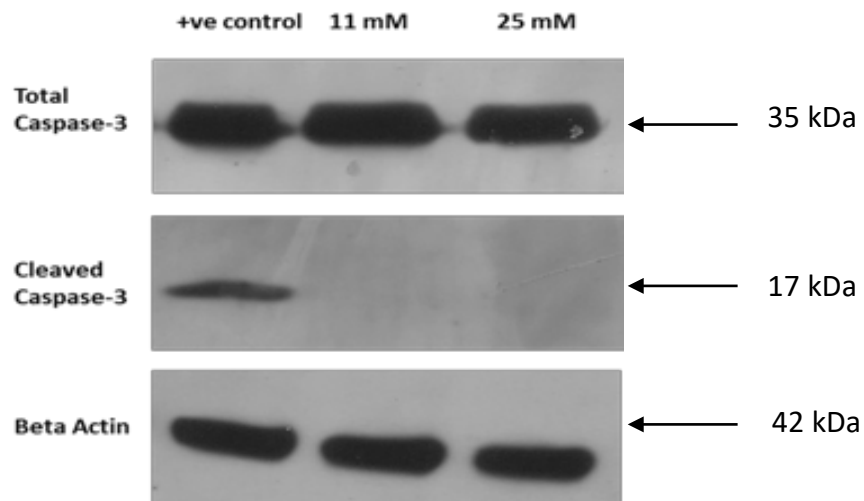


Figure 3.4 Western blotting analysis for cells in normal and high glucose culture.

Western blots were carried out for total and cleaved caspase-3 in both culture conditions. Wells were loaded with 40 μg protein. A 6-hour treatment with staurosporine was used as a positive control to activate caspase 3. Beta actin was used as a loading control. Image shown is representative of 3 biological repeats.

3.3.2 Impact of glucotoxicity on beta cell function

Testing of HbA1c (a test to measure the glycosylation of red blood cells) in patients with diabetes has been shown to correlate with diabetic complications and increased fasting glucose levels alongside insulin resistance, sensitivity and beta cell function (104, 105). To investigate whether glucotoxicity has a direct impact on beta cell function, and may therefore influence beta cell dysfunction in patients with diabetes, glucose stimulated insulin secretion assays (GSIS) were performed to measure basal and stimulated insulin secretion in response to different glucose challenges (Figure 3.5). Cells were first cultured for 48 hours in the respective glucose conditions before GSIS was carried out using low (2 mM) or high (25 mM) glucose stimulation. Insulin secretion was measured using insulin ELISA kits and function of the cells from both culture conditions were compared. Following high glucose culture, INS1E cells showed a marked decrease in stimulated insulin secretion (Figure 3.5) decreasing from 5348 ± 1791 ng insulin per μg protein in 11 mM glucose culture to $1562 \pm$ ng insulin per μg protein in 25 mM glucose culture. The basal insulin secretion was slightly, though not significantly, reduced. The stimulation index of the cells (worked out by the fold change in insulin secretion between high and low glucose stimulations) was decreased from 5.08-fold to 2.40-fold when cells were exposed to glucotoxic conditions (Figure 3.6). These

data provide evidence for glucotoxic conditions having a negative effect on beta cell function.

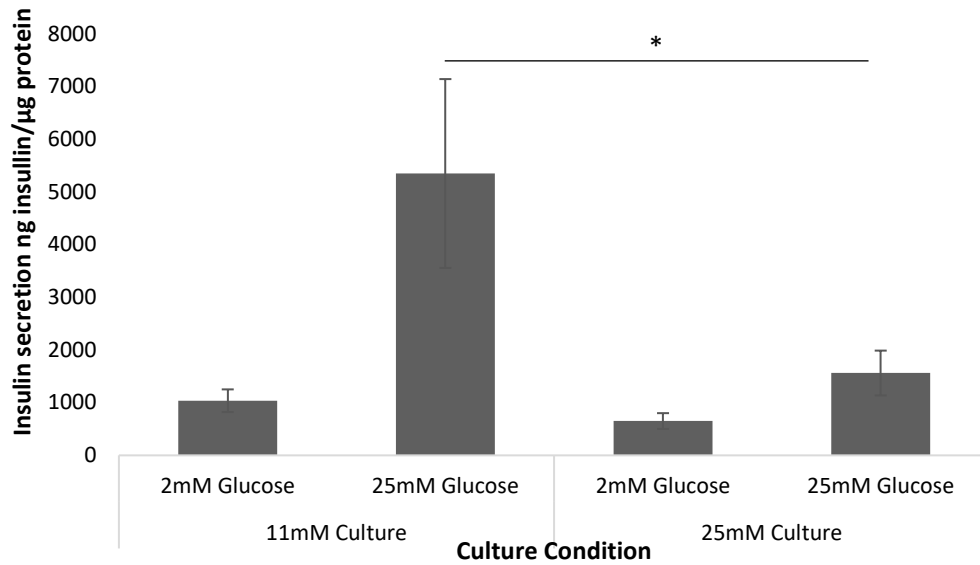


Figure 3.5 Glucose stimulated insulin secretion (GSIS).

Cells from both culture conditions were stimulated with a low glucose solution (2 mM) and high glucose solution (25 mM) and quantity of insulin secreted was measured using insulin ELISAs. Insulin values normalised to total protein. n=6 from 6 biological repeats *p<0.05 relative to normal glucose culture

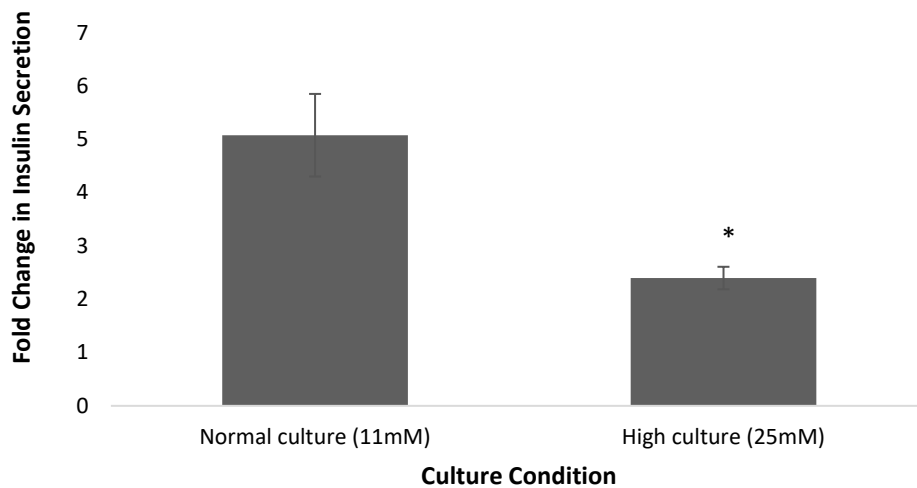


Figure 3.6 Stimulation Index for GSIS.

Stimulation index was calculated by calculating the fold change in insulin secretion from the high glucose treatment and the low glucose treatment (25 mM/2 mM). n=6 from 6 biological repeats *p<0.01 vs 11 mM glucose.

3.3.3 Effect of glucotoxicity on beta cell phenotype

As there was no evidence of increased apoptosis following culture in high glucose, and there was still a loss of beta cell function, qPCR was used to assess changes in gene expression to see whether expression of key beta cell genes were affected by prolonged high glucose exposure. Figure 3.7 shows decreased expression of the insulin 1 and 2 (*Ins1*, *Ins2*) genes in the INS1E cells, alongside a >2-fold increase in glucagon (*Gcg*) mRNA expression following high glucose culture for 48 hours (compared to cells cultured in normal glucose).

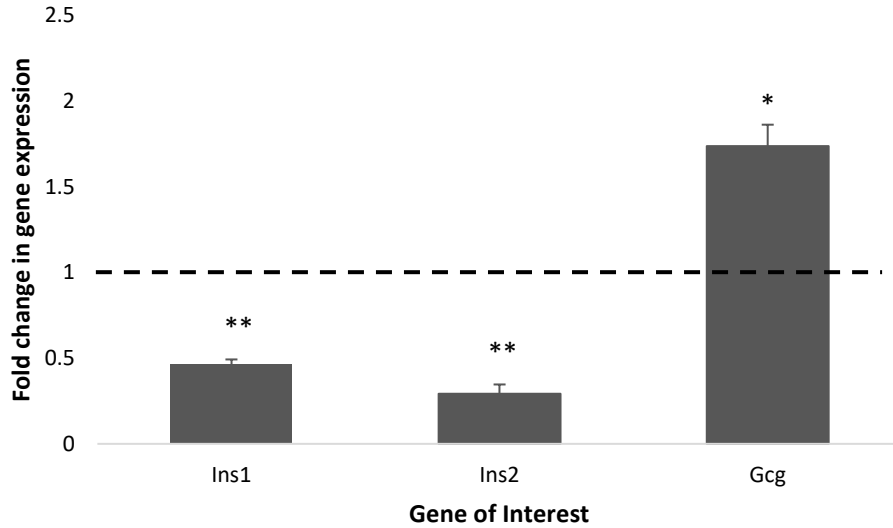


Figure 3.7 qPCR analysis of insulin and glucagon mRNA levels following culture in high glucose.

Levels of insulin 1, insulin 2 and glucagon were measured following culture in 25 mM glucose and normalised to cells from 11 mM glucose culture, as indicated by the dashed line. Data are representative of n=3 from 3 biological repeats. *p<0.05 and **p<0.01 vs normal glucose culture.

To then assess whether the changes in gene expression observed were translated to a protein level, insulin and glucagon ELISAs were used to look at protein content of the cells cultured in the two conditions (Figure 3.8 and Figure 3.9).

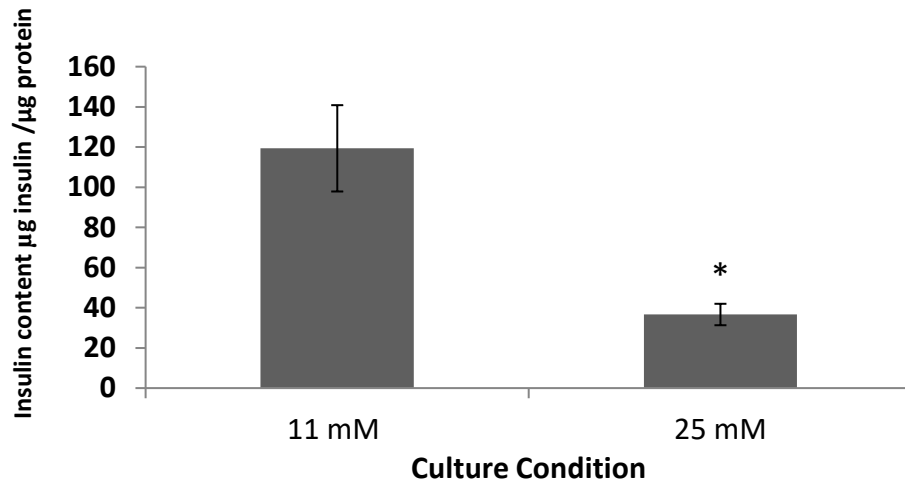


Figure 3.8 Insulin content ELISA from cells cultured in normal (11 mM) or high (25 mM) glucose.

Insulin content of cells was measured using ELISA kits. Data are normalised to total protein content and representative of n=3 from 3 biological repeats *p<0.01 vs 11mM glucose.

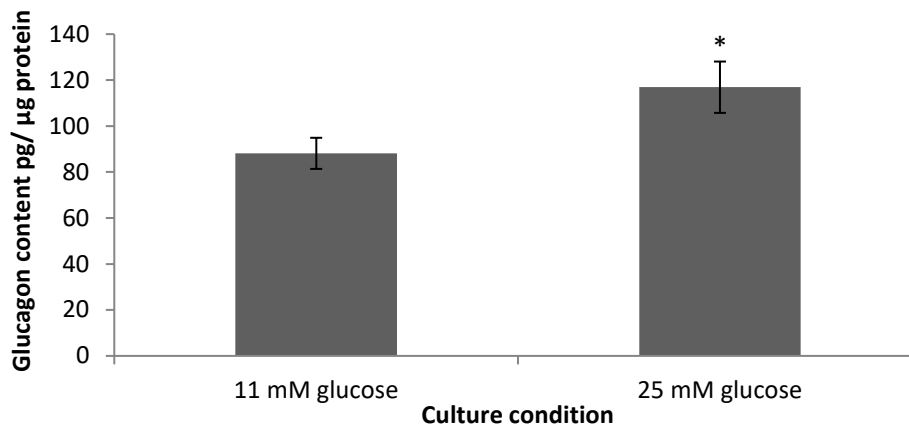


Figure 3.9 Glucagon content ELISA from cells cultured in normal (11 mM) or high (25 mM) glucose.

Glucagon content of cells was measured using ELISA kits. Data is normalised to total protein content and representative of n=3 from 3 biological repeats. *p<0.05 vs 11 mM glucose.

Figure 3.8 shows a 70% decrease in insulin content from 119 ± 21.5 to $36.6 \pm \mu\text{g insulin}/\mu\text{g protein}$ when INS1E cells cultured in 11 mM versus 25 mM glucose for 48 hours. This was coupled to a 1.3-fold increase in glucagon content from 88.1 ± 6.76 in cells cultured in high glucose medium to 116.9 ± 11.2 pg glucagon/ $\mu\text{g protein}$ in cells cultured in normal glucose medium (Figure 3.9). Increased glucagon content was also confirmed with western blotting and immunofluorescence staining (IF) by glucagon counts (Figure 3.10 and Figure 3.11) respectively. Glucagon could not be detected by western blotting in cells cultured in normal glucose medium. However, it could be detected in cells cultured in high glucose medium which suggests the upregulation of glucagon protein production. In conjunction with this, glucagon counts were carried out on the INS1E cell in both culture conditions and showed a 1.75-fold increase in glucagon positive cells following culture in high glucose medium. Representative images of cells used to perform glucagon counts are demonstrated in Figure 3.12. These changes support data gathered from mRNA expression analysis and help to demonstrate the shift from a beta to an alpha cell phenotype when cells are exposed to high glucose for prolonged periods of time.

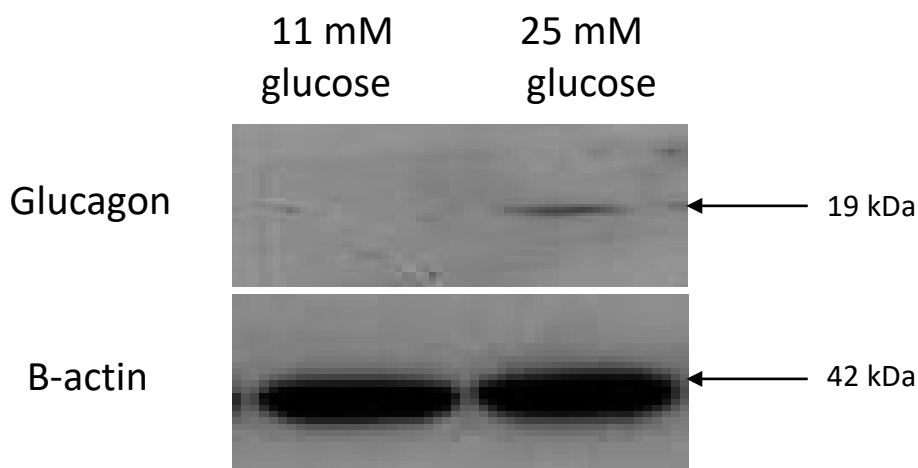


Figure 3.10 Western blot analysis of glucagon expression in cells cultured in normal glucose medium (NG) or high glucose medium (HG).

Wells were loaded with $40\mu\text{g}$ protein. Beta actin was used as a loading control. Image is representative of 3 biological repeats.

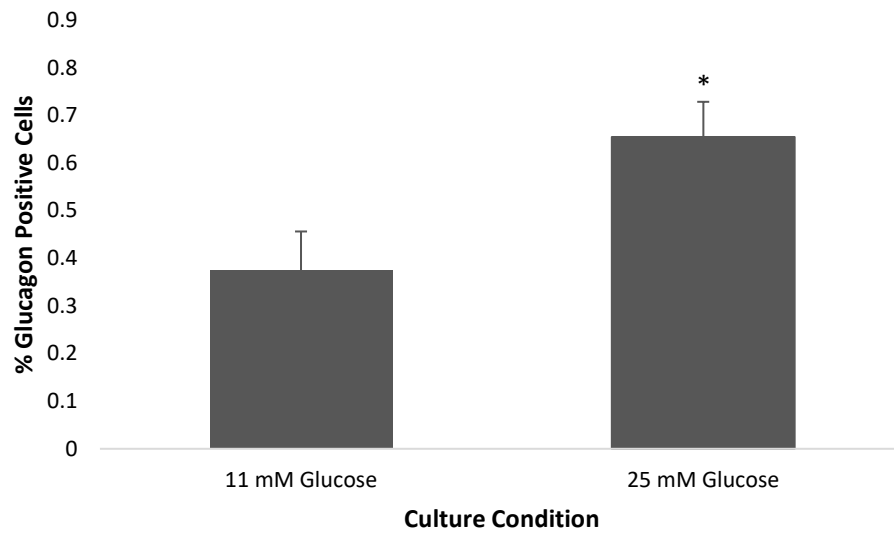


Figure 3.11 Glucagon counts were carried out on INS1E cells cultured in normal (11 mM) or high (25 mM) glucose. Cells were seeded on cover slips in 24 well plates.

Following 48 hours culture, cells were stained for glucagon and counterstained with DAPI. 3 wells were set up for each condition and 3 images were taken per well to perform counts. Data represents n=3 from 3 biological repeats. *p<0.05 vs 11 mM glucose

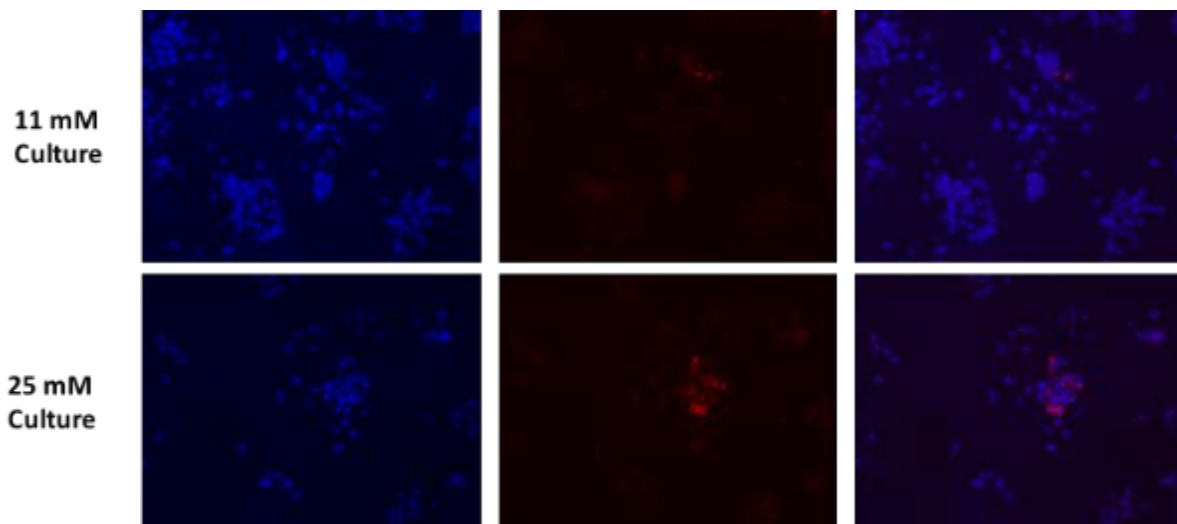


Figure 3.12 ICC analysis of glucagon expression in INS1E cells cultured in 11 mM and 25 mM glucose.

Cells were stained for glucagon (middle column) and number of glucagon positive cells were counted as % of total cell number. DAPI was used to mark out all cells (first column). A composite image is shown in the final column. ImageJ software was used to count cells. These images represent 1 of 3 images taken from 3 technical repeats per experiment (9 images per study). n=3 from 3 biological repeats.

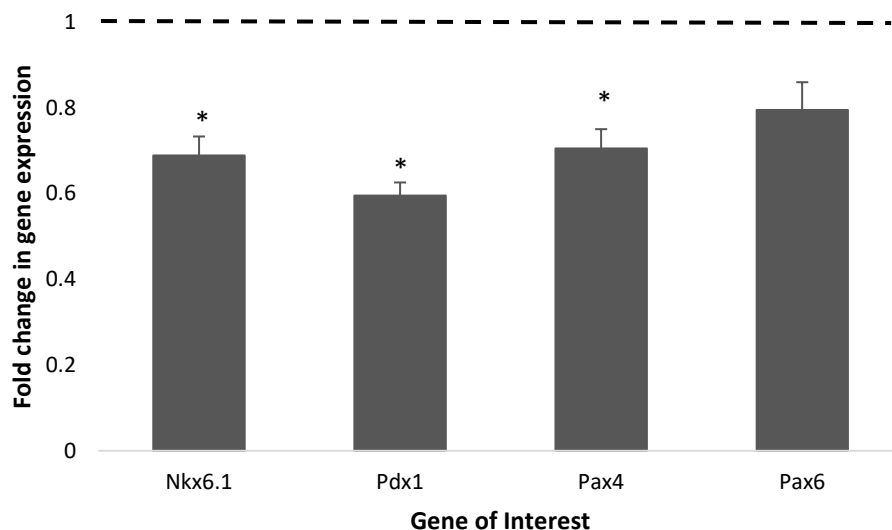


Figure 3.13 qPCR analysis of transcription factor mRNA levels following exposure to 25 mM glucose.

Levels of *Nkx6.1*, *Pdx1*, *Pax4* and *Pax6* were measured following exposure to 25 mM glucose and normalised to levels of cells exposed to 11 mM glucose, as indicated by the dashed line. Data are representative of n=3 from 3 biological repeats, *p<0.01 vs normal glucose.

To further investigate the loss of beta cell phenotype, expression of other key beta cell transcription factors was assessed. *Nkx6.1* and *Pdx1* are well established as important transcription factors in the identity and function of the pancreatic beta cell. For this reason, mRNA expression was carried out to detect and changes in gene expression following exposure to high glucose. Following 25 mM glucose culture, both *Nkx6.1* and *Pdx1* were significantly downregulated at an mRNA level. Alongside this, significant decreases in mRNA expression was observed for *Pax4* and, although it did not reach significance, *Pax6* also showed a trend towards downregulation (Figure 3.13). qPCR was also run for alpha cell transcription factor *Arx* however expression could not be detected in either 11 mM or 25 mM glucose culture. Figure 3.14 and Figure 3.15 show significant reductions in protein expression of *Nkx6.1* and *Pdx1* following high glucose culture compared to cells cultured in 11 mM glucose. Confirming changes in gene expression of these beta cell transcription factors was translated to a protein level.

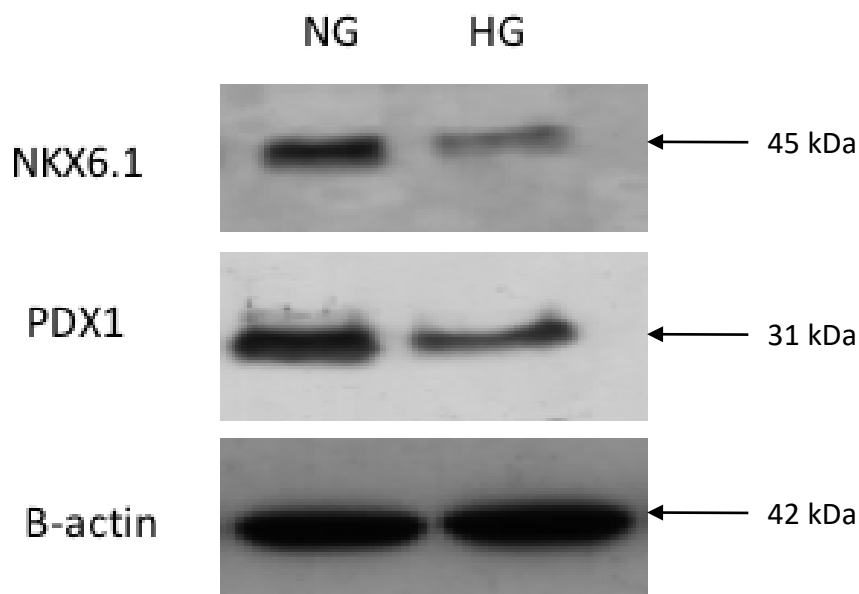


Figure 3.14 Representative Western blot analysis of *Nkx6.1* and *Pdx1* expression in cells cultured in normal glucose medium (NG) or high glucose medium (HG).

Wells were loaded with 40 μ g protein. Beta actin was used as a loading control. n=4 from 4 biological repeats.

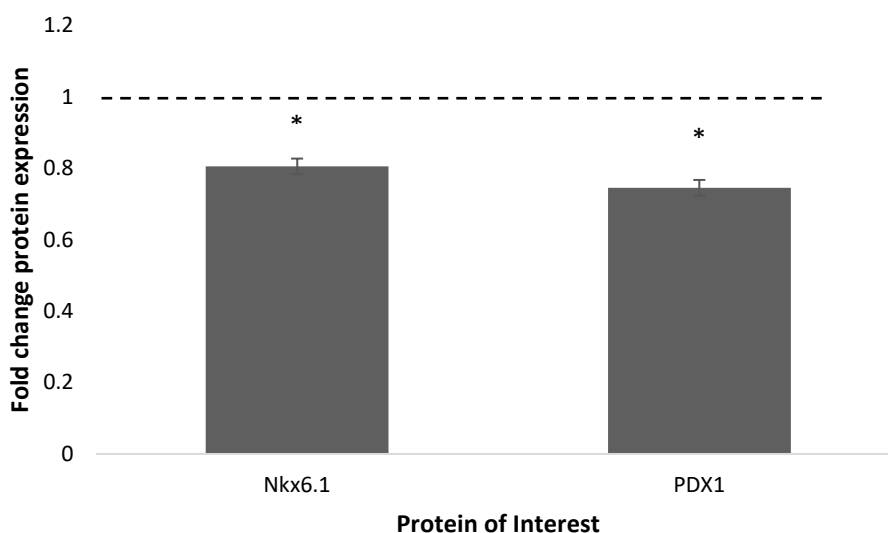


Figure 3.15 Analysis of Nkx6.1 and Pdx1 western blots following high glucose culture.

Protein levels of Nkx6.1 and Pdx1 were measured by western blotting following culture in 11 mM and 25 mM glucose and normalized to beta actin loading control. Fold change in protein expression following 25 mM glucose culture was worked out compared to levels in 11 mM glucose, as indicated by the dashed line. Data are representative of n=4 from 4 biological repeats. *p<0.01 vs normal glucose.

3.3.4 Effect of restoration of Pdx1 on changes observed in high glucose

It is well established that Pdx1 is an important beta cell transcription factor and is required for proper function of the beta cell. There have been studies that have shown that overexpression of Pdx1 in stem cells causes differentiation towards pancreatic lineages and increased *Ins1* gene expression and insulin production (106). Alongside this, studies looking at Pdx1 knockout in mice show that this transcription factor is required for generation of appropriate numbers of the endocrine cell types during embryogenesis, with loss resulting in reduced beta cell number and increases in alpha cell numbers (107). In light of these studies, adenovirus mediated *Pdx1* overexpression was used to see whether recovery of *Pdx1* expression could prevent, or reduce, the glucotoxicity-induced loss of the beta cell phenotype and help to retain adequate function of the cell.

Infection with adenoviral vector to induce ectopic expression of *Pdx1* showed increased intensity of Pdx1 staining in comparison with the cells treated with β -galactosidase control (B-gal) virus (Figure 3.16), suggesting successful overexpression of the *Pdx1* gene and translation to protein. qPCR and western blotting were used to measure Pdx1 expression

following treatment with increasing volumes of virus added per well (Figure 3.17 and Figure 3.18 respectively).

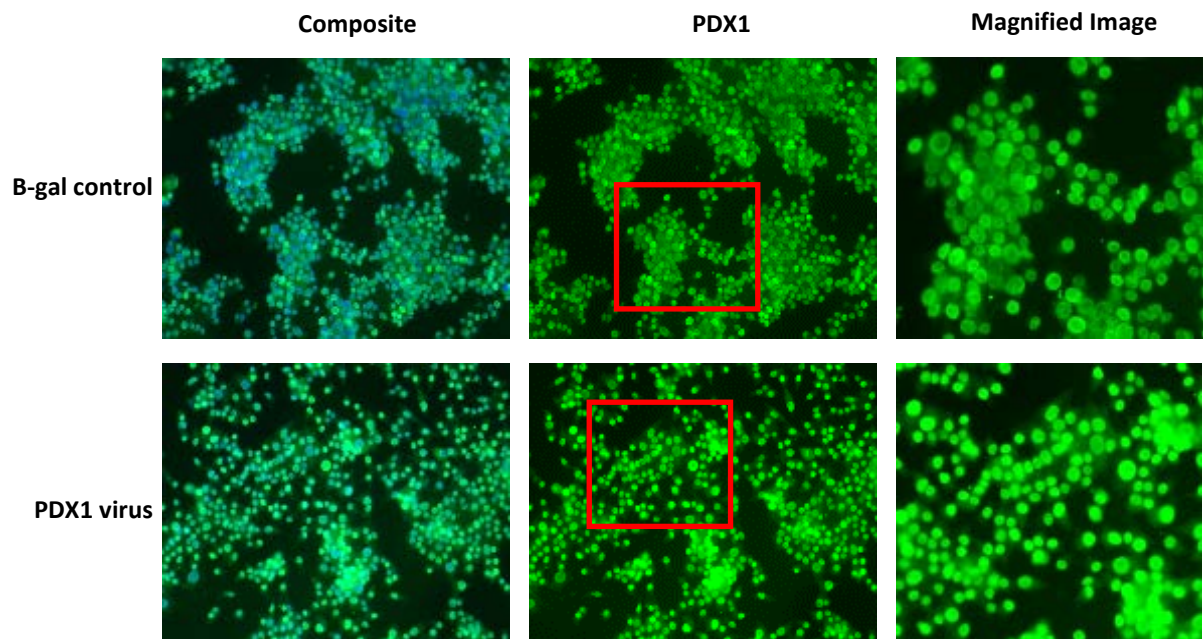


Figure 3.16 ICC of Pdx1 overexpression in INS1E cells. Infection with Pdx1 adenovirus caused increase in Pdx1 expression.

INS1E cells were stained for PDX1 following incubation with either B-gal control virus or PDX1 overexpression virus and counter stained with DAPI nuclear marker. All INS1E cells were positive for Pdx1 in control conditions. Images shown are 20x magnification.

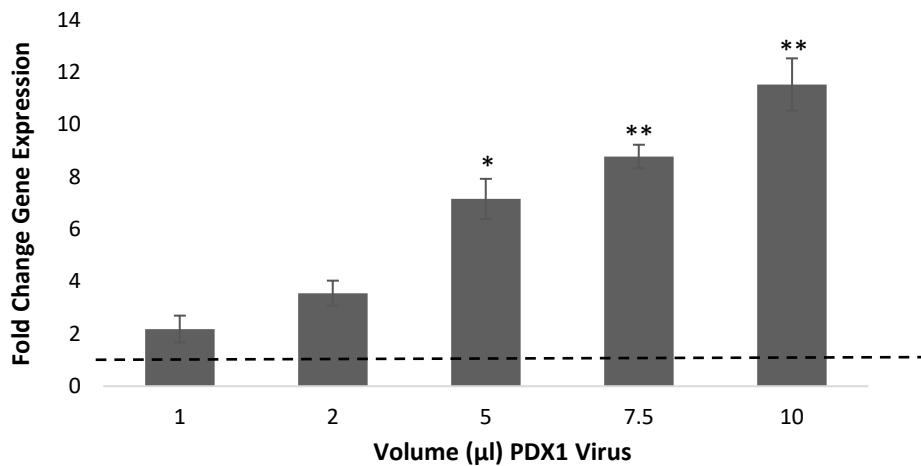


Figure 3.17 qPCR data of Pdx1 expression following 48 hour treatment with increasing volumes of adenovirus.

Levels of Pdx1 were measured following treatment with Pdx1 adenovirus and normalised to negative control (B-gal virus), as indicated by the dashed line. Data are representative of n=3 from 3 biological repeats, *p<0.05, **p<0.01 vs B-gal infected control.

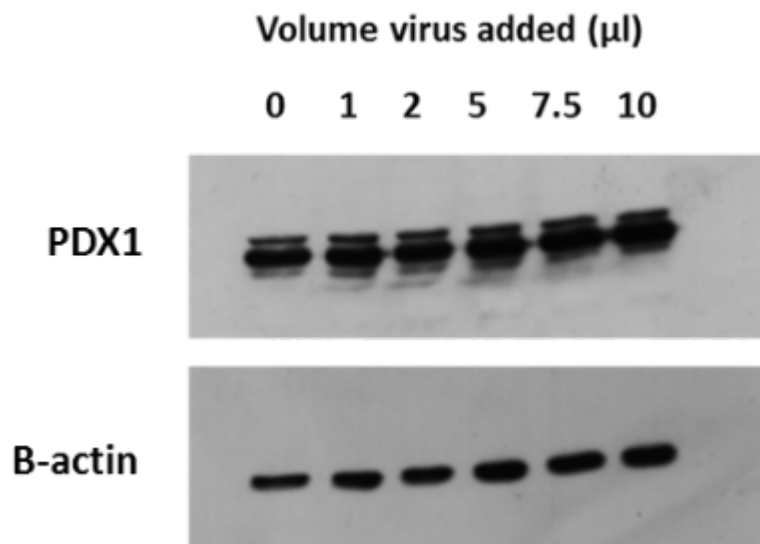


Figure 3.18 Western blot analysis of Pdx1 expression in cells treated with increasing volumes of Pdx1 adenovirus.

Wells were loaded with 40µg protein. Beta actin was used as a loading control. n=3 from 3 biological repeats.

With qPCR and western blotting showing successful overexpression of Pdx1, INS1E cells were then cultured in high glucose culture and infected with the Pdx1 virus or B-gal control virus. These conditions were then compared to normal glucose cultured cells infected with B-gal control virus, to see whether Pdx1 overexpression could prevent the beta cell gene expression changes seen following high glucose culture. qPCR was run to assess the changes in gene expression (Figure 3.19) between the B-gal and Pdx1 treated cells cultured in high glucose medium, relative to the control group (B-gal treated cells cultured in normal glucose medium) resulting in three different culture conditions: 11 mM glucose with B-gal virus, 25 mM glucose with B-gal virus and 25 mM glucose with Pdx1 virus. Firstly, there was successful overexpression of *Pdx1* in the treated group, with gene expression rising to almost 3-fold higher than in the control group. The overexpression of *Pdx1* in the high glucose culture, significantly increased the expression of *Ins2*, however levels were not fully recovered to those of the control group. *Ins1*, on the other hand, showed a slight decrease in mRNA expression however this change was not significant. Alongside the increase in *Ins2* expression, *Nkx6.1* showed recovery to just above normal levels when treated with the *Pdx1* overexpression virus in the high glucose culture, however the increase in levels compared to B-gal treated cells cultured in high glucose was not significant. Furthermore the 2.5-fold increase in glucagon expression that was observed when INS1E cells were cultured in the high glucose medium with the B-gal control virus compared to the control group was prevented upon treatment with the Pdx1 virus. This resulted in *Gcg* mRNA expression at 0.5-fold of that in the INS1E control cells cultured in normal glucose (Figure 3.19). These data suggest that overexpression of Pdx1 can prevent some of the changes seen in high glucose culture and retain, in part, expression of important beta cell genes.

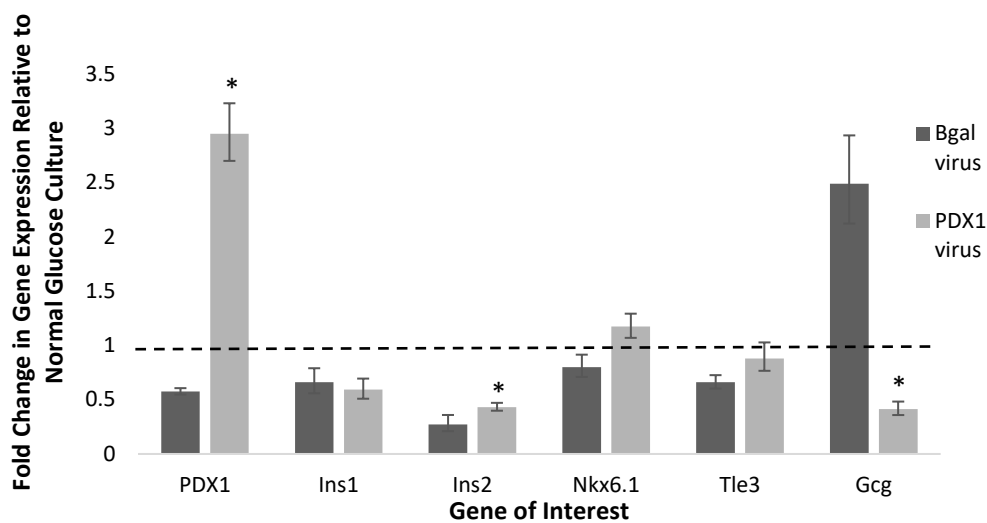


Figure 3.19 qPCR analysis of INS1E genes following high glucose culture and treatment with Pdx1 overexpression virus.

Levels of selected beta cell genes and alpha cell gene, glucagon was measured following 48 hours high glucose culture and treatment with Pdx1 adenovirus. Data are normalised to negative control (B-gal control virus) from cells cultured in normal glucose medium, as indicated by the dashed line. Data are representative of n=3 from 3 biological repeats, *p<0.01 relative to B-gal cells in high glucose medium.

To further analyse the effect of Pdx1 overexpression on the beta cell, insulin and glucagon content were measured following culture for 48 hours in high glucose medium. The overexpression of Pdx1 did not appear to have any effect on the insulin content of the cells (Figure 3.20). Following analysis of glucagon content however, there was a significant decrease with treatment of the Pdx1 virus, showing over a 2-fold decrease in content from 226.8 ± 16.62 to 89.81 ± 4.30 pg / μ g protein in untreated and treated cultures respectively (Figure 3.21).

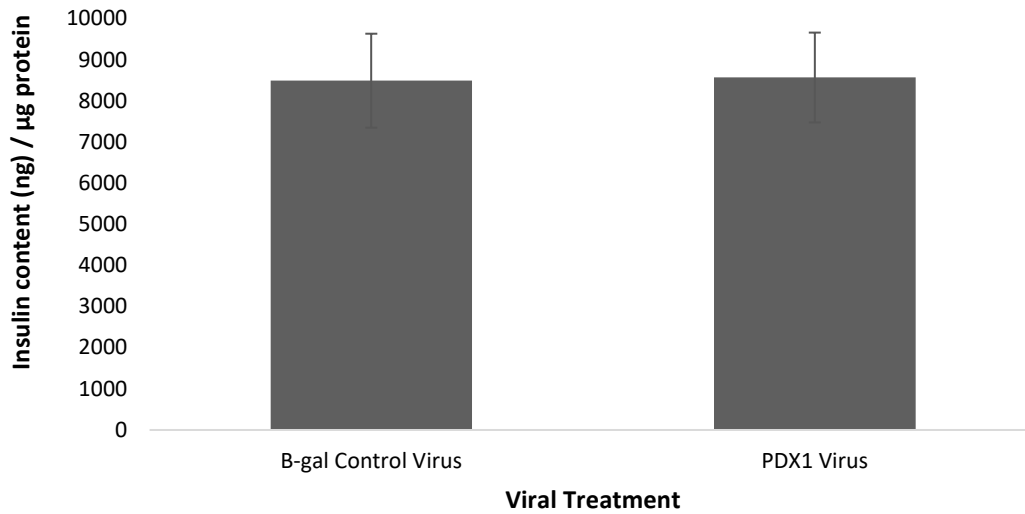


Figure 3.20 Insulin content following 48 hours in high glucose medium and treatment with Pdx1 overexpression virus or B-gal control virus.

Insulin content of cells was measured using ELISA kits. Data is normalised to total protein content and representative of n=3 from 3 biological repeats.

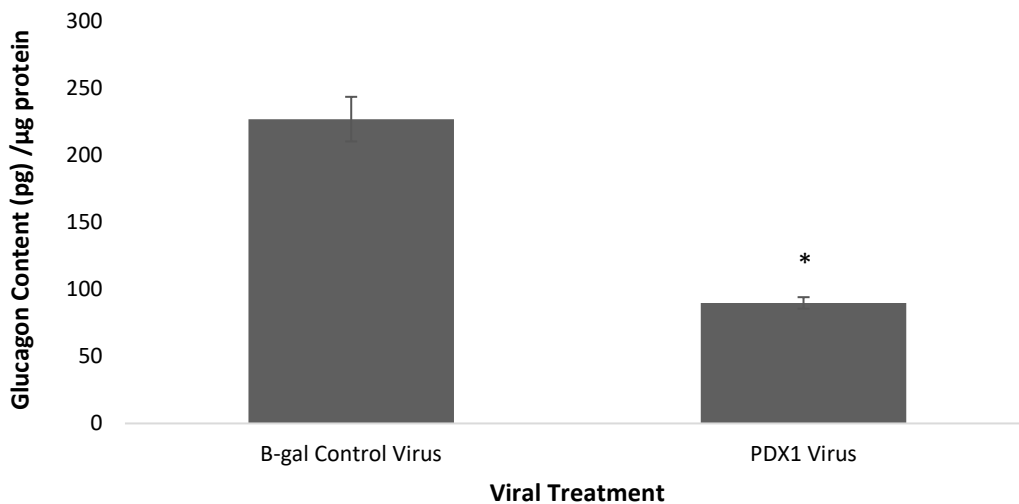


Figure 3.21 Glucagon content following 48 hours in high glucose medium and treatment with Pdx1 overexpression virus or B-gal control virus.

Glucagon content of cells was measured by ELISA. Data are normalised to total protein content and representative of n=3 from 3 biological repeats, *p<0.01.

To assess whether overexpression of Pdx1 could recover the function of INS1E cells cultured in high glucose, GSIS was carried out on the cells. No significant differences in function were observed following overexpression of Pdx1 in either normal or high glucose culture compared to cells infected with the B-gal control virus (Figure 3.22 and Figure 3.23 respectively). Although overexpression does not appear to be able to prevent the loss of function in the beta cell when cultured in high glucose medium, the insulin secreted for both basal and stimulated conditions was increased slightly with the Pdx1 overexpression. The basal level of insulin secretion was recovered from 296 ± 20.44 to 415 ± 19.26 ng/ μ g protein in the B-gal and Pdx1 treated cultures respectively, which was the same level of secretion shown in control cells cultured in 11 mM glucose (409 ± 60.24 ng/ μ g protein). Although the stimulated insulin secretion in cells cultured in high glucose medium showed an increase from 740 ± 100.85 (B-gal virus) to 902 ± 62.92 (Pdx1 virus) ng/ μ g protein, this was not a significant change and the levels remained less than half of that of the control cells cultured in normal glucose conditions. These data suggest that whilst overexpression of beta cell transcription factor Pdx1 can increase gene expression of some beta cell genes, and prevent increases in glucagon gene expression and content in high glucose, it is not sufficient to prevent the loss of beta cell function in high glucose culture.

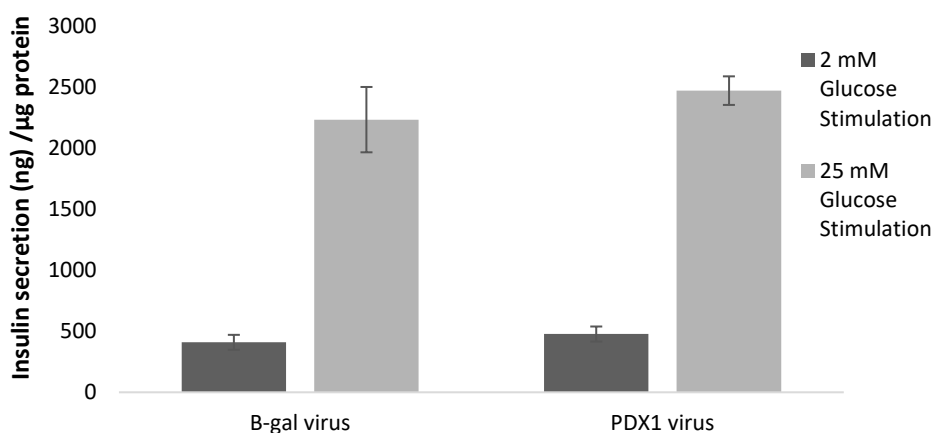


Figure 3.22 Glucose stimulated insulin secretion (GSIS) following normal glucose culture and treatment with Pdx1 overexpression virus.

Cells cultured at 11 mM for 48 hours were treated with a low glucose solution (2 mM) and high glucose solution (25 mM) and quantity of insulin secreted was measured using insulin ELISAs. Data was normalised to total protein. n=3 from 3 biological repeats.

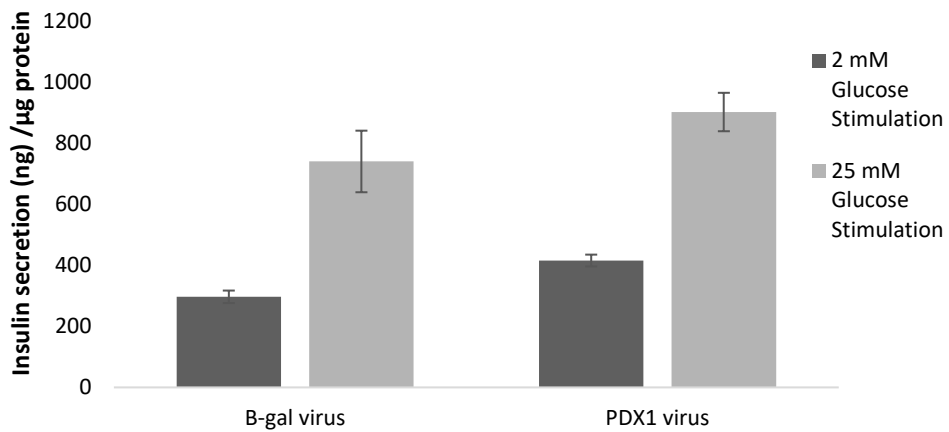


Figure 3.23 Glucose stimulated insulin secretion (GSIS) following high glucose culture and treatment with Pdx1 overexpression virus.

Cells cultured at 25 mM for 48 hours were treated with a low glucose solution (2 mM) and high glucose solution (25 mM) and quantity of insulin secreted was measured using insulin ELISAs. Data was normalised to total protein. n=3 from 3 biological repeats.

3.4 Discussion

In regard to the pancreatic beta cell, type 2 diabetes is associated with a progressive decline in function and can ultimately result in requirement for exogenous insulin injections (108). The decline in insulin secretion from pancreatic beta cells as the disease progresses, though originally thought to be due to apoptosis, is increasingly thought to be influenced by beta cell dysfunction. The importance of beta cell dysfunction has been highlighted in studies looking at different metabolic stresses such as hyperglycaemia. Using an inducible mouse model of type 2 diabetes, one study has shown that chronic hyperglycaemia causes a 70% reduction in insulin positive cells and an equivalent increase in glucagon positive cells. Furthermore, the study showed a 20-fold increase in cells positive for both insulin and glucagon (85). Although the cause of beta cell dysfunction could be numerous factors i.e. lipotoxicity, glucotoxicity, reactive oxygen species (ROS) or ER stress, we aimed to investigate the effect of exposure to chronic hyperglycaemia on the pancreatic beta cell to determine whether this symptom of diabetes directly contributes to further dysfunction of the beta cell.

Firstly, the studies described showed that culture of INS1E cells in high glucose did not seem to increase cell death (as shown by PI and caspase counts). Western blotting of the activated caspase protein, cleaved caspase-3, also remained absent in high glucose culture suggesting that glucotoxicity was not increasing cell death after 48 hours' culture. Upon exposure to high glucose levels, INS1E cells demonstrated a loss of beta cell specific transcription factors including *Pdx1* and *Nkx6.1*. The subsequent upregulation of both glucagon mRNA and protein levels in the cells is likely caused by de-repression of the glucagon gene by these transcription factors, rather than an induction by alpha cell genes. This is suggested by the inability to detect *Arx* gene expression in either normal glucose culture or high glucose culture, therefore the increase in glucagon expression is unlikely to be due to activation by *Arx*. This finding is in agreement with studies that have shown evidence of a subset of beta cells which convert to an alpha cell state through expression of glucagon when subjected to metabolic stresses, such as FoxO1 knockout (82) or hyperglycaemia (85). Although the INS1E cells had detectable levels of glucagon in normal glucose culture, the robust expression of beta cell transcription factors in the INS1E clones, in particular *Nkx6.1*, have been shown in other studies to repress higher levels of glucagon expression and help maintain the robust glucose responsiveness of a beta cell (63). The relatively low levels of glucagon expressed in

the cells cultured in normal glucose culture, along with the expression of beta cell transcription factors and glucose responsiveness suggest that these cells remain a viable model for these studies despite the basal level of glucagon expression.

The conversion of beta cells to alpha cells as a result of metabolic insult is an interesting concept. The transition to an alpha cell seems counter intuitive, as the production of more alpha cells would cause heightened glucagonaemia, putting further stress on the beta cell. However, one study has shown that alpha cells are more resistant to apoptosis than beta cells (109). This provides a possible explanation for this conversion to be a default mechanism to prevent the cells undergoing apoptosis following metabolic insult. Electron microscopy from control and type 2 diabetic patients in this study showed 6% of beta cells in type 2 donors were undergoing apoptosis compared to 0.4% in control donors. In contrast, the alpha cells, whilst some of the type 2 donors showed increased ER volume density (a sign of ER stress), showed no signs of cells undergoing apoptosis (109). Furthermore, this study also showed that rat alpha cells were more resistant to apoptosis than beta cells, expressing higher levels of the anti-apoptotic genes Bcl2 and Bcl2l1. When Bcl2l1 is silenced, alpha cells become sensitive to lipotoxicity to the same extent as beta cells, suggesting that it plays an important role in the resistance of alpha cells to apoptosis (109).

There are a few key beta cell transcription factors that have often been used in attempts to produce new insulin-producing cells from other cell types as a treatment for diabetes. One such transcription factor is Pdx1. Pdx1 has been used in conjunction with other transcription factors, such as Ngn3 and FoxA2, to produce insulin-producing cells from stem cells (106, 110), resulting in repression of glucagon expression and favouring a beta cell fate. As *Pdx1* is significantly decreased in this model of glucotoxicity, overexpression of Pdx1 using an adenoviral vector was carried out to see whether this could prevent the loss of beta cell phenotype and function and gain of alpha cell characteristics seen in the high glucose culture. The overexpression of Pdx1 in this model of glucotoxicity resulted in significantly reduced glucagon at both an mRNA and protein level, showing that Pdx1 may potentially act as a potent repressor of the alpha cell fate. In agreement with this, another study by Gao *et al.* showed that *Pdx1* knockout in beta cells lead to a transcriptional profile remarkably similar to that of an alpha cell (17). This suggests that loss of beta cell transcription factors contribute to the phenotypic changes seen in models of transdifferentiation.

In terms of maintaining the beta cell phenotype, the Pdx1 overexpression alone was not enough to recover the changes seen in high glucose. Whilst Pdx1 overexpression increased the gene expression of *Ins2* and *Nkx6.1*, the insulin content of the cells remained unchanged and, although there was a small improvement in insulin secretion, this was not enough to recover the function of the cells. The effectiveness of Pdx1 alone to induce cells that secrete insulin in response to glucose is not clear. While there are several studies that have shown combined overexpression of Pdx1 with other transcription factors producing pancreatic beta-like cells from stem cell lineages (106, 110), others have shown that although the overexpression of Pdx1 alone can induce mRNA expression of some beta cell genes, it is not sufficient to induce glucose stimulated insulin secretion in other cell types (61). In a study by Yamamoto *et al.* however, *Ins2^{Akita}* diabetic mice, with reduced Pdx1 expression compared to non-diabetic littermates, underwent transgenic overexpression of Pdx1 to preserve its expression. These diabetic mice showed improved glucose tolerance and increased expression of beta cell genes, alongside improved GLUT2 translocation (111). Whilst the retention of Pdx1 in this model of glucotoxicity did recover the expression of some key beta cell genes and reduce the glucagon content of the cells, it was not enough to rescue the function of the cells. It would be interesting to see whether combined Pdx1 expression with other beta cell transcription factors could protect against the changes seen in high glucose. Alternatively, it would also be of interest to see whether endogenous upregulation of *Pdx1* through a small molecule inducer could rescue the function of the beta cell to a greater extent than the exogenous adenoviral upregulation. Upregulation of Pdx1 through this method has been shown to induce both Pdx1 and insulin mRNA expression in both PANC-1 cells and human islets. This study also showed the induction of *Pdx1* expression in alpha cell line α TC1-6, however did not increase levels in beta cell line β TC, suggesting that it potentially acts on a process already active in beta cells (112). It would be interesting to see whether, following downregulation of Pdx1 expression in high glucose cultured cells, induction of endogenous *Pdx1* expression through a small molecule inducer could reverse the changes seen in high glucose more efficiently than infection with the adenoviral vector. If successful, this may provide a potential treatment for the preservation of beta cell function during times of hyperglycaemia.

The aims of this chapter were to establish a model of glucotoxicity, and investigate the changes in phenotype and function of the beta cell as a result of hyperglycaemia, with particular focus on the role of beta cell transcription factors in this process. The results shown demonstrate a loss of beta cell phenotype and gain of alpha cell characteristics as a result of hyperglycaemia. These studies also demonstrate a loss of beta cell transcription factors following prolonged exposure to high glucose, which may contribute to the transitional phenotype observed.

4 Results (2)

Investigating the role of Transducin-like Enhancer of Split 3 in pancreatic beta cell maintenance.

4.1 Introduction

To determine the end-fate of the endocrine lineages there are numerous transcription factors that need to be expressed at certain points in pancreatic development (Figure 1.2). This complex gene expression network gives rise to the different endocrine lineages and changes to these pathways have been shown to disrupt both pancreatic development and, more specifically, the differentiation of the different endocrine cells (13, 107, 113). In respect to the beta cell, key transcription factors such as *Pdx1*, *Nkx6.1* and *Nkx2.2* are needed to maintain the beta cell phenotype once in the end-differentiated state (17, 64, 66). Downregulation of these beta cell transcription factors have been shown to result in cellular reprogramming. Studies looking at the deletion of beta cell specific *Pdx1* in adult mice showed that, within a few days of deletion, there was not only a loss of beta cell identity but also a shift towards physiological and ultrastructural characteristics of alpha cells, indicating cellular reprogramming (17). This reprogramming to an alpha cell fate was thought to be, in part, due to the de-repression of *MafB* (the alpha cell transcription factor) by *Pdx1*, which was shown to be responsible for induction of glucagon expression (17). Other studies have highlighted the importance of *Pdx1* in correct proportions of endocrine cell types, showing large increases in glucagon positive cells and a depleted beta cell population following knockout (107). As well as its role as a repressor of the alpha cell fate, *Pdx1* has been shown to be important in activation of beta cell transcription factors, such as *Nkx6.1*, through induction of *Nkx6.1* expression following ectopic *Pdx1* expression (114).

Nkx6.1 is another protein which has been shown to be downregulated in beta cells of diabetic patients. Studies looking at deletion in beta cells have shown the important roles it plays in insulin processing of proinsulin to insulin and formation of insulin secretory vesicles (66). This was shown through the reduction in insulin plasma levels and loss of insulin content in mice following beta cell specific knockout of *Nkx6.1*, with no concurrent increases in cell death or transition to other endocrine lineages (66). Alongside this, it was also shown that knockdown of *Nkx6.1* increased expression of progenitor marker Neurogenin3 (*Ngn3*) and induced co-localisation of insulin and the delta cell hormone somatostatin (66). These studies, among others, have shown the importance of regulation of transcription factors in maintaining the functional beta cell. The downregulation of these key beta cell transcription factors in type 2 diabetes can provide possible explanation for some of the non-insulin

abnormalities seen in the diabetic state, for example, the hyperglucagonemia seen in some diabetic patients could potentially be the result of increased glucagon expression due to beta to alpha cell reprogramming.

In depth studies of the transcriptional targets of Pdx1 have shown that alongside activating a wide range of islet genes, Pdx1 is a potent repressor of numerous hepatic genes (115). Furthermore, the study suggested that Pdx1 can work in complexes with the likes of FoxA2 (a co-factor which has been shown to open compact chromatin to allow transcription of beta-cell genes) or Pbx1a/b to repress or activate genes involved in beta cell function depending on recruitment of other co-factors (115). Alongside the well-established beta cell transcription factors needed to maintain beta cell identity other, less well-studied proteins, may also be among those needed for adequate function of the beta cell.

The transducin-like enhancer of split (Tle) family of co-repressors have been implicated in numerous cell types and pathways as important proteins in gene regulation. This family of proteins have been shown to have important roles animal development, helping to regulate gene expression pathways in neurogenesis, haematopoiesis and adipogenesis among others (67). Tle3 has been shown to be recruited to act as a co-repressor with FOXA proteins (116). This, alongside the previously mentioned complex between Pdx1 and FoxA2, gives a potential way in which Tle3 and Pdx1 may work together in the beta cell. Although well established as a family of co-repressors more recent studies have also indicated a potential role for Tle3 as an activator of adipogenesis. Peroxisome proliferator-activated receptor γ (PPAR γ) is a key regulator of adipogenesis. The transgenic overexpression of Tle3 in *PPAR γ* knockout mice has been shown to act in a similar way to PPAR γ agonists to drive adipogenesis even in the absence of PPAR γ (117). This suggests that it is acting as an activator of the genes needed for adipogenesis.

The rodent Tle3 (and its human functional equivalent, TLE1) has been identified to play a role in the functional beta cell through repression of the alpha cell program. Alongside this, Tle3 has been shown to have a role in development of proper ratios of beta and alpha cells in the developing pancreas (61). This study also showed that lentiviral overexpression of Tle3 acts on the *Gcg* and *Arx* promoters to repress expression in the alpha cell line α TC1-6 through interaction with the beta cell transcription factor Nkx6.1 (61). Co-expression of Tle3 with Pdx1 in the α TC1-6 cell line has also been shown to induce glucose stimulated insulin secretion, whereas overexpression of Pdx1 or Tle3 alone did not, showing a potential role for

Tle3 is not only an alpha cell repressor, but also maintains the beta cell phenotype and function through interaction with Pdx1 (61).

4.2 Aims

The following studies aimed to further investigate the role of transducin-like enhancer of split 3 in beta cell identity and function.

Specific objectives were to:

1. Determine changes in gene expression of Tle3 following glucotoxicity
2. Further investigate the role of Tle3 in both repression of the alpha cell program and maintaining the beta cell program through siRNA mediated knockdown
3. Investigate long-term effects of reduced Tle3 expression on beta cell phenotype and function through development of stable knockdown cell lines
4. Use isolated rodent islets to look at how Tle3 expression affects the beta cell in a more physiological model through siRNA mediated knockdown

4.3 Results

4.3.1 The effect of high glucose culture on Tle3 expression

In Chapter 3, the model of glucotoxicity developed allowed for observation of changes in beta cell transcription factors and beta cell function. To investigate whether Tle3 is effected in this model, gene expression was measured to give an indication of whether expression levels are changed following glucotoxic culture. Figure 4.1 shows that mRNA levels of *Tle3* are downregulated in high glucose culture to ~0.55 fold.

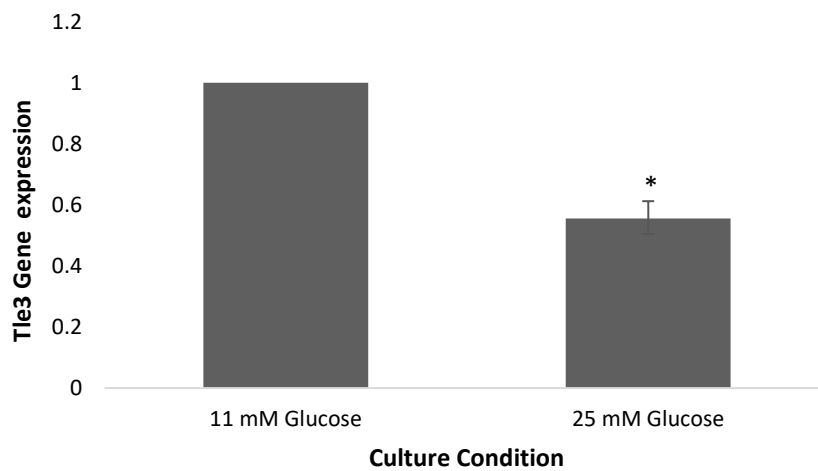


Figure 4.1 Gene expression of Tle3 in INS1E cell line following high glucose culture.

Cells were cultured for 48 hours in 11 mM or 25 mM glucose culture and fold change in mRNA expression was analysed in the 25 mM glucose culture compared to the 11 mM glucose culture. n=3 from 3 biological repeats, *p= <0.01 by student's t-test.

4.3.2 Interactions between Tle3 and Pdx1

Previous studies have shown interaction between Tle3 and the beta cell transcription factor Nkx6.1, and a potential interaction with Pdx1 (61). This suggests that Tle3 may play some role in maintaining beta cell function through interactions with key, well established beta cell transcription factors. To investigate relationship between Tle3 and Pdx1 gene expression analysis was carried out on INS1E cells that had been overexpressed with Pdx1, or B-galactosidase (B-gal), using an adenoviral vectors. Figure 4.2 demonstrates that cells overexpressing Pdx1 show increased *Tle3* gene expression in both normal and high glucose cultures compared to cells treated with the B-gal control virus. The significant reduction in *Tle3* gene expression shown in B-gal infected cells between the 11 mM and 25 mM cultures is prevented when cells are overexpressed with Pdx1, suggesting that Pdx1 can recover *Tle3* gene expression to a certain degree in high glucose culture.

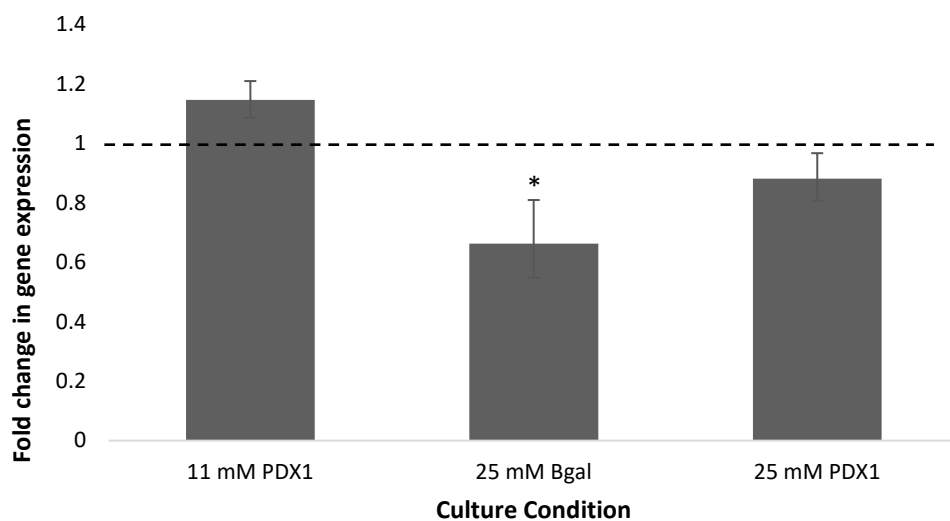


Figure 4.2 Tle3 gene expression following overexpression of Pdx1 in INS1E cells.

Gene expression analysis of Tle3 following Pdx1 overexpression in both 11 mM and 25 mM cultures. Results were normalised to 11 mM culture with B-gal expression as indicated by the dashed line. Data is expressed as mean value \pm SEM, n=3 from 3 biological repeats, *p= <0.05 by students t-test vs 11 mM B-gal.

To investigate whether there is an interaction between Pdx1 and Tle3, proximity ligation assays (PLA) were set up. PLA assays utilise immunofluorescent staining to enable visualisation of protein-protein interactions through use of secondary antibodies conjugated to complementary oligonucleotide probes. PLA assays were carried out to first establish interactions between Pdx1 and Tle3, and secondly to see whether this interaction was lost following exposure to high glucose. INS1E cells were seeded on cover slips and cultured at 11 mM and 25 mM glucose for 48 hours before the experiments were carried out. Interaction between Nkx6.1 and Tle3 was used as a positive control as previous studies have shown interactions between these two proteins in the beta cell (61) and IgG was used as a negative control. Figure 4.3 shows positive staining in INS1E cells cultured in 11 mM glucose suggesting strong interaction between Pdx1 and Tle3. In cells cultured in high glucose culture (bottom line) we see an apparent reduction in interaction between the two proteins suggesting that under conditions of hyperglycaemia the interaction between these proteins may be lost.

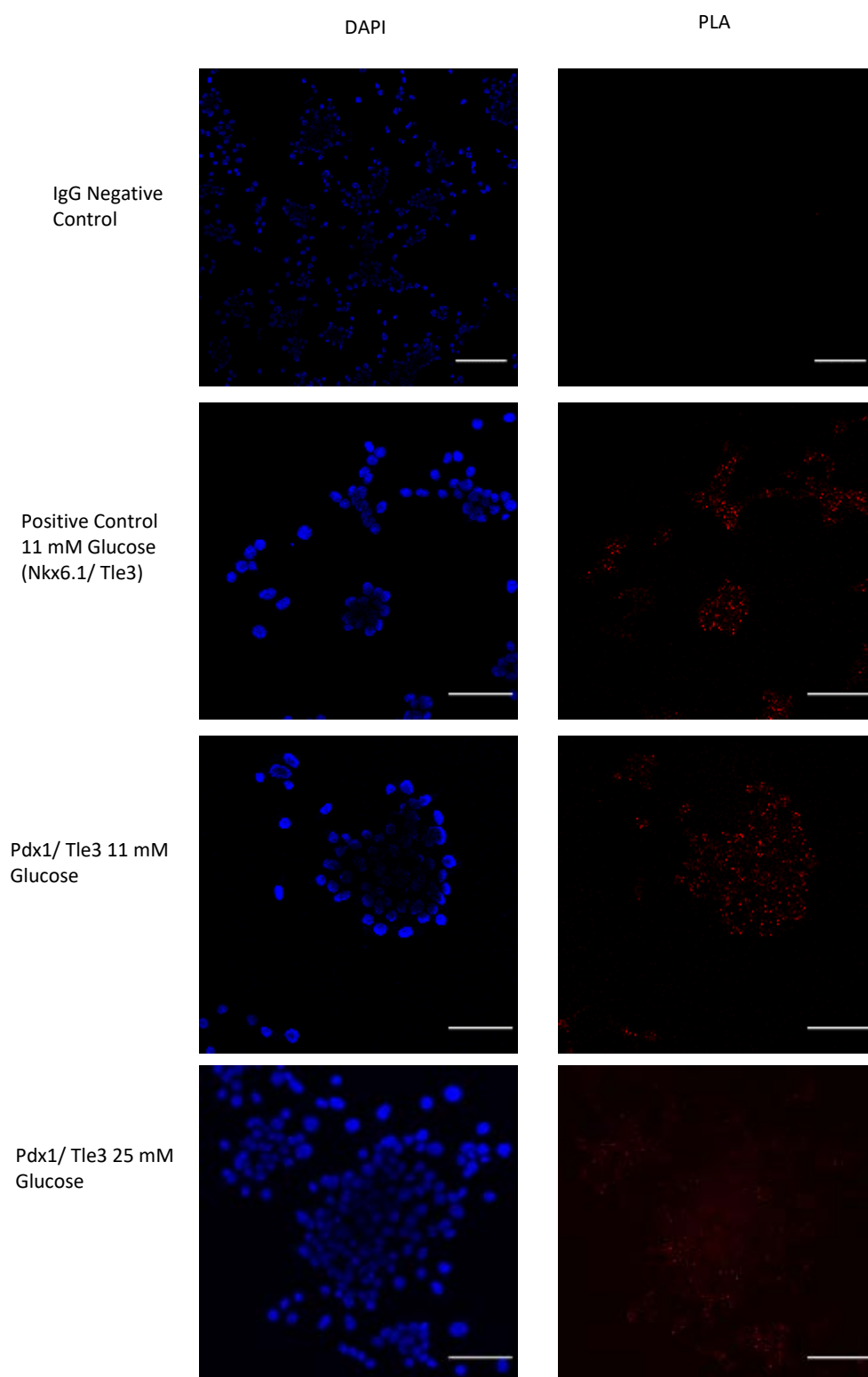


Figure 4.3 Proximity ligation assay assessing interactions between Pdx1 and Tle3 in INS1E cell line.

Following 48 hours in 11 mM or 25 mM glucose culture INS1E cells were assed for interaction between Tle3 and Pdx1. Interaction between Tle3 and Nkx6.1 was used as a positive control and IgG was used as a negative control and nuclei were stained for DAPI. Images are representative of 2 biological repeats. Scale bar= 50 μ m.

4.3.3 siRNA mediated knockdown of Tle3

To assess the role of Tle3 in the pancreatic beta cell, and determine the effects it has on the beta cell phenotype and function, siRNA mediated knockdown was carried out in the INS1E cell line. INS1E cells were seeded and left to settle overnight before siRNA-Lipofectamine complexes were used to knockdown *Tle3* gene expression. Fresh medium was added after 12-18 hours of transfection and cells were left for the remainder of the 48 or 72 hour incubation (for method see section 2.7.1).

Initially 3 different siRNA probes were used to assess efficiency at 48 and 72 hours of knockdown (Figure 4.4). Probe 3 was taken forward for further analysis as it showed the greatest degree of *Tle3* knockdown at both time points. Analysis of *Tle3* gene expression showed successful reduction in *Tle3* mRNA at both time points, achieving a ~60% knockdown at 48 hours and ~55% knockdown at 72 hours (Figure 4.5). Whilst confirmation of knockdown at a protein level was attempted through means of western blotting, discontinuation of the antibody used in other studies left no suitable antibodies for detection of the protein through this method. Due to successful and consistent knockdown of *Tle3* mRNA levels however, studies on phenotypic and functional changes were still assessed. Further analysis of other beta cell genes showed significant decreases at 48 hours of *Ins2* and *Pdx1*, however, the expression of these genes increased again at 72 hours (Figure 4.6). This is in support of Figure 4.5 that shows the level of Tle3 knockdown was less effective at 72 hours than 48 hours. Although Figure 4.6 shows *Nkx6.1* expression was decreased slightly this was not significant at either time point. Slight increases in *Ins1* expression are also observed at 48 hours and, significantly so, at 72 hours. This could be a result of decreased *Ins2* expression as previous studies have shown a compensation mechanism between the *Ins1* and *Ins2* genes in rodents (118). As Tle3 has been shown to act as a repressor on the glucagon promoter, gene expression for glucagon was also analysed. Modest increases of glucagon were observed at both 48 and 72 hours of Tle3 knockdown. These results support the hypothesis that Tle3 not only plays a role in repressing the alpha cell phenotype but also maintaining the beta cell phenotype. *Arx* was also run following knockdown however no detectable levels were observed for either control or knockdown groups. Further knockdown experiments were

set up to assess the changes in cell content of insulin and glucagon, and function by means of glucose stimulated insulin secretion.

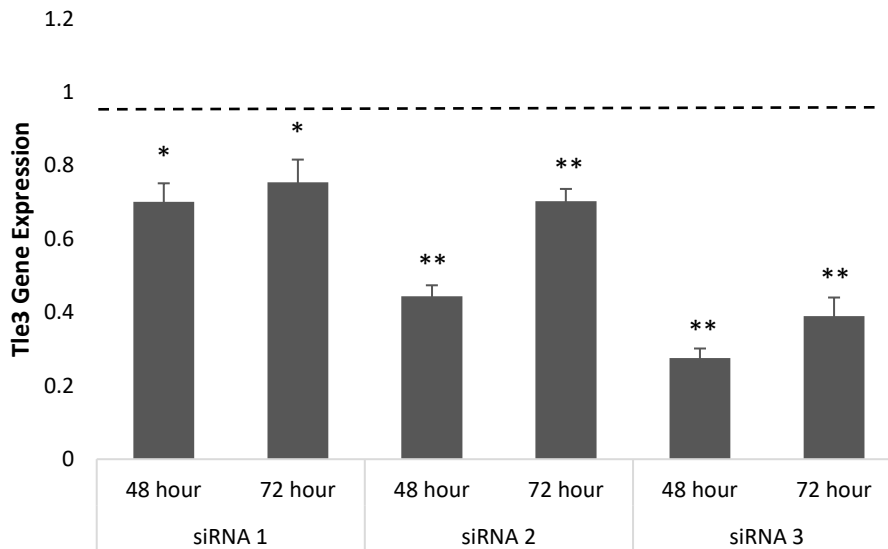


Figure 4.4 Gene expression analysis of Tle3 following siRNA mediated knockdown at 48 and 72 hours of 11 mM glucose culture using 3 different siRNA probes.

Efficiency of 3 different siRNA probes were initially tested at 48 and 72 hour transfection periods before choosing one to carry forward for further analysis. Results were normalised to scrambled control at respective time points as indicated by the dashed line. Data is expressed as mean value \pm SEM, n=3 from 3 biological repeats, *p= <0.01 by students t-test.

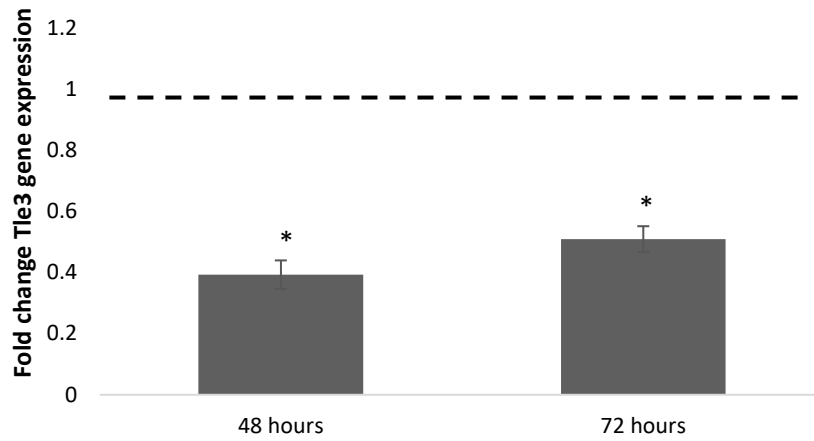


Figure 4.5 Gene expression analysis of Tle3 following siRNA mediated knockdown at 48 and 72 hours of 11 mM glucose culture using siRNA probe 3.

qPCR analysis of Tle3 gene expression following knockdown in INS1E cells using siRNA probe 3 as chosen from previous studies. Results were normalised to scrambled control at respective time points as indicated by the dashed line. Data is expressed as mean value ± SEM, n=3 from 3 biological repeats, *p= <0.01 by students t-test.

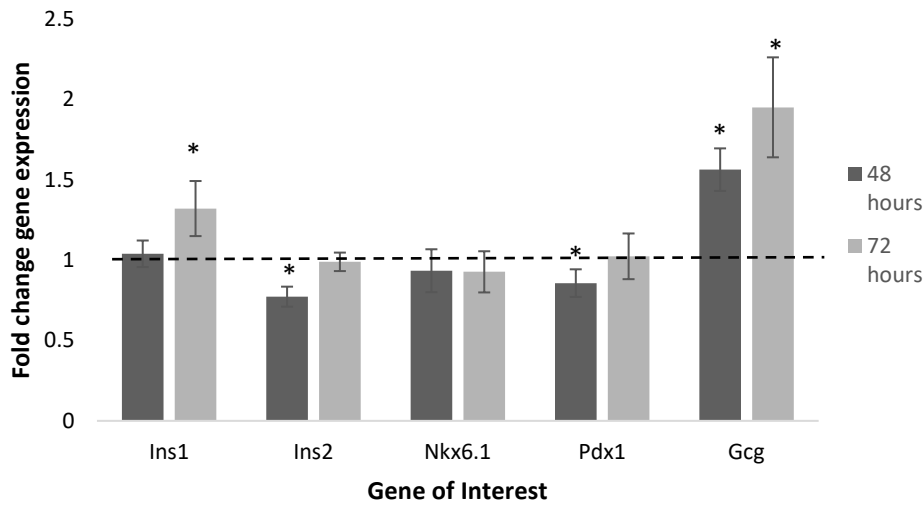


Figure 4.6 Gene expression analysis of p80+ INS1E cells following siRNA mediated *Tle3* knockdown at 48 and 72 hours of 11 mM glucose culture.

qPCR analysis of gene expression following knockdown in INS1E cells. Results were normalised to scrambled control at respective time points as indicated by the dashed line. Data is expressed as mean value \pm SEM, n=3 from 3 biological repeats *p= <0.01 by students t-test.

Assessment of insulin and glucagon content was carried out on the cells following *Tle3* knockdown to see whether changes in insulin and glucagon gene expression were translated into changes in protein content. As shown in Figure 4.7 there was a trend towards an increase in cellular insulin content following *Tle3* knockdown at both time points, however these results did not reach significance. Significant increases in glucagon expression however, were observed at both time points with a ~1.3-fold increase in glucagon expression in the *Tle3* knockdown culture compared to the scrambled control (Figure 4.8).

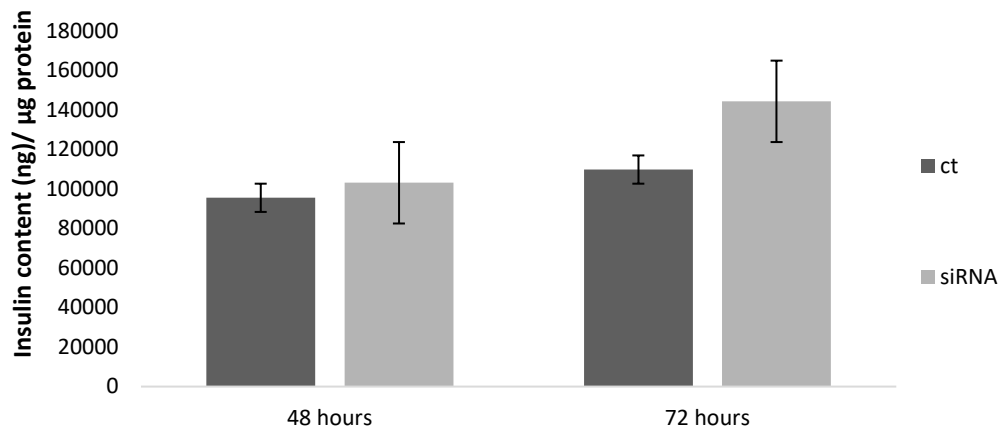


Figure 4.7 Insulin content ELISA from p80+ INS1E cells following 48 or 72 hours of Tle3 knockdown.

Data comparing insulin content following transfection with scrambled control siRNA (dark grey) or Tle3 siRNA (light grey) at 48 and 72 hours of Tle3 knockdown. Data is expressed as mean value \pm SEM and normalised to total protein content. n=3 from 3 biological repeats.

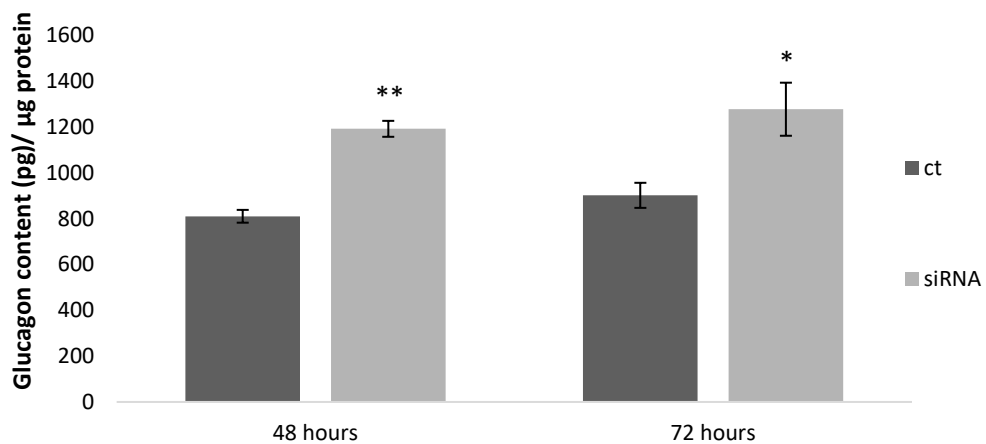


Figure 4.8 Glucagon content of p80+ INS1E cells following 48 or 72 hours of Tle3 knockdown.

Data comparing insulin content following transfection with scrambled control siRNA (dark grey) or Tle3 siRNA (light grey) at 48 and 72 hours of Tle3 knockdown. Data is expressed as mean value \pm SEM and normalised to total protein content. n=3 from 3 biological repeats *p<0.05 **p<0.01 by students t-test.

Glucose stimulated insulin secretion (GSIS) was employed to assess changes in beta cell function following *Tle3* knockdown. Figure 4.9 shows assessment of beta cell function through measuring secreted insulin at different levels of glucose stimulation. While there appeared to be slight increases in basal insulin secretion following *Tle3* knockdown at both time points, there were no significant changes observed and the function of the beta cell remained relatively similar between the two transfection conditions.

The results from the transfection studies confirm a role for *Tle3* in repressing glucagon expression in the beta cell and indicate a potential role for it in maintaining beta cell phenotype, however the results on the role it plays in beta cell function remain undetermined. These previous studies were carried out in highly passaged cells (p80+), so to ensure that the results were not affected by the passage of the cells and progressive loss of phenotype, further experiments were set up using a younger passage of INS1E to confirm these findings.

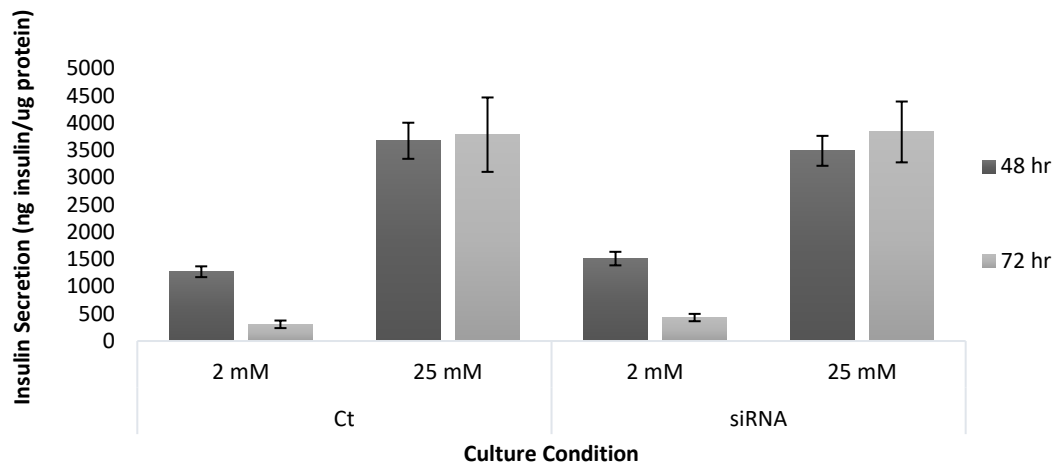


Figure 4.9 Glucose stimulated insulin secretion of p80+ INS1E cells following 48 or 72 hours of Tle3 knockdown.

Data comparing beta cell function following transfection for 48 hours (dark grey) or 72 hours (light grey) with either scrambled control or Tle3 siRNA. Secreted insulin levels were measured using ELISA method from supernatant collected following a low glucose stimulation (2 mM) and a high glucose stimulation (25 mM). Data is expressed as mean value \pm SEM and normalised to total protein content. n=3 from 3 biological repeats.

Analysis of younger INS1E cells (p40+) were carried out using the same experimental procedures as the higher passage cells. siRNA probes 2 and 3 were initially carried forward to test efficiency with the younger passage of cells as siRNA 1 showed less effective knockdown in the older passage of cells. Gene expression analysis was carried out on the cells following transfection with two different siRNAs alongside a scrambled control at 48 hours of transfection. The results showed that both siRNA probes successfully knocked down *Tle3* (Figure 4.10). Subsequent functional studies were conducted using probe 2, as although the changes in gene expression of selected beta and alpha cell genes were similar between the two probes, probe 2 gave more consistent and significant results (Figure 4.11)

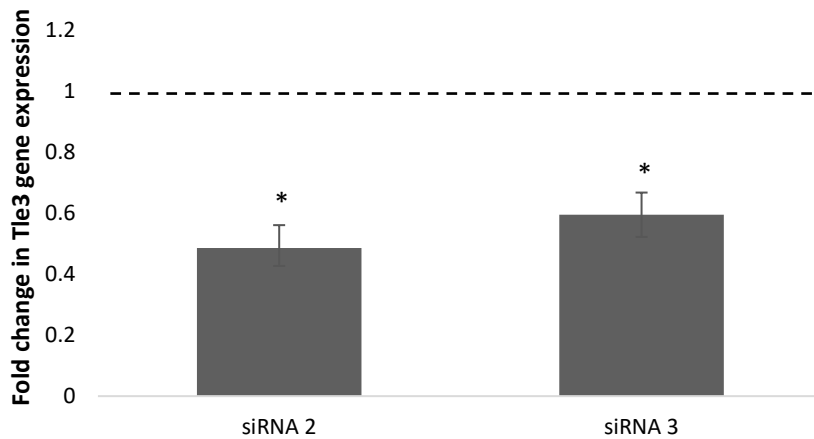


Figure 4.10 Gene expression for Tle3 following 48 hours knockdown in p40+ INS1E cells.

qPCR analysis used to assess gene expression of Tle3. Results were normalised to scrambled control as indicated by the dashed line. Data is expressed as mean value \pm SEM, n=4 from 4 biological repeats *p= <0.01 by students t-test.

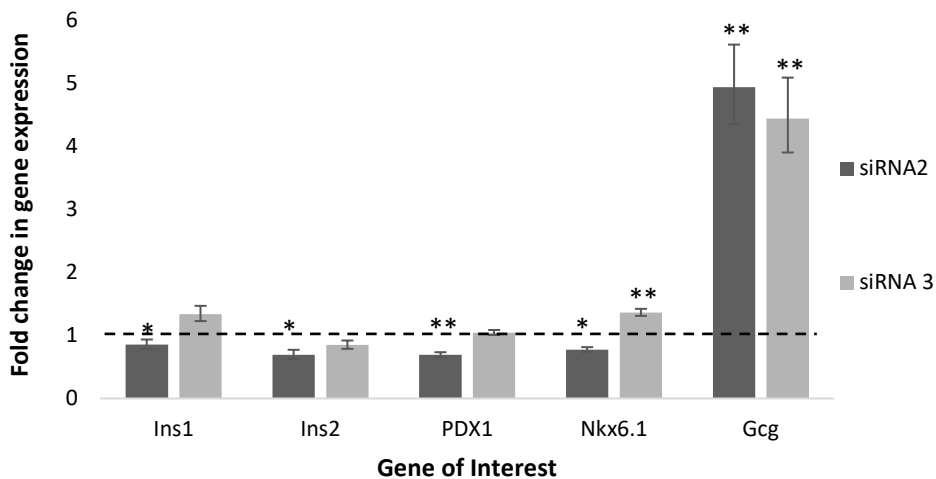


Figure 4.11 Gene expression in (p40+) INS1E cells following 48 hours Tle3 knockdown.

qPCR analysis of gene expression following Tle3 knockdown in INS1E cells. Results were normalised to scrambled control as indicated by the dashed line. Data is expressed as mean value \pm SEM, n=4 from 4 biological repeats *p= <0.05 and **p= <0.01 by students t-test.

Following gene expression analysis, cells were analysed for insulin and glucagon content with and without *Tle3* knockdown. In the young INS1E the average insulin content was significantly reduced between the two culture conditions (Figure 4.12). Interestingly, the insulin content in the younger INS1E cells was about 50x lower than the higher passage cells at 2042 ± 205.5 ng/ μ g protein compared to almost 95525 ± 67092 ng/ μ g protein in the older cells when looking at control conditions. Alongside this, Figure 4.13 shows significantly increased glucagon content after *Tle3* knockdown. In addition to this, when looking at the total quantities in older and younger cells there was also a marked difference in glucagon content between the two passages decreasing from 6242 ± 477.7 pg/ μ g protein in the lower passage to 810 ± 27.9 ng/ μ g protein in the older cells.

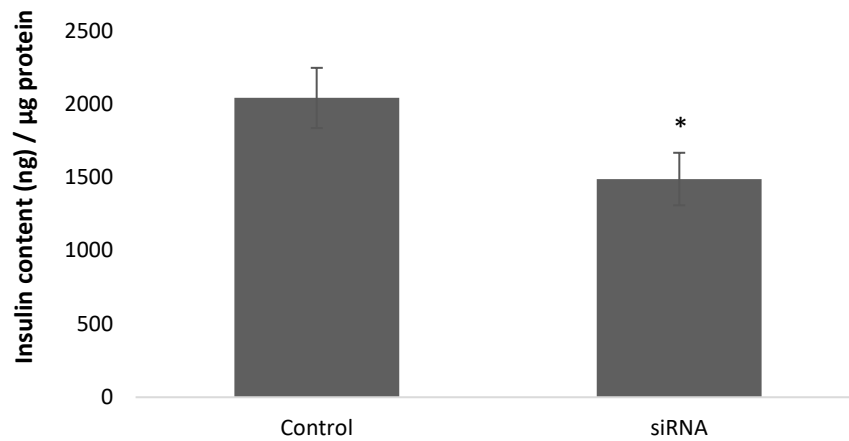


Figure 4.12 Insulin content ELISA from p40+ INS1E cells following 48 hours of Tle3 knockdown.

Data comparing insulin content following transfection with scrambled control siRNA Tle3 siRNA at 48 hours of Tle3 knockdown. Data is expressed as mean value \pm SEM and normalised to total protein content. n=3 from 3 biological repeats.

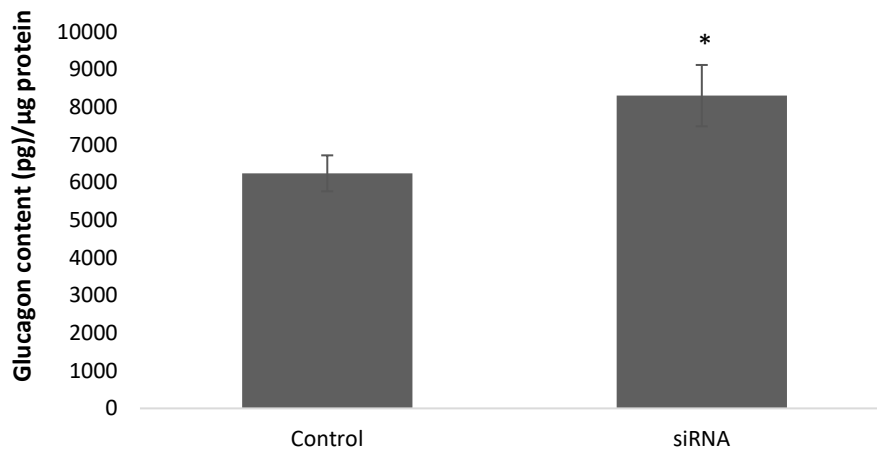


Figure 4.13 Glucagon content of p40+ INS1E cells following 48 hours of Tle3 knockdown.

Data comparing insulin content following transfection with scrambled control siRNA or Tle3 siRNA at 48 hours of Tle3 knockdown. Data is expressed as mean value \pm SEM and normalised to total protein content. n=3 from 3 biological repeats.

When analysing the function of the younger INS1E cells following *Tle3* knockdown, a significant decrease in function of the cells when stimulated with high glucose solution (25mM) was observed (Figure 4.14). Although the amount of insulin secreted by the younger passage cells is much lower compared to the older cells (646 ± 103.7 ng/ μ g protein and 3673 ± 331.2 ng/ μ g protein in control conditions respectively), the impact of the *Tle3* knockdown on cell function was much greater. In the older passage the stimulation index after 48 hours of transfection was 0.97-fold (Figure 4.9) whereas the stimulation index in the younger cells was 0.58-fold (Figure 4.15).

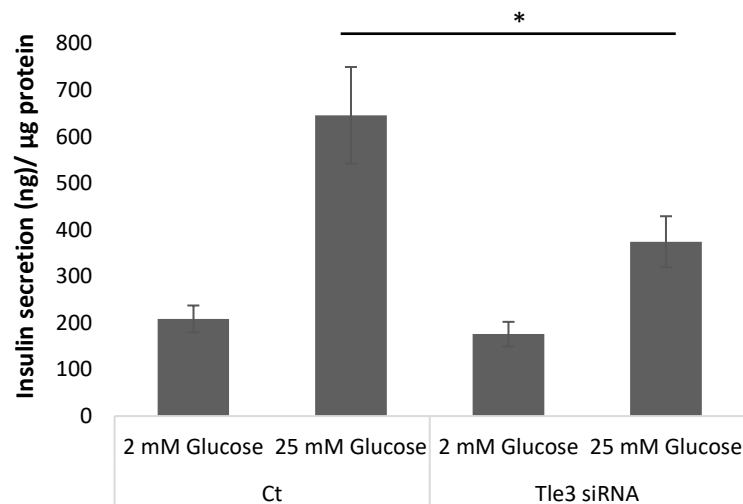


Figure 4.14 Glucose stimulated insulin secretion of p40+ INS1E cells following 48 hours of *Tle3* knockdown.

Data comparing beta cell function following transfection for 48 hours with either scrambled control or *Tle3* siRNA. Secreted insulin levels were measured using ELISA method from supernatant collected following a low glucose stimulation (2 mM) and a high glucose stimulation (25 mM). Data is expressed as mean value \pm SEM and normalised to total protein content. n=3 from 3 biological repeats, *p<0.05

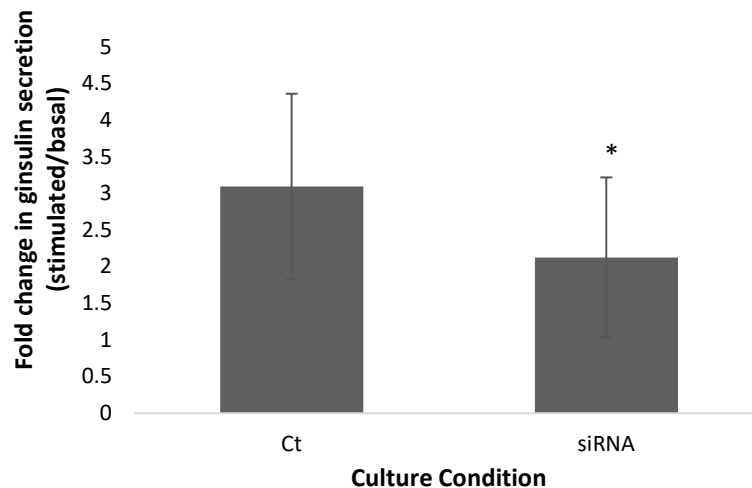


Figure 4.15 Stimulation Index of young INS1E cells following 48 hours of Tle3 knockdown.

Data comparing beta cell function following transfection for 48 hours with either scrambled control or Tle3 siRNA. Insulin secretion was quantified using ELISA and stimulation index was worked out by stimulated insulin secretion/basal insulin secretion. Data is expressed as mean value \pm SEM and normalised to total protein content. n= 3 from 3 biological repeats, *p<0.05

4.3.4 Generation of a stable Tle3 knockdown cell line

To help further elucidate the role of Tle3 the beta cell identity and function, stable knockdown cell lines were generated to look at the impact of loss of Tle3 over a longer period of time. The data from the siRNA mediated knockdown showed increases in Tle3 expression after 72 hours when compared to 48 hour transection therefore, generation of a stable knockdown cell line would ensure the loss of Tle3 expression is maintained through multiple passages. For this, the INS1E cell line was treated with polybrene to counter the electrostatic charge between the virus and the cell membrane and allow easier entry into the cell. Cells were then infected with lentivirus containing shRNA constructs for Tle3 as stated in methods 2.2.3). shRNA is used to generate stable knockdown cell lines as the RNA is integrated into the hosts' genome and processed in the same way as native miRNA. The integration into the genome also means that the knockdown is maintained in dividing cells

whereas the effect of siRNA is diluted as the cells divide (88). Four different lentivirus were used alongside a scrambled control to allow us to choose the virus with the best infection efficiency.

Cells that have stable integration of the shRNA construct contain a puromycin resistance gene. To ensure a pure population of stably integrated cells, they were exposed to puromycin in order to kill any cells which do not have the shRNA integrated. Initially, a puromycin kill curve was set up to determine the lowest concentration that killed all cells without the shRNA integrated (Figure 4.16). For this, non-infected INS1E cells were cultured in 6 well plates and treated with increasing concentrations of puromycin until the cells were fully confluent (~1 week). The concentration chosen was 0.02 $\mu\text{g/ml}$. Further to this, these vectors contained a Green fluorescent protein (GFP) cassette to enable visualisation of transduced cells (Figure 2.1). Following transduction, the cells were cultured in complete medium + 0.02 $\mu\text{g/ml}$ of puromycin as chosen by the puromycin kill curve experiment to maintain a pure knockdown population.

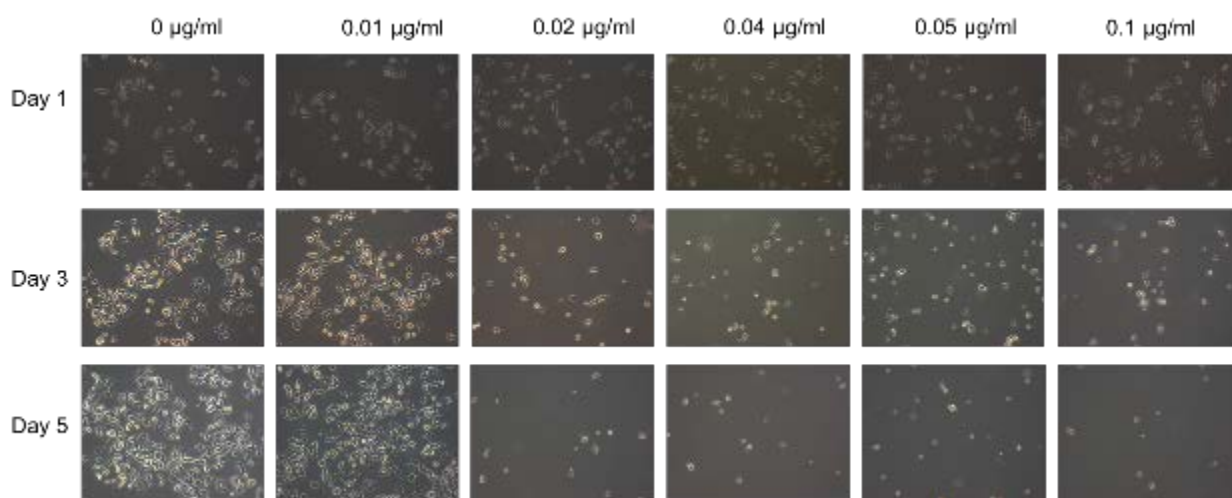


Figure 4.16 Puromycin kill curve.

The stable knockdown cell lines contain puromycin resistance. To ensure a pure population of the modified cell line culture in puromycin is required to kill those cells without genetic modification. A range of concentrations of puromycin was tested on non-modified INS1E cells to pick the lowest concentration that killed all cells.

Following infection and culture of the cells through several passages, images were taken to look at efficiency of each of the viruses (Figure 4.17). The viruses with the best efficiency were shRNA constructs C and D. Western blots were carried out following establishment of ~80% GFP+ populations (~4 weeks passaging and selecting with puromycin) to look at the protein level of Tle3 following knockdown (Figure 4.18). Non-modified INS1E cells were used as a positive control (Lane 1). The blot confirmed that constructs C and D had the highest level of knockdown. qPCR analysis was used to confirm these findings at an mRNA level (Figure 4.19).

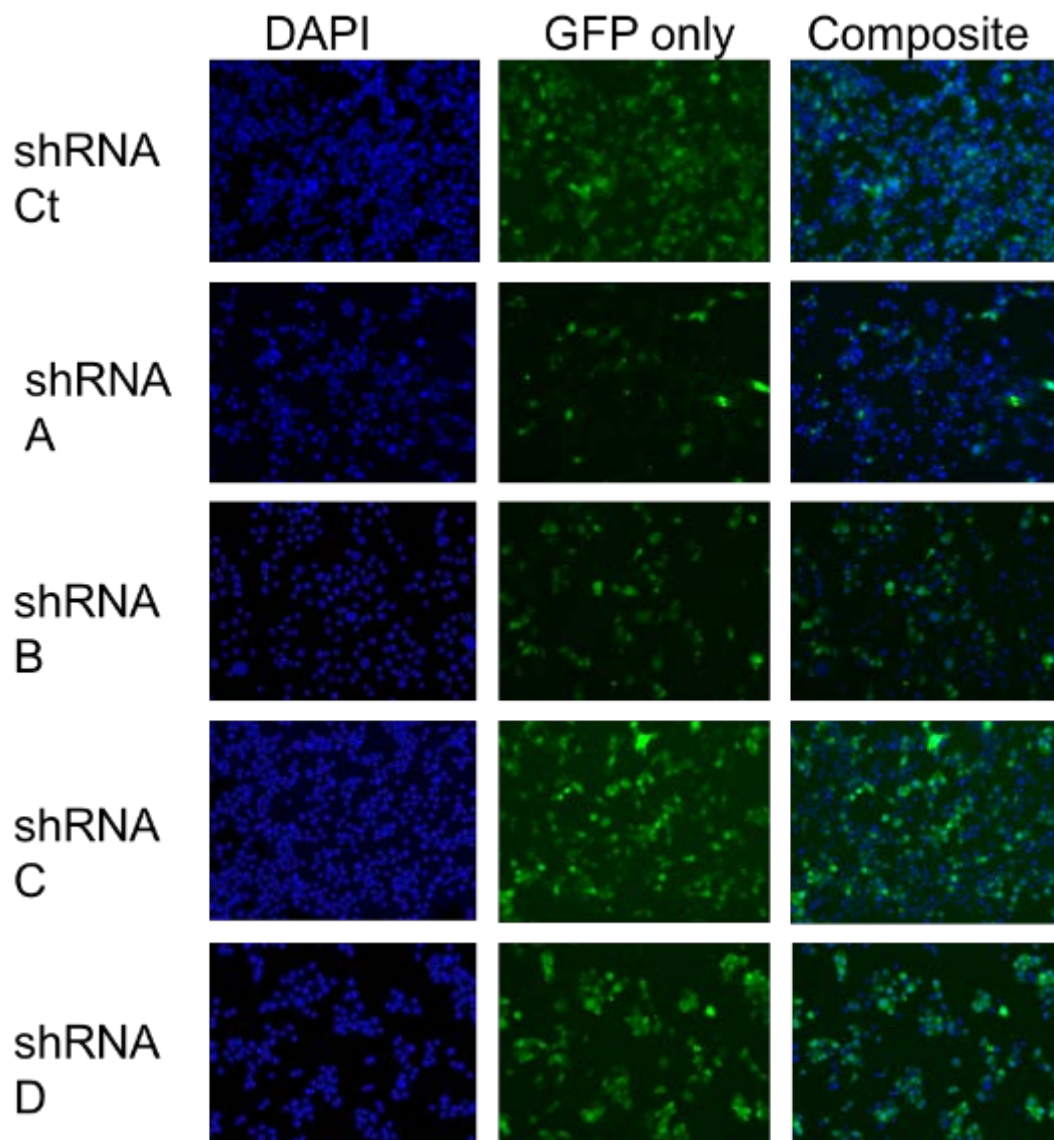


Figure 4.17 Images of INS1E cells following infection with lentivirus containing shRNA for Tle3.

Lentiviral particles containing four different shRNA constructs to different loci on the Tle3 gene alongside a scrambled control, were used to infect the INS1E cells. Each plasmid contained GFP sequence to allow observation of virus efficiency. Images were taken at 10x magnification.

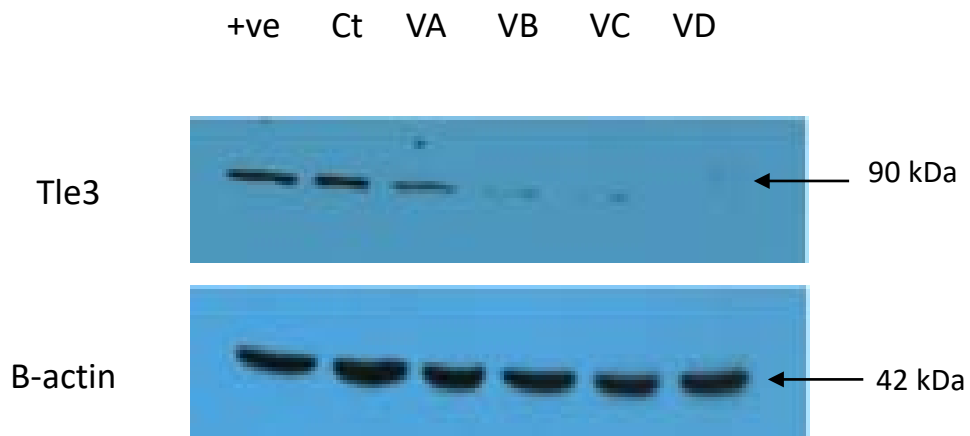


Figure 4.18 Western blot of lentiviral mediated knockdown of INS1E cells with no knockdown, a control vector and four different Tle3 vectors.

Western blotting was used to confirm knockdown of Tle3 in INS1E cells. 40 μ g of protein was loaded onto 10% SDS gels. Blots were incubated at 1:100 concentration of Tle3 primary antibody or 1:10 000 concentration for beta actin, 1:1000 concentration of secondary antibody was used for both Tle3 and beta actin blots. n=3 from 3 biological repeats.

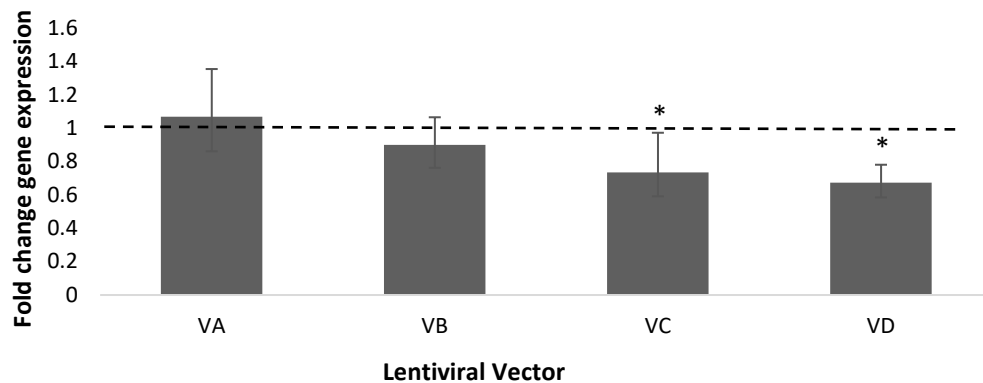


Figure 4.19 qPCR analysis of stable cell lines.

mRNA levels of each construct were measured using qPCR analysis. Values were normalised to the scrambled control as indicated by the dashed line. Data is expressed as mean value \pm SEM, n=3 from 3 biological repeats *p<0.01.

Considering transduction efficiencies of the four shRNA vectors alongside the changes in *Tle3* knockdown at an mRNA and protein level, viruses C and D were taken forward, alongside the scrambled control, for further analysis. Gene expression patterns of the other beta cell genes, alongside glucagon, were observed to see the impact of longer term *Tle3* knockdown (continual knockdown over ~5-7 weeks of passage). Figure 4.20 shows vector D (VD) had significant decreases in *Ins2* expression while *Ins1* was significantly upregulated. Vector C (VC) showed this same pattern in insulin gene genes however the downregulation of *Ins2* did not reach significance. Alongside these changes, significant increases in glucagon were observed for both VC and VD. *Pdx1* was shown to be consistently upregulated following *Tle3* knockdown with both vectors although neither VC nor VD reached significance. Interestingly, *Nkx6.1* was the only gene that showed different changes between the different constructs. In the case of VC, *Nkx6.1* was significantly downregulated however VD showed no change in gene expression for *Nkx6.1*.

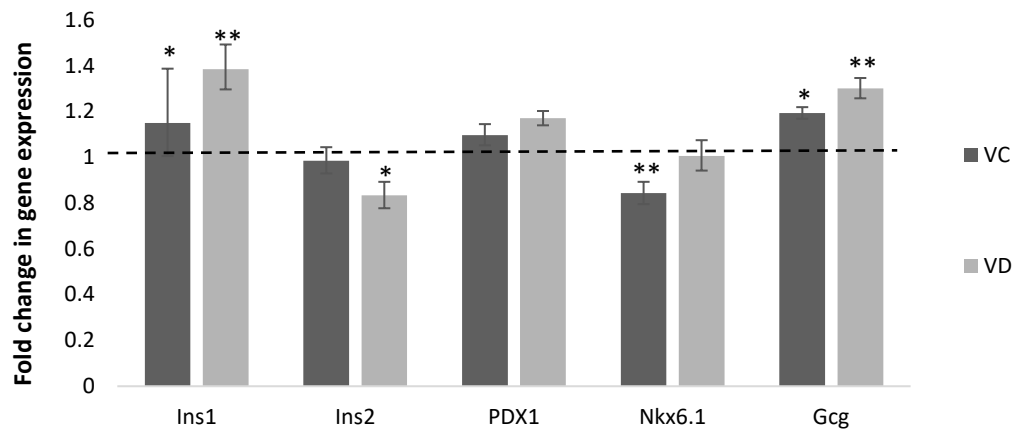


Figure 4.20 Gene expression analysis of INS1E cells following shRNA mediated Tle3 knockdown.

qPCR analysis of gene expression following knockdown in INS1E cells. Results were normalised to scrambled control as indicated by the dashed line. Data is expressed as mean value \pm SEM, n=3 from in 3 biological repeats, *p<0.05 and **p= <0.01 by students t-test.

When observing changes in insulin and glucagon protein content of the stable knockdown cell lines, the same pattern was seen for both VC and VD. Although there was a similar reduction in insulin content following Tle3 knockdown with shRNA C and D (from 881.37 ± 219.63 ng/ μ g protein in control cells to 591.88 ± 174.17 and 624.45 ± 212.78 ng/ μ g in VC and VD respectively), only VC reached significance as the levels of insulin measured were more consistent over the 3 individual experiments (Figure 4.21). Glucagon content was increased in both VC and VD when compared to the scrambled control (from 7869.78 ± 1941.28 pg/ μ g protein in control cells to 10286.47 ± 2099.70 and 11859.59 ± 2383.79 pg/ μ g protein for VC and VD respectively), however this did not reach significance in either knockdown lines. Although not always reaching significance, the patterns of changes seen following *Tle3* knockdown agreed with our hypothesis that Tle3 has a role in maintaining the beta cell phenotype whilst also suppressing the alpha cell phenotype.

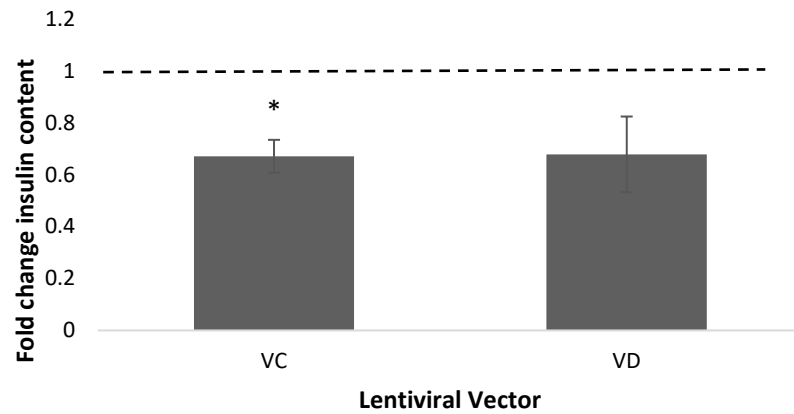


Figure 4.21 Insulin content ELISA from stable knockdown INS1E cells.

Data comparing insulin content following stable Tle3 knockdown with constructs C and D. Data is normalised to insulin content in cells infected with lentivirus carrying scrambled control as indicated by the dashed line. Data is expressed as mean value \pm SEM. n=3 from 3 biological repeats. *p<0.05.

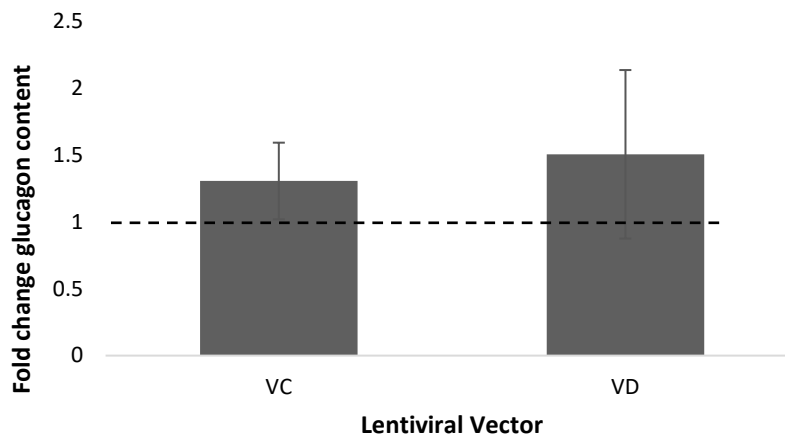


Figure 4.22 Glucagon content of INS1E cells following stable *Tle3* knockdown.

Data comparing insulin content following stable *Tle3* knockdown with constructs C and D. Data is normalised to glucagon content in cells infected with lentivirus carrying scrambled control as indicated by the dashed line. Data is expressed as mean value \pm SEM. n=3 from 3 biological repeats.

To see whether longer term *Tle3* knockdown has any effect on the function of the cells, changes in glucose stimulated insulin secretion were analysed (Figure 4.23). Following stimulation with 25 mM glucose VC showed a slight decrease in insulin secretion, however the changes did not reach significance. On the other hand, VD seemed to have an opposing effect, showing consistently increased stimulated insulin secretion compared to the scrambled control. Interestingly, when comparing the basal level of insulin secretion, significant increases were observed following knockdown of *Tle3* with VD, showing a 3.16 fold increase in insulin secretion compared to the scrambled control (Figure 4.23), resulting in a significantly reduced stimulation index (Figure 4.24). Although it did not reach significance, VC also showed a slight increase in basal insulin secretion compared to the scrambled control and a reduction in stimulation index (Figure 4.24). As a result of these changes in basal and stimulated insulin secretion the stimulation index for both cell lines were reduced however, due to the vast increase in basal insulin secretion with VD the resultant reduction in insulin secretion was significant, going from \sim 8-fold increase (from basal to stimulated conditions) in control cells to \sim 3.5-fold in VD knockdown cells. This provides evidence for the role of *Tle3* in beta cell function and suggests that loss of *Tle3* during diabetes may contribute to the loss of the beta cell phenotype.

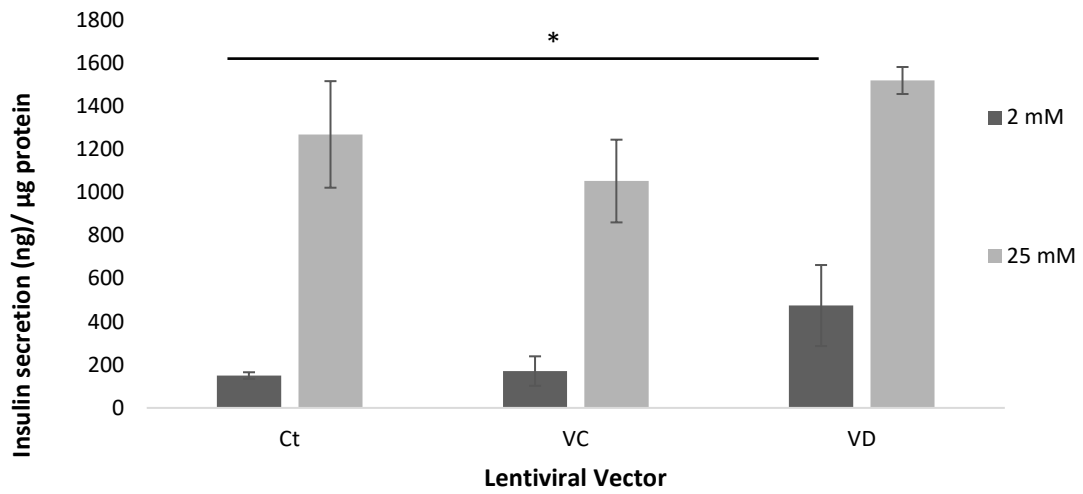


Figure 4.23 Glucose stimulated insulin secretion of INS1E cells following stable Tle3 knockdown.

Data comparing beta cell function of the two Tle3 knockdown cell lines with the scrambled control. Secreted insulin levels were measured using ELISA method from supernatant collected following a low glucose stimulation (2 mM) and a high glucose stimulation (25 mM). Data is expressed as mean value \pm SEM and normalised to total protein content. n=3 from 3 biological repeats, *p<0.05.

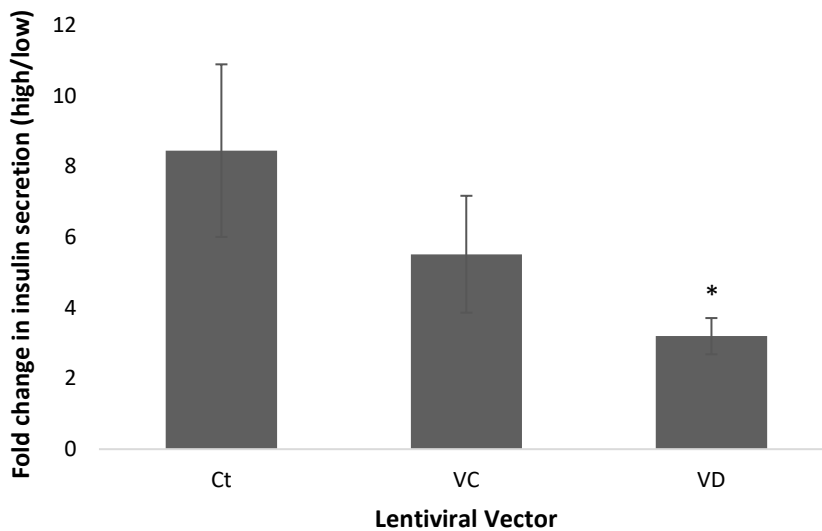


Figure 4.24 Stimulation index of control, and Tle3 knockdown cell lines.

Data comparing beta cell function following stable Tle3 knockdown. Stimulated insulin was quantified using ELISA and stimulation index was worked out by comparing secreted insulin in stimulated/basal conditions. Data is expressed as mean value \pm SEM and normalised to total protein content. n= 3 from 3 biological repeats, *p<0.05 vs control.

4.3.5 Tle3 knockdown in intact rodent islets

While the cell line models provide a good basis for understanding mechanisms occurring in the cell under different conditions and allow observation in a pure beta cell population, they lack the ability to depict what happens in a more physiological setting. As the INS1E cell line is an adherent rodent beta cell line, it does not replicate the normal niche of the beta cell i.e. in an islet, with multiple other cell types. Cell-cell interactions between the different cell types in the islet is a key factor in maintaining tight control of glucose homeostasis (119). For this reason, siRNA mediated knockdown of Tle3 was carried out using intact, isolated rodent islets. Tle3 has been previously shown to be specific to beta cells in mice (61) and therefore successful knockdown will provide insight into the role of Tle3 in the functioning of the beta cell within the islet.

Isolated islets were transfected with either scrambled control or mouse Tle3 siRNA (Table 2.3). For transfection, islets were incubated with 0.5x trypsin for 2 minutes to allow better transfection efficiency of cells in the centre of the islet. Following this, siRNA-lipofectamine complexes were set up for both probes and islets were treated in their respective conditions

(2.7.3) and left in transfection reagent for 2 days. After the initial 48 hours, islets were re-transfected (omitting the trypsin step) and left for a further 48 hours before experiments were carried out. Both the islet isolation and the transfection methods contain solutions which are harmful to cells. For this reason, viability of the islets was tested in each condition and compared to isolated, non-treated islets. Figure 4.25 shows little difference of propidium iodide (PI) staining in islets. These findings are confirmed with quantification of cell viability over several studies which shows no significant decrease in cell viability following treatment over the 5 days compared to Day 0 (Figure 4.26).

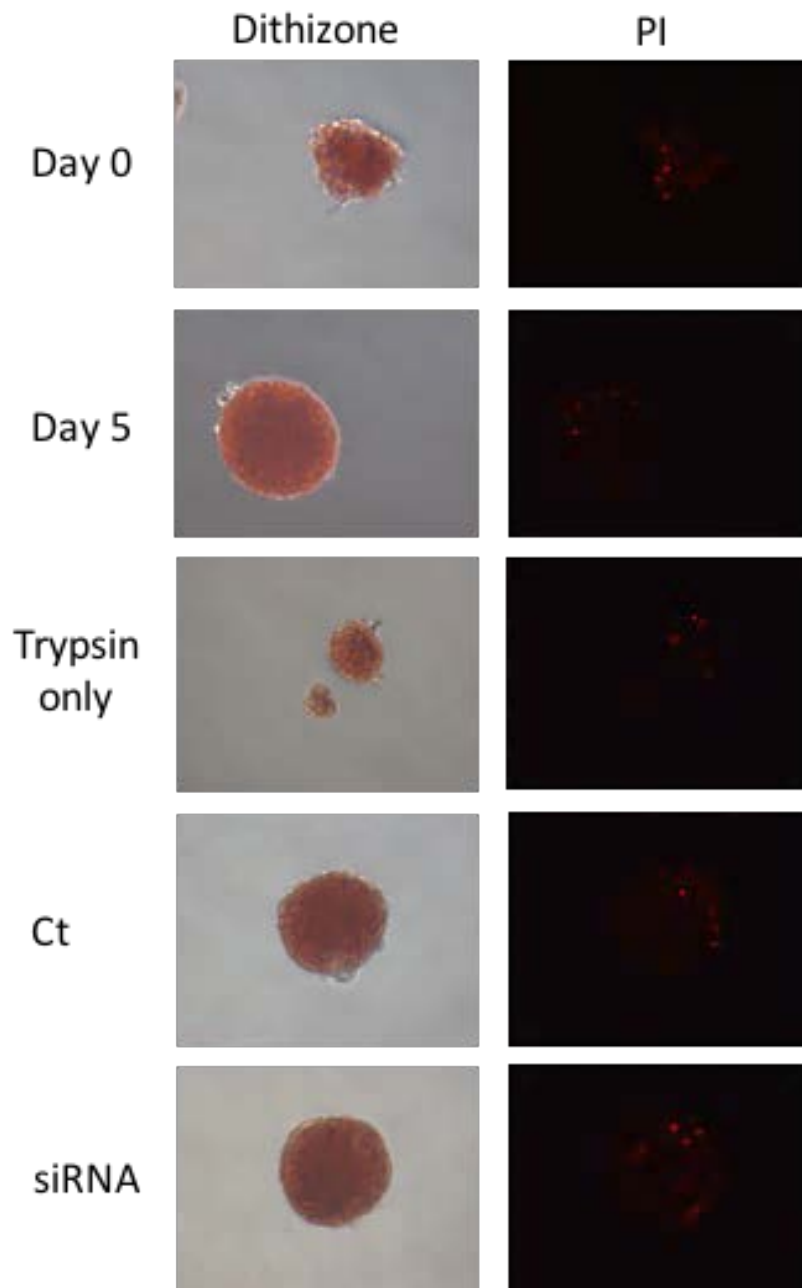


Figure 4.25 PI staining of isolated islets following different culture periods and treatments.

PI staining was set up to quantify levels of cell death. Cells were stained at Day 0 and Day 5 in the isolation process. Islets were also stained following treatment with trypsin but no transfection and following transfection with both probes. Dithizone was used identify islets. Images were taken at x20 magnification.

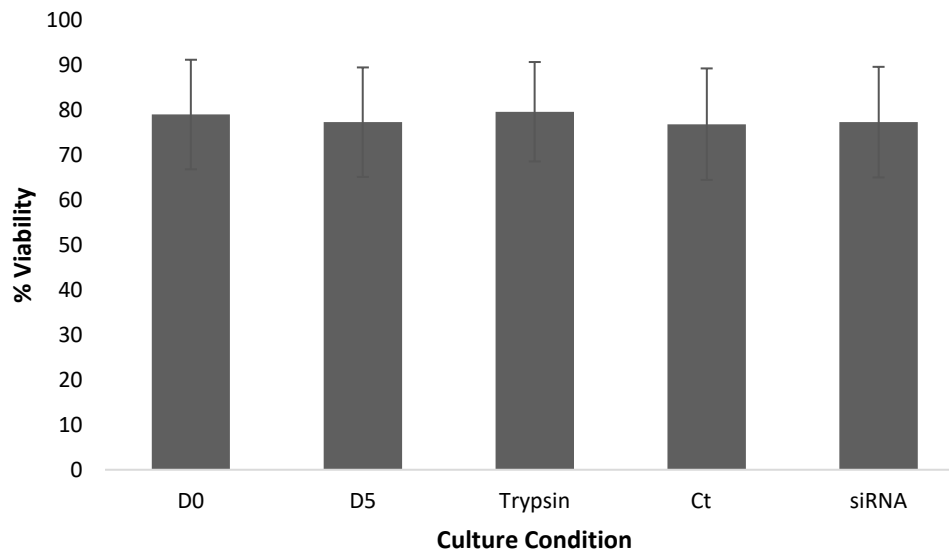


Figure 4.26 Assessment of cell viability following isolation and transfection.

Quantification of cell viability was assessed using PI staining across different conditions. All viability was carried out on Day 5 unless otherwise stated (Day 0 no transfection (D0), Day 5 no transfection (D5), Trypsin no transfection and transfection with Control (Ct) or Tle3 siRNA. A minimum of 25 islets were counted for each condition, in each individual experiment. Total % of PI positive cells were estimated for each islet and averaged over all experiments. Data is mean of three biological repeats \pm SEM.

Before proceeding with functional experiments, qPCR was carried out to see if the intact rodent islet transfections were successful. Figure 4.27 shows a significant decrease in *Tle3* mRNA expression with a 0.57-fold decrease compared to the scrambled control. Assessment of other islet cells genes were also quantified. Figure 4.28 shows gene expression for a range of beta cell genes (*Ins1*, *Ins2*, *Nkx6.1* and *Pdx1*) and alpha cell genes (*Gcg*, *Arx* and *MafB*), alongside gene expression of delta cell hormone somatostatin (*Sst*) and PP cell expressed pancreatic polypeptide (*Ppy*). All beta cell genes were downregulated apart from *Pdx1* which was consistently upregulated. *Ins1*, however, was the only gene that reached significance. When looking at the alpha cell genes there was upregulation of all three observed genes (*Gcg*, *Arx* and *MafB*), of which both *Arx* and *MafB* reached significance. No significant changes were observed for somatostatin or pancreatic polypeptide.

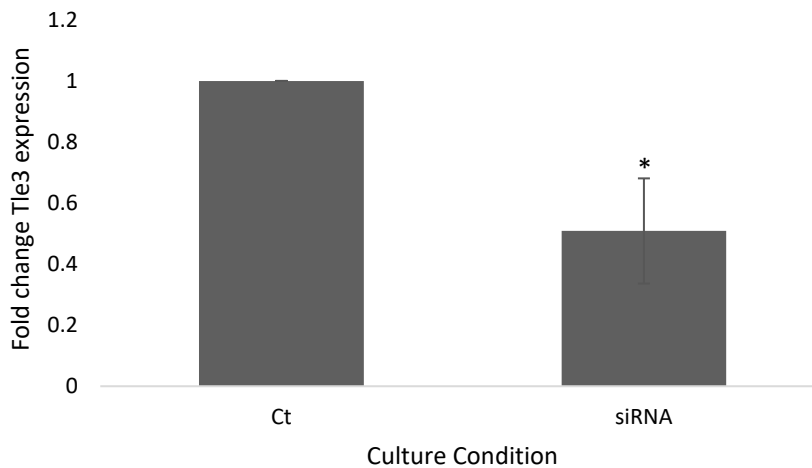


Figure 4.27 Gene expression analysis of Tie3 following siRNA mediated knockdown in intact rodent islets.

qPCR was used to detect changes in mRNA levels. Values were normalised to the scrambled control. Data is expressed as mean value \pm SEM. n=3 from 3 biological repeats, *p<0.01

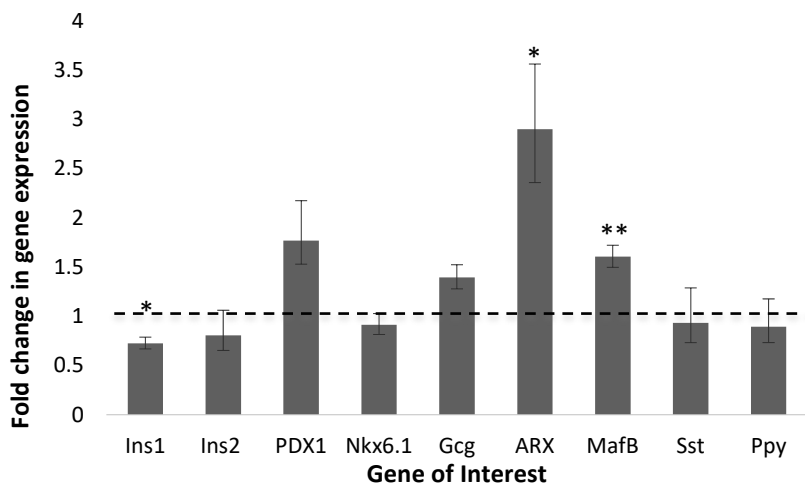


Figure 4.28 Gene expression analysis of islet genes following siRNA mediated knockdown in intact rodent islets.

qPCR was used to detect changes in mRNA levels of a range of islet cell genes. Values were normalised to the scrambled control as shown by the dashed line. Data is expressed as mean value \pm SEM. n=3 from 3 biological repeats, *p<0.05 and **p<0.01 vs scrambled control.

Alongside gene expression analysis, insulin and glucagon ELISAs were used to assess changes in islet hormone content following Tle3 knockdown. Figure 4.29 shows a modest decrease in insulin content in islets transfected with siRNA compared to the scrambled control. As seen in Figure 4.30 the fold change in insulin content was significantly decreased to 0.52x that of the control. Glucagon content is increased in islets with Tle3 knockdown (Figure 4.31). The average glucagon content significantly increased by 1.59-fold in islets with Tle3 knockdown when compared to the scrambled control (Figure 4.32).

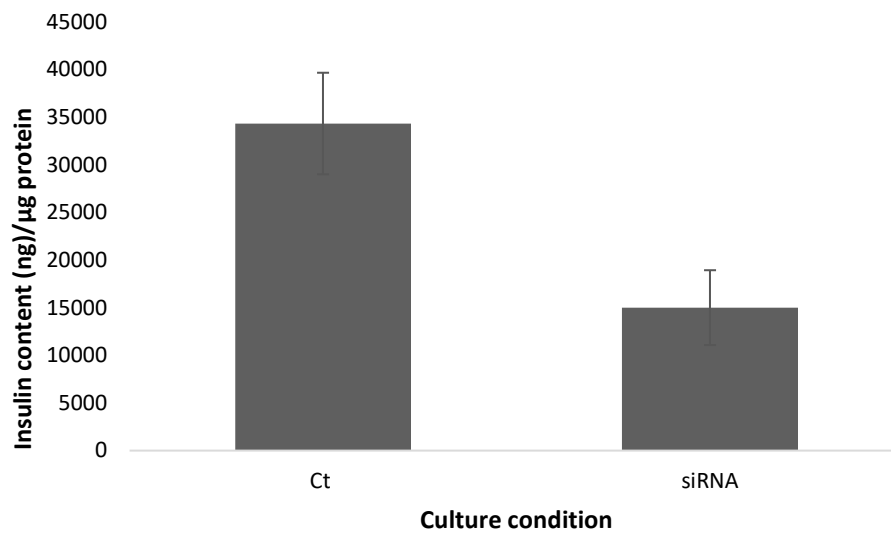


Figure 4.29 Insulin content following Tle3 knockdown in intact rodent islets.

Data comparing insulin content following Tle3 knockdown with siRNA or scrambled control. Data is normalised to total protein content. Data is expressed as mean value ± SEM. n=3 from 3 biological repeats.

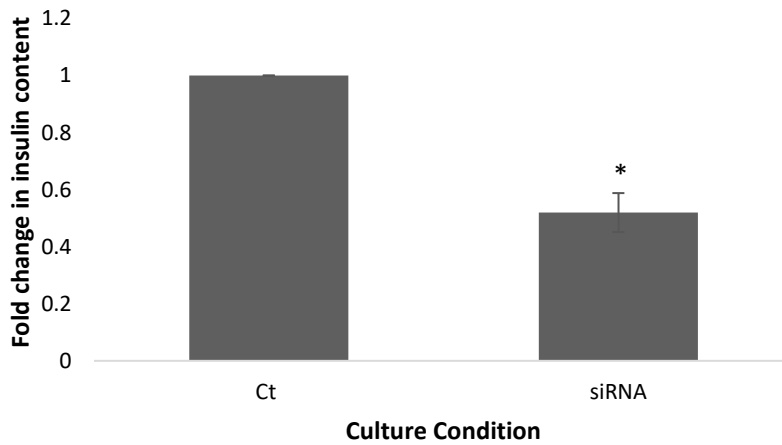


Figure 4.30 Fold change in insulin content following siRNA mediated knockdown of Tle3 in rodent islets.

Data comparing insulin content following Tle3 knockdown with siRNA or scrambled control. Data is normalised to total protein content. Data is expressed as mean fold change \pm SEM. n=3 from 3 biological repeats. *p<0.01 relative to scrambled control.

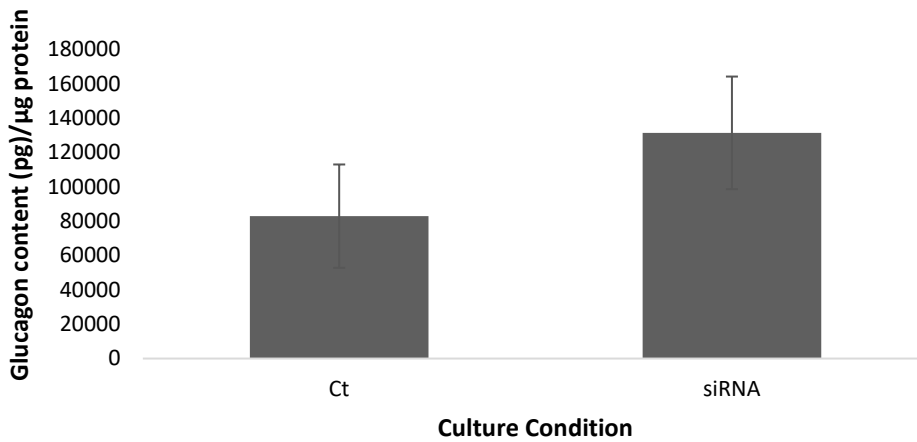


Figure 4.31 Glucagon content following Tle3 knockdown in intact rodent islets.

Data comparing glucagon content following Tle3 knockdown with siRNA or scrambled control. Data is normalised to total protein content. Data is expressed as mean value \pm SEM. n=3 from 3 biological repeats.

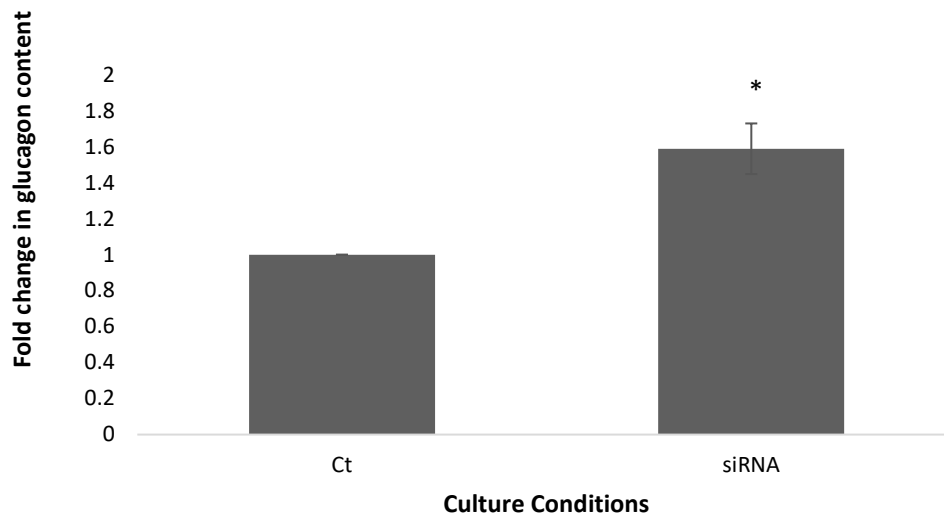


Figure 4.32 Fold change in glucagon content following siRNA mediated knockdown of *Tle3* in rodent islets.

Data comparing glucagon content following *Tle3* knockdown with siRNA or scrambled control. Data is normalised to total protein content. Data is expressed as mean fold change \pm SEM. n=3 from 3 biological repeats. *p<0.01 relative to scrambled control.

To assess the function of the islets following *Tle3* knockdown, glucose stimulated insulin secretion was employed (Figure 4.33). Basal insulin secretion was upregulated following *Tle3* knockdown by 2-fold whereas the stimulated insulin secretion was decreased to 0.59-fold. The resultant stimulation index of the rodent islets was worked out by calculating stimulated insulin secretion/ basal insulin secretion. The stimulation index was significantly decreased to 0.54-fold in transfected islets when compared to control islets. These data give evidence to support the hypothesis that *Tle3* not only suppresses the alpha cell program but also plays a role in maintaining the beta cell phenotype through regulation of beta cell genes, insulin production and the secretion of insulin in response to glucose stimulation.

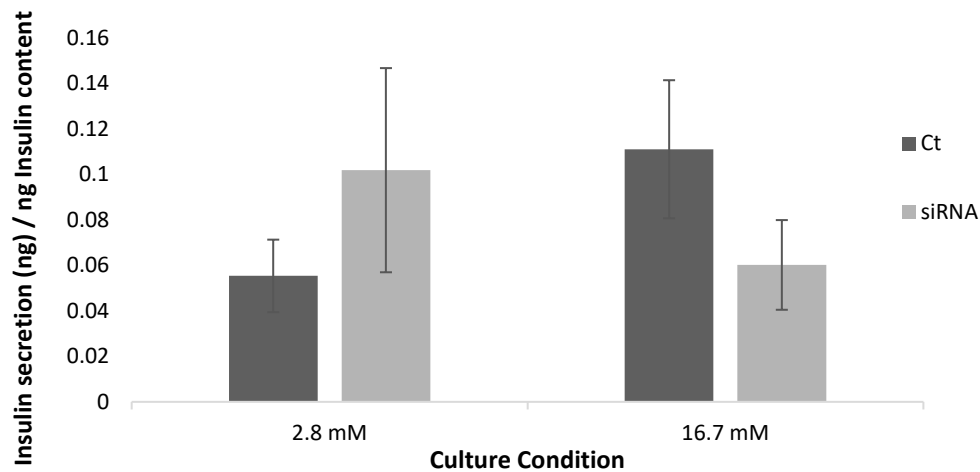


Figure 4.33 Glucose stimulated insulin secretion of rodent islets following siRNA mediated Tle3 knockdown.

Data comparing islet function of the rodent islets transfected with Tle3 siRNA or scrambled control. Secreted insulin levels were measured using ELISA method from supernatant collected following a sequential low glucose stimulation (2 mM) and high glucose stimulation (25 mM). Data is expressed as mean value \pm SEM and normalised to total protein content. n=4 from 4 biological repeats.

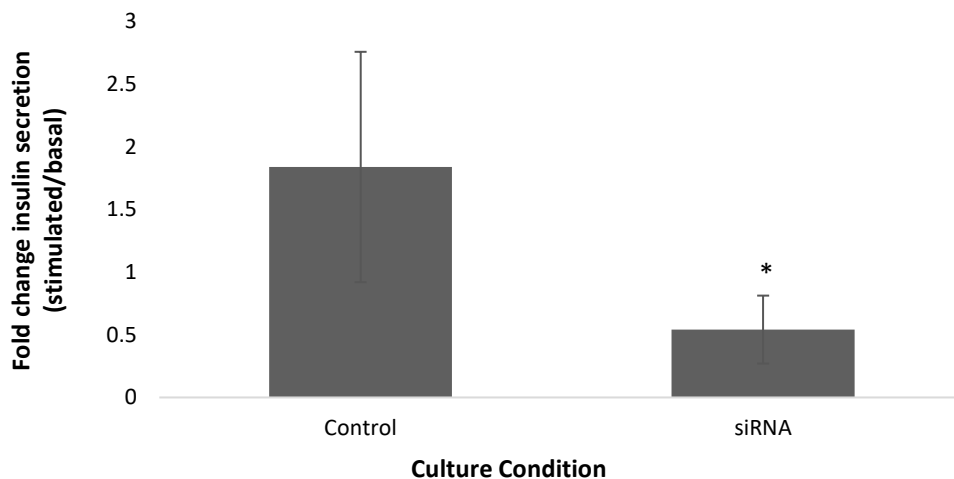


Figure 4.34 Fold change in glucagon content following siRNA mediated knockdown of Tle3 in rodent islets.

Data comparing stimulation index of rodent islets transfected with siRNA or scrambled control. Data is normalised to total protein content. Data are expressed as mean fold change \pm SEM. n=4 from 4 biological repeats. *p<0.05 vs control.

4.4 Discussion

In this chapter, the role of transducin-like enhancer of split 3 (Tle3) in maintaining beta cell function and phenotype was investigated. Gene expression analysis of *Tle3* in the INS1E model of glucotoxicity showed a significant reduction in *Tle3* gene expression (Figure 4.1) giving evidence of potential downregulation in response to glucotoxicity. A study by Metzger *et al.* indicated that interactions between Pdx1 and Tle3 were important for beta cell function (61). Specifically, ectopic expression of Pdx1 in alpha cells induced *Ins1* and *Ins2* mRNA however could not induce insulin secretion in response to glucose. In contrast, co-expression of ectopic Pdx1 and Tle3 in alpha cells not only increased *Ins1* and *Ins2* gene expression but also induced insulin secretion when stimulated with glucose (61). This study also showed that combined overexpression of Tle3 and Pdx1 in the α TC1.6 cell line generated detectable levels of C-peptide, whereas overexpression of Pdx1 and Tle3 individually did not (61). This suggests potential interaction or regulation of these proteins with the insulin processing enzymes. Looking at changes in gene expression levels of the insulin processing enzymes would be useful in future studies to help elucidate the role of Tle3 in the regulation of these proteins. This interaction between Pdx1 and Tle3 was investigated using PLA assay in INS1E cells. The results demonstrated an interaction between the two proteins which was reduced in high glucose cultured cells (Figure 4.3). This could potentially contribute to the loss of beta cell function and insulin content in high glucose cultured cells. The reduction in the interaction between Pdx1 and Tle3 may be due to either loss of interaction as a direct result of high glucose or, alternatively, a reduction in interaction due to downregulation of the two proteins in the high glucose. It would be interesting to test the loss of interaction by using techniques such as co-immunoprecipitation in the two culture conditions.

The reduction of Tle3 expression was shown to cause a shift in beta cell phenotype through reduction in beta cell genes such as *Ins2* and *Pdx1*, and increases in glucagon mRNA and protein. This apparent transdifferentiation towards an alpha cell phenotype was not unexpected as previous studies showed that Tle3 directly represses both *Gcg* and *Arx* (61, 69) to prevent activation of the alpha cell program in pancreatic beta cells. The knockdown of Tle3 in INS1E cells did not induce *Arx* expression, suggesting perhaps a loss of direct repression at the glucagon promoter rather than induction of expression through *Arx*

activation. The potential role for Tle3 in stimulated insulin secretion in response to glucose was observed in younger INS1E cells following 48 hours of Tle3 knockdown and, although there was also a slight decrease in stimulated insulin release from older cells at 48 hours, this could not be observed following 72 hours of Tle3 knockdown (Figure 4.9 and Figure 4.14). This could be explained by the increase of Tle3 expression at 72 hours compared to 48 hours which may have allowed recovery of insulin secretion.

Previous studies have shown the important role of Tle3 in endocrine differentiation, providing evidence that expression is needed immediately after Neurogenin3 (*Ngn3*) expression ceases in the developing pancreas to develop all the endocrine cell types (68). This was shown in a study looking at *Tle3*^{-/-} mice. Although most embryos die at E14.5 due to placental defects, pancreata were explanted at E12.5 from control and *Tle3*^{-/-} mice embryos to observe differentiation (68). In control pancreata, explants showed development of all endocrine cell types alongside ductal and acinar differentiation. In contrast to this, *Tle3*^{-/-} explants showed acinar and ductal differentiation but lacked almost all endocrine cell types (68). This suggests that expression of Tle3 is important in differentiation of all endocrine cell types but non-beta cell types are more likely to express Tle3 transiently, during development, whereas expression remains in the beta cell to maintain a mono-hormonal phenotype. The long-term loss of Tle3 through development of stable knockdown cell lines demonstrated changes in phenotype and function of the beta cell that suggests transition away from the beta cell phenotype. The loss of Tle3 led to downregulation of different key beta cell genes such as *Ins2* (VD) and *Nkx6.1* (VC), alongside a downregulation of insulin content, and an upregulation of glucagon gene expression and protein levels. Interestingly, although overall insulin content was decreased following stable Tle3 knockdown, gene expression for *Ins1* was shown to be upregulated in both VC and VD. It has been previously shown that *Ins1* is upregulated in *Ins2*^{-/-} null mice as a compensatory mechanism (118) which provides potential explanation for what was observed. Another possible explanation is a role for Tle3 in the regulation of the insulin processing enzymes in conjunction to gene regulation, as suggested by the previously mentioned study by Metzger *et al.* (61).

Another area of interest would be to look at *Tle3* gene regulation by *Pdx1*, as *Pdx1* was consistently upregulated following Tle3 knockdown. A possible explanation for the upregulation of *Pdx1* is as a compensation mechanism to increase Tle3 levels and restore expression to near control levels. The *Pdx1* overexpression studies demonstrated that when

INS1E cells cultured in high glucose medium *Tle3* levels are significantly reduced, however, with overexpression of *Pdx1*, there was recovery of *Tle3* levels to 0.9-fold of that of control cells.

Long term knockdown of *Tle3* in the INS1E cell line showed a bigger impact on beta cell function. In agreement with previously mentioned studies that gave evidence for a potential role of *Tle3* in beta cell function (61), the function of the beta cell was decreased in the stable cell lines with the stimulation index decreasing from 10.7- to 6.6- and 4.4-fold in control, VC and VD respectively (Figure 4.24). Although the stimulation index was decreased for both stable knockdown cell lines, VD showed over 3-fold increase in basal insulin secretion compared to the control (Figure 4.23). A study by Nagaraj *et al.* provided evidence for the increased basal insulin secretion in a rodent model of type 2 diabetes being caused by reduction in membrane rafts, which are platforms at the cell membranes of pancreatic beta cells which spatially organise membrane ion channels and proteins involved in exocytosis (80). A potential area of interest would be to look at *Tle3* mediated regulation of proteins involved in the membrane rafts to see whether this provides explanation for the increased basal insulin secretion observed. Alternatively, defects in insulin secretion could be due to changes in regulation of key proteins such as GLUT2 and glucokinase, which are both highly important proteins in glucose sensing and defects in either protein can lead to impaired beta cell development and changes in glucose stimulated insulin secretion (120, 121). Gene expression analysis of these proteins following *Tle3* knockdown would also be another area to explore.

The studies in the INS1E cell line allowed a basic understanding of the role of *Tle3* in the beta cell, however *in vitro* models using cell culture lines have limitations in representing the physiological situation of the beta cell and interactions that occur between endocrine cell types. To better explore the role of *Tle3* in the beta cell, rodent islets were used to more closely represent the microenvironment of the islets of Langerhans. Similar to the results in the cell line model, the majority of beta cell genes were decreased following *Tle3* knockdown, with the exception of *Pdx1*. Agreeing with the results from the stable *Tle3* knockdown, *Pdx1* was consistently upregulated (Figure 4.28). This gives further reason to explore the potential action of *Pdx1* at the *Tle3* promoter to induce gene expression.

The loss of beta cell gene expression was coupled to a decrease in insulin content (Figure 4.29) in islets with *Tle3* knockdown. This supports evidence provided in previous studies for

the role it may have in production of the mature insulin protein (61). Similar findings of transcription factors having dual roles in the beta cell have been shown for transcription factors such as Pax6, which showed through RNA-sequencing, ChIP-sequencing and reporter assays that Pax6 simultaneously activates transcription of beta cell genes such *Slc2a2* (which encodes the GLUT 2 transporter), *Pdx1*, *MafA* whilst also directly repressing transcription of genes required for other endocrine cell types including glucagon, somatostatin and ghrelin (87). The data presented here suggests a similar role for Tle3 as both a repressor and activator of genes in the beta cell.

Alongside the downregulation of beta cell genes, the increases in alpha cell genes for *Arx* and *MafB*, alongside elevated glucagon gene and protein expression provide further evidence a role for Tle3 in beta to alpha cell transition and support previously published studies (61). Although the INS1E cells and rodent islets showed different effects on expression of the alpha cell transcription factors, with INS1E cells showing upregulation of glucagon without *Arx* expression and the rodent islets showing upregulation of *Arx* and *MafB* expression, it may be that the expression of glucagon is affected by both the loss of repression by beta cell transcription factors (as demonstrated in the INS1E cells) and the induction of expression through alpha cell transcription factors (shown by the rodent islets). As Tle3 has been shown to act as both a co-activator and repressor in adipose tissue (122), it is possible that it is playing a similar role with the co-activation of beta cell transcription factors and repression of alpha cell transcription factors.

The function of the rodent islets following Tle3 knockdown showed marked changes to regulation of insulin secretion. In type 2 diabetes basal insulin secretion is often increased to compensate for insulin resistance alongside a decreased insulin release following glucose stimulation (123). The results observed from the rodent studies agree with this and show a potential role for Tle3 in the insulin secretion process, showing ~2-fold increase in basal insulin secretion along with a 40% reduction in stimulated insulin secretion (Figure 4.33). This led to an overall decrease in stimulation index from ~1.5 in control islets to ~0.6 in islets following Tle3 knockdown.

This chapter aimed to elucidate the role of Tle3 in maintaining the phenotype and function of the pancreatic beta cell in both a rodent cell line and isolated rodent islets. These studies have shown that Tle3 expression is reduced in high glucose and that a loss of Tle3 can affect the function of the cells and expression of some beta cell genes. These data also confirm

previous finding that Tle3 plays a role in the repression of the alpha cell lineage as loss of Tle3 resulted in increased glucagon gene expression and content in cell line models and an increase in all alpha cell genes in rodent models. Figure 4.35 demonstrates the main findings for the role of Tle3 in rodent beta cells from these studies, with effects on beta cell gene expression, hormone content and function. The potential for further studies in this area is great. The impact of Tle3 knockdown, both short and long-term, on rodent beta cell function provides evidence of its importance as a regulator of the beta cell phenotype, expanding on current publications in this area of research. The mechanisms by which Tle3 functions are yet to be elucidated and current research provides numerous possible mechanisms in which it may be involved. These are pathways such as: 1. Reduction in insulin processing enzyme production or function, resulting in lowered insulin content (61). 2. Reduced fatty acid and cholesterol production for membrane rafts, contributing to impairment in insulin secretion (80). 3. Reduced expression or function of the glucokinase enzyme, potentially resulting in reduced beta cell function (62). Further studies are needed to investigate the potential role of Tle3 in these pathways however the studies presented here show preliminary evidence of its role as a regulator of beta cell phenotype and function.

In conclusion, the data shown provides potential evidence for the role of Tle3 in beta cell maintenance, not only in repression of the alpha cell program as previous studies have indicated, but also in the regulation of key beta cell genes and in insulin secretion in response to glucose challenges.

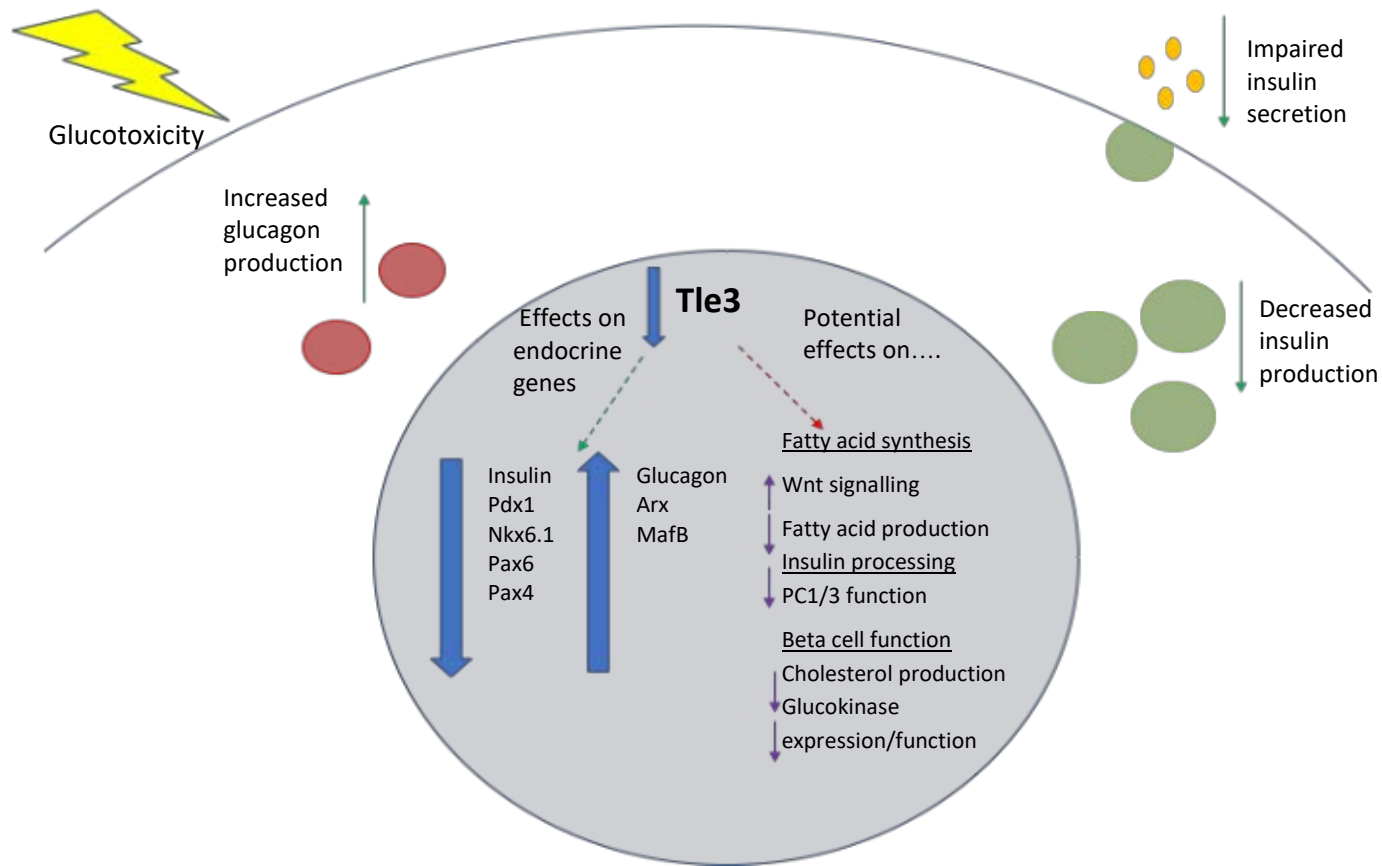


Figure 4.35 Effects of Tle3 knockdown on rodent beta cells and potential mechanisms by which these effects may occur.

Down regulation of Tle3 gene expression results in reduction in beta cell genes and increases in alpha cell genes, alongside changes in production of their respective hormones and impairment of both basal and stimulated insulin secretion (green arrows). Potential mechanisms by which this may occur (red arrow) are those such as dysregulation of cholesterol and fatty acids for use in membrane rafts or through effecting production/function of key beta cell enzymes such as glucokinase.

5 Results (3)

Assessing the impact of the loss of TLE1 on beta cell phenotype in human type 2 diabetes

5.1 Introduction

There has been increasing evidence over the past few years of beta cell plasticity in human diabetes which supports the hypothesis that beta cell dysfunction contributes greatly to the decline in insulin secretion in type 2 diabetes. A study by Spijker *et al.* looking at human pancreas sections demonstrated a marked increase in insulin and glucagon co-expressing cells from $0.52 \pm 0.18\%$ in control donors to $4.05 \pm 1.37\%$ in type 2 diabetic donors. To confirm that the pancreatic beta cells were undergoing identity change, pancreas sections were analysed for presence of glucagon expressing cells containing nuclear NKX6.1 as further confirmation of transdifferentiation (124). The presence of bihormonal cells has been confirmed in other studies using different cohorts of control and diabetic patients (100) and also in a study looking at sections from patients who had undergone islet transplantation (125). These both showed co-localisation of insulin and glucagon in human islets following different the stresses. This provides evidence that transdifferentiation may be a common default pathway in human beta cells to avoid different metabolic stresses, such as hyperglycaemia associated with type 2 diabetes or hypoxia associated with islet transplantation.

The role of the Groucho proteins in animal pancreas development is important to ensure production of all endocrine cell types (116). Although all of the Groucho proteins are thought to be expressed at some point during pancreatic development, Tle2 and Tle3 have been shown to be important in determining the beta cell phenotype in rodent models of animal development (67). This has been backed up by studies showing the importance of Tle3 in maintaining mono-hormonal beta cell identity through *Tle3* knockout in a beta cell line, resulting in increased *Gcg* and *Arx* expression (61). This study also demonstrated that overexpression of *Tle3* in an alpha cell line resulted in repression of *Arx* and *Gcg* alongside glucose stimulated insulin secretion when co-expressed with *Pdx1* (61). Alongside these rodent studies, Metzger *et al.* provided evidence that the Groucho protein TLE1 is the human functional equivalent of Tle3 in rodents, showing abundant TLE1 staining in human beta cells but not in alpha cells. Overexpression of *TLE1* also repressed *GCG* and *ARX* in alpha cells in a dose-dependent manner (61). In support of the function of TLE1 in beta cell maintenance, a study of 5739 European subjects found a single nucleotide polymorphism (SNP) in the *TLE1* loci to be a risk allele for type 2 diabetes (126). Another study of European woman showed TLE1 being associated with increased risk of gestational diabetes (127).

Gestational diabetes is known to be a result of the insulin resistance associated with pregnancy, therefore woman who are already predisposed to insulin resistance may develop the disease (128). If the *TLE1* loci is associated with increased risk of gestational diabetes this suggests that TLE1 could play a role in sensitivity to insulin as SNPs in this region predisposes patients to insulin resistance.

Although these studies suggest a role for TLE1 in beta cell maintenance, most of these studies are rodent models and evidence for the role of TLE1 in human beta cells is lacking both in control and diabetic patients.

5.2 Aims

How TLE1 is affected during type 2 diabetes is yet to be elucidated. Given its suggested role in maintaining the beta cell phenotype and previous findings investigating the rodent functional equivalent, Tle3, it is important to determine the role of TLE1 in the human beta cell. In this chapter, studies using human pancreas sections were set up to see whether TLE1 plays a role in changes in beta cell phenotype during type 2 diabetes.

Specific aims were:

1. To investigate changes in TLE1 expression in human type 2 diabetes
2. To see whether these changes are associated with a shift in beta cell phenotype
3. To assess the impact of loss of TLE1 on the beta cell phenotype and function

5.3 Results

The recent clinical evidence of reversal of type 2 diabetes through restoration of beta cell function warrants further study to understand the mechanisms behind beta cell dysfunction in diabetes. Evidence from previously mentioned studies, showing co-localisation of insulin and glucagon in human diabetic patients (129), give strength to the hypothesis of beta cell plasticity playing a part in the loss of function. Although evidence for bihormonal beta cells has been shown, it is not clear what regulatory mechanisms are changing in the beta cell to make it express more than one hormone. The role of the Transducin-like enhancer 3 (Tle3) protein has been shown, in rodent models, to play a part in maintaining the beta cell phenotype through repression of the alpha cell phenotype (61). The studies shown in Chapter 4 provide supporting evidence to these previously published studies, demonstrating interactions with key beta cell transcription factors Pdx1 and Nkx6.1, alongside a role in glucose stimulated insulin secretion. However investigation of its human counterpart, TLE1, and the role it plays in the beta cell, still remains relatively unexplored. The identification of the *TLE1* loci as a potential diabetes risk allele (126) provides a basis for further investigation. The following studies aim to investigate the expression of TLE1 in two different cohorts of human pancreas sections from deceased donors with type 2 diabetes and controls without diabetes.

5.3.1 Cohort 1- Donor information

Cohort 1 consisted of 16 donors, 7 control donors and 9 type 2 diabetic donors (Table 5.1 and Table 5.2 respectively). Where possible, the controls were age-matched with the diabetic patients.

Study Number	Age	Description
132/67	46	ND adult; cirrhosis
77/87	57	Pneumonia
44/66	60	ND adult; CVA, renal failure
202/75	60	ND adult; cerebral vascular accident
64/67	69	ND adult; Gall bladder cancer
37/66	70	ND adult; Myocardial infarction
329/66	76	ND adult; PTE

Table 5.1 Cohort 1- Donor information for control pancreas sections sourced from Exeter Archival Diabetes Biobank.

Study Number	Age	Description
261/67	46	T2D; Recently diagnosed died of hyperglycemia
38/66	56	T2D; 3/12 months duration
150/87	58	T2D; myocardial infarction
184/66	60	T2D; myocardial infarction
230/66	69	T2D; Newly diagnosed; diverticulitis
168/69	70	Type II Diabetes; Uncertain at PM
364/66	73	T2D; 13y duration, meningitis
PM28/70	74	Type II Diabetes; heart failure
379/71	75	T2D; diabetic coma

Table 5.2 Cohort 1- Donor information for diabetic pancreas sections sourced from Exeter Archival Diabetes Biobank.

5.3.2 Cohort 1- Counting and analysis

Following staining of sections with insulin, glucagon and TLE1 (for method see 2.9.1), analysis of the cells was carried out independently by two different observers. Cells in the islet were marked for expression of each protein on their individual channels using the cell counter tool in the ImageJ software. This tool enabled cells expressing each protein to be labelled with a different colour marker (2.10.1). Once all cells on each channel were marked, the number of cells with each phenotype could be counted (i.e. How many cells were Ins⁺/Tle⁺/Gcg⁻, Ins⁺/Tle⁻/Gcg⁻, Ins⁺/Tle⁺/Gcg⁺, Ins⁺/Tle⁻/Gcg⁺, Ins⁻/Tle⁺/Gcg⁺ and Ins⁻/Tle⁻/Gcg⁺). Where possible, 50 islets were counted per donor. Both observers were blinded from which donors were control patients and which donors had type 2 diabetes.

5.3.3 Cohort 1- Does glucagon expression increase in type 2 diabetes?

If pancreatic beta cells undergo a transition from a beta- to an alpha-like cell phenotype during the type 2 diabetes, it would be expected that islets from diabetic donors would contain a higher number of glucagon positive cells. To investigate this, the average percentage of all glucagon expressing cells per islet was calculated for both observers 1 and 2 and were compared between control and diabetic donors (Figure 5.1). Significant increases in the number of glucagon expressing cells were seen by both observers.

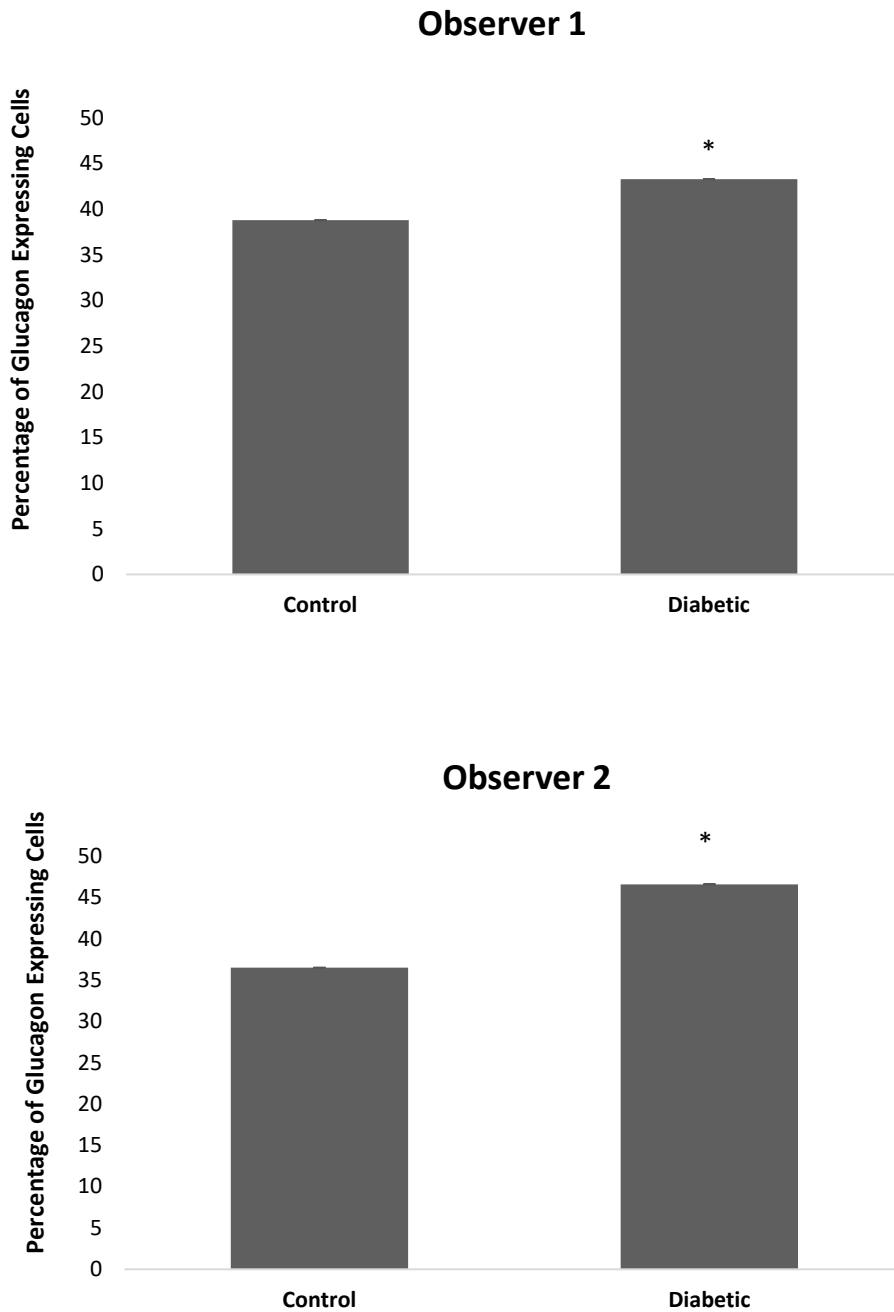


Figure 5.1 Average percentage of glucagon expressing cells per islet in control and diabetic patients.

Graphs show data for observer 1 and 2. Data are expressed as average of all islets in all control donors and all islets in all diabetic donors±SEM. n=348 islets for control donors, n=472 islets for diabetic donors, *p<0.01 vs control using unpaired student's t-test.

5.3.4 Cohort 1- Is there an increase in bihormonal cells in type 2 diabetes? In conjunction with an increase in glucagon expressing cells, if beta cells undergo transdifferentiation from beta to an alpha cell type, it would be expected that there would be a subset of cells that could be identified as expressing both insulin and glucagon in the type 2 diabetic donor tissue. Figure 5.2 and Figure 5.3 depict the average insulin, bihormonal and glucagon cells as percentage of total cell number in control and diabetic donors counted for observers 1 and 2 respectively. Observer 1 identified $7.7 \pm 0.07\%$ in type 2 diabetic donors versus $4.4 \pm 0.06\%$ in control tissue (a 1.75-fold increase in number of bihormonal cells). This finding is supported by Observer 2 which showed $5.8 \pm 0.07\%$ in type 2 diabetic donors versus $3.5 \pm 0.05\%$ in control donors (a 1.65-fold increase in bihormonal cells).

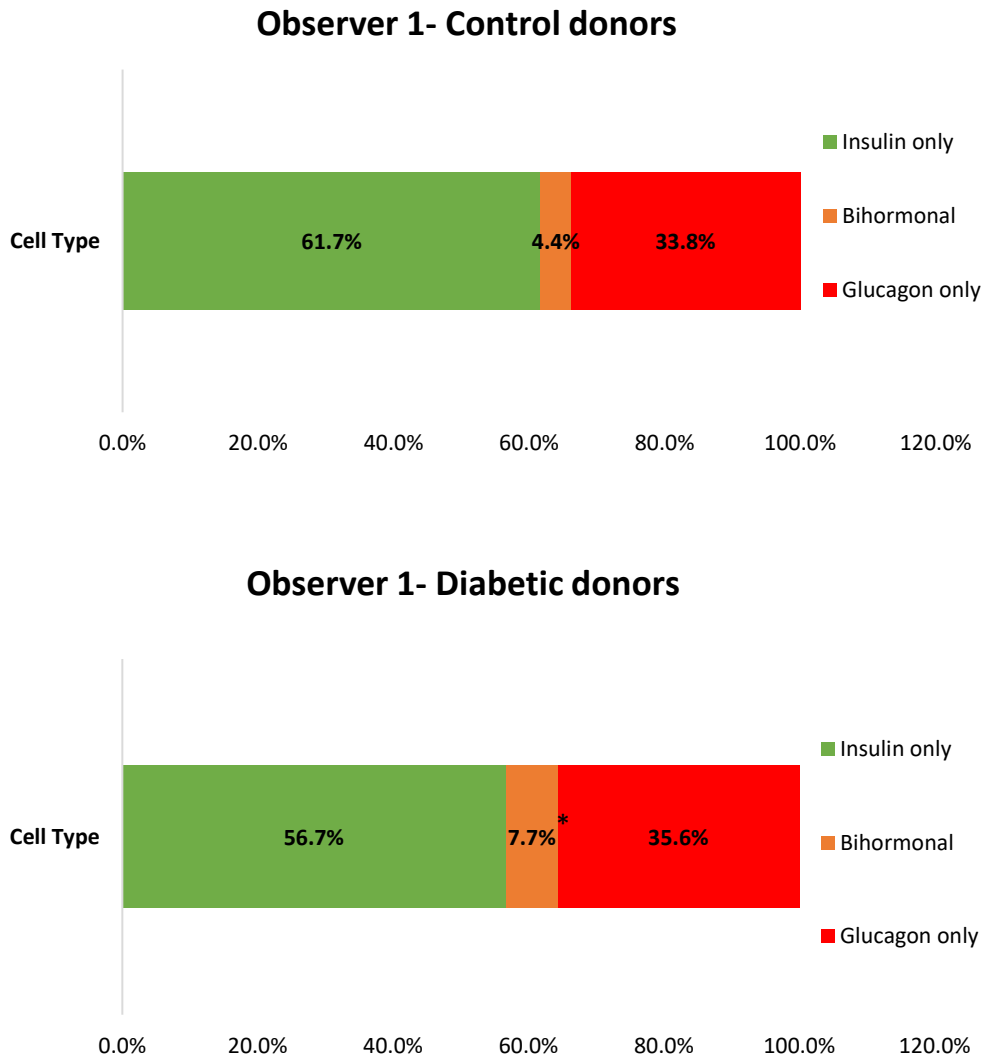
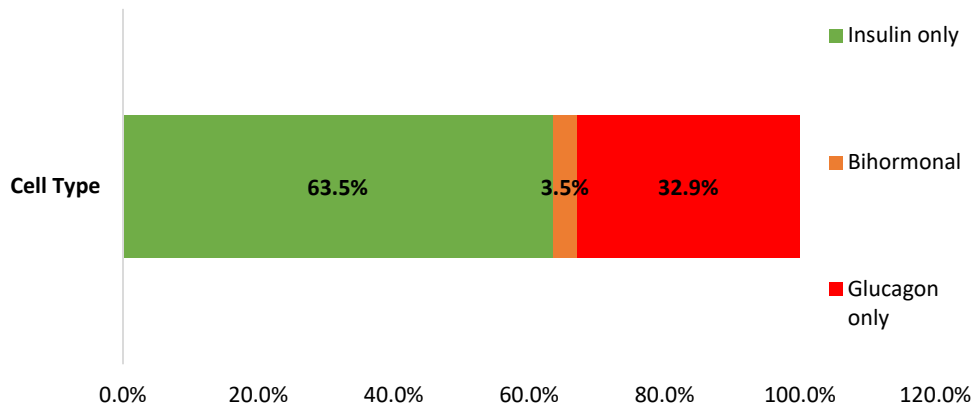


Figure 5.2 Average percentage of cell types in control and diabetic donors for Observer 1.

Data show combined average percentage of each cell type for all donors in either group. Bihormonal cells = $4.4 \pm 0.07\%$ for control and $7.7 \pm 0.06\%$ for diabetic donors, $*p < 0.01$ vs percentage of bihormonal cells in control donors using an unpaired student's t-test. n=348 control donors and n=472 diabetic donors.

Observer 2- Control Donors



Observer 2- Diabetic Donors

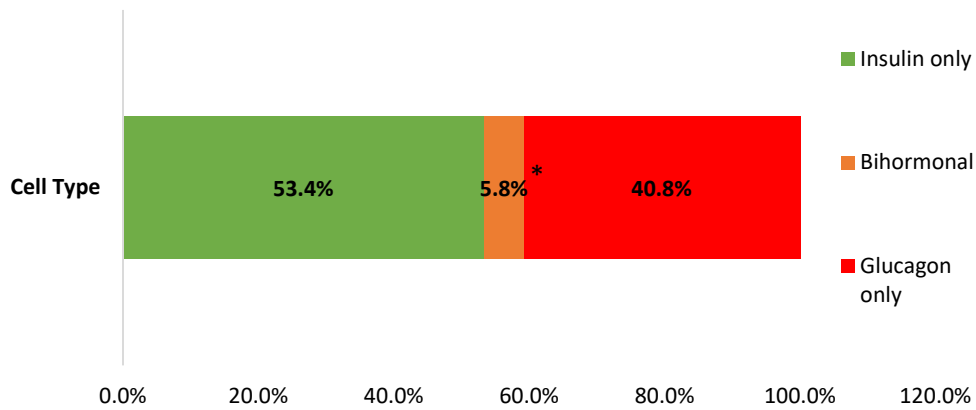


Figure 5.3 Average percentage of cell types in control and diabetic donors for Observer 2.

Data show combined average percentage of each cell type for all donors in either group. Bihormonal cells = $3.5 \pm 0.05\%$ for control and $5.8 \pm 0.07\%$ for diabetic donors, $*p < 0.01$ vs percentage of bihormonal cells in control donors using an unpaired student's t-test. $n=348$ control donors and $n=472$ diabetic donors.

5.3.5 Images of islets from tissue with and without type 2 diabetes

Examples of islets from both control and diabetic tissue can be seen in Figure 5.4. This image demonstrates consistent staining across 4 donors from control tissue (top line) and 4 from the diabetic tissue (bottom line) for both insulin and glucagon expression. Examples of the different phenotypes can be found in Figure 5.5. The top row shows an islet from a control donor. Control donors showed separate staining for insulin and glucagon and only few bihormonal cells were identified across all donors. The bottom row shows an islet from a diabetic donor. Although most cells are either glucagon or insulin positive, there were some cells identified that appeared to express both endocrine hormones (yellow arrow). A further example of islets in control and diabetic tissue can be seen in Figure 5.6. The top line shows a control islet that shows no co-localisation of insulin and glucagon. The bottom row shows an islet from a diabetic donor. A bihormonal cell co-expressing insulin and glucagon is indicated by the white arrow. Further analysis of the higher magnification image shows the expression profile for the cell cross-sectioned by the pink arrow. This confirmed overlapping expression of insulin and glucagon. These images are representative of the different phenotypes counted to produce the data for Figure 5.2 and Figure 5.3.

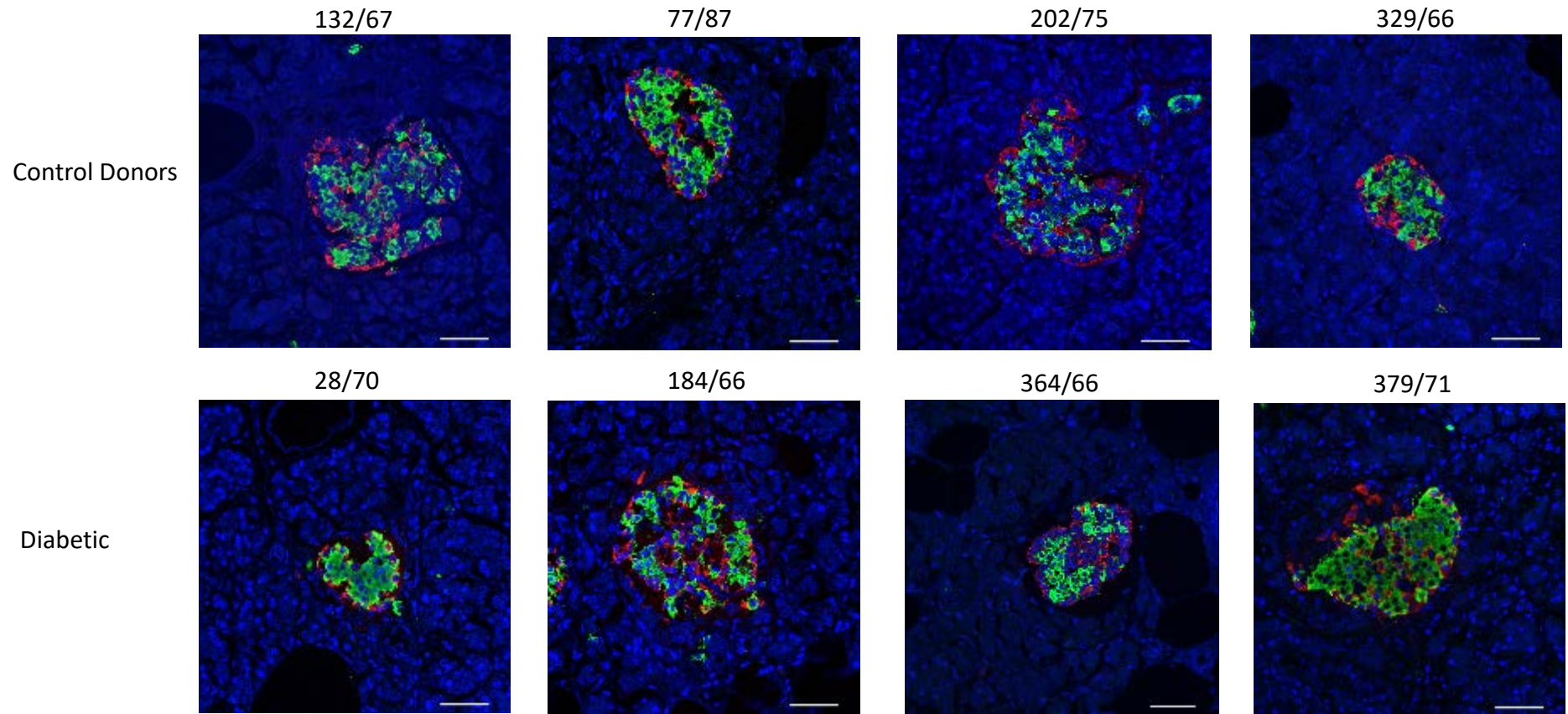


Figure 5.4 Representative images from a range of donors in Cohort 1.

Islets from 4 control donors (top line) and 4 type 2 diabetic donors (bottom line) show consistent staining of insulin (green) and glucagon (red) stain throughout the cohort alongside nuclear counterstain DAPI (blue). Although there was some variation in intensity, all stains could be easily identified for all donors. Scale bar =50 μ M.

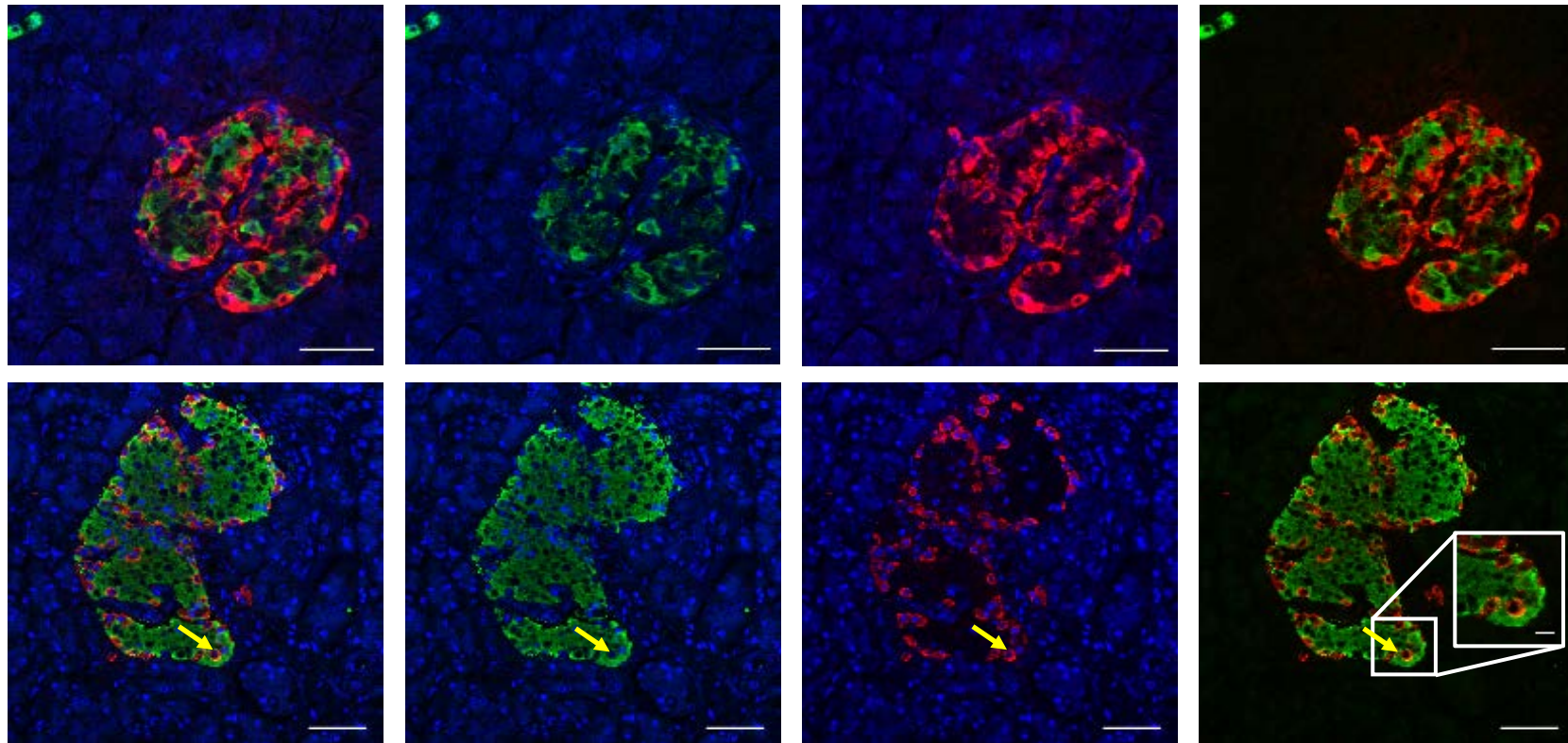


Figure 5.5 Example islet from control donor (top line) and diabetic donor (bottom line).

Images were stained with insulin (green) and glucagon (red) and counterstained with nuclear stain, DAPI (blue). Control tissue showed no cells expressing both insulin and glucagon. In type 2 diabetic tissue, bihormonal cells were observed, expressing both insulin and glucagon (yellow arrow). Scale bar = 50 μ M, higher magnification inset scale bar = 10 μ M.

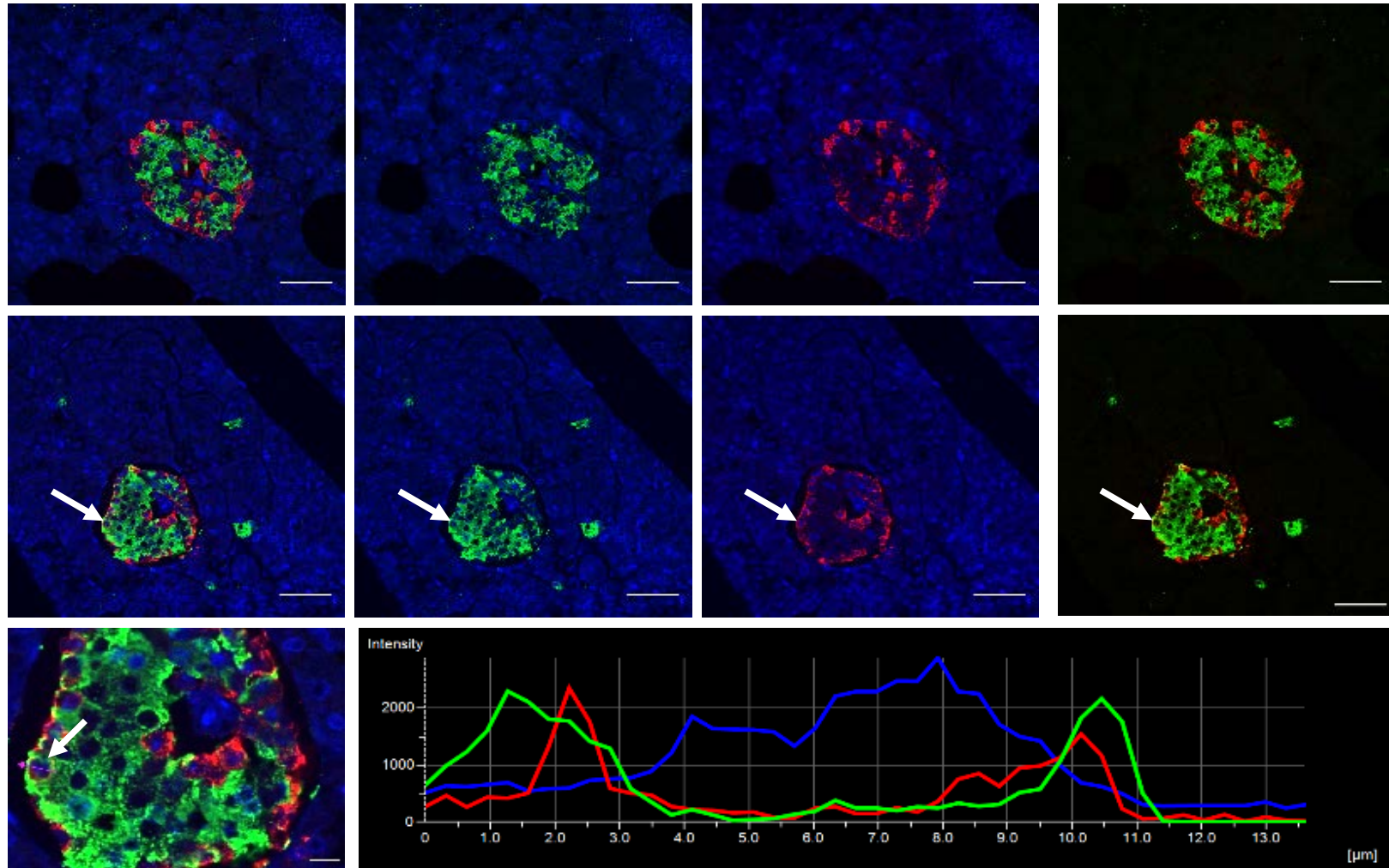


Figure 5.6 Images of insulin and glucagon co-localisation Cohort 1.

Islet from a control donor (top line) shows no insulin/glucagon co-localisation. Islet from diabetic donor (middle line) identifies cell expressing both insulin and glucagon (white arrow). The magnified image shows further identification of bihormonal cell, as indicated by pink arrow and expression profile (bottom line). Scale bar =50 μM . Magnified image scale bar =10 μM .

5.3.6 Cohort 1- Is TLE1 reduced in Type 2 diabetes?

To determine the role of TLE1 in human type 2 diabetes, TLE1 counts were carried out alongside insulin and glucagon. The TLE1 counts between count 1 and 2 were far more varied and often differed significantly. The staining for TLE1 was carried out using horseradish peroxidase (HRP) staining rather than immunofluorescent (IF) staining due to the inability to detect the protein using the latter technique. This could potentially be because of the age and condition of the tissue used or the donor status (i.e. heart beating vs post-mortem). Previous studies looking at the cyclin-D1 and D3 transcription factors showed that, in post mortem donors, these transcription factors were translocated to the cytosol where, in the case of cyclin-D1, degradation may occur. In contrast to this, this study also showed that in heart-beating donors these transcription factors remained exclusively in the nucleus (130). It is possible that a similar translocation occurs with TLE1 post-mortem and this may have contributed to the difficulty in detecting the stain using IF. The identification of positively stained cells using HRP was not as clear as the IF stain. Alongside this, combined HRP and IF staining caused dampening of the IF signal making it harder to identify dual positive cells (Figure 5.7).

Examples of the TLE1 staining are shown in Figure 5.7 which shows 3 different islets from the same donor. The top row shows composite images with both insulin and TLE1 staining. This image is shown at a higher magnification on the bottom row. Overlaying the insulin and TLE1 channels makes the identification of the TLE1 easier to distinguish the positive stain from the background. Although the TLE1 is easier to identify from the background signal with the insulin channel on, the fluorescent signal for the insulin is dampened by the HRP. These images also provide examples of the variation of staining intensity within islets in the same donor. Islet 1 shows much weaker staining for TLE1 than islet 2 and 3. Alongside this, the intensity of staining within the same islet also differs greatly, making it hard to determine which cells are negative for TLE1 and which show a weak positive stain. As the identification of the weaker stained TLE1 positive cells was difficult to judge, this may have played a part in the variation between counts 1 and 2. For these reasons, the TLE1 data for Cohort 1 has been left out of further analysis.

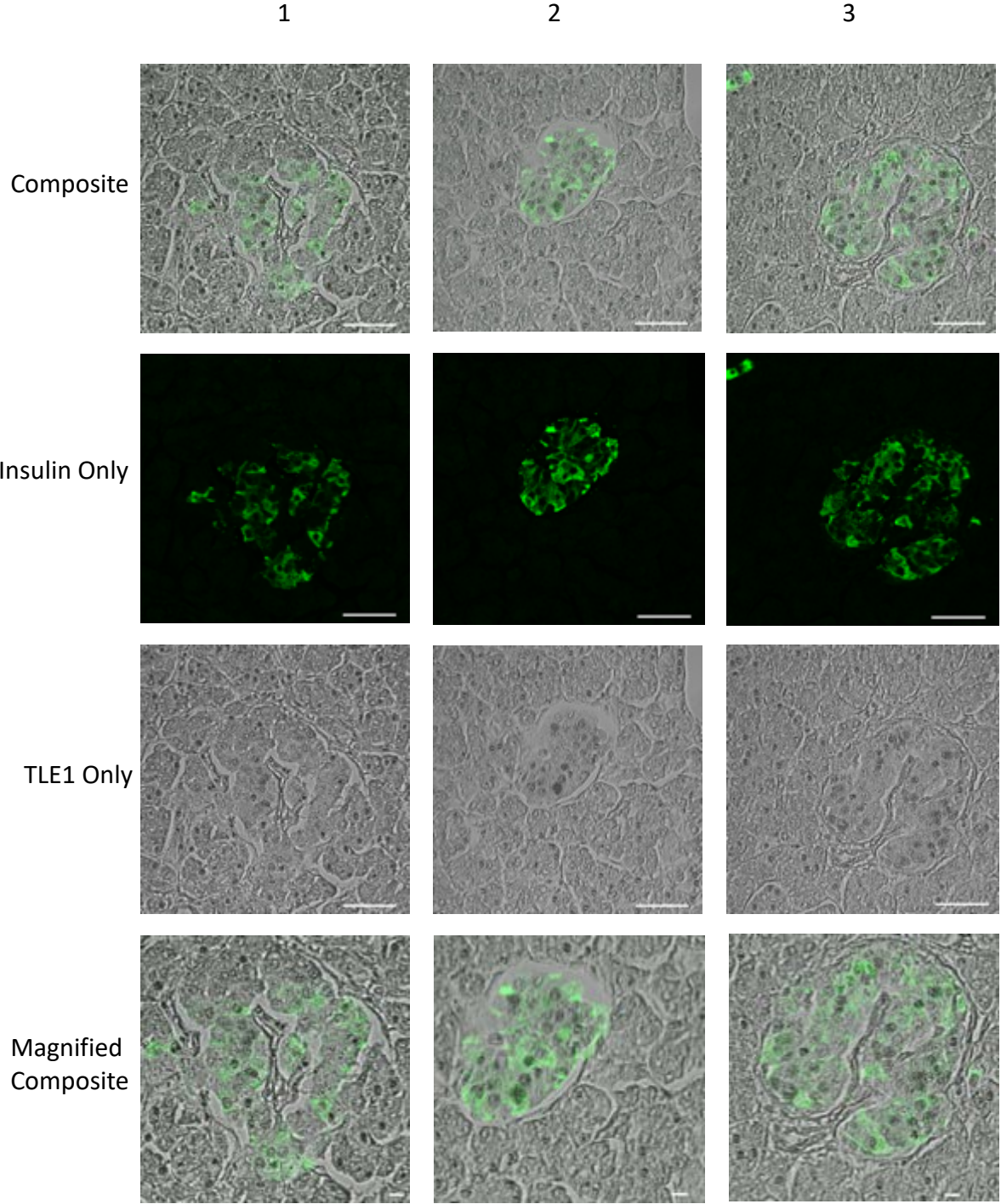


Figure 5.7 Islets showing TLE1 and insulin staining in 3 islets from a single donor.

Images show insulin (Green) and TLE1 (Grey). Scale bar = 50 μ m, magnified images scale bar = 10 μ m.

5.3.7 Cohort 2- Donor information

Due to the poor TLE1 staining in the first cohort of donors, the analysis was repeated on a second cohort of donors, provided by the MacDonald Islet Biology Laboratory at the University of Alberta, to assess TLE1 expression in the beta cell. This cohort of patients consisted of 10 type 2 diabetic donors with 9 age and BMI matched controls. The donor information is shown in Table 5.3 and Table 5.4.

Donor ID	BMI	Age	Sex	HbA1c	No. Islets Counted
R026	28.5	68	F	5.3	36
R044	24.7	38	M	5.9	46
R104	27.1	42	M	5.4	11
R146	25.3	52	M	5.5	49
R147	26	62	M	5.4	33
R149	41.2	47	M	5.9	63
R166	35.8	54	M		45
R194	32.3	54	M	5.7	63
R214	34.9	49	M	5.9	49

Table 5.3 Donor information from control tissue in cohort 2 sourced from University of Alberta Islet Core Biobank.

Average age = 51.78 ± 2.93 , Average HbA1c = 5.63 ± 0.08 mmol /L

Donor ID	BMI	Age	Sex	HbA1c	Duration (Years)	No. Islets Counted
R057	35.5	53	F	10.3	20	29
R059	28.1	68	F			42
R064	28.1	36	M	10.9	1.5	32
R068	26.7	45	F		5	43
R078	35.3	47	F	5.9	6	58
R110	26.8	41	M	9.3	2	35
R131	26	52	M	6.8		32
R133	34.1	53	M	5.6	2	50
R170	38.6	49	M	6.5	3	76
R192	26.9	63	M		15	54

Table 5.4 Donor information from diabetic tissue in cohort 2 sourced from University of Alberta Islet Core Biobank.

Average age = 50.7 ± 2.87 years, Average HbA1c = 7.9 ± 0.77 mmol /L

5.3.8 Cohort 2- Staining of TLE1

Due to the previous issue with the TLE1 stain, TSA protocol was employed to enhance staining of TLE1 and ensure easy identification for analysis. Below are shown representative islets from control and diabetic donors to demonstrate consistent staining across the whole cohort. Although there is some variation in intensity between donors, this is not unexpected and all positive cells were easy to identify on all channels (Figure 5.8). Figure 5.9 and Figure 5.10 show an islet from a control and diabetic donor respectively. Firstly, the images show that the IF TLE1 stain worked well with the TSA kit and it is easy to distinguish positively and negatively stained cells. This allowed further analysis of all phenotypes in the islet. By first observation there is a decrease in TLE1 staining in the diabetic islet, with a lot less TLE1 positive insulin+ cells compared to the control islet; which shows the majority of insulin+ cells positive for TLE1. There is also a marked increase in glucagon expression in the diabetic islet compared to the control. Alongside these apparent changes in TLE1 and glucagon expression there were insulin positive cells identified that had lost TLE1 expression and started to co-express glucagon (indicated by white arrow) in the diabetic islet (Figure 5.10). To further demonstrate the different phenotypes, Figure 5.11 shows another islet from control (top line) and diabetic (bottom lines) donor. The arrow on the diabetic islet indicates a bihormonal cell expressing both insulin and glucagon. This can be seen in the higher magnification image. The expression profile of this cell is shown in the spectral plot and confirms overlapping expression of the insulin and glucagon channels. To quantify these changes, an automated counting method using the Vectra system (2.10.2) was employed for all donors.

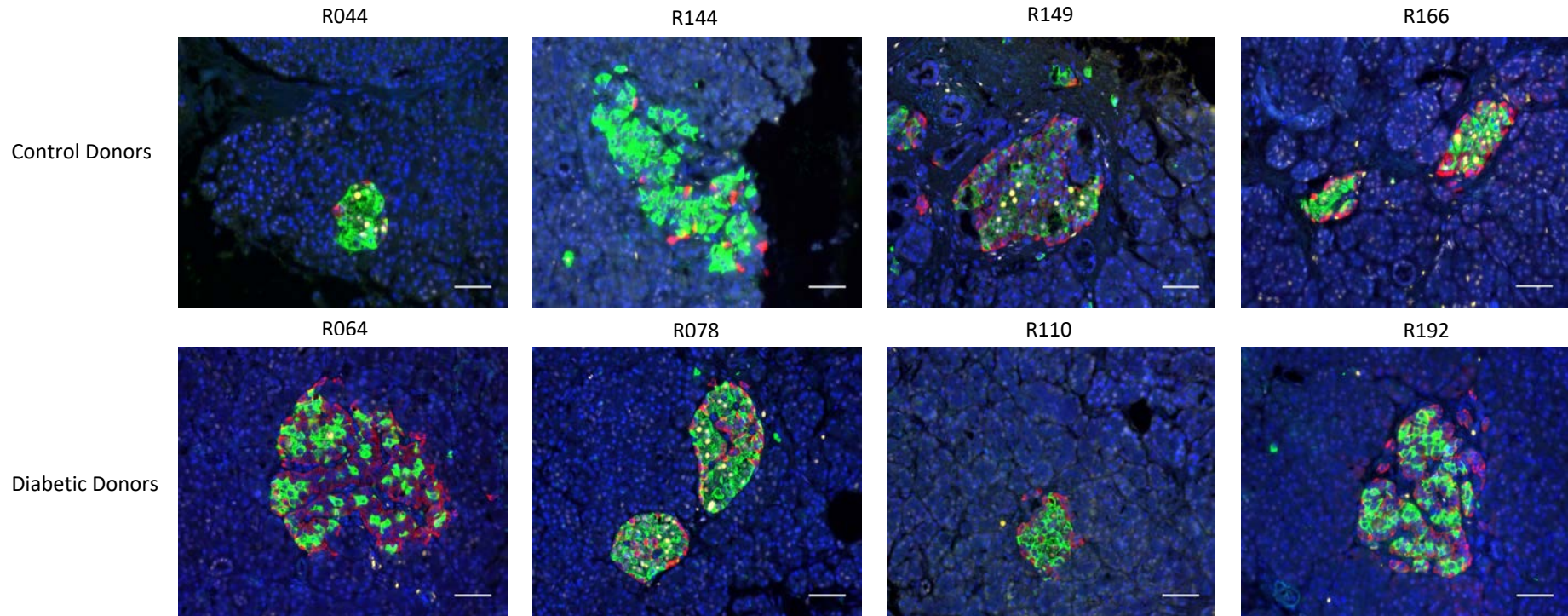


Figure 5.8 Islets from control and diabetic donors of cohort 2.

Islets were stained for insulin (green), glucagon (red), TLE1 (yellow) and counterstained with DAPI (blue). Islets from 4 control donors and 4 diabetic donors are shown as representative images of Cohort 2. Scale bar =50 μ M.

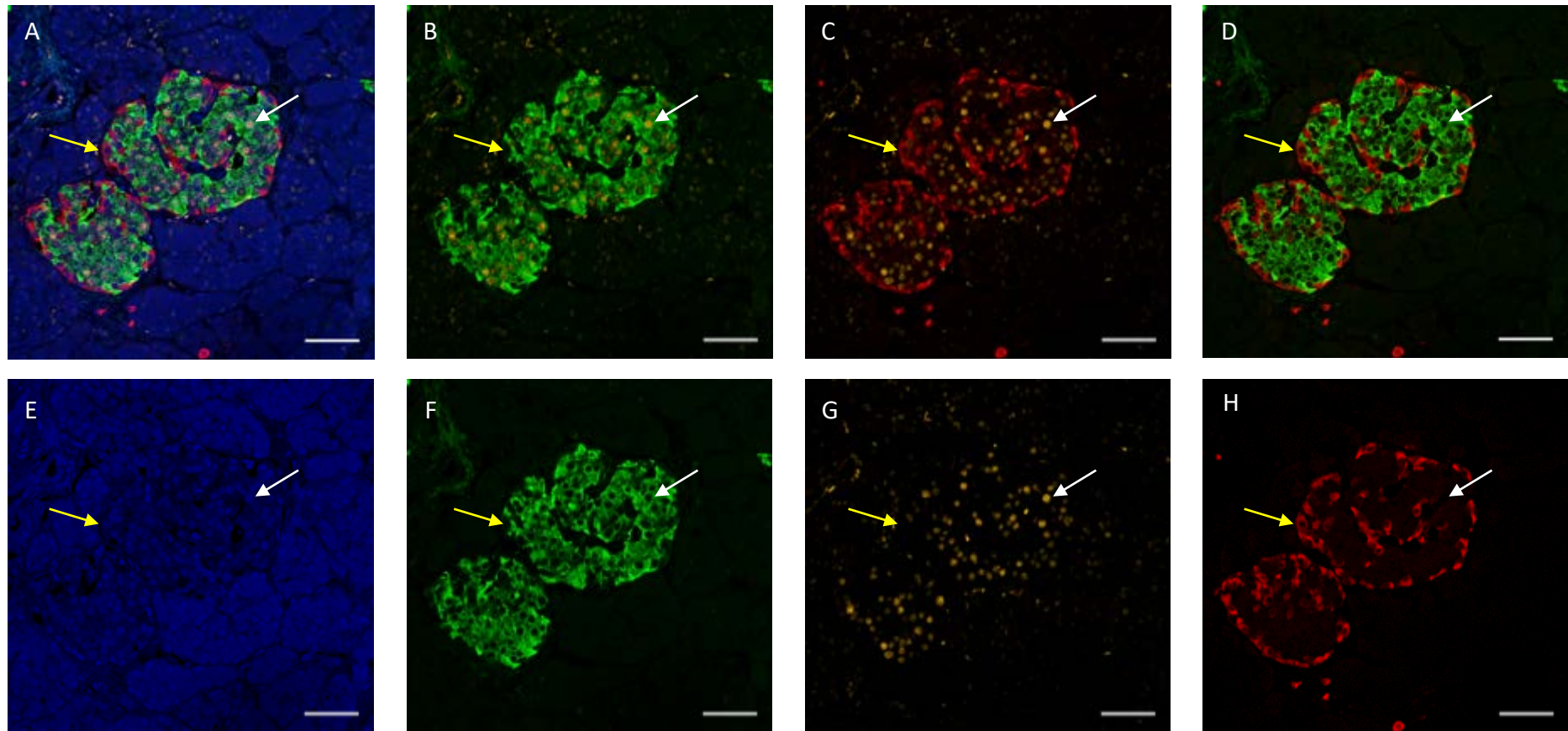


Figure 5.9 Islet from control donor of cohort 2.

Islets were stained for insulin (green), glucagon (red), TLE1 (yellow) and counterstained with DAPI (blue). Composite image is shown in A. The white arrow indicates a cell expressing insulin and TLE1 (B). Glucagon positive cells were almost always negative for TLE1 as indicated by the yellow arrow (C). Very few bihormonal cells were observed in control donors (D). Individual channels are shown in the bottom row (E-H). Scale bar = 50 μ M.

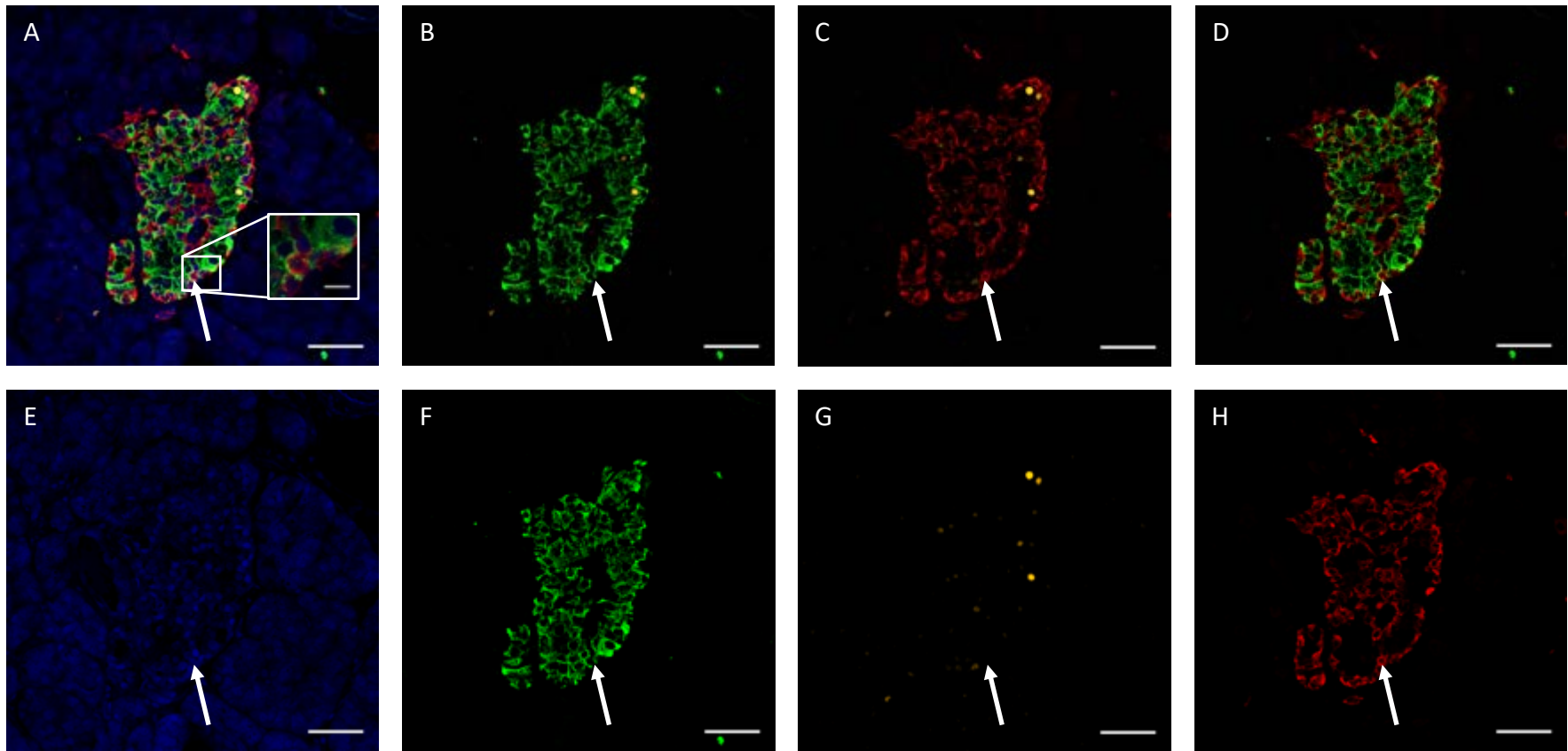


Figure 5.10 Islet from diabetic donor of cohort 2.

Islets were stained for insulin (green), glucagon (red), TLE1 (yellow) and counterstained with DAPI (blue). The composite image is shown in A. TLE1 was still mostly found in beta cells (B) and rarely in glucagon cells (C). The white arrow indicates an insulin positive cell that is negative for TLE1 and positive for glucagon and would be counted as a bihormonal cell (D). Individual channels are shown in images E-H. Scale bar = 50 μ M. Magnified image shows bihormonal cell. Scale bar = 10 μ M.

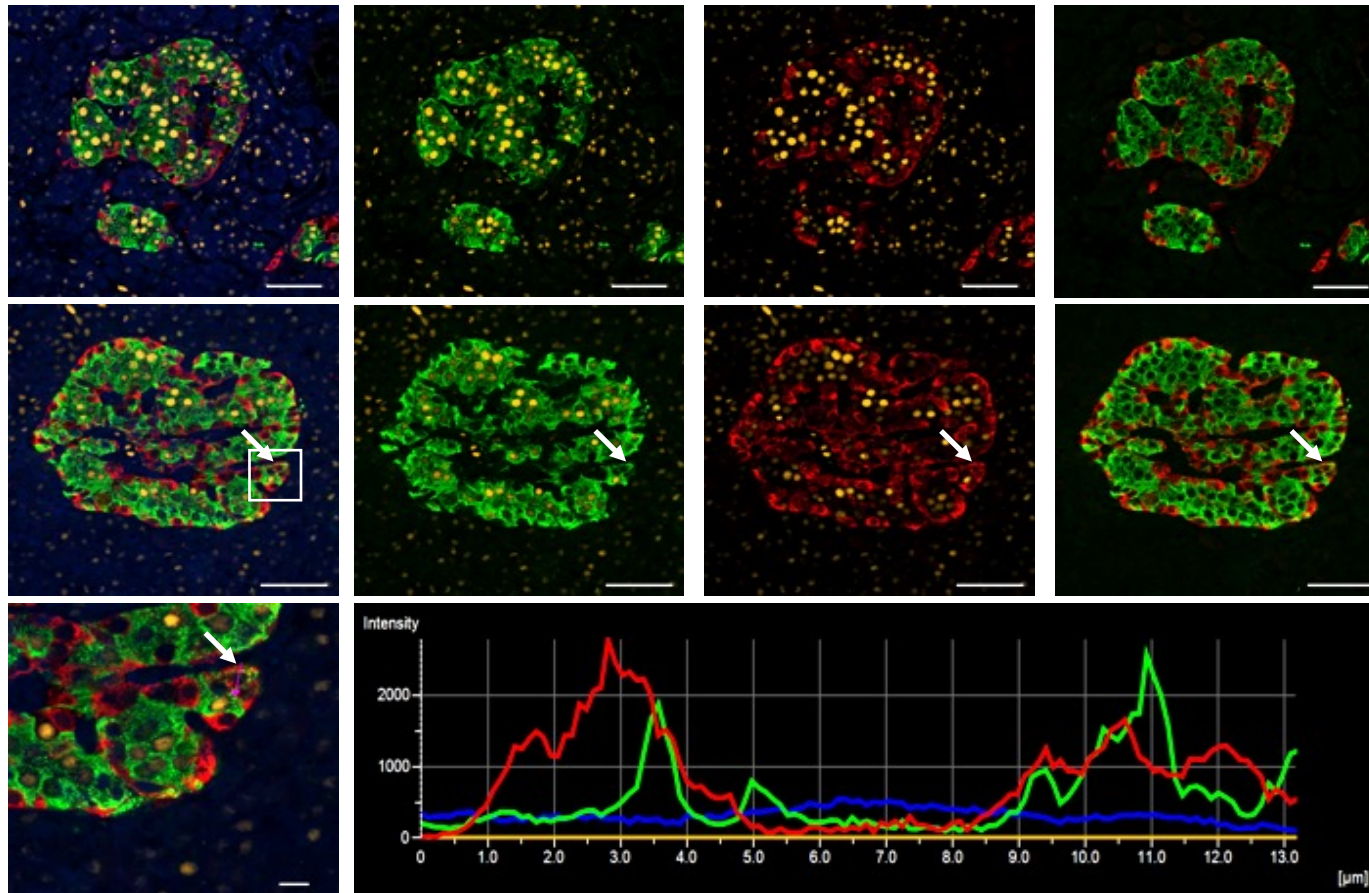


Figure 5.11 Co-expression of insulin and glucagon in human type 2 diabetes.

Representative image of a control (top line) and diabetic (bottom lines) islet. Islets are stained for insulin (green), TLE1 (yellow) and glucagon (red) all cells are stained with nuclear marker DAPI (blue). Box indicates area of higher magnification image. The spectral plot is provided for the cell indicated by the pink arrow in the high magnification image and shows overlapping expression of insulin and glucagon. Scale bar =50 μM . Magnified image scale bar =10 μM .

5.3.9 Cohort 2- Determining the validity of the automated counting method

Automated counting methods are very useful in studies such as these, where a large amount of data needs to be gathered and many cell types need to be analysed. In this study, the number of cells expressing six different phenotypes needed to be analysed for an average of 45 islets per donor across 19 different tissue samples. Using the Vectra system, the software was manually 'trained' to identify each phenotype and this was applied across all islets in that donor to give the number of cells for each phenotype and a percentage confidence of how sure the software is that it has correctly identified the phenotype of each cell (either 50, 70 or 90% confident). To ensure that the machine was correctly phenotyping the cells, a manual count was carried out on all islets from one control donor and one diabetic donor to see whether these could be compared.

One issue with the comparison of these manual and automated counts was that they were carried out on different images of islets and therefore were not directly comparable as the counts may have been done of different islets within the donors. Although these counts could not be statistically compared using the paired students' t-test, on the recommendation of statistician Dr. Pearce, Newcastle University, the counts could be used to compare trends using an unpaired t-test, and therefore could still be used to validate the automated counting method.

Figure 5.12 and Figure 5.13 show the average counts of each cell type; insulin positive (Ins+), bihormonal (Bih+) and glucagon positive (Gcg+) for a control donor and type 2 diabetic donor respectively. These data show the average number of the manual count versus the different automated confidence counts. In all instances, the control donor shows ~60-70% Ins+, ~25-35% Gcg+ and only ~2% bihormonal cells. When looking at the diabetic donor all of the counts show the same trend, with a decrease in Ins+ cells by about 15-25% and increases in Gcg+ cells by ~25%. There also seemed to be a consistent increase in bihormonal cells for all counts. Taking this into consideration, the similarity between the manual counts and the automated counts for both the control and diabetic tissue suggested that the automated counting was a reliable method and therefore the data was taken forward for further analysis.

R026

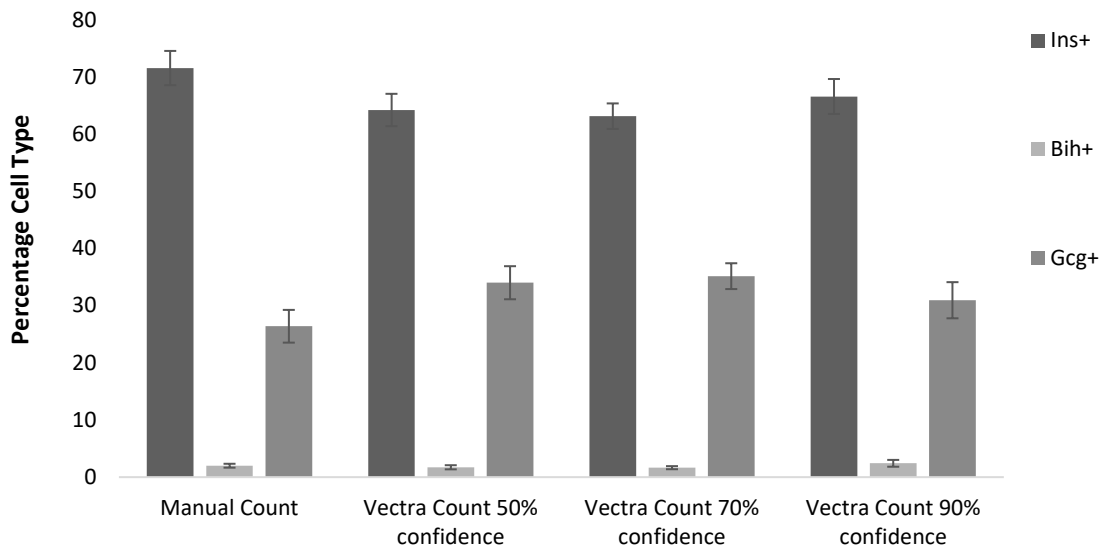


Figure 5.12 Comparison of manual counts versus automated counts at 50, 70 and 90% confidence for control donor.

The average percentage of insulin positive (Ins+), bihormonal (Bih+) and glucagon positive (Gcg+) was calculated for the chosen donor for all Vectra confidences and the manual counts. For manual counts n= 47, for automated counts n=36.

R064

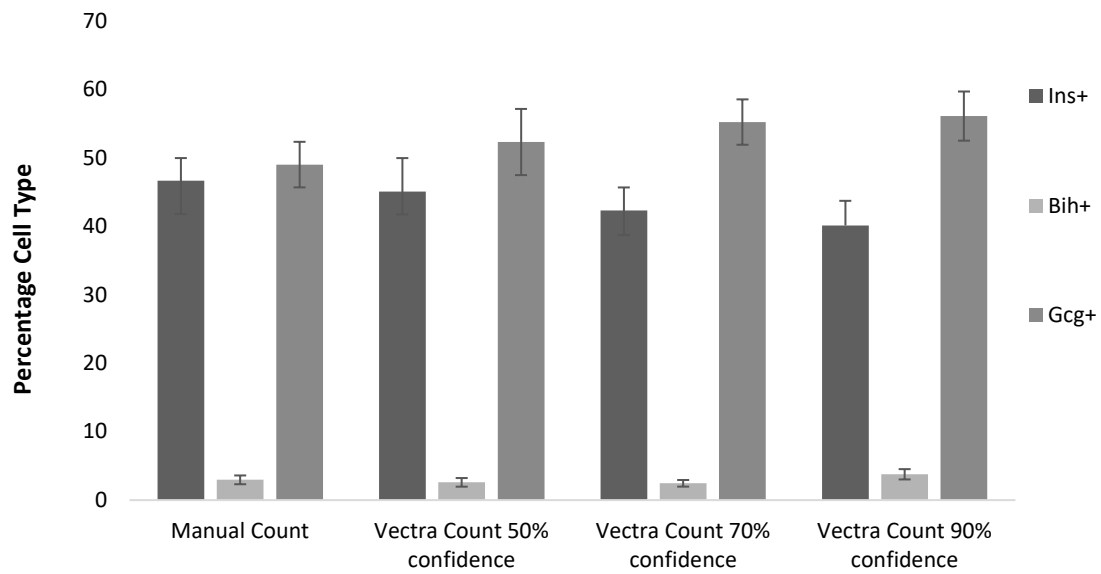


Figure 5.13 Comparison of manual counts versus automated counts at 50, 70 and 90% confidence for diabetic donor.

The average percentage of insulin positive (Ins+), bihormonal (Bih+) and glucagon positive (Gcg+) was calculated for the chosen donor for all Vectra confidences and the manual counts. For manual counts n= 35, for automated counts n=32.

5.3.10 Cohort 2- Does the number of glucagon expressing cells increase in type 2 diabetes?

The data for Cohort 2 was analysed in a similar way to Cohort 1. Firstly, it was of interest to see whether the data showed increases in glucagon positive cells when looking at the average number across all control or diabetic donors. Figure 5.14 shows the data for percentage of glucagon positive cells in all confidence intervals. As expected, there was a significant increase across all percentage confidences by ~4% when looking at the diabetic donors compared to the control donors.

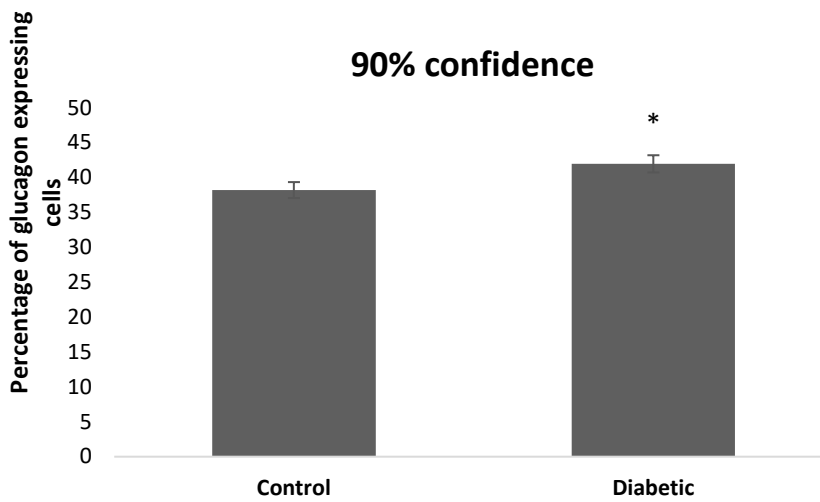
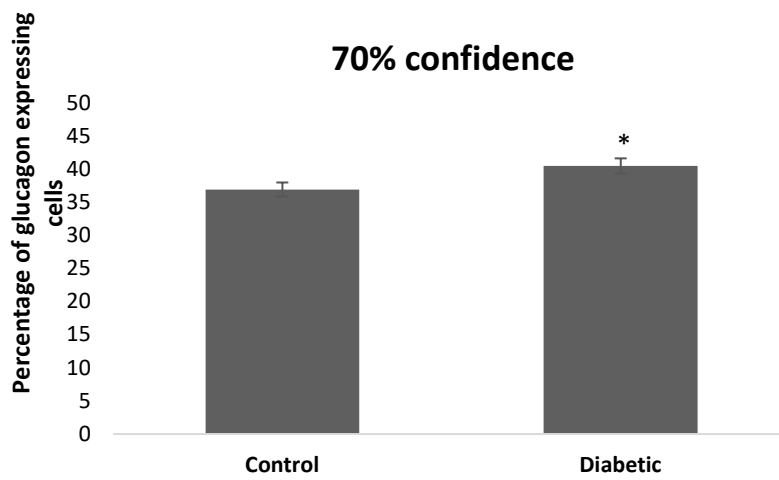
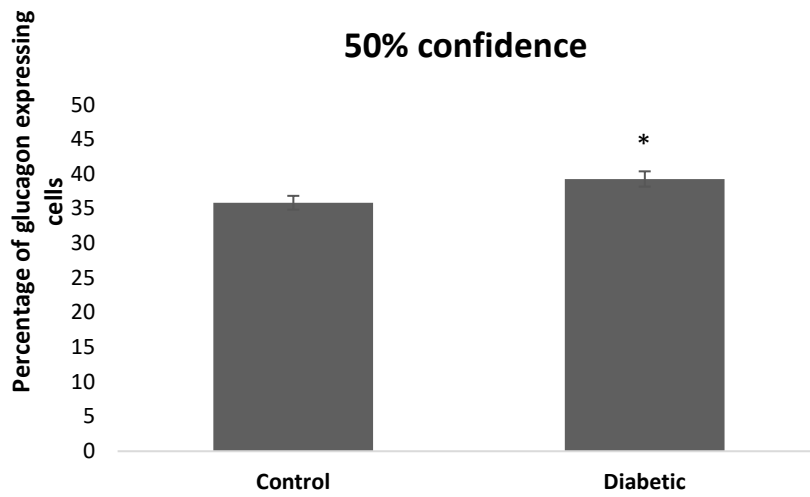
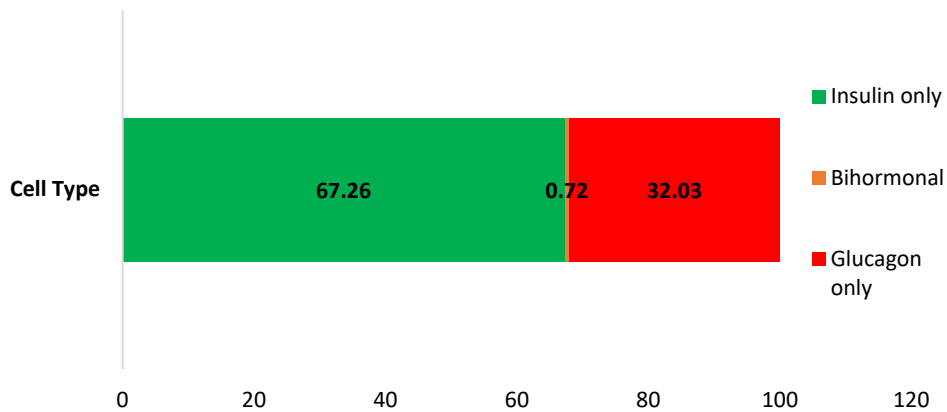


Figure 5.14 Average number of glucagon positive cells in control vs diabetic donors.

Data represent average value of all islets per condition \pm SEM. n=397 (control), 450 (diabetic), *p<0.05 vs control group.

5.3.11 Cohort 2- Do the number of bihormonal cells increase in diabetes?
Alongside increases in glucagon, the hypothesis that beta cell undergo transdifferentiation to an alpha cell phenotype would suggest that there would be an increased number of bihormonal cells in diabetic donors, as some cells may be in this transitional state upon time of death. To assess whether this is the case, counts for each cell type were carried out and compared between control and diabetic tissue. There was a significant increase in bihormonal cells in diabetic patients compared to control for 50, 70 and 90% confidence counts (Figure 5.15, Figure 5.16 and Figure 5.17 respectively) with 2.31-, 1.86-, and 1.6-fold increase in average percentage of bihormonal cells respectively. This data agrees with both the hypothesis presented and the data for Cohort 1.

Control donors



Diabetic donors

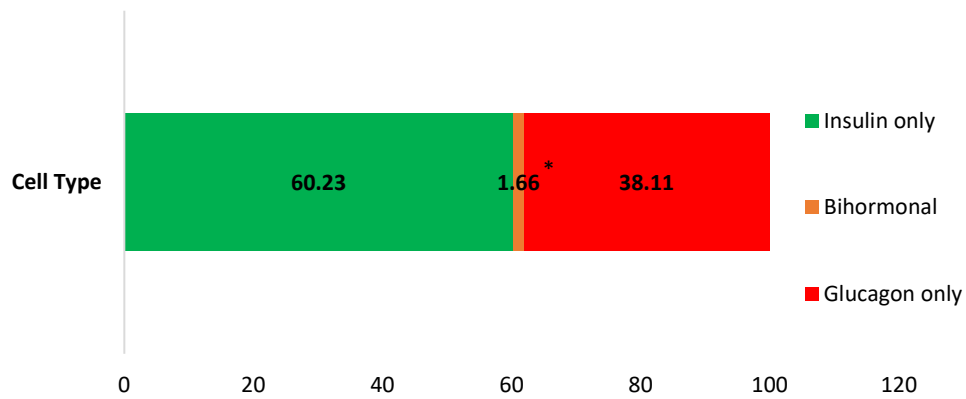
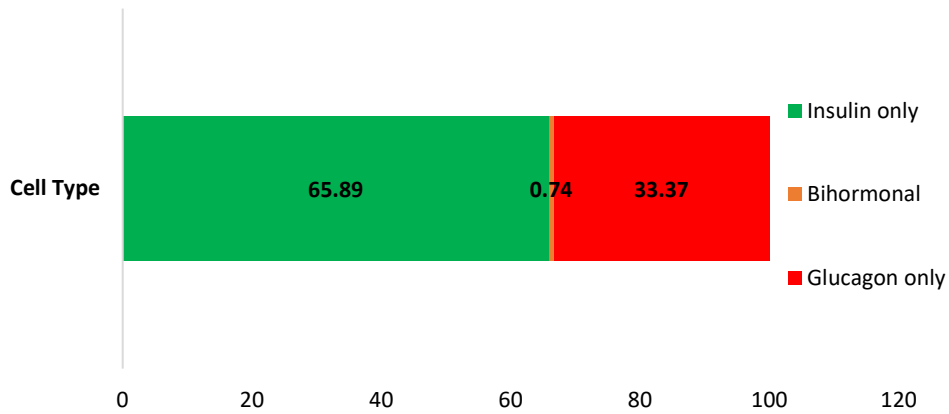


Figure 5.15 Average percentages of all insulin expressing cells, all glucagon expressing cells and bihormonal cells in control and diabetic donors for 50% confidence counts.

Data shows average percentage of each cell type per islet for control and diabetic donors, n= 397 (control) or 450 (diabetic), *p<0.05 for average percentage of bihormonal cells in diabetic donors vs control donors.

Control donors



Diabetic donors

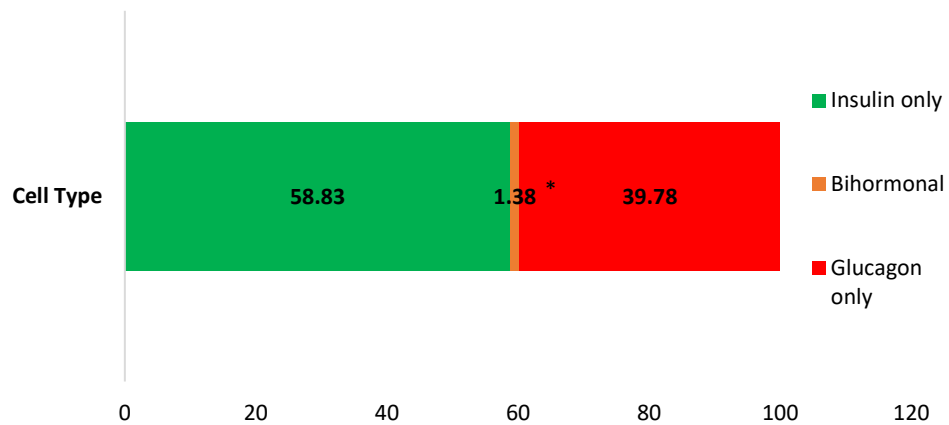
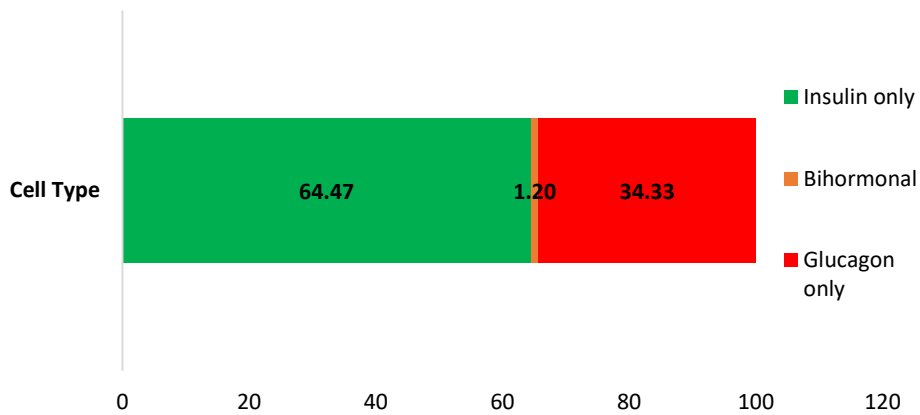


Figure 5.16 Average percentages of all insulin expressing cells, all glucagon expressing cells and bihormonal cells in control and diabetic donors for 70% confidence counts.

Data shows average percentage of each cell type per islet for control and diabetic donors, n= 397 (control) or 450 (diabetic), *p<0.05 for average percentage of bihormonal cells in diabetic donors vs control donors.

Control donors



Diabetic donors

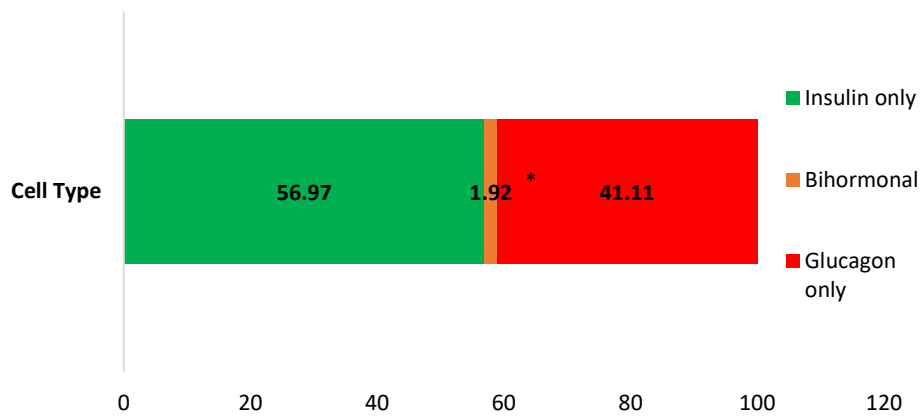


Figure 5.17 Average percentages of all insulin expressing cells, all glucagon expressing cells and bihormonal cells in control and diabetic donors for 90% confidence counts.

Data shows average percentage of each cell type per islet for control and diabetic donors, n= 397 (control) or 450 (diabetic), *p<0.05 for average percentage of bihormonal cells in diabetic donors vs control donors.

5.3.12 Cohort 2- Choosing a percentage confidence to continue with.

For Cohort 2, the TLE1 staining was very clear and therefore could be counted and analysed.

There was also a lot more donor information available to consider in the analysis for Cohort 2. To look at any correlations between donor information and the data gathered, a percentage confidence was chosen to move forward with. As the manual and automated counts were done from different images, a paired t-test could not be used to validate the automated counting method as it could not be definitively said that the same islets were counted. For this reason, an unpaired t-test was used to get an idea of the difference between the manual and automated counts and to see if there were different trends between control and diabetic patients for the different counting methods. When looking at the data for all conditions, the 90% confidence was the only one that did not approach significance for any cell types in both the control and the diabetic donors. For this reason, the data gathered from the 90% confidence counts were taken forward for analysis of TLE1 and using the donor information provided.

Ttest vs Manual Count	All Ins+ Cells	All Bih Cells	All Gcg+ Cells
Control 50%	0.050846742	0.560725026	0.068758673
Control 70%	0.028719303	0.465679758	0.041090151
Control 90%	0.254689582	0.505732135	0.23228137
Diabetic 50%	0.578522271	0.692230738	0.61892534
Diabetic 70%	0.291876457	0.59948684	0.327538848
Diabetic 90%	0.249812681	0.514922518	0.198698452

Table 5.5 Determining the percentage confidence to use.

Unpaired t-tests were carried out between all islets in manual count versus islets in each percentage confidence.

5.3.13 Cohort 2- Localisation of TLE1.

Previous work by Metzger *et al.* has shown that the rodent equivalent of TLE1 (Tle3) is localised mainly in the beta cell and very few glucagon+ Tle3 positive cells are found (68). To determine whether this is the case with Tle1 in humans, the data was analysed to show the proportion of TLE1 positive cells also expressing insulin, glucagon or both. In both the control and the diabetic donors almost all TLE1 cells expressed insulin, with very few expressing either glucagon or both hormones (Figure 5.18). Taking this into consideration, it is fair to assume that any changes seen in TLE1 between the control and diabetic donors is because of changes occurring in the beta cell as TLE1 is rarely present in the other cell types.

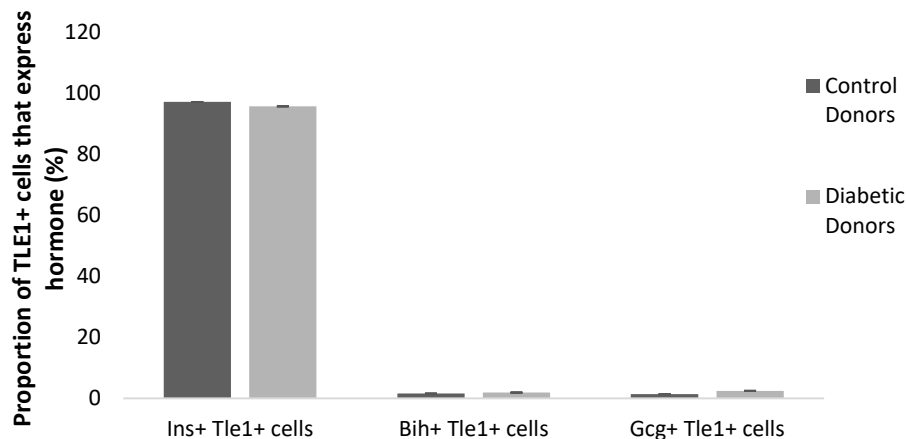


Figure 5.18 Localisation of TLE1 in human control and diabetic donors.

The average percentage of insulin, glucagon or bihormonal TLE1 cells was calculated per islet \pm SEM. n= 397 (control) or 450 (diabetic).

5.3.14 Cohort 2- Is TLE1 lost in type 2 diabetes?

This study aimed to explore TLE1 expression in type 2 diabetes and whether expression is lost in the beta cell during the disease state. It also aimed to identify whether loss of TLE1 encourages co-expression of insulin and glucagon and a subsequent transition to the alpha cell phenotype.

The overall expression of TLE1 is significantly reduced in donors with type 2 diabetes, as demonstrated in Figure 5.19. The average percentage of TLE1 negative cells was calculated

for each insulin, bihormonal and glucagon expressing cells. Glucagon+ cells remained almost completely TLE1 negative regardless of whether they were in control or diabetic tissue. This finding was expected, as TLE1 has been shown to repress glucagon expression (61) therefore should not be expressed in glucagon positive cells. The bihormonal cells showed a significant loss of TLE1 in diabetic tissue, with the proportion of Tle1 negative bihormonal cells rising from 66.67 to 69.32%. Finally, there was a significant increase in TLE1 negative insulin-positive cells in the diabetic tissue from 34.03 to 41.36% confirming that most of the loss of TLE1 expression during diabetes is as a result of downregulation in the beta cells (Figure 5.20).

To further assess the loss of TLE1 in insulin expressing cells, the average percentage of all insulin positive/TLE1 negative phenotypes were calculated i.e. cells expressing insulin only and cells expressing insulin and glucagon without TLE1 present. This showed that there was a significant increase in TLE1 negative insulin+ cells in type 2 diabetic donors (Figure 5.21). This supports the hypothesis that insulin+ cells lose TLE1 during diabetes and this may potentially play a role in the increased number of bihormonal cells found in diabetic donors.

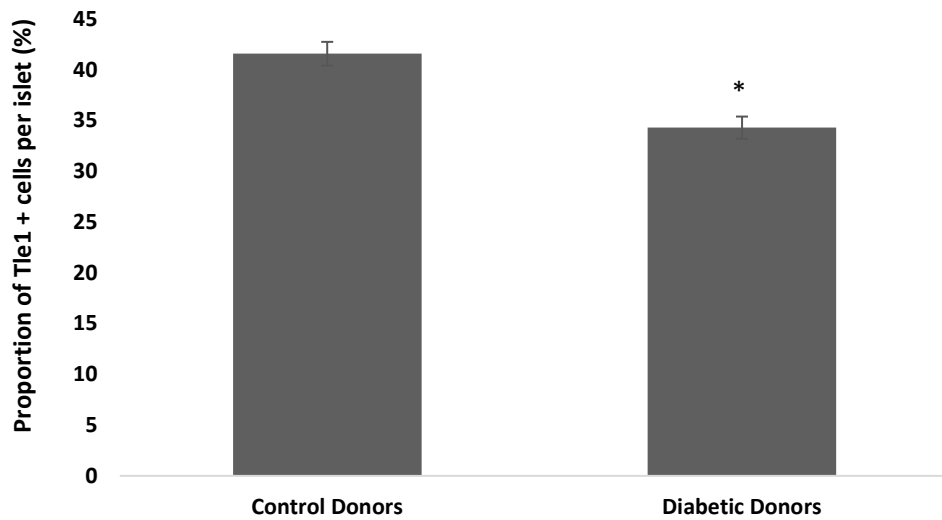


Figure 5.19 Total percentage of all Tle1+ cells in donors with and without type 2 diabetes.

All cells expressing TLE1 were counted in both donor groups. Data are expressed as average percentage of the number of cells per islet expressing TLE1±SEM. n=395 (control) and 450 (diabetic). *p<0.01 vs control donors using student's t-test

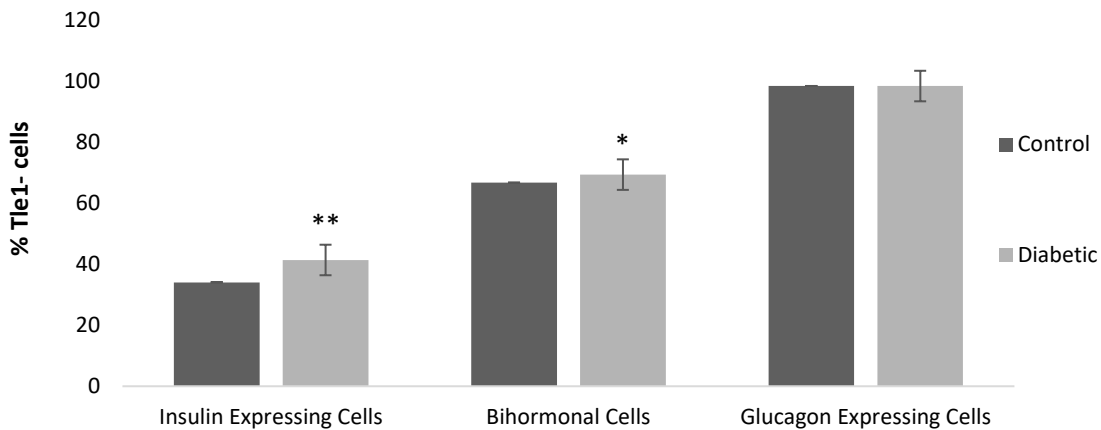


Figure 5.20 The percentage of TLE1 negative cells for each cell type in control versus diabetic tissue.

Control and diabetic tissue was compared for TLE1 expression in each of the three cell types of interest. Data expressed as the average percentage of TLE1 in each islet±SEM, for each cell type. n=395 (control) and 450 (diabetic). *p<0.05 and **p<0.01 vs control donors using student's t-test.

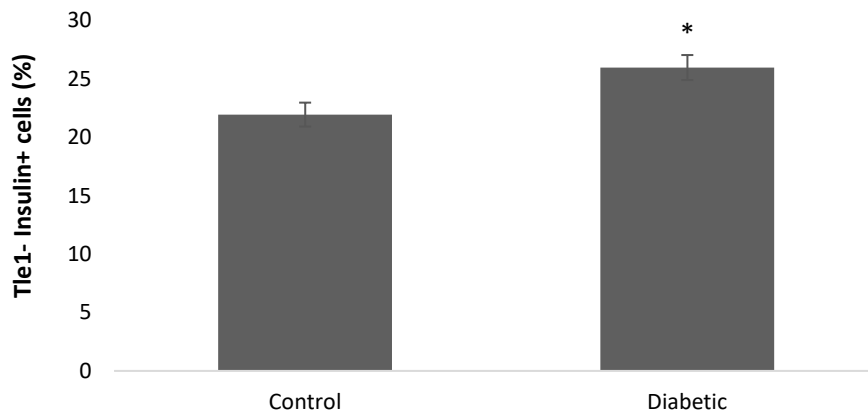


Figure 5.21 The average percentage of TLE1 negative insulin expressing cells.

Data is expressed as the average percentage of all insulin expressing cells that are negative for TLE1 \pm SEM (insulin only and insulin/glucagon cells) per islet. n=395 (control) and 450 (diabetic). *p<0.01 using student's t-test.

To see the range of TLE1 negative beta cells throughout the cohort, the average percentage of insulin only cells (i.e. insulin positive/TLE1 negative) was taken per donor (Figure 5.22). This shows the range of TLE1 expression between the donors in each group. The median value of insulin positive, TLE1 negative cells increased from 34.5% to 43.5% in diabetic donors. These data also show that the control donors had a lowest value of 15.8% TLE1 negative insulin+ cells whereas this value for the diabetic counterpart was roughly 10% higher at 24.14%. On the other hand, when looking at which donors contained the most TLE1 negative insulin+ cells, control tissue showed 51.2% TLE1 negative beta cells as the highest value but in diabetic tissue the donors showed up to 60.64% of beta cells negative for TLE1.

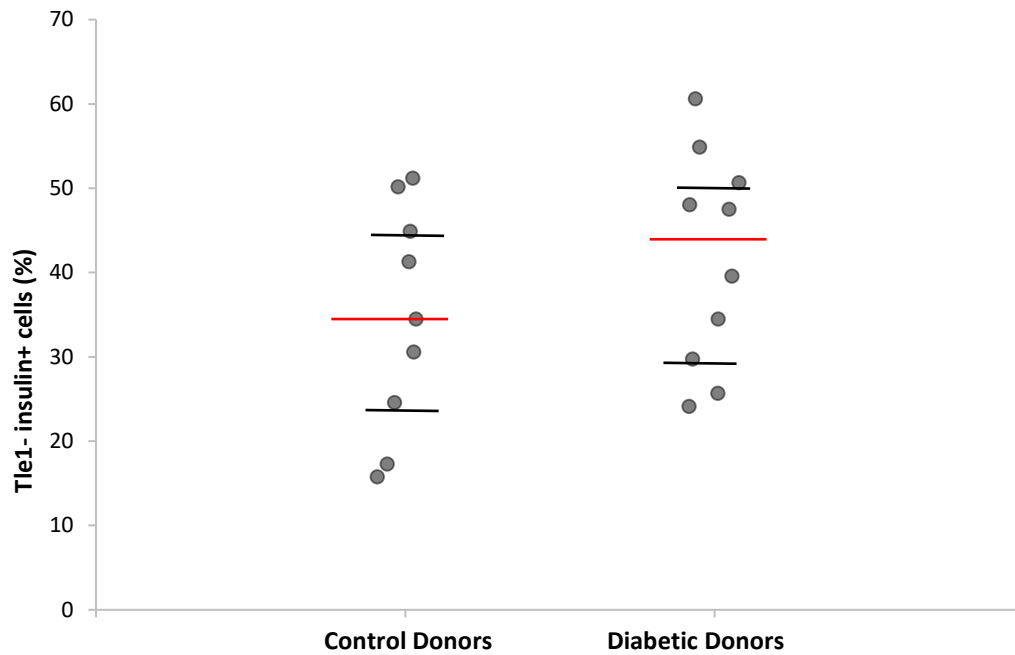


Figure 5.22 Average percentage of TLE1 negative beta cells per donor.

Data is expressed as the average percentage of TLE1 negative beta cells in control and diabetic tissue per donor. The red line represents the median value, 34.5% and 43.5% for control and diabetic respectively, the black lines represent interquartile ranges (1 and 3). n = 9 (control) and 10 (diabetic).

5.3.15 Cohort 2- Does the loss of TLE1 correlate to increased glucagon expression? As TLE1 is known to act as a repressor of glucagon, it would be expected that as TLE1 expression is lost, glucagon expression would increase. As shown in Figure 5.18, TLE1 expression is almost exclusively expressed in beta cells and therefore any correlation between loss of TLE1 and increased glucagon expression is likely to come from changes in the beta cell. To assess this, the average number of insulin positive/ TLE1 negative cells was compared to the average number of all glucagon expressing cells across all islets for each donor. Figure 5.23 shows a correlation between the loss of TLE1 in beta cells and the increase in glucagon expressing cells. Regression analysis gave a correlation coefficient (R) of 0.81 and R^2 value of 0.65. Although this shows a positive correlation between the two variables, this may have been stronger if outlying points, such as donor 104 (highlighted on graph), were excluded.

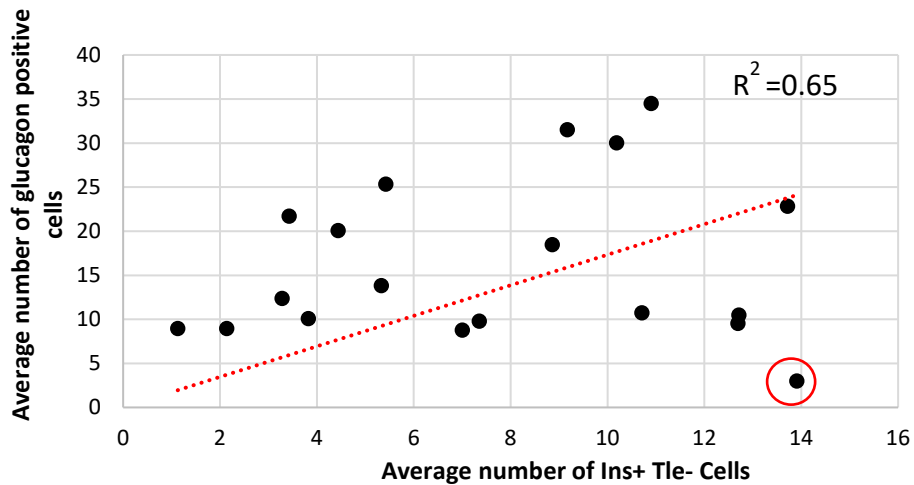


Figure 5.23 Relationship between the loss of TLE1 in insulin+ cells and increased glucagon expression.

The average number of insulin only cell per islet and the average number of all cells expressing glucagon cells per islet was calculated. The average of these numbers was worked out per donor for both control and diabetic tissue. Data represent n=19. Pearson's correlation coefficient (R) = 0.81.

5.3.16 Cohort 2- Is there a link between loss of TLE1 and other donor information? The data presented so far provides evidence for the loss of TLE1 from the beta cells during the diabetic state and provides a potential explanation for the increased proportion of glucagon expressing cells. To investigate whether loss of TLE1 in diabetes is linked to other attributes of diabetes, such as glycosylated haemoglobin (HbA1c) and body mass index (BMI), the level TLE1 expressed in beta cells was compared to the donor information provided with the tissue.

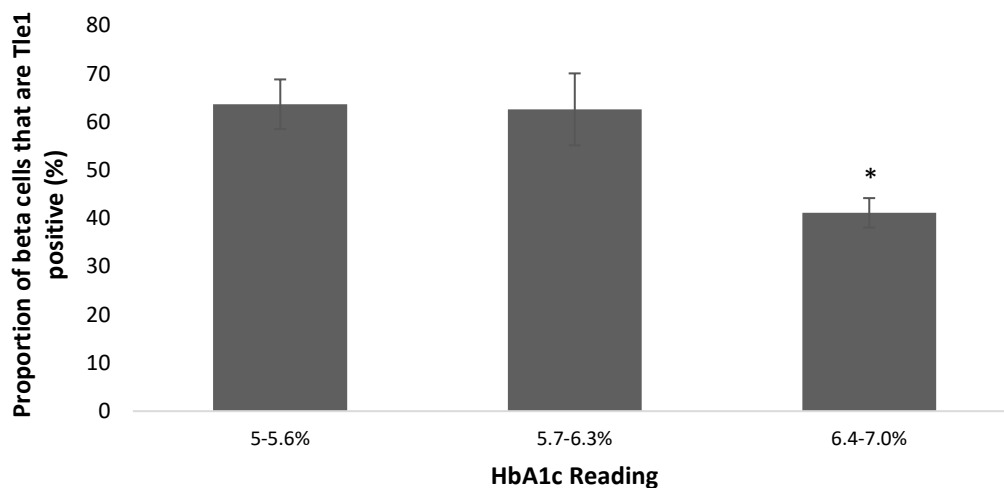


Figure 5.24 Relationship between the percentage of TLE1 expressing beta cells and glycosylated haemoglobin levels.

All donors with HbA1c readings provided were separated into three categories; HbA1c between 5-5.6%, 5.7-6.3 and 6.4-7%+. Data expressed are average % TLE1+ beta cells across all donors in category \pm SEM. n=5, *p<0.05 compared to normal category using student's t-test.

As shown in Figure 5.24, the level of TLE1+ beta cells are highest at the non-diabetic HbA1c level (5-5.6%). This decreases slightly as HbA1c increases to 5.7-6.3%, and is significantly reduced as HbA1c increases to between 6.4-7.0%. As HbA1c levels are a marker of long term blood glucose levels (104) this could mean that extended periods of glucotoxicity contribute to the loss of TLE1 in the beta cell. These findings support the rodent data presented in Chapters 3 and 4 that gave evidence for glucotoxicity driving the loss of the beta cell phenotype.

To assess expression of TLE1 throughout disease duration the total number of TLE1 positive cells in all islets was worked out per donor. Donors were separated into categories based on disease duration and the average number of TLE1 expressing cells across all donors in each group was worked out. Figure 5.25 shows a gradual decrease in TLE1 expression as the disease persists.

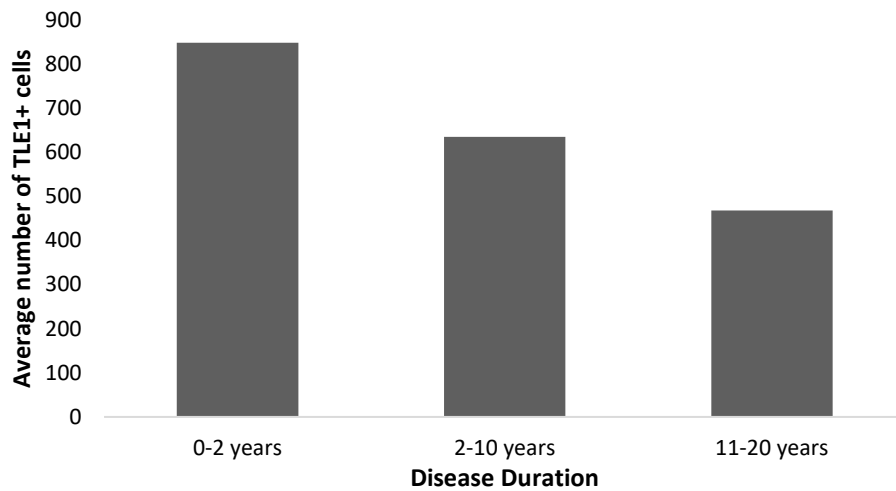


Figure 5.25 Loss of TLE1 expression with disease duration in diabetic donors.

The number of TLE1 expressing cells was worked out per donor. Donors were grouped by disease duration and an average was taken of the TLE1 counts for each group. n=3 for 0-2 years and 2-10 years. n=2 for 11-20 years.

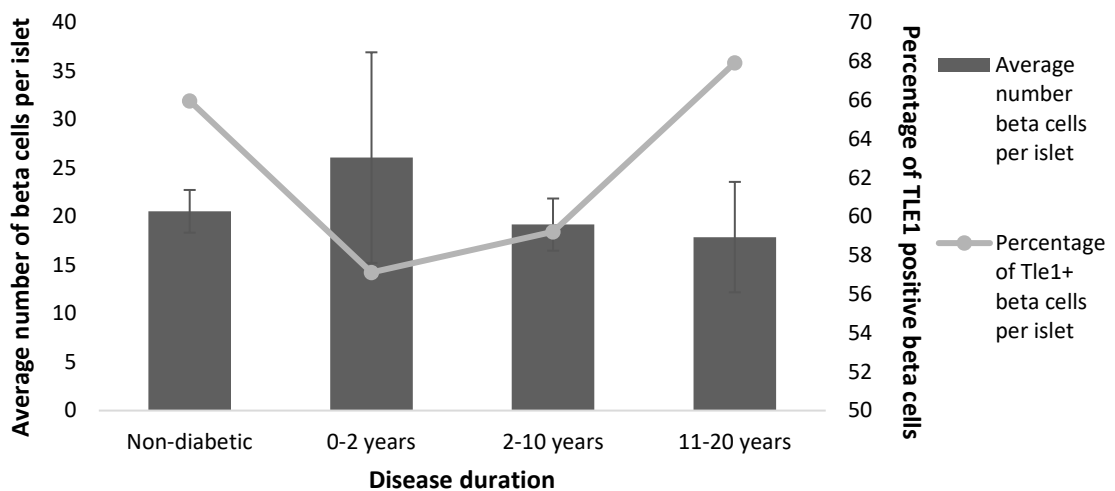


Figure 5.26 Relationship between disease duration and TLE1 expression.

The average percentage of TLE1 expression in beta cells (line graph) was worked out for non-diabetic donors and diabetic donors of different disease durations (0-2 years, 2-10 years and 11-20 years). This was compared to the average number of beta cells in islets of each category.

As this study aimed to elucidate the role of TLE1 in maintaining the beta cell phenotype, the average number of beta cells was plotted against the duration of the disease. This was then compared to the average number of TLE1+ insulin expressing cells in all donors for each duration group. Figure 5.26 shows that the average number of beta cells in the islets (bar graph) decreases as the disease progresses however, the overall percentage of TLE1+ beta cells increases (line graph). This suggests that the beta cells that remain during the disease progression are more likely to express TLE1, supporting the hypothesis that TLE1 is important in maintaining the beta cell phenotype.

5.3.17 Cohort 2- Is there a link between loss of TLE1 and bihormonal cells?

As TLE1 acts to repress glucagon and appears to be lost during diabetes, potentially resulting in a transition towards an alpha cell phenotype, it would be expected that the number of bihormonal cells (defined as cells expressing both insulin and glucagon) would increase during diabetes. Figure 5.17 supported this hypothesis and showed significantly increased bihormonal cells in diabetic donors. Figure 5.27 demonstrates the spread of data for average bihormonal cells in the control and diabetic groups. The spread of the diabetic group is far greater, with the highest percentage of bihormonal cells being 4.34% compared to 2.42% in the control group. The median value also increases from control to diabetic group from 0.99%-1.38%.

To assess whether there is a relationship between the presence of bihormonal cells and an absence of TLE1 expression, the percentage of TLE1 negative insulin positive cells in islets was compared with the average percentage of bihormonal cells across control and diabetic donors. Figure 5.28 shows the relationship between these two variables. Analysis of the correlation coefficient showed a slight correlation between loss of TLE1 and increased number of bihormonal cells, with an R value of 0.57 in control donors and 0.5 in diabetic donors with resultant coefficient of determination at an R^2 of 0.33 and 0.25 respectively.

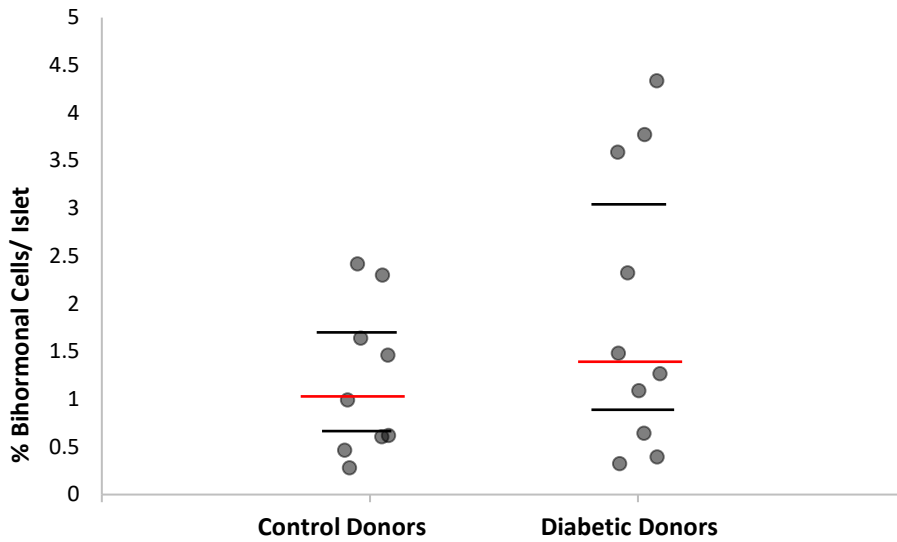


Figure 5.27 Average percentage of bihormonal cells per donor in control and diabetic donors.

Average number of bihormonal cells were calculated per donor. The red line indicates the median percentage of bihormonal cells for each condition and the black lines indicate interquartile ranges (1 and 3). n = 9 (control) and 10 (diabetic).

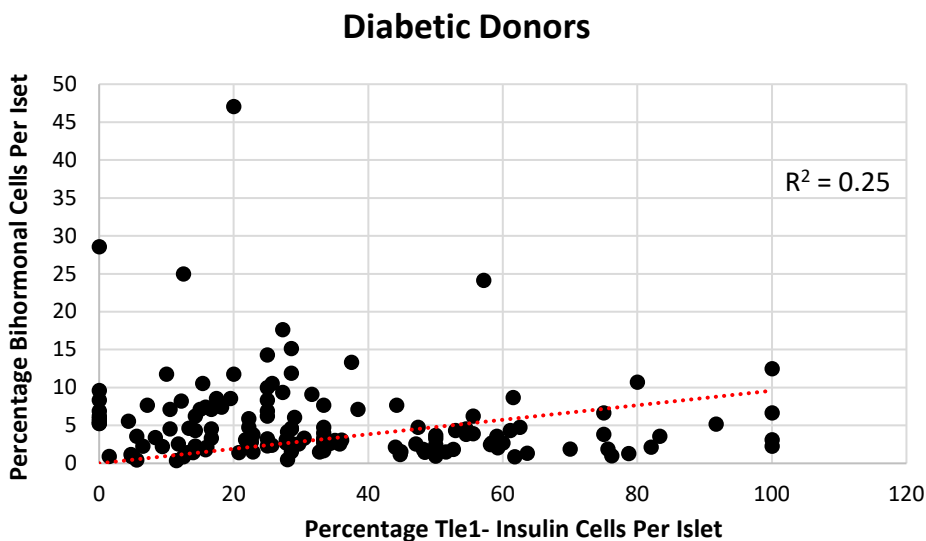
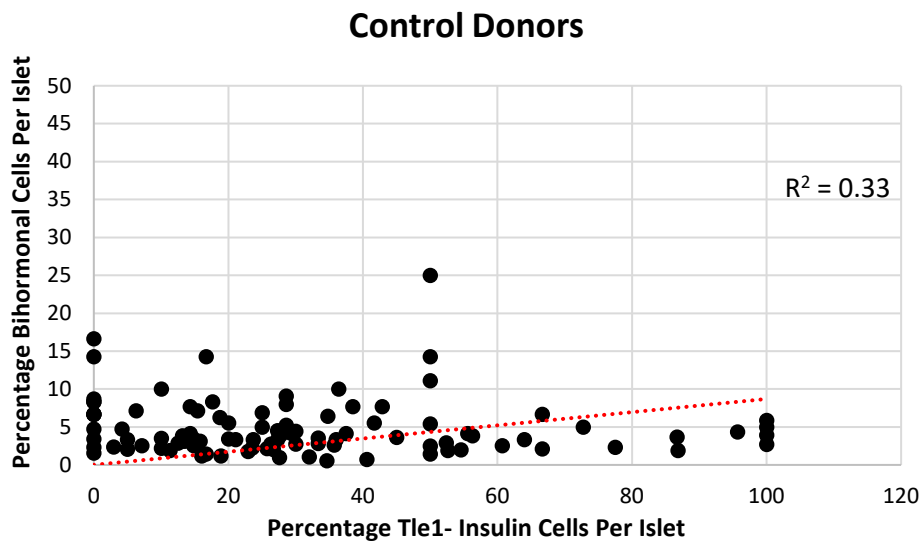


Figure 5.28 The relationship between loss of TLE1 expression and presence of bihormonal cells in islets from control and diabetic donors.

The percentage of insulin positive/TLE1 negative cells were plotted against the percentage of bihormonal cells per islet. Data represents all islets that contained bihormonal cells in both control and diabetic donors. $R^2 = 0.33$ (control donors) and 0.25 (diabetic donors).

Although there did not appear to be a strong link between the loss of TLE1 and increased bihormonal cells, it is possible that the increase of bihormonal cells is affected by multiple variants, for example, extended periods of high glucose as suggested by data shown in the glucotoxicity model. To investigate this further, the average percentage of bihormonal cells present were compared to other donor information. Looking at trends between the number of bihormonal cells and disease duration showed a trend towards increasing during the first 10 years of disease. After 10 years of disease duration however there was a decrease in

presence of bihormonal cells, potentially a result of overall reductions in insulin positive cells (Figure 5.29).

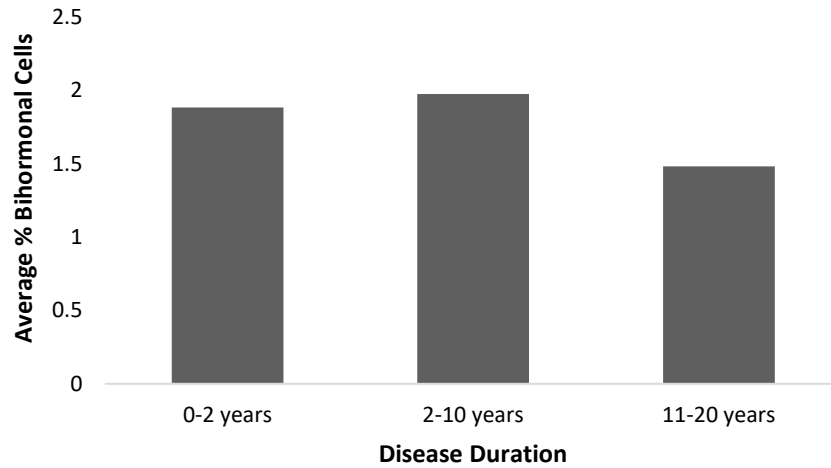


Figure 5.29 Relationship between percentage of bihormonal cells and disease duration.

The percentage of bihormonal cells was compared to BMI per donor for control and diabetic patients. n=3 (0-2 years), 3 (2-10 years) and 2 (10+ years).

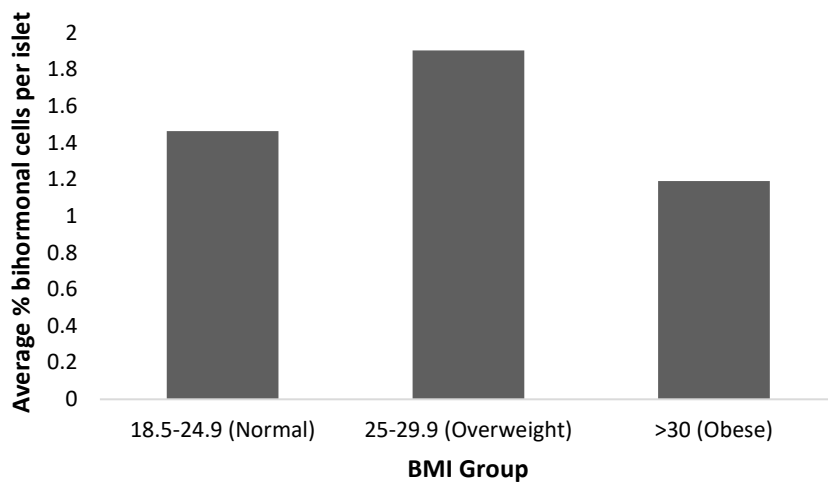


Figure 5.30 Relationship between percentage of bihormonal cells and Body Mass Index (BMI) in control and type 2 diabetic donors.

The percentage of bihormonal cells was compared to the disease duration for diabetic donors where this information was known. n=1 (Normal), 10 (Overweight) and 8 (Obese).

Figure 5.30 shows the relationship between number of bihormonal cells and Body Mass Index. These data show an average increase from 1.4-1.8% bihormonal cells per donor when looking at the normal weight group compared to the overweight group. Looking at the obese group however, there appeared to be a decrease in bihormonal cells on average. This may also be as a result of reduced insulin positive cells overall or potentially may be influenced by other factors.

To assess the impact of extended periods of hyperglycaemia on bihormonal expression, the percentage of bihormonal cells was compared to HbA1c levels in all donors where this information was provided. Figure 5.31 shows an increase in percentage of bihormonal cells with increasing HbA1c levels. When looking at the data for each individual donor there is a correlation coefficient of 0.485 for type 2 diabetic donors suggesting a moderate correlation between sustained high glucose levels and percentage of bihormonal cells (Figure 5.32).

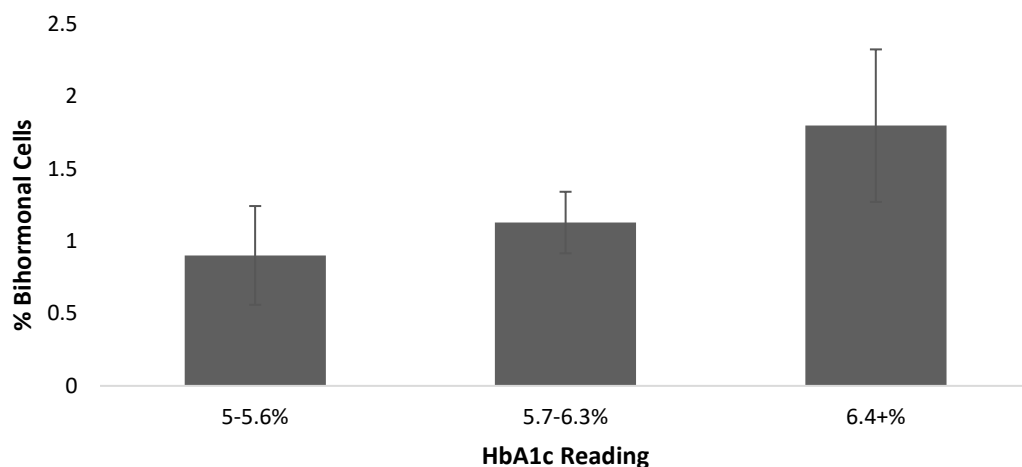


Figure 5.31 Relationship between HbA1c and presence of bihormonal cells.

Average percentage of bihormonal cells were calculated for three categories of HbA1c reading (Normal (5-5.6%), dysglycaemia (5.7-6.3%) and diabetes (6.4+ %)). Data represents n=5 for each group.

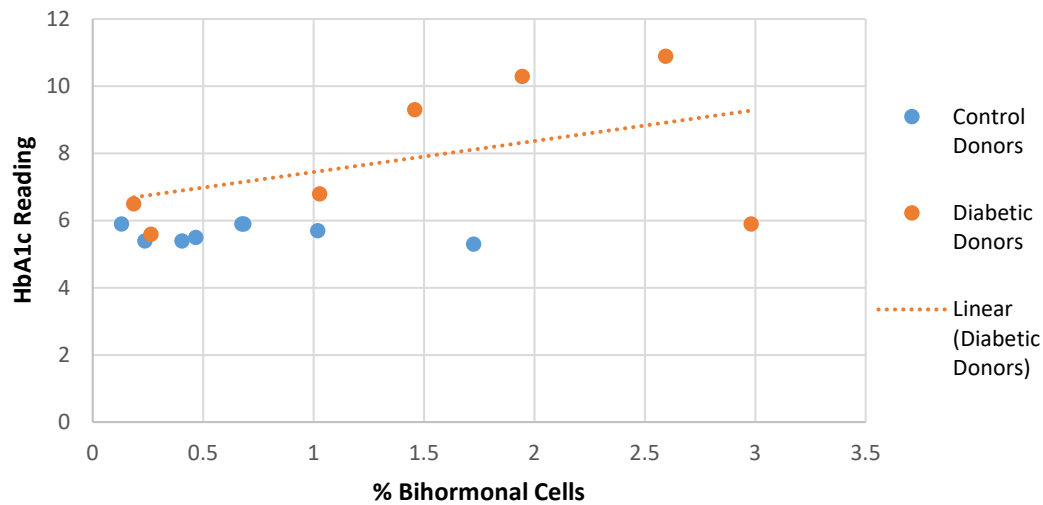


Figure 5.32 Relationship between HbA1c and presence of bihormonal cells per donor.

Average percentage of bihormonal cells were calculated for control and diabetic donors that provided HbA1c reading. Data represents n=15. Pearson's correlation coefficient for diabetic donors =0.455.

5.3.18 Development of an in vitro model of TLE1 knockdown in intact human islets. To further investigate the effect of the loss of TLE1 has on the islet, a model of TLE1

knockdown was developed in isolated human islets using the previously described method (2.7.2). This model provides further insight into how the absence of TLE1 expression in beta cells affect the function and characteristics of human islets.

Initially, four different shRNA plasmids for TLE1 and one scrambled control were used to transfect intact human islets. Transfection efficiency could be visualised under the microscope as plasmids contained GFP sequence. qRT-PCR was then used to assess the efficiency of each plasmid. Figure 5.33 shows the level of *TLE1* knockdown with each shRNA. Plasmids A and C had the most efficient knockdown with ~52% and ~55% decrease in *TLE1* expression respectively.

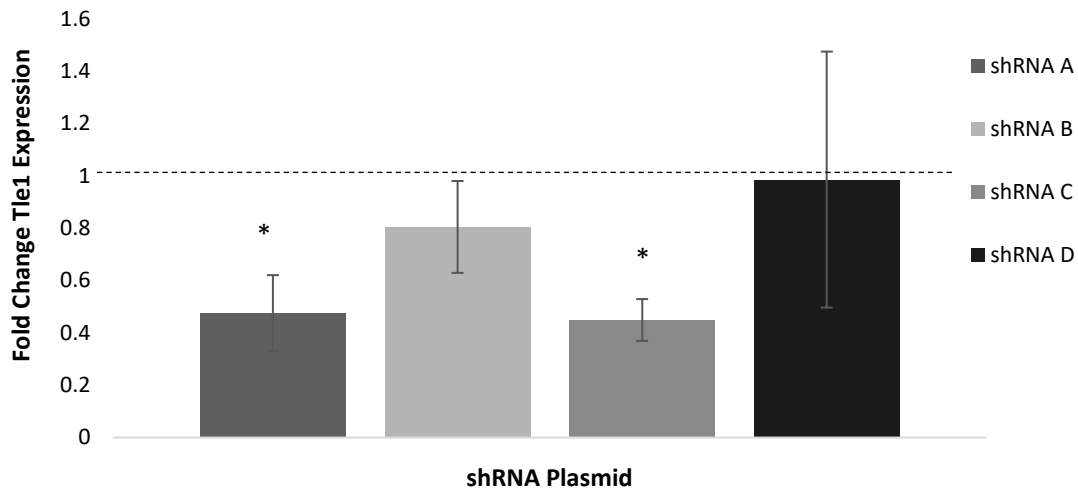


Figure 5.33 Knockdown of *TLE1* in intact human islets by transfection with shRNA plasmids.

Islets were transfected over 5 days with either scrambled control or *TLE1* shRNA. ~500 IEQ per well was used to gather RNA. Data represents average gene expression for *TLE1*±SEM. Results are normalised to the scrambled control. n=3 from 3 biological repeats.

Assessment of other islet genes was carried out for plasmid A and C. Plasmid C showed significant reduction of *INS* expression, in contrast to plasmid A which showed significant upregulation of *INS* mRNA. The expression of *PDX1*, *NKX6.1* and *MAFB* showed no significant changes following *TLE1* knockdown for either plasmid, however, gene expression for alpha cell gene *ARX* was highly upregulated following *TLE1* knockdown with both plasmids. Interestingly, *GCG* expression showed the opposite of what was expected, with downregulation of mRNA expression across both plasmids however neither reached significance (Figure 5.34).

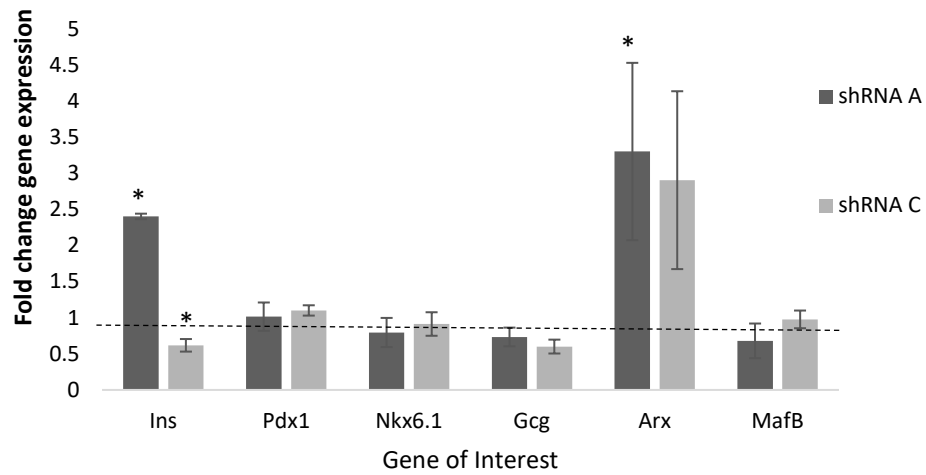


Figure 5.34 Changes in gene expression following knockdown of TLE1 in intact human islets.

Islets were transfected over 5 days with either scrambled control or TLE1 shRNA. ~500 IEQ per well was used to isolate RNA. Data represents average gene expression \pm SEM. Results are normalised to the scrambled control as indicated by the dashed line. n=3 from 3 biological repeats.

5.4 Discussion

These studies have aimed to elucidate the role of TLE1 in maintaining the beta cell phenotype and to observe any changes seen in human type 2 diabetes. Previously published studies have shown an increase in the number of bihormonal cells in tissue sections obtained from patients with type 2 diabetes compared to those without the disease (131). This is in support with other studies giving evidence for the hypothesis of transdifferentiation from beta to alpha cell transition in both rodent (85) and human studies (124). This study has provided further insight into this hypothesis using two cohorts of patients and explores the potential role for TLE1 in this phenomenon.

Cohort 1 showed significant increases in both glucagon expressing cells and bihormonal cells in diabetic donors compared to age-matched controls (Figure 5.1-Figure 5.3) suggesting that there may be some transdifferentiation from a beta to an alpha cell type occurring during type 2 diabetes. This is also demonstrated in Figure 5.5 which showed an example of co-localisation of insulin and glucagon in a diabetic islet. Although the results presented here show potential for beta- to alpha- cell transdifferentiation, one drawback with analysis of human pathology sections is the interpretation by the user. Some studies have suggested that co-localisation of insulin and glucagon expressing cells in rodent models of beta cell ablation is evidence of alpha to beta cell transdifferentiation as a mechanism of renewing the beta cell population (132). Further to the mouse model, subsequent analysis of both human type 1 diabetic and type 2 diabetic tissue alongside control donors explained the co-localisation of insulin and glucagon as alpha to beta cell transition, with potential further transdifferentiation to the delta cell type (133). The evidence for alpha to beta cell transdifferentiation is largely from models of beta cell ablation and one study looking into this phenomenon following different levels of beta cell ablation showed that only with >95% beta cell loss was there significant alpha to beta cell conversion (75). In these studies, a loss of beta cells to this extent was not observed therefore bihormonal cells were thought to be as a result of beta to alpha cell transition.

The role of TLE1 is relatively unexplored in human diabetes. Its rodent counterpart, Tle3, has been shown to have a role in repression of the alpha cell program, specifically *Arx*, and a potential activating role in maintaining adequate beta cell function through interactions with the likes of *Pdx1* (61). The studies shown in chapter 4 give support to the role of Tle3 in

maintaining beta cell identity and, given that TLE1 has been proposed to be the human equivalent, suggest that the loss of TLE1 in human diabetes may impact on the dysfunction of the beta cell during type 2 diabetes. To investigate this, sections were stained with TLE1 alongside insulin and glucagon. The TLE1 staining proved difficult to do as no immunofluorescence could be detected despite successful optimisation in control tissue. To overcome this issue, TLE1 was stained using HRP-techniques however this again, was not without problems. The suspected reason for these issues with the TLE1 staining was that the age and quality of the tissue mean that this protein could not be detected. Although the latter method of HRP-staining enabled detection of TLE1, this, combined with the immunofluorescent stains of insulin, glucagon and DAPI caused these signals to be dampened and therefore made analysis of co-localisation very difficult (Figure 5.7). As a result, the analysis of TLE1 expression in cohort 1 was not carried out.

The second cohort of donors was stained for the same as that of the first cohort. This cohort gave a higher quality of staining as all proteins were probed using immunofluorescent staining and amplification of the TLE1 stain was carried out through the use of tyramide signal amplification. The initial analysis of insulin and glucagon cells gave support to the findings from the first cohort of donors and showed significant increases in both glucagon expressing cells and bihormonal cells expressing both insulin and glucagon. Some studies have shown that there is a certain degree of alpha cell proliferation in the pancreas, particularly in young adults which gradually decreases over time. This study found a subset of cells positive for proliferation marker Ki67, alongside alpha cell marker ARX in both control and type 1 diabetic tissue (134). Although alpha cell proliferation may account for the increased glucagon expressing cells seen in the human donors, the decrease in proportion of insulin positive cells that was coupled to the increase in both glucagon and bihormonal cells is more suggestive of a switch from beta to alpha cell phenotype. Whether there is a role for TLE1 in this transdifferentiation still requires further investigation. While these studies have shown that there is an increased number of insulin positive cells that do not express TLE1 in donors with type 2 diabetes, and a suggested link between the loss of TLE1 and increased glucagon expression, the relationship between loss of TLE1 and bihormonal expression does not seem as clear cut. The evidence provided by Metzger *et al.* for the role of Tle3 as a repressor of glucagon in rodent beta and alpha cell-line models would suggest that the loss of TLE1 in human beta cells would give rise to increased bihormonal cells. These studies have shown an increase in glucagon expression following the

loss of TLE1, alongside a general increase in bihormonal cells overall, however the relationship between the loss of TLE1 and increase in bihormonal cells showed only a moderate correlation. This may potentially be influenced by the small number of bihormonal cells present on average. Furthermore, this analysis is carried out assuming that the relationship between number of TLE1 negative insulin+ cells and the number of bihormonal cells will not be affected by other variables however this may not be the case.

The larger amount of donor information provided with cohort 2 allowed for other trends to be assessed. It is widely accepted that obesity is linked to type 2 diabetes, and therefore observing links between BMI and other factors may be useful. A study of non-diabetic adults showed that even in the absence of diabetes, increased BMI can be linked to abnormal glucose metabolism with almost 20% of the population with a BMI $<25\text{kg/m}^2$ having worsened glucose metabolism (135). As cohort 2 only had one subject in the normal BMI range, due to the donors being both age and BMI matched as closely as possible, it would be interesting to have more non-obese diabetic donors and BMI matched controls to see whether there is a link between BMI and loss of TLE1.

The studies presented in chapter 3 and the beginning of chapter 4 showed the effect of high glucose on the beta cell phenotype, and gave evidence for transdifferentiation of beta cells during extended periods of high glucose. HbA1c readings are used to determine the amount of glycosylated haemoglobin in the blood and can be used to give an idea of the level of glucose in the blood over a 3 month period. It has been shown that HbA1c can be useful in determining the prognosis of several factors influenced by diabetes, such as being used as a good predictor of lipid profile and risk of cardiovascular problems (104). The data presented in these studies not only show a significantly reduced percentage of TLE1+ INS+ cells in donors with higher HbA1c, but also show a strong link between HbA1c and number of bihormonal cells present.

The hypothesis that TLE1 plays a role, not only in repression of the alpha cell phenotype, but also in the maintenance of the beta cell phenotype can be supported by looking at the number of beta cells and the percentage of these expressing TLE1 as the disease progresses. Figure 5.26 shows that as the disease progresses, the average number of beta cells per islet is reduced, however by looking at the expression of TLE1, these studies demonstrate that

cells which retain the beta cell phenotype are far more likely to express TLE1. This suggests a role for TLE1 in maintaining the beta cell phenotype.

As demonstrated in these studies, there is evidence for transdifferentiation taking place in human diabetes and a potential role for TLE1 in this mechanism. To further investigate this, the knockdown of TLE1 in human islets was carried out to determine the role that loss of TLE1 may have on the human beta cell. The knockdown of TLE1 showed a decrease in insulin gene expression with only one of the shRNA plasmids, whereas all of the plasmids resulted in increased *ARX* expression. As Metzger *et al.* have shown previously, *Tle3* acts to repress *Arx* at the promoter region in rodents (61) and therefore this result is in agreement with the theory that TLE1 is the human functional equivalent. The changes in *NKX6.1* and *PDX1* expression were not significant however with both plasmids, *PDX1* showed a trend towards increased expression. This result is consistent with the *Tle3* knockdown studies in rodent islets and beta cell lines. Unexpectedly the expression of *GCG*, although not significant, was decreased with all shRNA plasmids. One potential explanation for this may be that the isolation process itself, alongside islet culture, causes adverse effects on the gene expression which has been investigated in pancreatic beta cells (136) but effect on alpha cells remains unclear. Whether these changes in gene expression are translated to a protein level are yet to be determined and therefore it would be interesting to carry out further studies investigating the knockdown of *TLE1* on insulin and glucagon content. Alongside this, glucose stimulated insulin secretion could be carried out to assess any impact that loss of *TLE1* has on human islet function. The upregulation of *ARX* in the human islet knockdown is very interesting and is in agreement with data from the rodent islet studies. Although glucagon expression was not upregulated in the human islets, perhaps with further culture, gene expression would have changed. The de-repression of *ARX* following *TLE1* knockdown may suggest that changes seen in the human tissue, with increased numbers of glucagon expressing cells, may be due to direct activation of glucagon through *ARX* activation as opposed to indirect expression through loss of repression by beta cell transcription factors. It would be interesting to investigate this further through analysis of *ARX* expression in the human tissue samples.

These studies aimed to investigate the loss of TLE1 in human type 2 diabetes and whether loss of expression lead to an increase in beta to alpha cell transition. These data have shown that there is a loss of TLE1 expression in type 2 diabetes which is concurrent with an increase in bihormonal and glucagon expressing cells alongside a loss of insulin expressing cells. This may suggest that the loss of TLE1 may encourage the transitional phenotype and the switch from a beta to an alpha cell lineage. Finally, these studies have also shown that the loss of TLE1 and subsequent increase in bihormonal cells may be influenced by disease factors such as HbA1c.

6 General discussion

6.1 Discussion

The work presented in these studies aimed to investigate the effect of exposure to high glucose on the function and phenotype of the pancreatic beta cell. The findings have shown that exposure to high glucose causes a loss of the beta cell phenotype and gain of alpha cell characteristics. To further investigate the mechanisms behind these changes, the studies also aimed to elucidate the role of Tle3 as a novel transcription factor required to maintain the function and phenotype of the functional beta cell. Although the majority of work was carried out using cell line and *in vitro* islet models, the acquisition of human control and diabetic pancreas sections allowed evaluation as to whether these changes also occur in human diabetes.

The loss of the beta cell phenotype as a mechanism of beta cell dysfunction has become a well-established theory over the past few years. Talchai *et al.* provided convincing evidence of this theory in their FoxO1 knockout model of metabolic stress, showing beta cells reverting to a progenitor like state, and some cells adopting an alpha cell fate, using lineage tracing methods (82). Since then, increasing evidence has been provided in support of this hypothesis showing that non-human primates on a high sugar/high fat diet showed loss of insulin and other beta cell transcription factors such as *NKX6.1*, *NKX2.2* and *PDX1* compared to those on a standard diet (137). Furthermore, loss of beta cell phenotype and gain of alpha cell characteristics, known as transdifferentiation, has been seen in human pancreas sections, from both patients with type 2 diabetes and patients who had undergone islet transplantation through co-localisation of insulin glucagon (125, 129). The studies presented here suggest a role for transdifferentiation in beta cell dysfunction during type 2 diabetes, giving evidence that extended periods of high glucose cause the beta cells to lose key transcription factors such as *Nkx6.1* and *Pdx1* and gain more alpha cell characteristics such as increased levels of glucagon. Through staining of human tissue, these data provide supporting evidence for previous studies, with a subset of cells with bihormonal expression of insulin and glucagon, suggesting a transitional state. Previous publications, alongside the evidence presented here, suggest that the loss of phenotype in the pancreatic beta cell may be a common pathway to deal with a number of metabolic stresses, including exposure to high glucose, high fat (55) or hypoxia (125). In these instances, the transition to a more alpha cell like phenotype means the cells would not have to constantly produce insulin in response to constitutively elevated glucose levels, and therefore prevent themselves from being 'worn

out' and undergoing apoptosis. Alongside this, published studies have shown that alpha cells have a higher resistance to stresses such as lipotoxicity and glucotoxicity and also express more anti-apoptotic genes (109), giving an advantage to cells that may undergo this transition.

Following the theory that beta cell dysfunction has a bigger role to play in the dysregulation of glucose during diabetes than cell death does, several studies looking at patients who underwent bariatric surgery (54) or took part in a restricted calorie diet (55) have shown reversal of diabetes. Due to the rapid nature of the reversal these studies suggest that the beta cells may not have died but had reverted from their end-differentiated state until metabolic stress was alleviated and regain of function could occur. To investigate the possible prevention of changes seen in the model of glucotoxicity discussed throughout these studies, overexpression of beta cell transcription factor Pdx1 was carried out in INS1E cells using an adenoviral vector. The role of Pdx1 has been well established as an important beta cell transcription factor and been shown to maintain the beta cell phenotype through repression of the alpha cell program (17). Studies looking at islet cell differentiation have shown that loss of *Pdx1* is important in progression to the alpha cell lineage, more so than expression of alpha cell markers such as *Brain4* (138). Whilst other papers have shown that with overexpression of Pdx1 and other transcription factors the beta cell lineage can be adopted in stem cells (106, 110), whether Pdx1 alone is enough to cause beta cell differentiation in other cell types is not clear. A study by Yang *et al.* showed that reprogramming alpha cells through forced expression of *Pdx1* alone was dependant on the maturity of the cells. This study demonstrated that when *Pdx1* was expression was forced during pancreas development there was a loss of glucagon cells and gain of beta cells around E16.5 (139). A further reduction of glucagon cells was found in the postnatal pancreas in mice that had *Pdx1* overexpressed from development. This caused an almost total loss of alpha cells with a transitional period of cells positive for insulin and glucagon and resulting in an alpha cell-derived beta cell population indistinguishable from the original beta cell population (139). Although this shows Pdx1 alone is capable of deriving beta cells from an alpha cell lineage this study also showed that when *Pdx1* was overexpressed in mature alpha cells they were more resistant to reprogramming, and although most cells showed loss of glucagon (>96%), only around 14% of cells showed any insulin expression and the Pdx1 overexpression failed to repress *Arx* (139). In agreement with this study, and others (17),

that show Pdx1 is able to repress the alpha cell program, the data presented showed that overexpression of exogenous *Pdx1* in high glucose can prevent the upregulation of glucagon seen at an mRNA and protein level. Although the upregulation of some beta cell genes did occur, the function of the beta cells in high glucose could not be rescued, suggesting that overexpression of Pdx1 alone is not sufficient for preventing the loss of beta cell phenotype in hyperglycaemic conditions. An alternative reason for the lack of induction of beta cell genes and function upon overexpression of Pdx1 could be that expression of exogenous Pdx1 acts in a negative feedback loop to reduce levels of endogenous *Pdx1*. This has been previously reported by a study that showed a 3-fold decrease in endogenous *Pdx1* expression following exogenous overexpression of *Pdx1* in the insulinoma cell line (140).

The Groucho (Gro) family of co-repressors and their mammalian equivalent, the Transducin-like Enhancer (Tle) of split family of proteins, have been implicated as important co-repressors in several pathways including the Wnt and Notch signalling pathways (67). Tle3 has been shown to be involved in adipogenesis, osteogenesis, kidney development and development of the pancreas (67). Evidence for the specific role of Tle3 in the pancreatic beta cell was provided by Metzger *et al.* who showed that not only did Tle3 interact with Nkx6.1 to repress *Gcg* and *Arx* genes in beta cells (61). This study also showed that overexpression of Pdx1 and Tle3 could induce *Ins1* and *Ins2* mRNA expression and secretion of insulin in response to glucose in the alpha cell line α TC1-6. Furthermore, the control cells (beta cell line β TC6) and alpha cells overexpressing Pdx1 and Tle3 were positive for C-peptide whereas alpha cells overexpressing Pdx1 alone showed no detectable levels (61). This suggests a role for Tle3 in the processing of insulin and the production of the mature protein. To support this evidence for potential interaction between Pdx1 and Tle3, this study used a proximity ligation assay to determine positive interactions between Pdx1 and Tle3 in the pancreatic beta cell. Following this finding, it would be interesting to see whether the combined overexpression of Pdx1 and Tle3 in the INS1E cells could prevent the loss of beta cell function seen in high glucose. Another important beta cell transcription factor that has been shown to be important in repressing the alpha cell fate is Pax4. Whilst Tle3 has been shown to repress the alpha cell lineage, only some of the potential mechanisms of this have been explored. It is not known exactly how many beta cell transcription factors Tle3 interacts with. Another potential interaction may be with Pax4, a protein which has been shown to be involved in repressing the alpha cell fate. Loss of *Pax4* in rodent pancreas

results in increased *Arx* expression due to loss of repression and as a result, increased alpha cell number (102). As these studies have shown that *Pax4* is downregulated in high glucose, it would be interesting to explore the potential recruitment by *Pax4* to repress *Arx* expression. These studies showed loss of *Tle3* results in upregulation of *Arx* and therefore this could be another potential mechanism by which *Tle3* helps to repress the alpha cell fate in beta cells.

Although the groucho family of proteins are widely known for their roles in gene repression, a recent paper by Villanueva *et al.* has shown that *Tle3* also has a role of an activator of adipogenesis through working to enhance the action of PPAR γ on its target promoters (122). Taking this into consideration, and the evidence that overexpression of *Pdx1* and *Tle3* can promote glucose stimulated insulin secretion (61), it is possible that *Tle3* also has a dual role in the beta cell as a repressor of the alpha cell program and activation and maintenance of the beta cell phenotype. Along with the confirmation of interaction between *Pdx1* and *Tle3*, these studies showed reduced interaction between the two proteins in high glucose conditions. Although it is not determined whether this loss in protein-protein interaction is a result of the high glucose directly, or reduced expression of the genes in question, it may provide explanation for the loss of beta cell phenotype and has the potential to be an early marker of beta cell dysfunction. The loss of *Tle3* shown in high glucose can provide a reason for the upregulation of glucagon as it has previously been shown to be a potent repressor of the *Gcg* gene (61) thus, the downregulation of the protein causes a de-repression of the glucagon gene and allows activation of its expression.

To further investigate the hypothesis that *Tle3* plays a role in the maintenance of the beta cell phenotype alongside the repression of the alpha cell fate, knockdown of the gene was carried out in the INS1E cell line and rodent islets. The short-term knockdown showed significant increases in glucagon gene expression and protein levels as expected. Some beta cell genes were also down regulated in both passages tested, suggesting the loss of beta cell phenotype. Interestingly the function of the cells showed different results across the two passages. The older passage, although there were no significant changes in function showed increased basal insulin secretion whereas the younger cells showed significant decreases in stimulated insulin secretion. Although the two passages showed different results, the reason for this is unclear. Investigation into long term use of the INS1 cell line showed that the cells retain their phenotype and function throughout 116-passages (141) and therefore this is

unlikely to have affected the results. The overall insulin content and secretion was lower in the younger passage, which also showed slightly higher glucagon content which may suggest that these cells were less well differentiated and therefore may have been more susceptible to changes induced by high glucose culture. Although the previously mentioned study showed good glucose response over 116-passages, they also showed the function of the cells to have a normal distribution, with passages 54-95 having the highest insulin content and glucose stimulated insulin secretion (141). This could potentially explain the lower insulin content and GSIS from the younger passage of cells.

The development of stable *Tle3* knockdown cell lines using the INS1E cells and lentiviral vectors allowed further investigation into the role of *Tle3* in the beta cell. The two most effective vectors were taken forward to assess the impact of loss of *Tle3*. Again, these studies showed downregulation of beta cell genes such as *Ins2* and *Nkx6.1* alongside reduced insulin content. There was also significant upregulation of glucagon mRNA and protein. Following the long term knockdown of *Tle3*, the stimulation index of both vector cell lines were reduced. In both cases, data showed upregulation of basal insulin secretion, agreeing with data gathered from the short-term knockdown in the older INS1E cells. Although only one of the viral vectors showed reduced stimulated insulin secretion, these data show that the loss of *Tle3* may indeed have a negative impact on the function of the beta cell.

While the data from cell lines is useful in determining the role of proteins in the cells, in the case of the pancreatic beta cell, they do not give a representative microenvironment of that in which they are physiologically found. For this reason, knockdown of *Tle3* was also carried out in isolated rodent islets. Due to the heterozygous nature of the islets of Langerhans, it is undetermined whether the knockdown of *Tle3* is because of a reduction in the beta cell or other cell types, however previously published data (61), alongside observations in these studies, suggest that almost all *Tle3* is expressed in the beta cell and therefore it is assumed that reductions in *Tle3* is due to loss in the beta cells.

The loss of *Tle3* in the rodent islets caused downregulation of all beta cell genes apart from *Pdx1* which showed consistent upregulation. There was also significant upregulation of alpha cell genes *Arx* and *MafB*. *Gcg* also showed an upregulation of mRNA levels alongside a 1.59-fold increase in protein expression. The impact of *Tle3* knockdown on function of the cells significantly decreased from a stimulation index of ~2-fold in control islets to ~0.5-fold in islets with *Tle3* knockdown. Again, the basal level of insulin secretion was vastly upregulated

and the stimulated insulin secretion showed a marked decrease. This suggests that Tle3 may help to regulate both basal and stimulated insulin secretion in the rodent islet.

Taken together this data provides evidence for the role of Tle3 as a repressor of the alpha cell program and also supports the hypothesis that it has a dual role as an activator of the beta cell program, both in gene regulation and cell function. The concept of transcription factors having dual repressive and activating activity in a single cell type is not unheard of. In respect to the beta cell, studies have shown that Nkx2.2 acts as a repressor of *Arx* through recruitment of Tle3 and HDAC1 in mice (63) whilst others have shown that without expression of *Nkx2.2*, mice can develop beta-like cells that express markers such as *Pdx1* but do not express insulin, suggesting that *Nkx2.2* also plays a role in activation of genes required for terminal beta cell differentiation (64).

The data presented also suggests that Tle3 may be needed in more than one process in the beta cell to retain its phenotype as knockdown showed changes in gene expression, protein expression and insulin secretion. The mechanisms by which it may work are still to be investigated and there are several potential pathways to explore.

Firstly, as previously mentioned, Tle3 works in adipose tissue to encourage expression of PPAR γ target genes (122) and therefore may be playing a similar role in the activation of beta cell genes. The proximity ligation assay carried out showed interactions between *Pdx1* and Tle3 which makes the target genes of *Pdx1* a possible candidate for this. Alongside exploring this pathway to uncover the role of Tle3 in the function of the beta cell, the known role of Tle3 as a co-activator of downstream PPAR γ target genes also provides reason to investigate its involvement in the function of the group of drugs known as thiazolidinediones (TZDs). Thiazolidinediones act to increase insulin sensitivity through acting as agonists of PPAR γ in several tissues, particularly adipose tissue where TZDs encourage safe storage of lipids, reducing free fatty acid levels and insulin resistance (142, 143). Due to the role of Tle3 as a co-activator of PPAR γ , it would be interesting to see whether Tle3 is involved in the mechanism of action of this class of drugs, which is yet to be fully understood. A study looking into the role of beta cell specific ABCA1 protein (a protein involved in cholesterol homeostasis), showed that this protein is required for the drug Rosiglitazone (a member of the TZD family) to have its beneficial effects on glucose tolerance (144). Rosiglitazone is known to be an activator of PPAR γ , of which ABCA1 has been shown to be a downstream

target (145), which gives a potential mechanism by which Tle3 may be involved in the effect of these drugs. The stable Tle3 knockdown cell lines will be useful in future studies to determine whether Tle3 plays a role in the mechanism of action of the Thiazolidinediones.

Secondly, the suggested role of Tle3 in the processing of the insulin protein in the study by Metzger *et al.*, which looked at combined overexpression of Pdx1 and Tle3 (61), may provide an explanation as to why insulin content was downregulated following Tle3 knockdown. It would be interesting to investigate insulin processing following loss of Tle3. The interaction with Pdx1 may be a way in which Tle3 activates beta cell specific genes, therefore when the proteins are downregulated in times of high glucose (or the interaction between the two proteins are lost), the loss of these beta cell transcription factors and their involvement in insulin gene expression/processing may contribute to the decrease in insulin content and secretion seen in the high glucose model. To investigate this, studies could be set up using the stable *Tle3* knockdown cell lines to analyse expression of the insulin processing enzymes alongside assays such as C-peptide ELISA to determine whether insulin processing is affected by loss of *Tle3*.

Finally, the role of Tle3 in insulin secretion is yet to be elucidated. The combined overexpression of Pdx1 and Tle3 in alpha cells causing cells to secrete insulin in response to glucose is an indication of its importance in insulin secretion as this was not achieved by expressing Pdx1 alone (61). The studies presented here give strong evidence for its role in regulating not only stimulated insulin secretion but also basal insulin secretion. A study looking at human diabetic patients showed a dysregulation of basal insulin secretion with an increased plasma insulin level in patients with impaired glucose tolerance, compared to patients with normal glucose tolerance (123). Another study suggested that this dysregulation of basal insulin secretion could be due to a reduced level of cholesterol at membrane rafts, which are used to spatially organise proteins involved in exocytosis, including the release of insulin from pancreatic beta cells (80). Due to the role of Tle3 in adipose tissue as a regulator of adipogenesis (122), and the observation that loss of Tle3 encourages increased basal insulin secretion, its role in the production of cholesterol and phospholipids for membrane rafts is an area that may warrant investigation. A potential involvement of Tle3 in this pathway is depicted in Figure 6.1. Tle3 is known to act as a repressor of the Wnt pathway through antagonising β -catenin activation of LEF/TCF receptor

and the subsequent transcription of the Wnt target genes (122), thereby reversing β -catenin based repression of adipocyte gene activation. With the downregulation of Tle3, the loss of this antagonism on the Wnt genes may result in lowered cholesterol and fatty acid production for use in membrane rafts. TCF7L2 has also been shown to be a susceptibility gene for type 2 diabetes and the regulation of this pathway is important in pancreatic beta cells to encourage proper insulin secretion (146). A study by Zhai *et al.* showed that the β -catenin pathway contributes to the inhibition of sterol regulated element binding protein 1c (SREBP-1c) in hepatic stellate cells (147). Given the role of SREBP-1c in the generation of lipids and formation of cholesterol esters in the cell (148) it is possible that the loss of Tle3-mediated repression of the β -catenin pathway contributes to the changes in lipid production for membrane rafts in the pancreatic beta cell during diabetes. Another study looking at the inhibition of SREBP-1c by β -catenin in hepatic stellate cells showed that stabilisation of the β -catenin protein in the cytosol caused a reduction in expression and activity of SREBP-1c (147). This may also contribute to the reduced action of SREBP-1c in activating genes needed for lipogenesis. Furthermore, inhibition of endogenous cholesterol production in the pancreatic beta cell of mouse islets caused a marked decrease in stimulated insulin secretion through disruption of the voltage-gated calcium channel function (149). If, therefore, Tle3 plays a role in the proper production of lipids and cholesterol for membrane rafts in the pancreatic beta cell, this may provide a possible explanation as to the changes in beta cell function observed in the Tle3 knockdown studies.

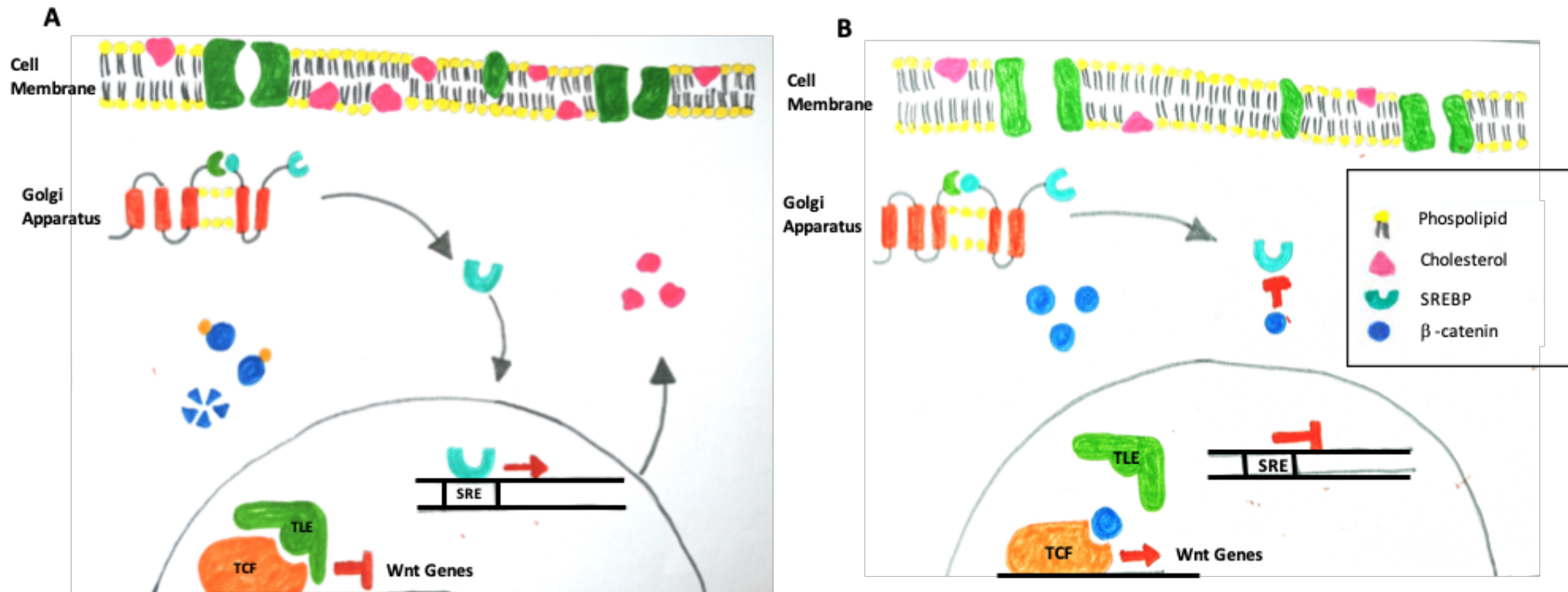


Figure 6.1 A suggested role for Tle3 in regulating insulin secretion in the pancreatic beta cell.

(A) Tle protein prevents binding of β -catenin to the LCF/TCF receptor, thereby preventing transcription of Wnt genes, which are known inhibitors of lipogenesis. Phosphorylation of β -catenin in the cytoplasm marks it from degradation and Tle continues to repress Wnt gene expression. SREBP protein is cleaved from its complex in the Golgi and moves to the nucleus to bind to the sterol regulatory element (SRE) and activate transcription of genes involved in lipogenesis and cholesterol production, allowing cholesterol and lipids to be produced and used for formation of the membrane rafts and allows for proper regulation of insulin release in the beta cell. (B) Downregulation of Tle3 may result in loss of competitive inhibition of LCF/TCF, allowing β -catenin to bind and activate transcription of Wnt genes, resulting in a suppression of lipogenesis. Stabilisation of β -catenin may result in β -catenin-based inhibition of SREBP causing downregulation of cholesterol production, thereby reducing the availability for formation of membrane rafts and resulting in dysregulation of insulin secretion.

TLE1 has been implicated as a risk allele for type 2 diabetes in recent GWAS studies (126) and has been shown to be the human functional equivalent of Tle3 (61). Although it is thought that TLE1 is likely to have the same role as Tle3, there has been little evidence provided by human studies which confirms this. Here, we aimed to elucidate, for the first time, the role of TLE1 in maintaining the beta cell phenotype during diabetes. To investigate this, tissue from two cohorts of patients with and without diabetes were evaluated for expression of insulin, glucagon and TLE1. A common finding in both cohorts studied was that the average number of insulin+ cells was reduced in diabetes and the number of bihormonal cells and glucagon cells were increased. These data give support to the hypothesis that pancreatic beta cells undergo transdifferentiation to an alpha like phenotype under diabetic conditions. To assess the role of TLE1 in these changes, expression of TLE1 in all cell types was also calculated using data from cohort 2. The findings showed that overall expression of TLE1 is reduced in diabetes. In line with the theory that TLE1 actively maintains the beta cell phenotype, these studies showed that although the number of insulin positive cells was reduced per islet as diabetes progressed, the beta cells that remained mono-hormonal showed increased likelihood of TLE1 expression. Alongside this, the loss of TLE1 in insulin positive cells showed a moderate correlation to the increase in glucagon expression which is in agreement with the previously established role of TLE1/3 as a repressor of the alpha cell program (61).

Subsequent analysis with the donor information provided showed that the loss of TLE1 and the increase in bihormonal cells correlated with an increased HbA1c. HbA1c is a measure of glycosylated haemoglobin which can give an average blood glucose reading for a period of roughly 3 months. For this reason it is often used as a determination of prognosis and diagnosis of diabetes (104). Previous studies have shown the value of HbA1c as an indicator of beta cell function and glucose sensitivity (150), and a link between glucose sensitivity and increased bihormonal cells in human patients without diabetes (151). The findings observed in these studies suggest that TLE1 may play a role in this relationship as there was a significant decrease in TLE1+ beta cells in donors in the highest HbA1c category. To further explore the role of TLE1 in the beta cell, transient knockdown of TLE1 was carried out in human islets. This data gave preliminary evidence that agreed with rodent studies and showed downregulation of some beta cell genes alongside upregulation of alpha cell gene, *Arx*, suggesting a loss of beta cell phenotype and gain of alpha cell characteristics upon loss of *TLE1* expression. Published data by Papizan *et al.* have suggested that, in rodents, Tle3 is

recruited by Nkx2.2 alongside HDAC1 to the promotor of the *Arx* gene as a mechanism of repression. Mutations in the Nkx2.2 tinman (TN) domain caused expression of *Arx* in pancreatic beta cells suggesting beta to alpha cell reprogramming (69). If TLE1 acts as the functional equivalent of Tle3 in rodents, this mechanism may explain the upregulation of *Arx* seen in the TLE1 human islet studies.

Although more research is needed into the role of TLE1/3 in the function and maintenance of the beta cell, these studies show evidence of a dual role as a repressor of the alpha cell program and a novel role in maintaining the beta cell phenotype. The collective *in vitro* and human pathology data has shown that loss of TLE1/3 in human and rodent cells can cause an upregulation of glucagon and increased bihormonal expression. The human data has also shown a potential role for TLE1 in maintaining glucose sensitivity and the mono-hormonal phenotype of the beta cell as the disease progresses. Further research should focus on determining the mechanisms of action of TLE1/3 in the beta cell and whether the increase in glucagon expression following loss of TLE1/3 is caused by activation of resultant *ARX* expression, or through indirect de-repression by downregulated beta cell transcription factors. Another area of interest would be to investigate its potential involvement in the action of current therapeutics, such as Thiazolidinediones, which would provide further insight into mechanisms of action and may help to improve treatments for patients. Further understanding of the role of TLE1/3, and the maintenance of its expression in the diabetic state, could help to develop treatments that prevent changes in phenotype and loss of function of the pancreatic beta cell.

6.2 Future work

There are numerous studies that require further investigation to properly establish the role of TLE1/3 in the beta cell.

Firstly, the interaction between Pdx1 and Tle3 can be carried out in rodent cell lines to establish whether interactions between these two proteins encourage transcription of beta cell genes. Overexpression of these two proteins individually and combined will give an idea as to whether Tle3 is needed for the proper function of the beta cell and whether it can help prevent loss of function seen during hyperglycaemia. Alongside this, analysis of C-peptide levels, alongside changes in proteins involved in insulin processing enzymes (PC2 and PC3), may indicate the role Tle3 has in insulin processing.

Secondly, the involvement of Tle3 in generation of lipids and membrane raft conservation may also provide insight into the dysregulation of both basal and stimulated insulin secretion seen in diabetic patients. Use of the stable knockdown cell lines will be useful for looking at levels of proteins involved in lipid homeostasis alongside observing changes in membrane rafts through immunostaining. The stable knockdown cell lines will also be useful in determining what role, if any, Tle3 has in the mechanism of action of the TZD class of drugs used in diabetes treatment.

Lastly, further analysis of TLE1 knockdown in intact human islets will provide information as to its role in beta cell function in humans and show whether this is similar to the role of Tle3 in rodents. Further staining of ARX in the human cohorts will also elucidate whether the loss of TLE1 may result in increased glucagon cell number due to induction by ARX, and looking at lean type 2 diabetic donors and matched controls will further understanding of loss of TLE1 in relation to different donor factors.

Taken together, these future studies could build on those presented here to elucidate the role of the novel transcription factor, TLE1/3, in the maintenance of the pancreatic beta cell and potentially provide a target for future therapeutics to help maintain the function of the beta cell during diabetes.

7 Bibliography

7.1 References

1. Mergenthaler P, Lindauer U, Dienel GA, Meisel A. Sugar for the brain: the role of glucose in physiological and pathological brain function. *Trends in neurosciences*. 2013;36(10):587-97.
2. Bernard K, Logsdon NJ, Ravi S, Xie N, Persons BP, Rangarajan S, et al. Metabolic Reprogramming is Required for Myofibroblast Contractility and Differentiation. *The Journal of biological chemistry*. 2015.
3. Rui L. Energy metabolism in the liver. *Comprehensive Physiology*. 2014;4(1):177-97.
4. Aronoff SL, Berkowitz, K., Shreiner, B. and Want, L. Glucose Metabolism and Regulation- Beyond Insulin and Glucagon. *Diabetes Spectrum*. 2004;17(3):183-90.
5. DeFronzo RA, Tripathy D. Skeletal muscle insulin resistance is the primary defect in type 2 diabetes. *Diabetes Care*. 2009;32 Suppl 2:S157-63.
6. Abdul-Ghani MA, DeFronzo RA. Pathogenesis of insulin resistance in skeletal muscle. *Journal of biomedicine & biotechnology*. 2010;2010:476279.
7. Adeva-Andany MM, Perez-Felpe N, Fernandez-Fernandez C, Donapetry-Garcia C, Pazos-Garcia C. Liver glucose metabolism in humans. *Biosci Rep*. 2016;36(6).
8. Agius L. Glucokinase and molecular aspects of liver glycogen metabolism. *Biochem J*. 2008;414(1):1-18.
9. Santoro N, Zhang CK, Zhao H, Pakstis AJ, Kim G, Kursawe R, et al. Variant in the glucokinase regulatory protein (GCKR) gene is associated with fatty liver in obese children and adolescents. *Hepatology*. 2012;55(3):781-9.
10. Havel PJ. Regulation of Energy Balance and Carbohydrate/Lipid Metabolism. *Diabetes*. 2004;53(S1):9.
11. Wendy M. Mueller KLS, * Francine Gregoire,† Joseph L. Evans,‡ and Peter J. Havel*. Effects of Metformin and Vanadium on Leptin Secretion from Cultured Rat Adipocytes. *Obesity Research*. 2000;8(7):10.
12. HAVEL BAAPJ. Leptin inhibits insulin secretion induced by cellular cAMP in a pancreatic B cell line (INS-1 cells). *American Journal of Physiology*. 1999;227:7.
13. Bonal C, Herrera PL. Genes controlling pancreas ontogeny. *Int J Dev Biol*. 2008;52(7):823-35.
14. Marcela Brissova MJF, Wendell E. Nicholson, Anita Chu, Boaz Hirshberg, David M. Harlan, and Alvin C. Powers. Assessment of Human Pancreatic Islet Architecture and Composition by Laser Scanning Confocal Microscopy. *Journal of Histochemistry and Cytochemistry*. 2005;53(9):10.
15. Da Silva Xavier G. The Cells of the Islets of Langerhans. *J Clin Med*. 2018;7(3).
16. Saltiel AR, Kahn, R. Insulin signalling and the regulation of glucose and lipid metabolism. *Nature*. 2001;414:799-806.
17. Gao T, McKenna B, Li C, Reichert M, Nguyen J, Singh T, et al. Pdx1 Maintains β Cell Identity and Function by Repressing an α Cell Program. *Cell Metabolism*. 2014;19(2):259-71.
18. Hauge-Evans AC, King AJ, Carmignac D, Richardson CC, Robinson IC, Low MJ, et al. Somatostatin secreted by islet delta-cells fulfills multiple roles as a paracrine regulator of islet function. *Diabetes*. 2009;58(2):403-11.
19. Aragon F, Karaca M, Novials A, Maldonado R, Maechler P, Rubi B. Pancreatic polypeptide regulates glucagon release through PPYR1 receptors expressed in mouse and human alpha-cells. *Biochim Biophys Acta*. 2015;1850(2):343-51.
20. Rorsman P, Ashcroft FM. Pancreatic β -Cell Electrical Activity and Insulin Secretion: Of Mice and Men. *Physiological reviews*. 2018;98(1):117-214.

21. Rorsman P, Renstrom E. Insulin granule dynamics in pancreatic beta cells. *Diabetologia*. 2003;46(8):1029-45.
22. Seino S, Shibasaki T, Minami K. Dynamics of insulin secretion and the clinical implications for obesity and diabetes. *The Journal of clinical investigation*. 2011;121(6):2118-25.
23. American Diabetes A. Diagnosis and classification of diabetes mellitus. *Diabetes Care*. 2008;31 Suppl 1:S55-60.
24. Guariguata L, Whiting DR, Hambleton I, Beagley J, Linnenkamp U, Shaw JE. Global estimates of diabetes prevalence for 2013 and projections for 2035. *Diabetes Res Clin Pract*. 2014;103(2):137-49.
25. Larissa Eiselein HJS, and John C. Rutledge. The Challenge of Type 1 Diabetes Mellitus. *ILAR Journal*. 2004;45(3):231-6.
26. G.R.Vreugdenhil AG, T.H.M. Ottenhoff, W.J.G. Melchers, B.O. Roep, J.M.D. Galama. Molecular mimicry in diabetes mellitus. The homologous domain in coxsackie B virus protein 2C and islet autoantigen GAD is highly conserved in the coxsackie B-like enteroviruses and binds to the diabetes associated HLA-DR3 molecule. *Diabetologia*. 1998;41:6.
27. Morgan NG, Richardson SJ. Enteroviruses as causative agents in type 1 diabetes: loose ends or lost cause? *Trends Endocrinol Metab*. 2014;25(12):611-9.
28. Winkler C, Lauber C, Adler K, Grallert H, Illig T, Ziegler AG, et al. An interferon-induced helicase (IFIH1) gene polymorphism associates with different rates of progression from autoimmunity to type 1 diabetes. *Diabetes*. 2011;60(2):685-90.
29. Parkkola A, Laine AP, Karhunen M, Harkonen T, Ryhanen SJ, Ilonen J, et al. HLA and non-HLA genes and familial predisposition to autoimmune diseases in families with a child affected by type 1 diabetes. *PLoS One*. 2017;12(11):e0188402.
30. Barrett JC, Clayton DG, Concannon P, Akolkar B, Cooper JD, Erlich HA, et al. Genome-wide association study and meta-analysis find that over 40 loci affect risk of type 1 diabetes. *Nat Genet*. 2009;41(6):703-7.
31. GRAEME I. BELL SH, AND JOHN H. KARAM. A Polymorphic Locus Near the Human Insulin Gene Is Associated with Insulin-dependent Diabetes Mellitus. *Diabetes*. 1984;33:8.
32. Fazeli Farsani S, van der Aa MP, van der Vorst MM, Knibbe CA, de Boer A. Global trends in the incidence and prevalence of type 2 diabetes in children and adolescents: a systematic review and evaluation of methodological approaches. *Diabetologia*. 2013;56(7):1471-88.
33. Jana Tumova MA, Jan Trnka. Excess of Free Fatty Acids as a Cause of Metabolic Dysfunction in Skeletal Muscle. *Physiological Research*. 2015.
34. de Ferranti S, Mozaffarian D. The perfect storm: obesity, adipocyte dysfunction, and metabolic consequences. *Clin Chem*. 2008;54(6):945-55.
35. Ali O. Genetics of type 2 diabetes. *World journal of diabetes*. 2013;4(4):114-23.
36. Fuchsberger C, Flannick J, Teslovich TM, Mahajan A, Agarwala V, Gaulton KJ, et al. The genetic architecture of type 2 diabetes. *Nature*. 2016;536(7614):41-7.
37. AHMED H. KISSEBAH NV, ROBERT MURRAY, DAVID J. EVANS, ARTHUR J. HARTZ, RONALD K. KALKHOFF, AND PETER W. ADAM. Relation of Body Fat Distribution to Metabolic Complications of Obesity. *Journal of Clinical Endocrinology and Metabolism*. 1982;54(2):7.
38. Tol A, Sharifirad G, Shojaezadeh D, Tavasoli E, Azadbakht L. Socio-economic factors and diabetes consequences among patients with type 2 diabetes. *J Educ Health Promot*. 2013;2:12.
39. Kelly SJ, Ismail M. Stress and type 2 diabetes: a review of how stress contributes to the development of type 2 diabetes. *Annu Rev Public Health*. 2015;36:441-62.

40. Pozzilli P, Strollo R, Bonora E. One size does not fit all glycemic targets for type 2 diabetes. *Journal of diabetes investigation*. 2014;5(2):134-41.
41. Boulton AJM. Management of Diabetic Peripheral Neuropathy. *Clinical Diabetes*. 2005;23(1):9-15.
42. Montero RM, Covic A, Gnudi L, Goldsmith D. Diabetic nephropathy: What does the future hold? *Int Urol Nephrol*. 2015.
43. Curtis TM, Gardiner TA, Stitt AW. Microvascular lesions of diabetic retinopathy: clues towards understanding pathogenesis? *Eye (Lond)*. 2009;23(7):1496-508.
44. Delplace V, Payne S, Shoichet M. Delivery strategies for treatment of age-related ocular diseases: From a biological understanding to biomaterial solutions. *J Control Release*. 2015.
45. R. Paul Robertson JH, Phuong Oanh T. Tran, and Vincent Poitout. Beta cell glucose toxicity, lipotoxicity, and chronic oxidative stress in type 2 diabetes. *Diabetes*. 2004;53(S1):6.
46. S. Jacqueminet IB, C. Rouault, G. Reach, and V. Poitout. Inhibition of Insulin Gene Expression by Long-term Exposure of Pancreatic Beta cells to Palmitate is Dependent on the Presence of a Stimulatory Glucose Concentration. *Metabolism*. 2000;49(4):5.
47. Jamie S. Harmon CEG, Yoshito Tanaka, Vincent Poitout, and R. Paul Robertson. Antecedent Hyperglycemia, Not Hyperlipidemia, Is Associated with Increased Islet Triglycerol Content and Decreased Insulin Gene mRNA Level in Zucker Diabetic Faty Rats. *Diabetes*. 2001;50:6.
48. Gillespie SJ, Kulkarni KD, Daly AE. Using Carbohydrate Counting in Diabetes Clinical Practice. *Journal of the American Dietetic Association*. 1998;98(8):897-905.
49. Steve A White JAS, David E R Sutherland. Pancreas transplantation. *Lancet*. 2009;373:9.
50. A.M. JAMES SHAPIRO MB, B.S., JONATHAN R.T. LAKEY, PH.D., EDMONDA. RYAN, M.D., GREGORY S. KORBUTT, PH.D., ELLENTOTH, M.D., GARTHL. WARNOCK, M.D., NORMAN M. KNETEMA, M.D., ANDRAYV. RAJOTTE, PH.D. Islet transplantation in seven patients with type 1 diabetes mellitus using a glucocorticoid free immunosuppressive regimen. *The New England journal of medicine*. 2000;343(4):9.
51. Zhou G, Myers R, Li Y, Chen Y, Shen X, Fenyk-Melody J, et al. Role of AMP-activated protein kinase in mechanism of metformin action. *Journal of Clinical Investigation*. 2001;108(8):1167-74.
52. Fiona M. Gribble FR. Differential selectivity of insulin secretagogues. Mechanisms, clinical implications and drug interactions. *Journal of Diabetes and Its Complications*. 2003;17:11-5.
53. Sanchez-Garrido MA, Brandt SJ, Clemmensen C, Muller TD, DiMarchi RD, Tschop MH. GLP-1/glucagon receptor co-agonism for treatment of obesity. *Diabetologia*. 2017;60(10):1851-61.
54. Rubino F. Bariatric surgery: effects on glucose homeostasis. *Current Opinion in Clinical Nutrition and Metabolic Care*. 2006;9(4):497-507.
55. Lim EL, Hollingsworth, K.G., Aribisala, B.S., Chen, M.J., Mathers, J.C. and Taylor, R. Reversal of type 2 diabetes: normalisation of beta cell function in association with decreased pancreas and liver triacylglycerol. *Diabetologia*. 2011;54(10):2506-14.
56. Taylor R, Al-Mrabeh A, Zhyzhneuskaya S, Peters C, Barnes AC, Aribisala BS, et al. Remission of Human Type 2 Diabetes Requires Decrease in Liver and Pancreas Fat Content but Is Dependent upon Capacity for beta Cell Recovery. *Cell Metab*. 2018.
57. Zhao M, Amiel SA, Christie MR, Muiesan P, Srinivasan P, Littlejohn W, et al. Evidence for the presence of stem cell-like progenitor cells in human adult pancreas. *J Endocrinol*. 2007;195(3):407-14.

58. Jorgen Jonsson LC, Thomas Edlund and Helena Edlund. Insulin promoter factor 1 is required for pancreas development in mice. *Nature*. 1994;371:606-9.
59. Cano DA, Soria B, Martin F, Rojas A. Transcriptional control of mammalian pancreas organogenesis. *Cell Mol Life Sci*. 2014;71(13):2383-402.
60. Hoffman BG, Zavaglia B, Beach M, Helgason CD. Expression of Groucho/TLE proteins during pancreas development. *BMC Dev Biol*. 2008;8:81.
61. David E. Metzger CL, Amin Sam Ziaie, Ali Naji, and Kenneth S. Zaret. Grg3/TLE3 and Grg1/TLE1 Induce Monohormonal Pancreatic Beta-Cells While Repressing Alpha-Cell Functions. *Diabetes*. 2014;63:1804-16.
62. Babu DA, Deering TG, Mirmira RG. A feat of metabolic proportions: Pdx1 orchestrates islet development and function in the maintenance of glucose homeostasis. *Mol Genet Metab*. 2007;92(1-2):43-55.
63. Schisler JC, Jensen PB, Taylor DG, Becker TC, Knop FK, Takekawa S, et al. The Nkx6.1 homeodomain transcription factor suppresses glucagon expression and regulates glucose-stimulated insulin secretion in islet beta cells. *Proceedings of the National Academy of Sciences of the United States of America*. 2005;102(20):7297-302.
64. L. Sussel JK, D. J. Hartigan-O'Connor, J. J. Meneses, R. A. Pedersen, J. L. Rubenstein and M. S. German. Mice lacking the homeodomain transcription factor Nkx2.2 have diabetes due to arrested differentiation of pancreatic beta cells. *Development*. 1998;125:2213-21.
65. Schisler JC, Fueger PT, Babu DA, Hohmeier HE, Tessem JS, Lu D, et al. Stimulation of human and rat islet beta-cell proliferation with retention of function by the homeodomain transcription factor Nkx6.1. *Mol Cell Biol*. 2008;28(10):3465-76.
66. Taylor Brandon L, Liu F-F, Sander M. Nkx6.1 Is Essential for Maintaining the Functional State of Pancreatic Beta Cells. *Cell reports*. 2013;4(6):1262-75.
67. Agarwal M, Kumar P, Mathew SJ. The Groucho/Transducin-like enhancer of split protein family in animal development. *IUBMB Life*. 2015;67(7):472-81.
68. Metzger DE, Gasperowicz M, Otto F, Cross JC, Gradwohl G, Zaret KS. The transcriptional co-repressor Grg3/Tle3 promotes pancreatic endocrine progenitor delamination and β -cell differentiation. *Development*. 2012;139(8):1447-56.
69. Papizan JB, Singer RA, Tschen SI, Dhawan S, Friel JM, Hipkens SB, et al. Nkx2.2 repressor complex regulates islet beta-cell specification and prevents beta-to-alpha-cell reprogramming. *Genes Dev*. 2011;25(21):2291-305.
70. Abed M, Barry KC, Kenyagin D, Koltun B, Phippen TM, Delrow JJ, et al. Degringolade, a SUMO-targeted ubiquitin ligase, inhibits Hairy/Groucho-mediated repression. *EMBO J*. 2011;30(7):1289-301.
71. Hasson P, Egoz N, Winkler C, Volohonsky G, Jia S, Dinur T, et al. EGFR signaling attenuates Groucho-dependent repression to antagonize Notch transcriptional output. *Nat Genet*. 2005;37(1):101-5.
72. & AEBLC-MRGRAR, Butler ACCPC. Adaptive changes in pancreatic beta cell fractional area and beta cell turnover in human pregnancy. *Diabetologia*. 2010;53:9.
73. Lingohr MK, Buettner, R., Rhodes, C.J. Pancreatic beta cell growth and survival. A role in obesity linked type 2 diabetes. *Trends in Molecular Medicine*. 2002;8:9.
74. Yuval Dor JB, Olga I. Martinez & Douglas A. Melton. Adult pancreatic beta cells are formed by self-duplication rather than stem β -cell differentiation. *Nature*. 2004;429:6.
75. Thorel F, Nepote V, Avril I, Kohno K, Desgraz R, Chera S, et al. Conversion of adult pancreatic alpha-cells to beta-cells after extreme beta-cell loss. *Nature*. 2010;464(7292):1149-54.
76. Butler AEJ, J.; Bonnar-Weir, S.; Ritzel, R.; Rizza, R.A.; Butler, P.C. Beta-Cell Deficit and Increased Beta-Cell Apoptosis in Humans With Type 2 Diabetes. *Diabetes*. 2003;52:9.

77. Jones HB, Nugent D, Jenkins R. Variation in characteristics of islets of Langerhans in insulin-resistant, diabetic and non-diabetic-rat strains. *Int J Exp Pathol*. 2010;91(3):288-301.
78. Rahier J, Guiot Y, Goebbels RM, Sempoux C, Henquin JC. Pancreatic beta-cell mass in European subjects with type 2 diabetes. *Diabetes, obesity & metabolism*. 2008;10 Suppl 4:32-42.
79. & LMMSMDCMB, & FSLMDFFSFO, Marchetti FPMUBP. Are we overestimating the loss of beta cells in type 2 diabetes. *Diabetologia*. 2014;57:4.
80. Nagaraj V, Kazim AS, Helgeson J, Lewold C, Barik S, Buda P, et al. Elevated Basal Insulin Secretion in Type 2 Diabetes Caused by Reduced Plasma Membrane Cholesterol. *Molecular endocrinology*. 2016;30(10):1059-69.
81. JOHN D. BRUNZELL RPR, ROGER L. LERNER,, WILLIAM R. HAZZARD JWE, EDWIN L. BIERMAN ADP, JR. Relationships Between Fasting Plasma Glucose Levels and Insulin Secretion During Intravenous Glucose Tolerance Tests. *Journal of Clinical Endocrinology and Metabolism*. 1976;42(2):7.
82. Talchai C, Xuan S, Lin HV, Sussel L, Accili D. Pancreatic beta cell dedifferentiation as a mechanism of diabetic beta cell failure. *Cell*. 2012;150(6):1223-34.
83. Offield MF, Jetton, T.L., Labosky, P.A., Ray, M., Stein, R.W., Magnuson, M.A., Hogan, B.L.M. and Wright, C.V.E. PDX-1 is required for pancreatic outgrowth and differentiation of the rostral duodenum. *Development*. 1996;122(3):983-95.
84. Chakrabarti SKaM, R.G. Transcription Factors Direct the Development and Function of Pancreatic Beta Cells. *Trends in Endocrinology and Metabolism*. 2003;14(2):78-84.
85. Brereton MF, Iberl M, Shimomura K, Zhang Q, Adriaenssens AE, Proks P, et al. Reversible changes in pancreatic islet structure and function produced by elevated blood glucose. *Nat Commun*. 2014;5:4639.
86. Gutierrez GD, Bender AS, Cirulli V, Mastracci TL, Kelly SM, Tsigos A, et al. Pancreatic beta cell identity requires continual repression of non-beta cell programs. *The Journal of clinical investigation*. 2017;127(1):244-59.
87. Swisa A, Avrahami D, Eden N, Zhang J, Feleke E, Dahan T, et al. PAX6 maintains beta cell identity by repressing genes of alternative islet cell types. *The Journal of clinical investigation*. 2017;127(1):230-43.
88. Moore CB, Guthrie EH, Huang MT, Taxman DJ. Short hairpin RNA (shRNA): design, delivery, and assessment of gene knockdown. *Methods Mol Biol*. 2010;629:141-58.
89. RHONA SEIJFFERS OB-D, YAEL COHEN, AVRAHAM KARASIK, MEIR BEREZIN, CHRISTOPHER B. NEWGARD, AND SARAH FERBER. Increase in PDX-1 Levels Suppresses Insulin Gene Expression in RIN 1046-38 Cells. *Endocrinology*. 1999;140(7):7.
90. Carthew RW, Sontheimer EJ. Origins and Mechanisms of miRNAs and siRNAs. *Cell*. 2009;136(4):642-55.
91. Carmen María Jiménez-Moreno IdGH-G, 1 Livia López-Noriega,1 Petra Isabel Lorenzo,1 Nadia Cobo-Vuilleumier,1 Esther Fuente-Martín,1 José Manuel Mellado-Gil,1 Géraldine Parnaud,2 Domenico Bosco,2 Benoit Raymond Gauthier,1,* and Alejandro Martín-Montalvo1,*. A Simple High Efficiency Intra-Islet Transduction Protocol Using Lentiviral Vectors. *Current Gene Therapy*. 2015;15(4):10.
92. Bobrich MA, Schwabe SA, Brobeil A, Viard M, Kamm M, Mooren FC, et al. PTP1B51: a new interaction partner of the insulin receptor and PKA in adipose tissue. *J Obes*. 2013;2013:476240.
93. Komatsu H, Omori K, Parimi M, Rawson J, Kandeel F, Mullen Y. Determination of Islet Viability Using a Zinc-Specific Fluorescent Dye and a Semiautomated Assessment Method. *Cell Transplant*. 2016;25(10):1777-86.

94. Guidone C, Manco M, Valera-Mora E, Iaconelli A, Gniuli D, Mari A, et al. Mechanisms of recovery from type 2 diabetes after malabsorptive bariatric surgery. *Diabetes*. 2006;55(7):2025-31.
95. Gerber PA, Rutter GA. The Role of Oxidative Stress and Hypoxia in Pancreatic Beta-Cell Dysfunction in Diabetes Mellitus. *Antioxid Redox Signal*. 2017;26(10):501-18.
96. Peter Krippeit-Drews * CKA, Susanne Welker †, Florian Lang *, † HPTAaGD. Interference of H₂O₂ with stimulus-secretion coupling in mouse pancreatic beta cells. *Journal of Physiology*. 1999;514(2):10.
97. Waeber AAGNDFSAMFJYRRCWG. Human high-density lipoprotein particles prevent activation of the JNK pathway induced by human oxidised low-density lipoprotein particles in pancreatic beta cells. *Diabetologia*. 2007;50:10.
98. Cernea S, Dobreanu M. Diabetes and beta cell function: from mechanisms to evaluation and clinical implications. *Biochimica Medica*. 2013:266-80.
99. Brereton MF, Rohm M, Ashcroft FM. beta-Cell dysfunction in diabetes: a crisis of identity? *Diabetes, obesity & metabolism*. 2016;18 Suppl 1:102-9.
100. Cinti F, Bouchi R, Kim-Muller JY, Ohmura Y, Sandoval PR, Masini M, et al. Evidence of beta-Cell Dedifferentiation in Human Type 2 Diabetes. *J Clin Endocrinol Metab*. 2016;101(3):1044-54.
101. Giacca A, Xiao C, Oprescu AI, Carpentier AC, Lewis GF. Lipid-induced pancreatic beta-cell dysfunction: focus on in vivo studies. *Am J Physiol Endocrinol Metab*. 2011;300(2):E255-62.
102. Beatriz Sosa-Pineda KC, Miguel Torres, Guillermo Oliver and Peter Gruss. The Pax4 gene is essential for differentiation of insulin producing beta cells in the mammalian pancreas. *Nature*. 1997;386:4.
103. Crowley LC, Waterhouse NJ. Detecting Cleaved Caspase-3 in Apoptotic Cells by Flow Cytometry. *Cold Spring Harbor protocols*. 2016;2016(11).
104. Sherwani SI, Khan HA, Ekhzaimy A, Masood A, Sakharkar MK. Significance of HbA1c Test in Diagnosis and Prognosis of Diabetic Patients. *Biomark Insights*. 2016;11:95-104.
105. Srihardyastutie A, Soeatmadji DW, Fatchiyah F, Aulani Aa. The Relationship between HbA1c, Insulin Resistance and Changes of Insulin Secretion in Indonesian Type 2 Diabetic Subjects 2014. 25-30 p.
106. Kubo A, Stull R, Takeuchi M, Bonham K, Gouon-Evans V, Sho M, et al. Pdx1 and Ngn3 overexpression enhances pancreatic differentiation of mouse ES cell-derived endoderm population. *PLoS One*. 2011;6(9):e24058.
107. Gannon M, Ables ET, Crawford L, Lowe D, Offield MF, Magnuson MA, et al. pdx-1 function is specifically required in embryonic beta cells to generate appropriate numbers of endocrine cell types and maintain glucose homeostasis. *Dev Biol*. 2008;314(2):406-17.
108. Home P, Riddle M, Cefalu WT, Bailey CJ, Bretzel RG, Del Prato S, et al. Insulin therapy in people with type 2 diabetes: opportunities and challenges? *Diabetes Care*. 2014;37(6):1499-508.
109. Marroqui L, Masini M, Merino B, Grieco FA, Millard I, Dubois C, et al. Pancreatic alpha Cells are Resistant to Metabolic Stress-induced Apoptosis in Type 2 Diabetes. *EBioMedicine*. 2015;2(5):378-85.
110. Lavon N, Yanuka O, Benvenisty N. The effect of overexpression of Pdx1 and Foxa2 on the differentiation of human embryonic stem cells into pancreatic cells. *Stem Cells*. 2006;24(8):1923-30.
111. Yamamoto Y, Miyatsuka T, Sasaki S, Miyashita K, Kubo F, Shimo N, et al. Preserving expression of Pdx1 improves beta-cell failure in diabetic mice. *Biochem Biophys Res Commun*. 2017;483(1):418-24.

112. Yuan Y, Hartland K, Boskovic Z, Wang Y, Walpita D, Lysy PA, et al. A small-molecule inducer of PDX1 expression identified by high-throughput screening. *Chem Biol*. 2013;20(12):1513-22.
113. Gerard Gradwhol AD, Marianne LeMeur, Francois Guillemot. Neurogenin3 is required for the development of the four endocrine cell lineages of the pancreas. *Proceedings for the National Academy of Science* 2000;97(4):4.
114. Pedersen JK, Nelson SB, Jorgensen MC, Henseleit KD, Fujitani Y, Wright CV, et al. Endodermal expression of Nkx6 genes depends differentially on Pdx1. *Dev Biol*. 2005;288(2):487-501.
115. Teo AK, Tsuneyoshi N, Hoon S, Tan EK, Stanton LW, Wright CV, et al. PDX1 binds and represses hepatic genes to ensure robust pancreatic commitment in differentiating human embryonic stem cells. *Stem Cell Reports*. 2015;4(4):578-90.
116. Santisteban P, Recacha P, Metzger DE, Zaret KS. Dynamic expression of Groucho-related genes Grg1 and Grg3 in foregut endoderm and antagonism of differentiation. *Dev Dyn*. 2010;239(3):980-6.
117. Ortega FJ, Serrano M, Rodriguez-Cuenca S, Moreno-Navarrete JM, Gomez-Serrano M, Sabater M, et al. Transducin-like enhancer of split 3 (TLE3) in adipose tissue is increased in situations characterized by decreased PPARgamma gene expression. *J Mol Med (Berl)*. 2015;93(1):83-92.
118. Loïc Leroux PD, Luciane Lamotte, Bertrand Duvillié, Nathalie Cordonnier,, Malene Jackerott JJ, Danielle Bucchini, and Rajiv L. Joshi. Compensatory Responses in Mice Carrying a Null Mutation for Ins1 or Ins2. *Diabetes*. 2001;50(S1):4.
119. Jain R, Lammert E. Cell-cell interactions in the endocrine pancreas. *Diabetes, obesity & metabolism*. 2009;11 Suppl 4:159-67.
120. Marie-Therese Guillam EH, Elisabeth Schaerer, J.-Y. Wu, Morris J. Birnbaum, Friedrich Beermann, Andrea Schmidt, Nathalie Deriaz and Bernard Thorens Early diabetes and abnormal postnatal pancreatic islet development in mice lacking Glut-2. *Nature Genetics*. 1997;17:4.
121. Hou JC, Min L, Pessin JE. Chapter 16 Insulin Granule Biogenesis, Trafficking and Exocytosis. *Insulin and IGFs. Vitamins & Hormones*2009. p. 473-506.
122. Villanueva CJ, Waki H, Godio C, Nielsen R, Chou WL, Vargas L, et al. TLE3 is a dual-function transcriptional coregulator of adipogenesis. *Cell Metab*. 2011;13(4):413-27.
123. Stefano Del Prato PM, and Riccardo C. Bonadonna. Phasic Insulin Release and Metabolic Regulation in Type 2 Diabetes. *Diabetes*. 2002;51(S1):8.
124. H. Siebe Spijker HS, 1,2 Johanne H. Ellenbroek,1 Maaïke M. Roefs,1, Marten A. Engelse EB, 3 Abraham J. Koster,3 Ton J. Rabelink,1, Barbara C. Hansen AC, 5 Françoise Carlotti,1 and Eelco J.P. de Koning1,6. Loss of beta cell identity occurs in type 2 diabetes and is associated with islet amyloid deposits. *Diabetes*. 2015;64:11.
125. Anderson SJ, White MG, Armour SL, Maheshwari R, Tiniakos D, Muller YD, et al. Loss of end-differentiated beta-cell phenotype following pancreatic islet transplantation. *Am J Transplant*. 2018;18(3):750-5.
126. Harder MN, Ribel-Madsen R, Justesen JM, Sparso T, Andersson EA, Grarup N, et al. Type 2 diabetes risk alleles near BCAR1 and in ANK1 associate with decreased beta-cell function whereas risk alleles near ANKRD55 and GRB14 associate with decreased insulin sensitivity in the Danish Inter99 cohort. *J Clin Endocrinol Metab*. 2013;98(4):E801-6.
127. Huopio H, Cederberg H, Vangipurapu J, Hakkarainen H, Paakkonen M, Kuulasmaa T, et al. Association of risk variants for type 2 diabetes and hyperglycemia with gestational diabetes. *Eur J Endocrinol*. 2013;169(3):291-7.
128. Alfidhli EM. Gestational diabetes mellitus. *Saudi Med J*. 2015;36(4):399-406.

129. White MGM, H.L.; Rigby, R.; Huang, G.C.; Amer, A.; Booth, T.; White, S.; Shaw, J.A.M. Expression of Mesenchymal and a-Cell Phenotypic Markers in Islet b-Cells in Recently Diagnosed Diabetes. *Diabetes Care*. 2013;36(11):3.
130. Morgan¹ KTMARSJRN. The subcellular distribution of cyclin-D1 and cyclin-D3 within human islet cells varies according to the status of the pancreas donor. *Diabetologia*. 2015;58:8.
131. H. Siebe Spijker RBGR, A. Mieke Mommaas-Kienhuis, Aart A. van Apeldoorn,, Marten A. Engelse AZ, Susan Bonner-Weir, Ton J. Rabelink, Rob C. Hoeben,, Hans Clevers CLM, Françoise Carlotti¹ and Eelco J.P. de Koning,. Conversion of Mature Human Beta Cells Into Glucagon Producing Alpha Cells. *Diabetes*. 2003;62:10.
132. Chung CH, Hao E, Piran R, Keinan E, Levine F. Pancreatic beta-cell neogenesis by direct conversion from mature alpha-cells. *Stem Cells*. 2010;28(9):1630-8.
133. Piran R, Lee SH, Li CR, Charbono A, Bradley LM, Levine F. Pharmacological induction of pancreatic islet cell transdifferentiation: relevance to type I diabetes. *Cell Death Dis*. 2014;5:e1357.
134. Lam CJ, Cox AR, Jacobson DR, Rankin MM, Kushner JA. Highly Proliferative alpha-Cell-Related Islet Endocrine Cells in Human Pancreata. *Diabetes*. 2018;67(4):674-86.
135. Li S, Xiao J, Ji L, Weng J, Jia W, Lu J, et al. BMI and waist circumference are associated with impaired glucose metabolism and type 2 diabetes in normal weight Chinese adults. *J Diabetes Complications*. 2014;28(4):470-6.
136. Negi S, Jetha A, Aikin R, Hasilo C, Sladek R, Paraskevas S. Analysis of beta-cell gene expression reveals inflammatory signaling and evidence of dedifferentiation following human islet isolation and culture. *PLoS One*. 2012;7(1):e30415.
137. Jennifer L. Fiori¹, Yu-Kyong Shin¹, Wook Kim¹, Susan M. Krzysik-Walker¹, Isabel González-Mariscal¹, Olga D. Carlson¹, et al. Resveratrol prevents b-cell dedifferentiation in nonhuman primates given a high-fat/high-sugar diet. *Diabetes*. 2013;62(10):13.
138. Wang H, Maechler P, Ritz-Laser B, Hagenfeldt KA, Ishihara H, Philippe J, et al. Pdx1 level defines pancreatic gene expression pattern and cell lineage differentiation. *The Journal of biological chemistry*. 2001;276(27):25279-86.
139. Yang YP, Thorel F, Boyer DF, Herrera PL, Wright CV. Context-specific alpha- to-beta-cell reprogramming by forced Pdx1 expression. *Genes Dev*. 2011;25(16):1680-5.
140. Galbo T, Pedersen IL, Fløyl T, Bang-Berthelsen CH, Serup P, Madsen OD, et al. Novel monoclonal antibodies against Pdx1 reveal feedback regulation of Pdx1 protein levels. *European Journal of Histochemistry*. 2010;54(2).
141. Merglen A, Theander S, Rubi B, Chaffard G, Wollheim CB, Maechler P. Glucose sensitivity and metabolism-secretion coupling studied during two-year continuous culture in INS-1E insulinoma cells. *Endocrinology*. 2004;145(2):667-78.
142. KENDALL DM. Thiazolidinediones. The case for early use. *Diabetes Care*. 2006;29(1):4.
143. Soccio RE, Chen ER, Lazar MA. Thiazolidinediones and the promise of insulin sensitization in type 2 diabetes. *Cell Metab*. 2014;20(4):573-91.
144. Brunham LR, Kruit JK, Pape TD, Timmins JM, Reuwer AQ, Vasanji Z, et al. Beta-cell ABCA1 influences insulin secretion, glucose homeostasis and response to thiazolidinedione treatment. *Nat Med*. 2007;13(3):340-7.
145. Chinetti G, Lestavel S, Bocher V, Remaley AT, Neve B, Torra IP, et al. PPAR-alpha and PPAR-gamma activators induce cholesterol removal from human macrophage foam cells through stimulation of the ABCA1 pathway. *Nat Med*. 2001;7(1):53-8.
146. Gloyn AL, Braun M, Rorsman P. Type 2 diabetes susceptibility gene TCF7L2 and its role in beta-cell function. *Diabetes*. 2009;58(4):800-2.

147. Zhai X, Yan K, Fan J, Niu M, Zhou Q, Zhou Y, et al. The beta-catenin pathway contributes to the effects of leptin on SREBP-1c expression in rat hepatic stellate cells and liver fibrosis. *Br J Pharmacol*. 2013;169(1):197-212.
148. Eberle D, Hegarty B, Bossard P, Ferre P, Fouchelle F. SREBP transcription factors: master regulators of lipid homeostasis. *Biochimie*. 2004;86(11):839-48.
149. Xia F, Xie L, Mihic A, Gao X, Chen Y, Gaisano HY, et al. Inhibition of cholesterol biosynthesis impairs insulin secretion and voltage-gated calcium channel function in pancreatic beta-cells. *Endocrinology*. 2008;149(10):5136-45.
150. Arie Srihardyastutie DWS, Fatchiyah Fatchiyah, Aulanni'am Aulani. The relationship between HbA1c Insulin resistance and changes in insulin secretion in indonesian type 2 diabetic subjects. *Advances in Natural and Applied Sciences*. 2014;8(8):5.
151. Mezza T, Sorice GP, Conte C, Sun VA, Cefalo CM, Moffa S, et al. beta-Cell Glucose Sensitivity Is Linked to Insulin/Glucagon Bihormonal Cells in Nondiabetic Humans. *J Clin Endocrinol Metab*. 2016;101(2):470-5.

8 Appendix A. Published Papers